JANUARY 29 & 30 1976

Records File
F-893-28-8-2

DOE/SF/00893--T5

MASTER

PROGRAM FOR THE DEVELOPMENT OF DESIGN DATA

LMFBR STEAM GENERATOR MATERIALS

AM03-76SF00893

Prepared For The
ENERGY RESEARCH AND DEVELOPMENT ADMINISTRATION
Under Contract AT(04-3)-893
TASK 10-G and TASK 18

GENERAL ELECTRIC

NOTICE

This report was prepared as an account of work sponsored by the United States Government. Neither the United States nor the Energy Research and Development Administration, nor any of their employees, nor any of their contractors, subcontractors, or their employees, makes any warranty, express or implied, or assumes any legal liability or responsibility for the accuracy, completeness or usefulness of any information, apparatus, product or process disclosed, or represents that its use would not infringe privately owned rights.

TABLE OF CONTENTS

Contract No. AT(04-3)-893, Task 18, 189-SG028 (FY76)

STEAM GENERATOR PLANT MATERIALS DEVELOPMENT

Contract No. AT(04-3)-893-10, Task G, 189-SG029 (FY76)

STEAM GENERATOR MATERIALS QUALIFICATION

CONTRACT NO. AT(04-3)-893, TASK 18

189 No. SG028 FY76

STEAM GENERATOR PLANT MATERIALS DEVELOPMENT

CONTRIBUTORS

K. D. Challenger

J. F. Copeland

G. R. Dodson

L. V. Hampton

M. E. Indig

J. L. Krankota

P. P. Pizzo

P. Roy

Contract No. AT(04-3)-893, Task 18

189 No. SG028 FY76

STEAM GENERATOR PLANT MATERIALS DEVELOPMENT

1. FY76 HIGHLIGHTS

- Uniaxial creep tests on 2¼Cr-1Mo in strongly decarburizing sodium failed in much less time than control tests in Argon but with the same fracture strain.

- An undefined interaction between sodium and tubular 2¼Cr-1Mo weld metal creep specimens that resulted in severe weld porosity has occurred.

- Simulated tubes to tube sheet welds of 2¼Cr-1Mo tested in 482°C (900°F) superheated steam containing 5 to 10ppm dissolved caustic did not suffer stress corrosion cracking.

- No stress corrosion cracking was observed in straining electrode experiments on 2¼Cr-1Mo tested in 5% NaOH at 316°C (600°F) with applied potentials ranging from - 0.1 to + 0.4 volts.

- A single constant extension rate experiment has been completed with Incoloy 800 in the Grade 1 condition. Compared with the reference heat treatment, Grade 2, the alloy exhibited excellent resistance to caustic cracking at 316°C (600°F) in 5% caustic.

- Preliminary crack growth rates with up to 1 min. hold time determined for Type 316 SS in carburizing sodium indicate no degredation of this property. However, calculations relating crack growth to carburization rates indicate that for the condition of these tests a one hour hold time is required before carburization effects should be observed.

- The second run, B-2, of the Intermediate Heat Transport System Loop (ISML) has been completed; the total loop operation time is now $\sim$ 1500 hours.

- ORNL has submitted several revised materials property correlations for 2¼Cr-1Mo to the NSM Handbook for review and approval. These include: tensile and creep elongation and reduction in area, elastic properties, toughness for tensile instability, true stress/strain equations, cyclic and saturated stress/strain curves, bilinear yield strength, and stress/strain parameters for cyclically hardened materials.

- No degredation of heat transfer properties due to particulate deposition in loop 1 operating at 650°C (1200°F) with low oxygen sodium has been observed after 4,000 hours.

- Initial fracture toughness results on 2¼Cr-1Mo, both VAR and air melted, in several different heat treatment conditions tested at room temperature all fall above the ASME Code, Appendix G, K_{IR} curve indicating safe performance if Appendix G requirements are followed.

2. INTRODUCTION

The primary objective of Task 18 is characterization of materials, mainly 2¼Cr-1Mo and austenitic stainless steels, to assure that satisfactory materials compatibility is achieved with LMFBR steam generator environments.

Subtask A will determine the kinetics and magnitude of decarburization of 2¼Cr-1Mo in high temperature liquid sodium. In addition, this Subtask relates the degree of decarburization to subsequent effects on mechanical properties. Subtask B is an assessment of stress corrosion susceptibility of 2¼Cr-1Mo in water/steam environments of LMFBR steam generators; both normal and various upset conditions (caustic contamination) are being investigated. Subtask C is for study of stainless steel mechanical properties within a carbruizing sodium environment at high temperatures. The kinetics and magnitude of carburization and decarburization are being determined from a model loop of the Intermediate Heat Transport System (IHTS), Subtask D. Thus, Subtasks C and D define, respectively, the effect of carburization on mechanical properties and the magnitude of carburization.

In addition to these direct characterization programs, two activities are in progress that directly support LMFBR steam generator design and fabrication. Under Subtask E, General Electric heads the working committee on steam generator materials for the Nuclear Systems Materials Handbook. Subtask F, an experimental effort, is investigating thermal degradation effects produced by particulate deposition (in sodium) on heat transfer surfaces.

3. DECARBURIZATION KINETICS AND DESIGN METHODS VERIFICATION TESTING (SUBTASK A)

L. V. Hampton/J. L. Krankota/P. P. Pizzo

3.1 OBJECTIVE

The objective of this program is to define the decarburization kinetics of 2¼Cr-1Mo base metal and weld metal exposed to 510°C(950°F) sodium, and to evaluate the response of these materials to interrupted creep loading.

This is necessary because one of the major concerns with the use of 2¼Cr-1Mo for sodium-heated steam generators has been its susceptibility to decarburization. However, it has been shown that the decarburization kinetics of 2¼Cr-1Mo base metal are sufficiently slow to permit its use for steam generator tubing in the LMFBR with only a small (10%) design stress penalty. This small design penalty is possible because the creep/rupture properties of 2¼Cr-1Mo are relatively insensitive to bulk carbon content until the level drops below 0.03-0.04% C, a value which will not be reached in the design life of steam generator tubes under LMFBR secondary sodium conditions. Decarburization tests are being conducted in this task to confirm the predicted rates.

Since the allowable stresses for a welded tube are based on the strength properties of the weakeast part of that tube, a "weak" weld in a steam generator tube would govern the allowable stress for the entire tube. Therefore a series of decarburization and creep tests on welds are also being performed to confirm predicted behavior.

3.2 DECARBURIZATION KINETICS

The test matrix to obtain decarburization rate data for 2¼Cr-1Mo base and weld metal in 510°C (950°F) static, titanium-gettered sodium has been completed. With the conclusion of run DP-8, weld metal specimens with 7,000 hours total exposure time and base metal specimens with 12,500 hours exposure have been obtained. Chemical analyses to determine levels of carbon losses of these specimens are in progress.

Weld metal pin specimens (0.318 cm. dia. x 7.62 cm) were fabricated from a 2¼Cr-1Mo linear simulated tube-to-tube sheet weld made at ORNL.[1] After fabrication, the pins were stress-relieved according to Table 3.1. Carbon loss data for 1900 and 4500 hour exposures of weld metal specimens yields a rate constant of 5×10^{-8} g/cm^2-sec for this material. This interim rate is indicated in Figure 3.1, along with previously reported base metal data. Analysis of the 7,000 hour specimens will further improve confidence in the definition of the decarburization kinetics of 2¼Cr-1Mo weld metal.

Figures 3.2a, b, and c show microstructures of exposed base and weld metal. Figures 3.2 d and e show microstructures for 2¼Cr-1Mo base metal after annealing (Fig. 3.2d) and normalizing and tempering (Fig. 3.2e). Heat treatment details are shown in Table 3.1. Based on the data of Figure 3.1, the carbide dispersion shown in Figure 3.2 results in a more stable microstructure, as indicated in the last report. After 10,000 hours exposure in 510°C (950°F) sodium, carbides in both specimens tend to coarsen and the annealed material shows evidence of heavy carbide precipitation in the grain boundaries.

Decarburization studies are continuing with vacuum-arc and electroslag

remelted (RDT, CRBR reference melt practice) materials, including base metal and weld heat affected zones. These materials are being tested after several different annealing and normalized and tempering treatments in order to further investigate the effect of prior thermal history on the decarburization behavior of 2¼Cr-1Mo. Heat treatment has been found to effect rates of decarburization significantly, both as a result of this work and recent work done in Japan and France.

3.3 MECHANICAL PROPERTIES OF 2¼Cr-1Mo STEEL IN DECARBURIZING SODIUM

Progress continues in the characterization of the mechanical behavior of isothermal annealed 2¼Cr-1Mo steel in decarburizing sodium. Data for the current phase of the mechanical properties program have been analyzed and the results are presented in this report. The mechanical properties program consists of testing tubular specimens under uniaxial stress creep conditions, and pressure pins (sealed and pressurized cylinders) under biaxial stress test conditions.

Test parameters used in the uniaxial creep/fatigue program are presented in Table 3.2. Both constant load creep tests and cyclic load creep tests are performed. Cyclic tests consist of a sustained monotonic load, with a periodic load increase which results in an approximate 69 MPa (10ksi) stress increment. This peak load is applied once each twenty-four hours, and the load is applied over an approximate 10 second period. The results of the first phase of this test program are tabulated in Table 3.3. Calibration of instrumented tubular test specimens indicated sources of error in earlier analyses of the raw data. The data of Table 3.3 supersede results previously reported.

Minimum creep rates are illustrated in Figure 3.3. No clear differentiation was observed between the decarburized and control test data. Creep rupture data

from tubular creep specimens are shown in Figure 3.4. Again, the data are limited, and no clear decarburization effect is apparent. All data lie beyond the minimum expected value of time to rupture for a given applied stress, as approximated from ASME Code Case 1592.

Typical creep curves for both central (Argon) and Na/Ti exposed uniaxial tubular specimens are presented in Figure 3.5. Both specimens were tested at 241 MPa (35 ksi) and at 502°C (935°F). Another Na/Ti specimen (A14) was tested under equivalent conditions, and its fracture time and fracture strain have been plotted in Figure 3.5.

The creep curves of Figure 3.5 allow direct comparison of the behavior of both Na/Ti exposed and control specimens under equivalent creep conditions. On the basis of this isolated datum, a decarburizing effect is observed. The Na/Ti exposed specimens are less creep resistant than the control (helium exposed) specimens. This is true over a broad strain range. A creep strain of 2½% is attained after 180 hours for the Na/Ti exposed sample, while the control sample attains 2½% strain after approximately 1140 hours. If found to be a definite trend in subsequent tests, this would suggest that decarburizing has a direct influence on elevated temperature deformation processes.

Information on Table 3.3 and the creep curves of Figure 3.5 indicate that the fracture strain is essentially constant, irrespective of the test environment. The fracture strain is a common measure of the creep ductility of an alloy. A constant strain to failure suggests that the decarburizing environment does not have a first order effect on fracture processes. If however, fracture processes take place over a more limited range of strain (5 to 10%), as would be the case for a more triaxial stress state, important influences on fracture

properties may be masked. In subsequent testing, reduction of area at the fracture plane, (known to be more sensitive to fracture processes) will be used to monitor the influence of the decarburizing environment on tertiary creep events and fracture.

In the next phase of creep testing, 2¼Cr-1Mo steel will be tested at 500°C (932°F) and at an applied stress level of 241 MPa (35ksi). Pre-exposure to the decarburizing environment prior to testing will be introduced as an experimental parameter. Major effort will be concentrated in quantifying decarburizing influence under monotonic creep stress conditions.

Test parameters for the biaxial creep program are summarized in Table 3.4. In this probram, cylindrical test specimens 15.9 mn (.625") diameter by 95.4 mn (3.75") long were pre-exposed in decarburizing sodium or exposed to pure argon. The selected test temperature was 510°C (950°F). Both base metal specimens ("B" designation) and weld metal specimens ("W" designation) were tested.

Weld metal specimens were fabricated in the following sequence:

(1) 2¼Cr-1Mo stee weld overlays were deposited on ¼"-Schedule 80, 2¼Cr-1Mo steel pipe.

(2) The I.D. of the specimens was enlarged to remove the base metal/pipe material.

(3) Specimens were further fabricated to meet the established dimensional tolerances and pressure pin configuration.

(4) After fabrication, the specimens were post weld heat treated at 732°C (1350°F) for 4 hours.

The current results of the biaxial stress creep program are tabulated in Table 3.5. The data of Table 3.5 are graphically illustrated in the logarithmic stress versus rupture time plot of Figure 3.6. The trends evident in this test program are as follows:

(1) The rupture life for a given applied stress is found to be displaced to shorter times for the Na/Ti exposed specimens versus control specimens.

(2) A ten-fold rupture strength reduction for Na/Ti versus control specimens data is observed for specimens pre-exposed at 510°C (950°F) for 950 hours.

(3) Data from specimens not exposed prior to testing fall above the minimum rupture strength limit established in ASME Code Case 1592, irrespective of test environment.

The biaxial creep data of Figure 3.6 must further be analyzed in order to quantitatively access the loss in rupture strength suffered by the decarburized 2¼Cr-1Mo steel. Metallographic examination and compositional analysis will be conducted on failed pressure pins. Effort will be devoted to determine the critical exposure to Na/Ti (equivalently, the critical bulk carbon content reduction) required for accelerated loss of creep rupture strength. Deformation morphology studies will be correlated with the mechanical properties data in order to investigate the mechanism responsible for creep rupture strength reduction. Mechanical properties data will be compared with the decarburization studies being conducted in this subtask to determine the properties degradation that can be expected in the service life of the LMFBR.

The rupture properties data for the weld metal specimens are inconclusive in the present study. Although the data of Figure 3.6 appear to indicate essentially equivalent behavior for the base metal and weld metal specimens, a variation in failure mode was noted for the weld metal specimens. Base metal failures in the pressurization tests were characterized by longitudinal tearing (the type of failure mode to be expected in this type of testing). Weld metal specimens failed by either longitudinal tearing or by pinhole perforations through the wall. An example of this latter failure mode is illustrated in Figure 3.7. Figure 3.7a illustrates a failed pressure pin (weld metal specimen). In Figure 3.7b, details of surface perforations are depicted. A transverse section through typical pore-like defects is presented in Figure 3.7c. This section depicts large pores, open in the outer weld overlay (last pass). Reexamination of micrographs obtained during weld overlay characterization indicate that weld porosity was not excessive, however, inclusion particles, approximately 1-2 μm in diameter were dispersed throughout the weld metal. Weld metal samples pre-exposed to Na for 950 hours prior to testing leaked upon pressurization. Detailed evaluation of these weld samples has been initiated to determine the cause for the apparent degredation of the weld metal during exposure to Na.

REFERENCES

1) Communication, P. Patriara to D. Weinstein, "Linear-Simulated 2¼Cr-1Mo Steel Tube-to-Tube Sheet Weldments" May 16, 1974

Table 3.1 Decarburization Rate Constants for 2¼Cr-1Mo Exposed to Static Sodium, 510°C (950°F) (titanium-gettered)

		$K(gmc/cm^2 - sec^{\frac{1}{2}})$	
		10,000 hrs.	4100 hrs.
Annealed*	½ hr. - 924°C (1695°F) fce. cool to RT	$9.4X10^{-9}$	$12X10^{-9}$
Normalized & Tempered	½ hr. 924°C (1695°F) AC to RT 1 hr. 677°C (1250°F) AC to RT	$2.5X10^{-9}$	$3.5X10^{-9}$

* Both treatments received a final stress relief anneal 1 hr. @ 732°C (1350°F) with subsequent air cooling to room temperature.

Table 3.2 Creep Fatigue Test Parameters
Tubular Creep Specimens

Environment	- Titanium-gettered sodium or helium (inside diameter)
	- Air (outside diameter)
Test Temperature	- 502°C (935°F)
Material	- 2¼Cr-1Mo Steel Isothermal Annealed
Loading Modes	- Constant load for creep
	- Periodic load increase of approximately 69 MPa (10ksi) for creep fatigue
Peak Load Frequency	- 1 cycle per 24 hours
Hold Time at Peak Load	- 10 seconds

Table 3.3 Uniaxial Creep/Fatigue Tests 502°C (935°F)

Specimen	Test Environment	Stress MPa	Stress ksi	Stress Peak MPa	Stress Peak ksi	Rupture Time (hr)	Rupture Strain (%)	Minimum Creep Rate (MCR) (%/hr)
A02	Helium	310.2	45	-		39.9	18.2	2.7×10^{-1}
A04	Helium	241.3	35	-		2296	29.2	1.9×10^{-3}
A05 (a)	Helium	172.4	25	-		1000 (a)		2.5×10^{-4}
A13	Na/Ti	241.3	35	310.2	45	248.5	27.0	-
A14	Na/Ti	241.3	35	-		1021.6	25.0	-
A15	Na/Ti	241.3	35	-		397.3	26.8	6.9×10^{-3}
A03	Helium	206.8	30	276	40	928	20.6	-

(a) Test of specimen A05 discontinued after 1000 hours

Table 3.4 Biaxial Creep Parameters
Pressure Pin (cylindrical) Specimens

Environment	-	high pressure argon 25 MPa/3630 psi (interior surface)
		titanium-gettered sodium or argon (exterior surface)
Test Temperature	-	510°C (950°F)
Material	-	2¼Cr-1Mo Steel Isothermal annealed designated "B" for base metal
		2¼Cr-1Mo Steel Weld Metal Post weld heat treated (732°C/1350°F for 4 hours); designated "W" for weld metal
*Pre-exposure Conditions	-	510°C (950°F) for 950 hours Control and Na/Ti Specimens

* 7 of 21 tests to date have been pre-exposed prior to testing

Table 3.5 Biaxial Creep Program (T = 510°C/950°F)

Specimen	Env.	Stress MPa	Stress ksi	Rupture Time (hrs.)
B40-07	Helium	223.37	32.4	248.2
B40-08	Sodium	223.37	32.4	98.2
B45-07	Helium	251.63	36.5	116.2
B45-08	Sodium	251.63	36.5	168.5
B40-01	Helium	275.76	40.0	4.0
B40-02	Sodium	275.76	40.0	1.3
B45-01	Helium	310.23	45.0	0.5
B45-02	Sodium	310.23	45.0	0.4
W40-07	Helium	223.37	32.4	200.0
W40-08	Sodium	223.37	32.4	116.2
W45-07	Helium	251.63	36.5	172.5
W45-08	Sodium	251.63	36.5	108.0
W40-01	Helium	275.76	40.0	0.1
W40-02	Sodium	275.76	40.0	0.9
W45-01	Helium	310.23	45.0	0.3
*B40-10	Sodium	223.37	32.4	17.1
*B40-09	Helium	223.37	32.4	234.5
*B40-04	Sodium	223.37	32.4	5.4
*B40-03	Helium	223.73	32.4	152.9
*B40-06	Sodium	223.73	32.4	5.9
*B45-09	Helium	251.63	36.5	154.8
*B35-01	Helium	195.44	28.35	473

B = Base Metal
W = Weld Metal
* Pre-exposed to sodium for 950 hours at 510°C (950°F)

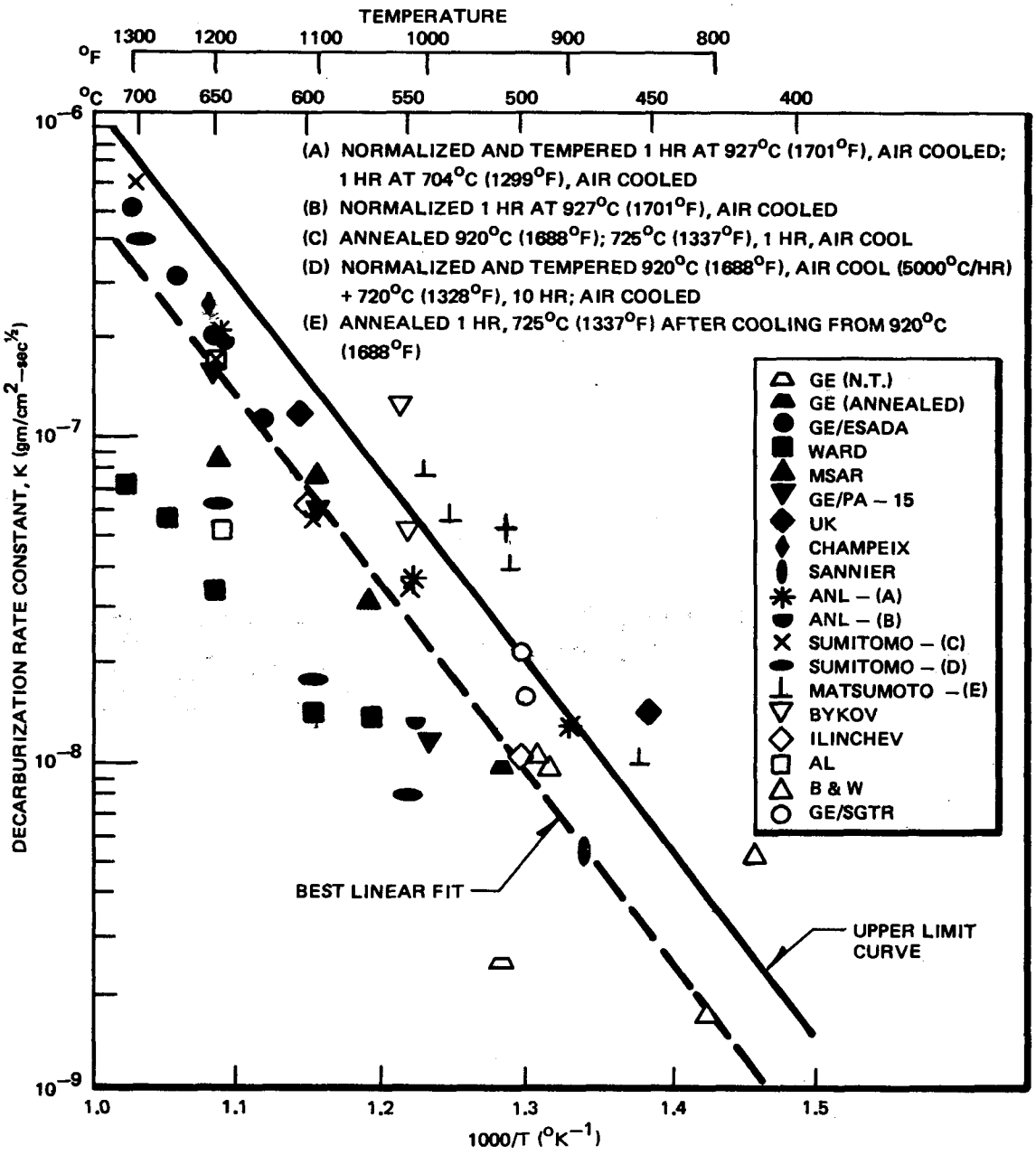

Figure 3.1. Decarburization Rate Constants for All Investigations

+ GE (weld metal-interim)

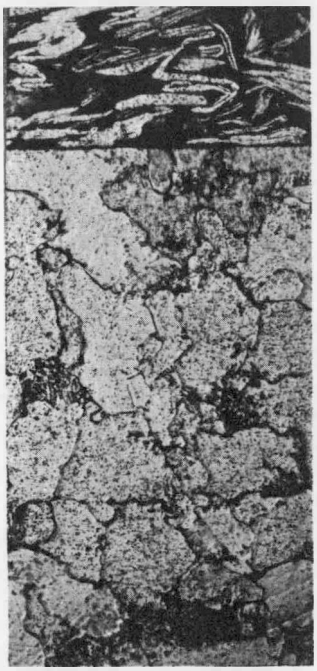

(a) annealed material after 10,000 hours

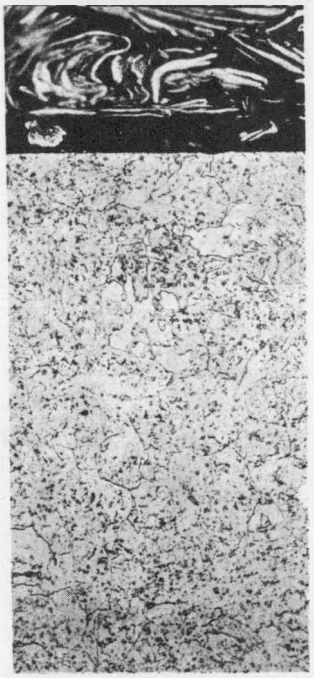

(b) N&T material after 10,000 hours

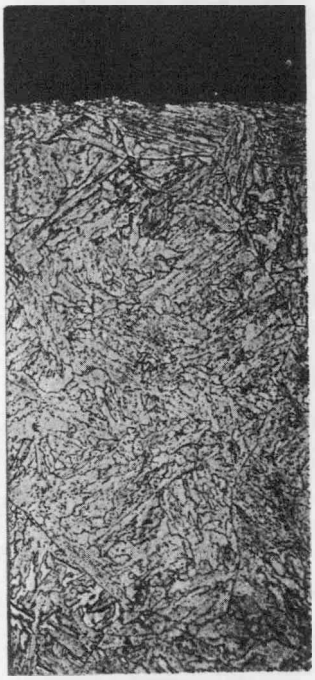

(c) stress-relieved weld metal after 4,500 hours

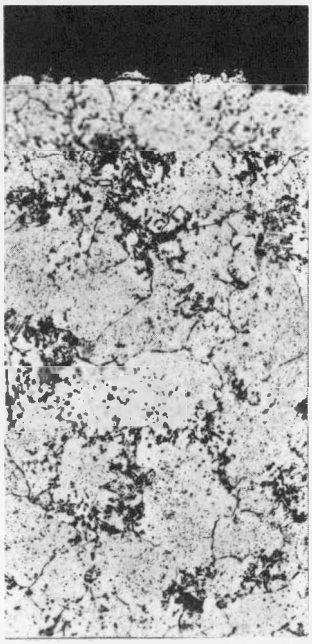

(d) base metal as-annealed

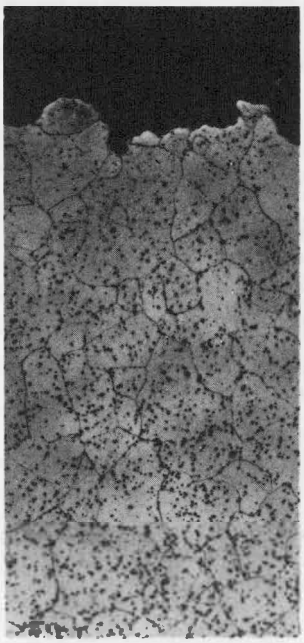

(e) base metal as normalized & tempered

Figure 3-2. Decarburization of 2-1/4 Cr-1Mo Base and Weld Metal, 510° C) (950° F) Ti-gettered Sodium (400X)

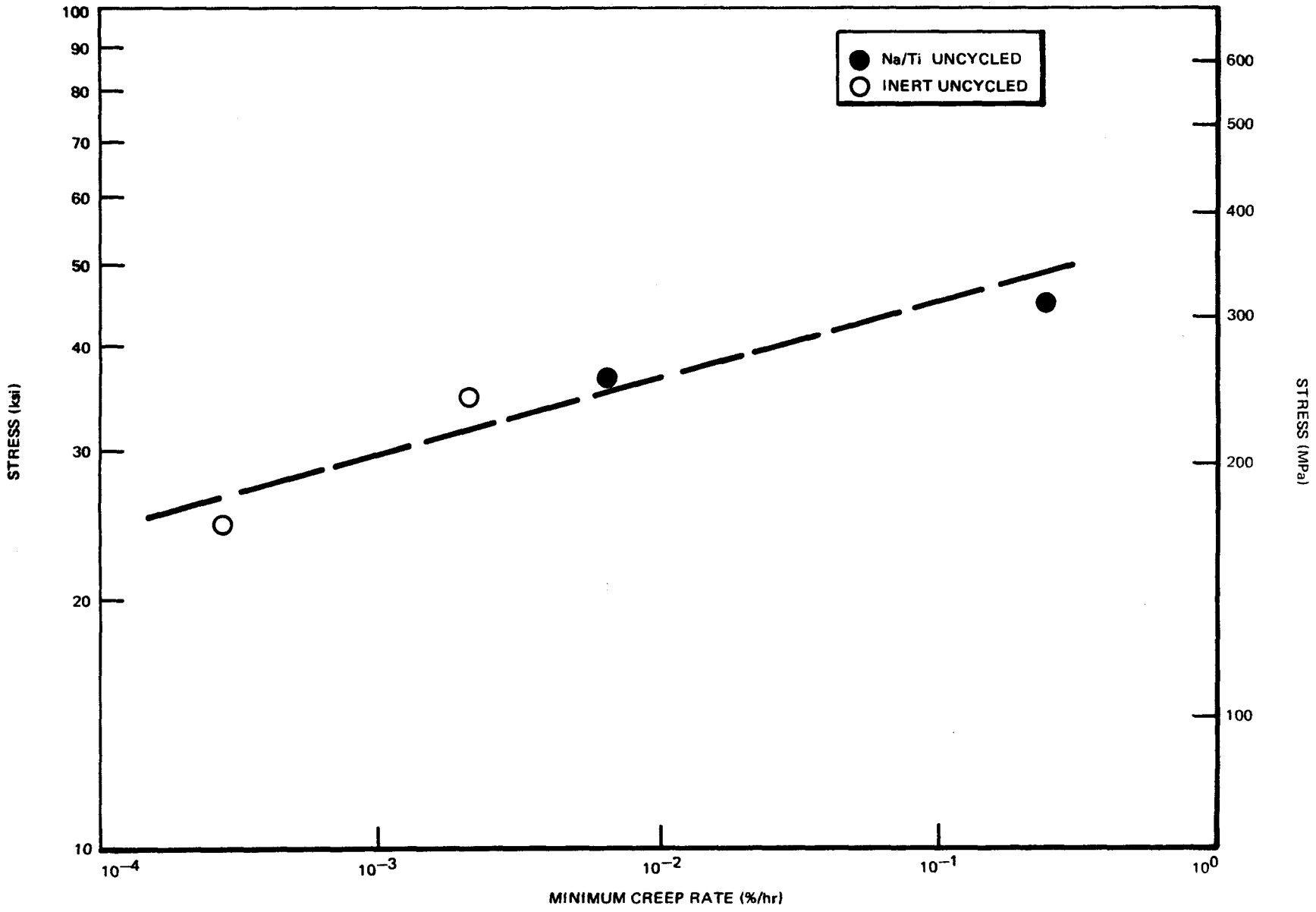

Figure 3-3. Minimum Creep Rate Results for Isothermal Annealed 2-1/4 Cr-1Mo Steel Tubular Creep Specimens

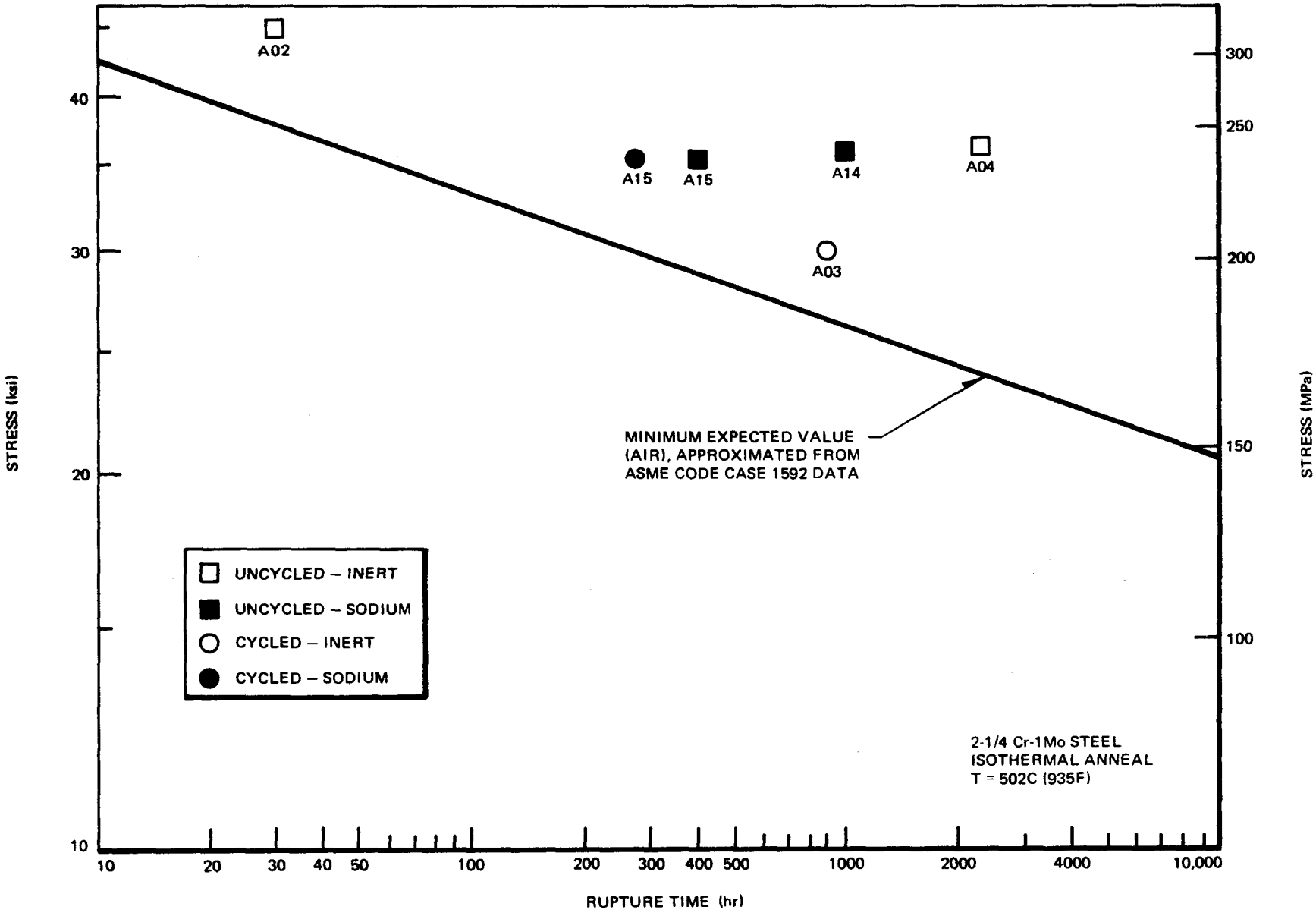

Figure 3-4. Stress Rupture Data for Isothermal Annealed 2-1/4 Cr-1Mo Steel Tubular Creep Specimens

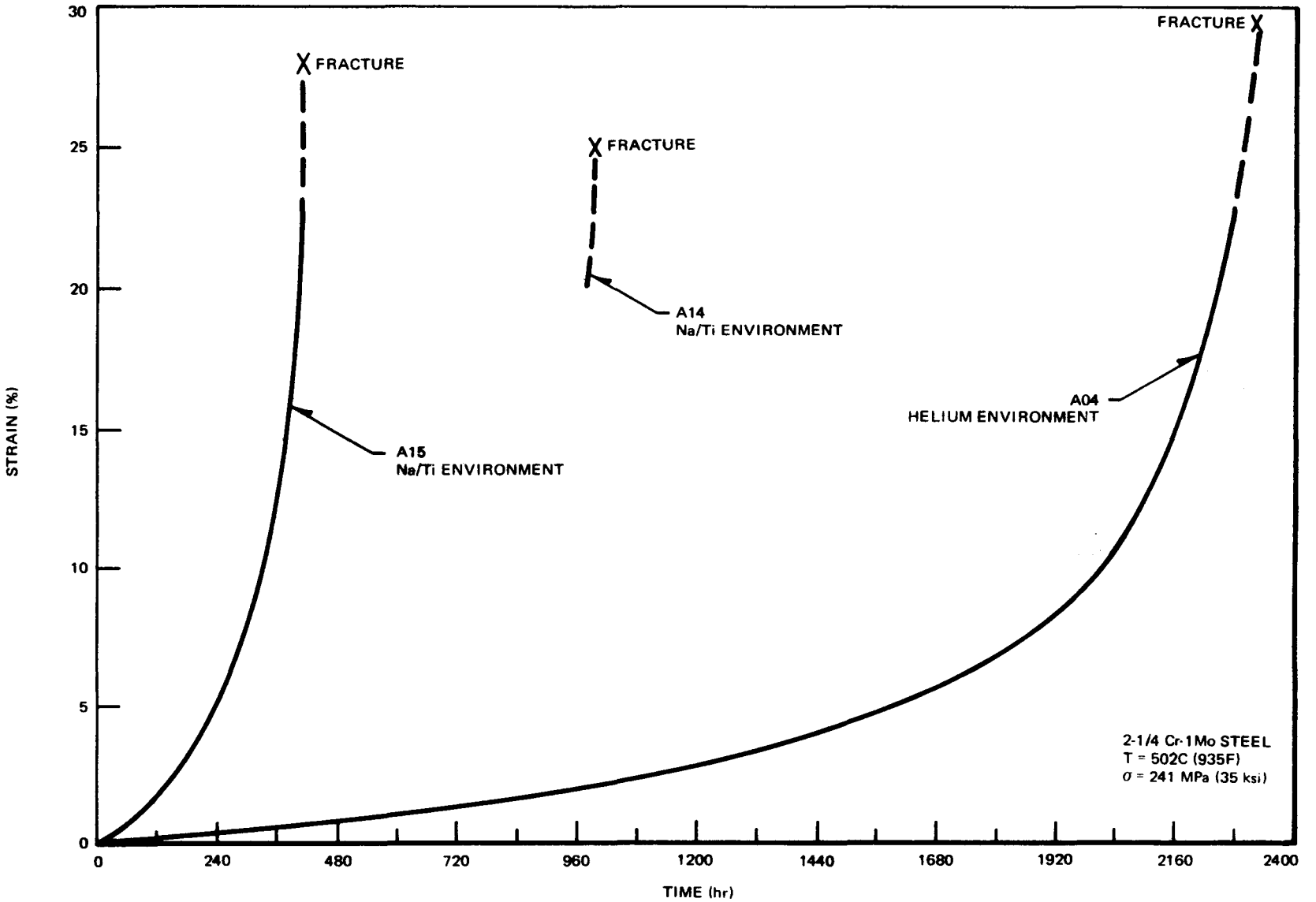

Figure 3-5. Strain versus Time Creep Behavior for Isothermal Annealed 2-1/4 Cr-1Mo Steel

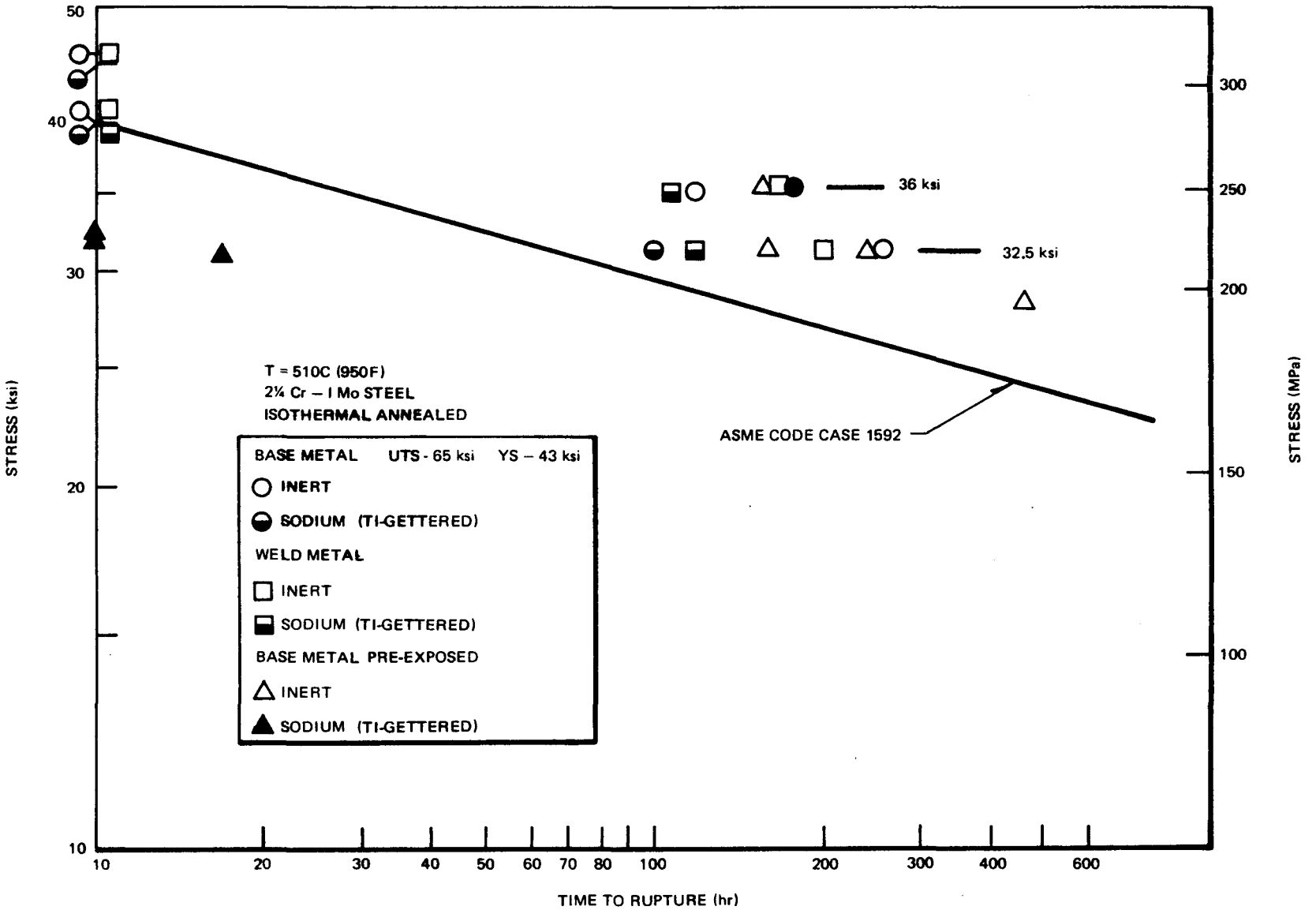

Figure 3.6. Biaxial Creep Tests, 2-1/4 Cr-1Mo Steel: Rupture Data

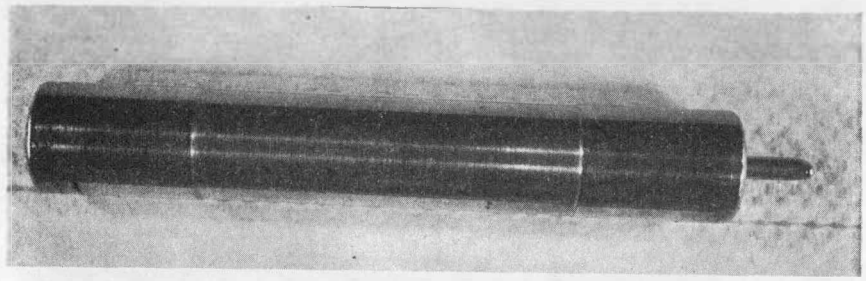

(a) 1X

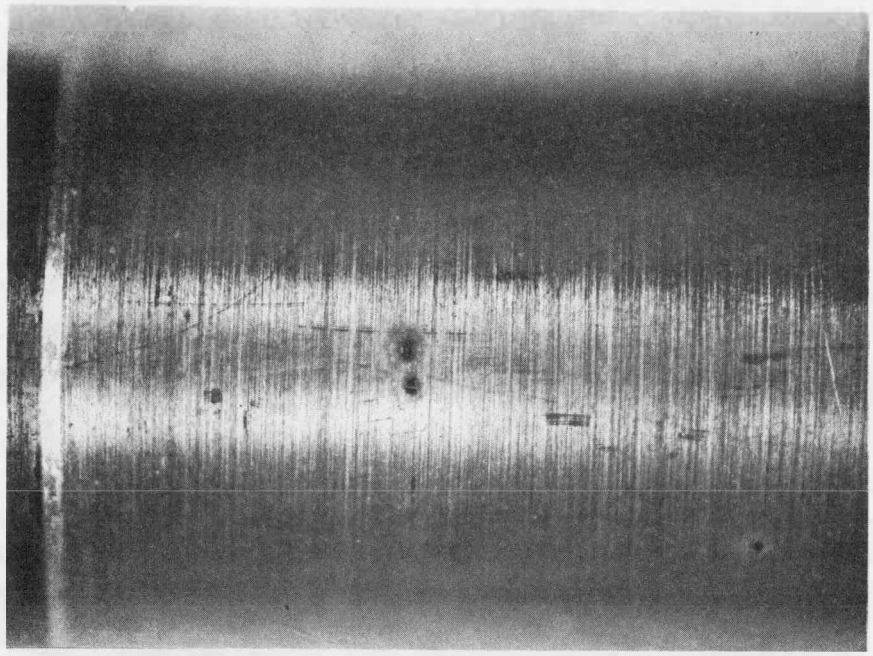

(b) details of surface perferations (5X)

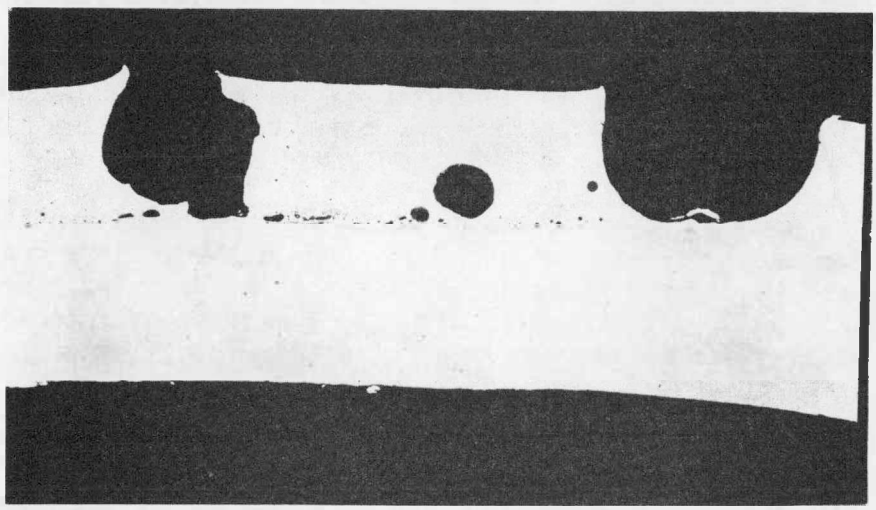

(c) transverse section (80X)

Figure 3-7. 2-1/4 Cr-1Mo All-weld Metal Pressure Pins. Pre-exposed to 950°F (510°C) Static Sodium for 950 Hours.

4. AQUEOUS STRESS CORROSION-WATER/STEAM SIDE CORROSION (SUBTASK B)

M. E. Indig

Subtask B studies caustic stress corrosion cracking and corrosion fatigue damage for simulated LMFBR evaporator and superheater environments. These studies, with the reference m aterial 2¼Cr-1Mo, and the alternate material Alloy 800 H, are concerned with the water/steam side portions of the steam generator. More specifically, the corrosion fatigue studies are planned to assess and predict damage in an environment that mechanically and chemically simulates the Departure from Nucleate Boiling (DNP) region of the evaporator section of the steam generator.

In all of these studies high concentrations of caustic are used to simulate off-chemistries in local regions. The high concentrations can occur as a result of in-leakage and normal concentrating mechanisms that can exist in LMFBR steam generators. Highlights for this reporting period are as follows:

- The final stress corrosion experiments with welded 2¼Cr-1Mo in superheated steam have been completed. This completes milestone B-5 and successfully terminates all planned testing in superheated steam under faulted conditions.
- Straining electrode experiments have been completed for annealed 2¼Cr-1Mo in 5% NaOH at 316°C (600°F) over the entire range of required potentials.
- The electronic control and external hardware for the high temperature corrosion fatigue facility has been ordered. In addition, the load frame design work has been completed.
- A single constant extension rate experiment (no applied potential) has been completed with Incoloy 800 in the Grade 1 condition (Alloy 800). Compared to the reference metallurgical treatment. Grade 2 (Alloy 800 H), the alloy with the lower temperature anneal (Grade 1) exhibited excellent resistance to caustic cracking at 316°C (600°F) in 5% caustic.

4.1 Straining Electrode Studies

The stress corrosion studies for 2¼Cr-1Mo at 316°C (600°F) in 5% NaOH at controlled potentials have been completed. Separate experiments were conducted at -0.100, 0.050, 0.100, 0.150, and 0.400 volts vs. a platinum reference electrode. All of the experiments were conducted at approximate extension rates of 0.025 mm/hr (0.001"/hr) or strain rates of 10^{-5}/min.

Although the results of the last experiment conducted at -0.100 volts are not yet available, all other sample examinations from the straining electrode experiments indicate no stress corrosion. Metallographic examination indicates that the positive potentials resulted in some increase of oxide formation, specifically manifested by the formation of fingers of oxides which penetrated several grains into the metal before terminating. Figures 4.1a and b are examples of this localized attack. Table 4.1 summarizes the mechanical, electrochemical and stress corrosion results available from the 5% caustic tests. The major effect of potential appears to be the lowering in reduction in area values, probably caused by the localized attack shown in Figures 4.1a and b.

In addition to the testing of 2¼Cr-1Mo samples, a single constant extension rate experiment was conducted with Incoloy 800 in the Grade 1 (Alloy 800) condition (927°C (1700°F) anneal) in 5% NaOH. Previously, it had been determined that Incoloy in the Grade 2 condition was quite susceptible to caustic cracking during constant extension rate testing and we had thought similar behavior could be expected from the lower temperature anneal. The test with the Grade 1 condition was terminated at the onset of plastic instability (before mechanical fracture) and thus reduction in area is not available. However, only minor stress corrosion cracks were observed in the necked area, and the material appeared quite resistant to stress corrosion. Table 4.2 compares the results obtained with the two metallurgical conditions. Figure 4.2 shows the appearance of the Grade 1 sample after testing, compared to a similar untested sample.

In the future, straining electrode experiments with annealed 2¼Cr-1Mo will be conducted in 10% NaOH, and Incoloy 800 will be tested in 5 and 10% NaOH in both the Grade 1 and Grade 2 conditions. After conclusion of the straining electrode experiments, the experimental portion of the stress corrosion program for simulated LMFBR evaporator and superheater operational conditions will be completed.

4.2 Superheat Stress Corrosion Studies, Weldments

The final stress corrosion experiment with pressurized 2¼Cr-1Mo tubes in superheated steam at 482°C (900°F) has been completed. In this experiment, fifteen tubes stressed from 103 (15)to 276 (40) MPa (ksi) were exposed to steam at 12.1 (1750) MPa (psi) containing 5 to 10 ppm dissolved caustic. ORNL prepared the tubes with center orbital welds. End cap weldments and capillary connections to the tubes were completed at GE.

The run was terminated after 133 hrs. and the results are tabluated in Table 4.3. In general, in this rather agressive environment, some mechanical failures resulted from general corrosion, which caused tube thinning and eventual stress rupture. Initial observations indicated no stress corrosion of the orbital welds. Metallographic examination is in progress to determine the extent of the general corrosion and whether any sign of stress corrosion can be detected.

4.3 Corrosion Fatigue Studies

Significant progress in the development of a high temperature aqueous corrosion fatigue facility in support of the DNB testing program has been made. The electronic control package with external hardware has been designed and ordered. A functional diagram of the system is shown in Figure 4.3. The load frame and specimen arrangement method for conducting 0 to tension, or tension to tension fatigue tests in simmulated DNB environments are shown in Figures 4.4 and 4.5. Cycling of the specimen will be under load control although cyclic strain will be monitored by an LVDT in the actuator. Specimens will be tested singly or in series with different internal arrangement. The system will be capable of operation up to 343^{o}C (650^{o}F).

Fabrication of the load frame assembly and autoclave modification will begin shortly.

4.4 STEAM/WATER-SIDE CORROSION TESTING OF 2¼Cr-1Mo (SNE/ORNL/GE) - L. V. Hampton

4.4.1 Introduction

This program is a cooperative program between GE and ORNL and was undertaken to provide an engineering assessment of the corrosion rates of 2¼Cr-1Mo steel under simulated CRBRP superheater conditions. Under these conditions, material degradation will occur by two corrosion mechanisms, isothermal and heat transfer. High temperature isothermal corrosion of the superheater tubes can be expected at the steam exit end of the module where no heat is tranferred by the sodium. For the heated length of the superheater tubes, however, heat transfer effects will tend to compound normal steam corrosion behavior of 2¼Cr-1Mo and lead to higher corrosion rates, especially at the sodium-inlet to the module where metal temperatures as high as 493°C (920°F)

Preliminary design correlations for the corrosion of 2¼Cr-1Mo in superheated steam are provided by the Nuclear Materials Systems Handbook[1]. The handbook derives a correlation based on previous corrosion experiments performed on 2¼Cr-1Mo by several independent investigators (see ref. 1 for references). The design equation derived from these studies relates the isothermal corrosion rate, Γ, to temperature as shown below:

$$\Gamma = 551.6 \exp(-10460/RT)$$

where

Γ = steady state corrosion rate, mil/yr

R = gas constant = 2 cal/mole-deg.

T = temperature, °K

To account for heat transfer effects in the corrosion process, a factor of 1.5 was applied to the isothermal corrosion rate data. This factor was derived from previous heat transfer tests conducted on Alloy 800 where a factor of 2

accounted for the increased heat transfer corrosion rate of this material over isothermal rate data. At the other extreme, it was found that there was no effect of heat transfer on the corrosion rate of plain carbon steel (see ref. 1 for references). Thus, for the low-alloy steel, 2¼Cr-1Mo, a 1.5 heat transfer factor was postulated. To confirm the NSM Handbook correlation for 2¼Cr-1Mo steam corrosion, heat transfer corrosion testing of this material is being conducted at the Florida Power Test Facility (Bartow Plant) operated by N.U.S. Corporation.

Materials

The chemical composition of the air-melted 2¼Cr-1Mo material used is listed in Table 4.4. The tubes were made from seamless pipe 2.23 cm (0.875 in.) O.D. with 0.434 cm (0.171 in.) wall. The pipe was reduced in diameter to 1.45 cm (0.570 in.) O.D. and 1.23 cm (0.484 in.) I.D. by a combination of swaging and honing steps. The specimens were annealed in an inert atmosphere at 913°C (1675°F) for one-half hour, furnace cooled to 704°C(1300°F) and held at this temperature for 2 hours. The final length of the heat transfer specimens was 80 cm (31.5 in.) while the isothermal specimens (which were cut from the same tubing) had a length of approximately 7.1 cm (2.8 in.). Prior to exposure, the specimens were pickled in inhibited sulfuric acid and weighed.

Facilities

The High Pressure Steam Corrosion Loop operated by Souther Nuclear Engineering (SNE), under the direction of, and funded by, the Oak Ridge National Laboratory was ued for the heat transfer and isothermal corrosion testing. The loop was modified to simulate the actual steam generator conditions as closely as possible.

A calrod heater through the heat transfer specimen I.D. provided the heat input necessary to obtain a heat transfer corrosion mode in the superheated steam. A list of the design test conditions is shown in Table 4.5. From the parameters listed in Table 4.5, metal wall temperatures at the entrance and exit of the specimen were calculated.

Water and steam quality measurements for the Florida Loop are shown in Table 4.6.

During the heat transfer run, two specimens were tested simultaneously. One specimen was exposed to a specified time point (500, 1000, 2000, 3000, 6000 hours) while the other accumulated exposure time. This method of testing eliminated the need of starting from zero time to obtain the longer term data.

As indicated in Table 4.5, only 610mm (24 inches) of the total specimen length was corroding. There was a 28°C(50°F) temperature difference between the heated entrance and the heated exit of the tube and a design temperature difference of 50°F between the metal and the steam at any point along the tube.

The isothermal specimens were placed at the 499°C(930°F) steam temperature region of the corrosion loop. These specimens were corroded on both the inside and outside diameters as opposed to the heat transfer specimens which were corroded only on the outside.

4.4.2 Results

The corrosion rates reported are derived from data generated at ORNL. The total amount of metal involved in the corrosion process is obtained by

subtracting the descaled specimen weight from the initial weight and mormalizing with the corroding area. The results for both isothermal and heat transfer specimens tested to date are shown in Figure 4.6.

There is a linear variation in metal temperature along the length of the heat transfer tube section. The data shown in Figure 4.6 for the heat transfer test would therefore represent corrosion of 2¼Cr-1Mo at an average temperature of 524°C (975°F) while the isothermal curve was obtained in 499°C (930°F) steam.

From the graph, an obvious disparity in the behavior of the isothermal and heat transfer curves is apparent. After 3,000 hours the isothermal corrosion rate has dropped off to 0.0076 mm/yr[3] (0.3 mil/yr), contrasting the 0.0152 mm/yr (0.6 mil/yr) predicted by the Handbook. The heat transfer corrosion rate is 0.051 mm/yr (2.0 mil/yr) at 524°C(975°F) as opposed to 0.030 mm/yr (1.2 mil/yr) from the Handbook correlation.

4.4.3 Discussion

The data obtained to date are inconclusive relative to the Clinch River superheater corrosion rate because the tests have been conducted at non-prototypic conditions: There is a linear temperature variation along the length of each transfer test section from 510°C (950°F) to 538°C (1000°F) and a 22°C (72°F) temperature difference between the steam and the metal at any point along the tube. Each heat transfer section operated at a heat flux of approximately 126,000 W/m^2 (40,000 $^{Btu}/_{hr\text{-}ft^2}$). Whereas the present thermal hydraulic design of the superheaters for CRBRP results in maximum metal temperatures of approximately 493°C (920°F) and the steam/metal ΔT of about 15°F at the

maximum temperature. The average heat flux expected in the superheaters will be ~ 250,000 W/m^2 (80,000 $Btu/hr\text{-}ft^2$). Thus, the corrosion rates resulting from the present experiment are higher than would be expected in the CRBRP. Attempts to develop a corrosion model to extrapolate these data to the CRBRP conditions has been unsuccessful due to a lack of information regarding the relationship amoung corrosion rates and metal temperature, steam/metal ΔT, and heat flux.

Therefore, longer term testing (> 10,000 hours) under the conditions listed in Table 4.7 is currently being conducted in an effort to further define the heat transfer behavior shown in Figure 4.6. As shown in the table, the critical parameters of metal wall temperature and steam-to-metal temperature difference have been reduced to more closely simulate the conditions in superheaters of the CRBRP. The tubing to be tested in this phase of the experiment is vacuum arc remelted 2¼Cr-1Mo manufactured to the CRBRP steam generator tubing specification, RDT M3-33.

4.5 EVAPORATOR CORROSION RATES

Numerous programs have been initiated to investigate the effects of the incorporation of the departure from nucleate boiling (DNB) in the evaporator tubes of the Clinch River Plant.[3] These programs are concerned, however, with the localized effects of DNB relative to enhanced exfolication and/or increased metal corrosion rates in the DNB zone. There is no program currently being run to yield overall evaporator corrosion rates.

The need for such a program is warranted in the light of new corrosion data coming from the French Phenix breeder reactor project.[4] The steam generator of this plant consists of a Type 321 stainless steel superheater and reheater

and a 2¼Cr-1Mo evaporator section. Sodium-side hydrogen measurements indicate an overall corrosion rate of 16 microns/year (0.64 mil/yr) for the Phenix steam generator[5] (the NSM Handbook correlation[1] predicts ~ 0.1 mil/yr corrosion under these conditions). The rate value is not conservative because it assumes that all of the corrosion product hydrogen diffuses through the steam generator tube walls into the sodium. However some of the hydrogen can be expected to enter the steam and, therefore, not give a good indication of the overall corrosion.

It is also expected that the less resistant evaporators are corroding at a much faster rate than the higher temperature superheater and reheater modules of the Phenix system.

In an all 2¼Cr-1Mo system (such as CRBRP), the flux of hydrogen into the sodium due to corrosion would be expected to be much greater due to the higher temperature operation of the superheater. Cold trap design for the CRBRP is attendant upon a knowledge of the amount of hydrogen expected to enter the sodium from the water-side of each module.

Experiments are being conducted at NUS-SNE to determine maximum superheater corrosion rates and, therefore, tube lifetimes for this module. These steam corrosion tests cannot predict the high temperature water corrosion rates of the evaporator module, however. The basic corrosion mode of each module will be different due to the differences in fluid characteristics of the superheater and evaporator.

Chemical corrosion of the evaporator due to the deposition of caustic species and the intrusion of condenser salts can lead to highly localized corrosion in this module as opposed to the general attack expected in the super-

heater. DNB enhanced damage mechanisms can also be expected to increase the corrosion of the evaporator tube wall in this region. A list of possible mechanisms is shown below:

(1) The temperature oscillations may cause thermal fatigue damage to, and exfoliation of, the protective oxide layer on the steam side of the boiler tube, leading to increased water-side corrosion.

(2) The temperature oscillations may cause cyclic thermal strain fatigue of the boiler tube wall with possibly attendant corrosion fatigue.

(3) Water impurity concentration caused by recirculation, evaporation in the boiler tube and local dryout at the critical heat flux point may cause greatly accelerated corrosion, possibly augmented by local porous deposits of corrosion products such as iron oxide acting as concentrating sites.

(4) Local buildup of precipitated deposits may lead to unpredicted local heat transfer perturbations which could adversely affect corrosion and/or fatigue potential.

A program to determine evaporator corrosion rates under simulated Clinch River water conditions is proposed. The experiment will be conducted in cooperation with ORNL at the Bull Run Steam Plant operated by the T.V.A.

REFERENCES

1) NSM Handbook, Water Side Corrosion, Vol II, pp. 1-14

2) Chakiaborty, A.K., "Literature Review and Test Plan on General Corrosion of Ferritic and Austenitic Steam Generator Materials in Superheated Steam Under Isothermal and Heat Transfer Conditions" NEDG 13860, May 1972

3) Memo to P. Lowe from D. Dutina/J. R. Peterson "Interrelationship of Ongoing and Proposed DNB Damage Support Testing" April, 1975

4) Cambillard, E., LaCroix, A. et al, "Phenix Steam Generators Measuring Hydrogen Concentration of Sodium For Tightness Inspection of Water-Steam Tubes." Paper presented at I.A.E.A. Study Group Meeting on LMFBR Steam Generators, Bensberg, Oct. 1974

5) Private Communication: M. G. Robin (Commissariat à L'Énergie Atomique) to P. Roy (G.E.-F.B.R.D.) August 1975

TABLE 4.1

Straining Electrode Results, Annealed
2¼Cr-1Mo, 5% NaOH, 316°C (600°F)
2×10^{-5}/min Strain Rate

Applied Potential Versus Pt, Volts	Tensile Strength MPa	(ksi)	Elognation %	Red. in area %	Observation
0*	492	(71.3)	22.0	53	No SCC**
0	491	(71.2)	18.0	31	
.050	>434	(>63)+	11.6	27.4	
.100	510	(74)	11.4	31.0	
.150	504	(73.1)	12.5	33	
.400	487	(70.7)	14.2	39.6	

* Standard in pure water, tested at 10^{-4}/min strain rate.

** Stress corrosion cracking.

+ Electronic malfunction in load cell after a load equivalent to 434 MPa was reached; test was continued to failure of the sample.

TABLE 4.2

Constant Extension Rate Testing of
Grade 1 and Grade 2 Incoloy 800 316°C (600°F),
5% NaOH $2x10^{-5}$/min Stran Rate

Metallurgical Condition	Tensile Strength MPa	(ksi)	Elongation %	Reduction in area %	Observation
Grade 2	302	(43.8)	38	15	Failure by IGSCC**
Grade 1	506	(73.4)	44.7	38.2*	Ductile failure

* Measurement obtained at the neck of unfailed sample

** IGSCC - Intergranular Stress Corrosion Cracking

TABLE 4.3

Summary of Caustic-Superheat Stress Corrosion Run
508, 482°C (900°F) 12.1 (1750) MPA (ksi), 133 hrs., 2¼Cr-1Mo Weldments*

Sample No.	Stress MPa	(ksi)	Results
1290	138	(20)	No failure
1291	138	(20)	Mechanical failure, between 99 and 113 hrs.
1292	138	(20)	"
1293	172	(25)	No failure
1294	172	(25)	"
1295	172	(25)	"
1296	207	(30)	Mechanical failure, between 49 and 65 hrs.
1297	207	(30)	Mechanical failure, 120 hrs.
1298	207	(30)	No failure
1299	241	(35)	Mecahnical failure, 98.5 hrs.
1300	241	(35)	Mechanical failure, 120 hrs.
1301	241	(35)	Mechanical failure, between 73 and 89 hrs.
1302	276	(40)	Mechanical failure, between 15.5 and 18 hrs.
1303	276	(40)	Mechanical failure, between 42 and 43.5 hrs.
1304	276	(40)	Mechanical failure, between 49 and 65 hrs.

* Annealed sections of 2¼Cr-1Mo tube joined in an orbital weld, followed by by a stress relief at 732°C (1350°F)

NOTE: Metallography in progress to determine any stress corrosion in weldments.

Table 4.4

Composition of 2¼Cr-1Mo Materials (Weight Percent) for Superheat Corrosion Tests

Carbon	0.11
Manganese	0.43
Sulphur	0.017
Phosphorous	0.017
Silicon	0.29
Chromium	2.36
Molybdenum	0.93
Iron	Balance

Table 4.5

Specimen Design and Test Requirements
General Corrosion Under Heat Transfer (Reference 2)

System Requirements

Steam to each test section	$0.038\frac{kg}{s}$ (300 lbs/hr.)
Temperature Steam into test section	468°C (875°F)
Heater Power with Variac Control	3.5KW - 220V
Temperature difference between steam and heated specimen (ΔT)	40°C (72°F)
Temperature Steam out of test section	499°C (930°F)
Velocity at outlet of test section	34.4m/sec (113 ft/sec)
Specimen metal temperature - inlet end	510°C (950°F)
Specimen metal temperature - outlet end	538°C (1000°F)

Heater Requirements

Outer diameter	12.662 $\pm$ 0.013mm (0.4985 $\pm$ 0.0005")
Length	25mm (32.5")
Heated Length	610mm (24")
Power	5KVA at 230V, 60 cycle
Non-heated length - both ends	109mm (4.25")

Speciment Requirements

Outer diameter	14.40 $\pm$ 0.05mm (0.567 $\pm$ 0.002")
Inner diameter	12.727 $\pm$ 0.013mm (0.5005 $\pm$ .0005")
Length	800mm (31.5")

Table 4.6

Allowable Ranges of Impurities and Chemical Analyses of Boiler Water and Steam at Bartow Plant (Ref. 3)

	Boiler Water Allowable ranges of concentrations	Saturated Steam
pH	10.1 - 10.7	8.8 - 9.0
Impurities, ppm		
Na_2SO_3	0.6 - 1.0	
NaCl	3 - 10	
PO_4	1.0 - 5.0	
Na_2SO_4	5 - 25	
S_iO_2	0.12 - 0.20	0.005 max
NH_3	---	1.0 max
Cl	---	0.5 max
Conductance, micromhos	---	2.2 - 4.5
TDS	30 - 50	0.5 - 1.0

Chemical Analyses at Random Dates

pH	10.7	10.7	10.3	8.8	8.9
Impurities, ppm					
Na_2SO_3	1.0	0.6	0.7	---	---
NaCl	4	3	4	---	---
PO_4	5	2	3	---	---
Na_2SO_4	8	13	14	---	---
S_iO_2	0.14	0.13	0.15	0	0
NH_3	---	---	---	0.153	0.180
Conductance, micromhos	---	---	---	4.5	4.0
TDS	---	---	---	0.7	0.7

Table 4.7 Test Requirements
General Corrosion Under Heat Transfer

Steam to each test section	0.061 $\frac{kg}{s}$ (483 lb/hr)
Temperature steam into test section	486°C(906°F)
Heat Power with Variac control	3.5 KW
Temperature difference between steam and heated specimen (ΔT)	16.7°C(30°F)
Temperature steam out of test section	507°C(945°F)
Velocity at outlet of test section	34.14 mps(112fps)
Specimen metal temperature - inlet end	502°C(936°F)
Specimen metal temperature - outlet end	524°C(975°F)

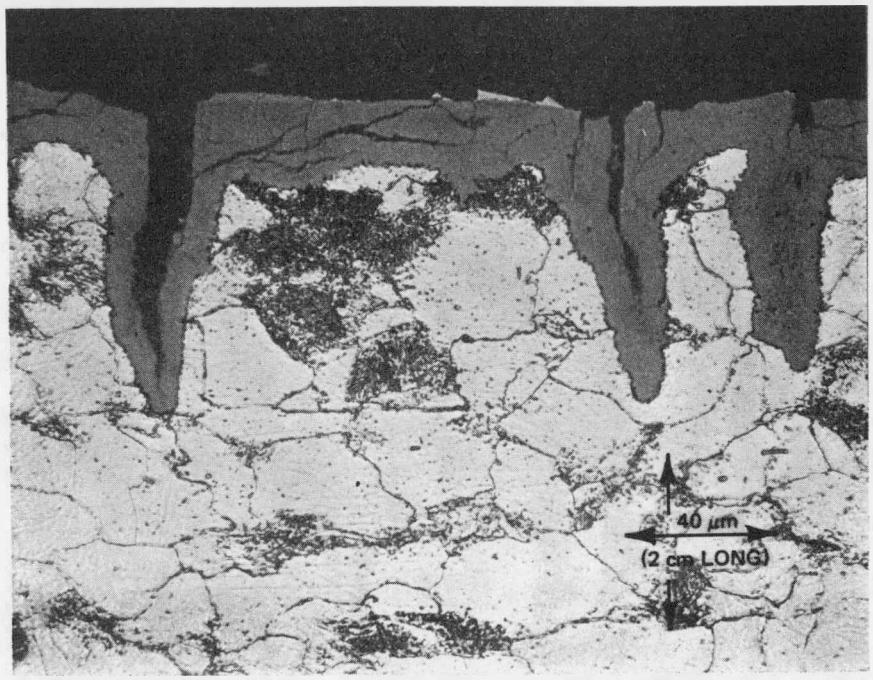

Figure 4.1a. 2 1/4 Cr-1 Mo Annealed, 5% NaOH, 316°C (600°F), 10^{-5}/Min Strain Rate, 0.100 Volts Versus Pt

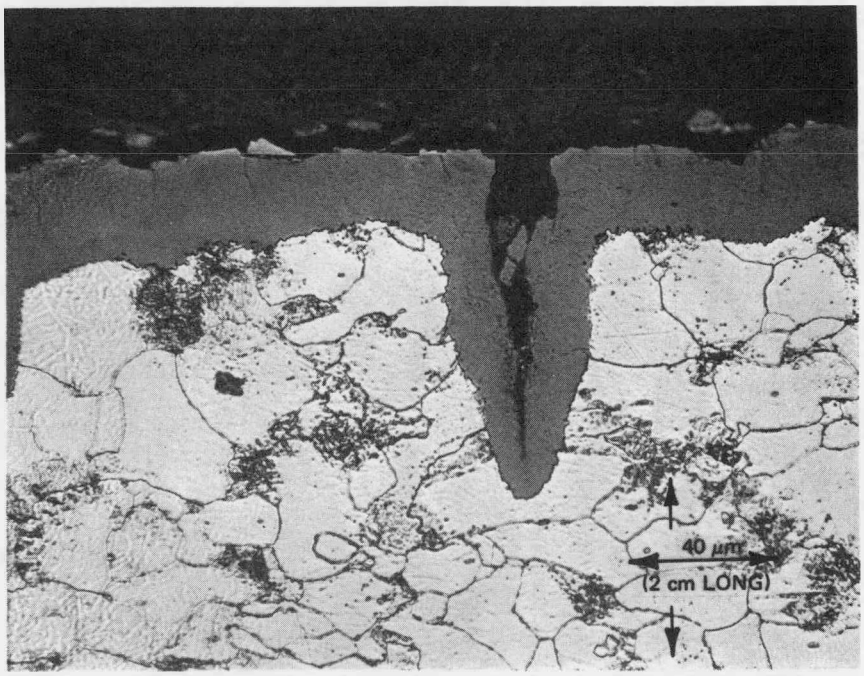

Figure 4.1b. 2 1/4 Cr-1 Mo Annealed, 5% NaOH, 316°C (600°F), 10^{-5}/Min Strain Rate, 0.150 Volts Versus Pt

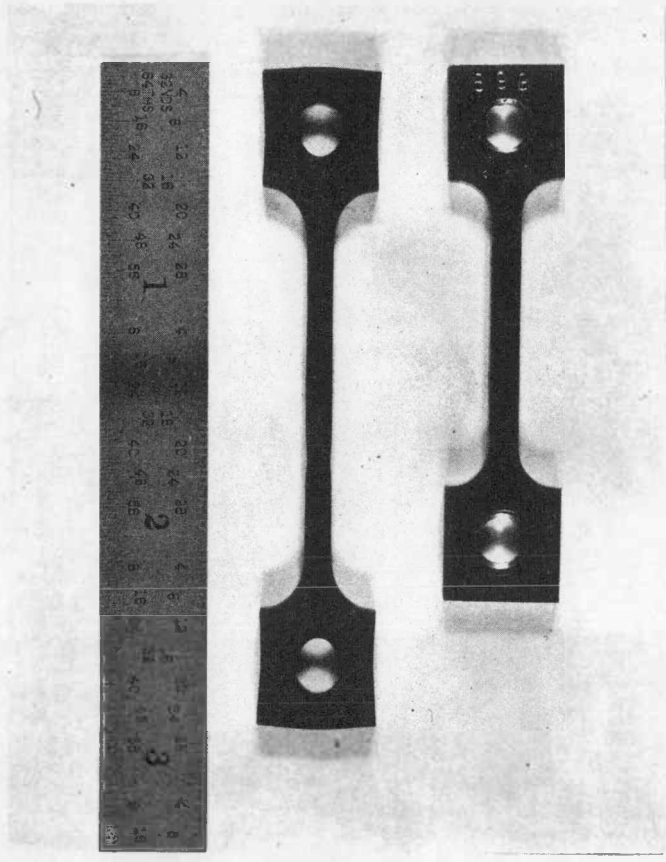

Figure 4.2. Incoloy 800, Grade 1, Before and After Constant Extension Testing, 316°C (600°F) 5% NaOH, 10^{-5}/Min Strain Rate

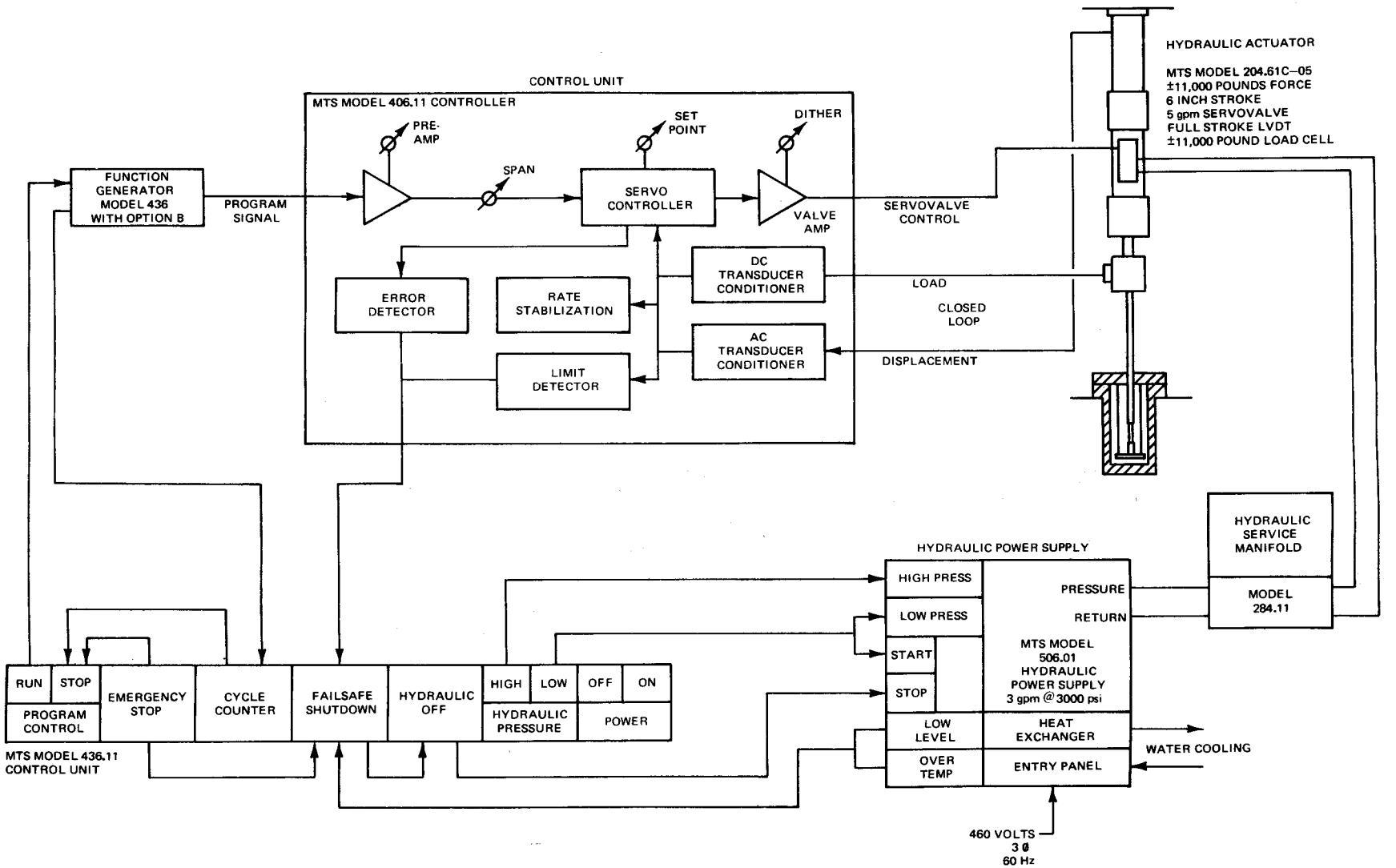

Figure 4-3. Corrosion Fatigue Test Functional Diagram

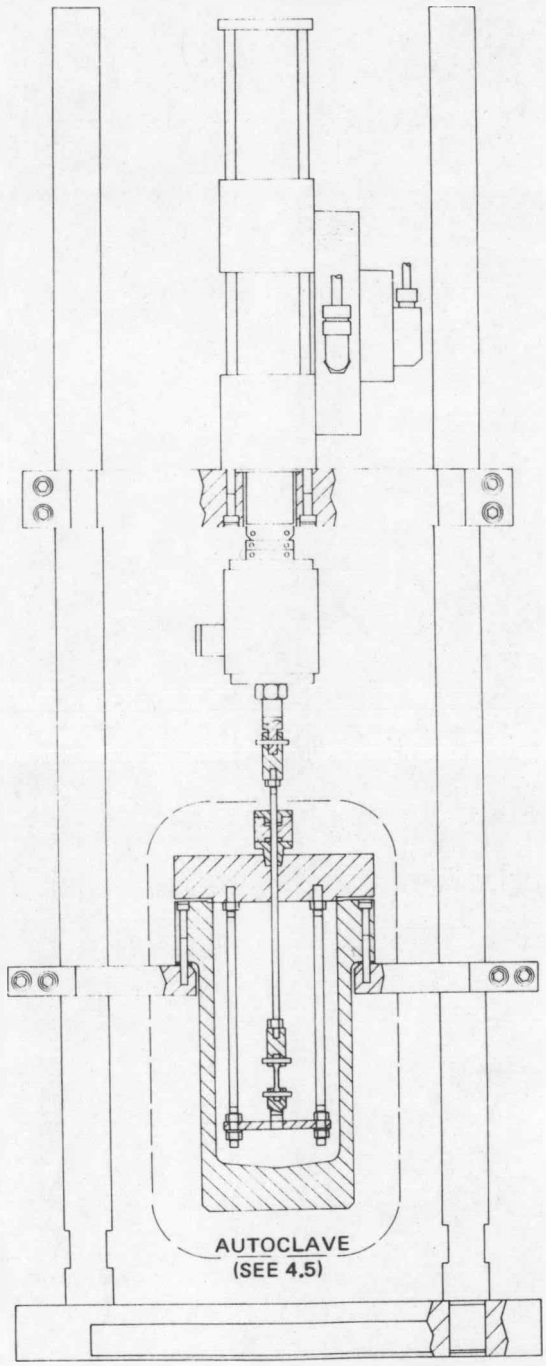

Figure 4.4. Load Frame

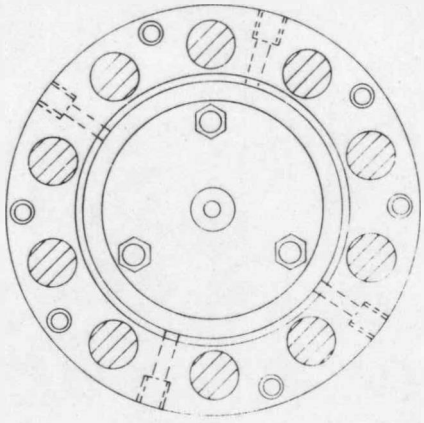

AUTOCLAVE VESSEL

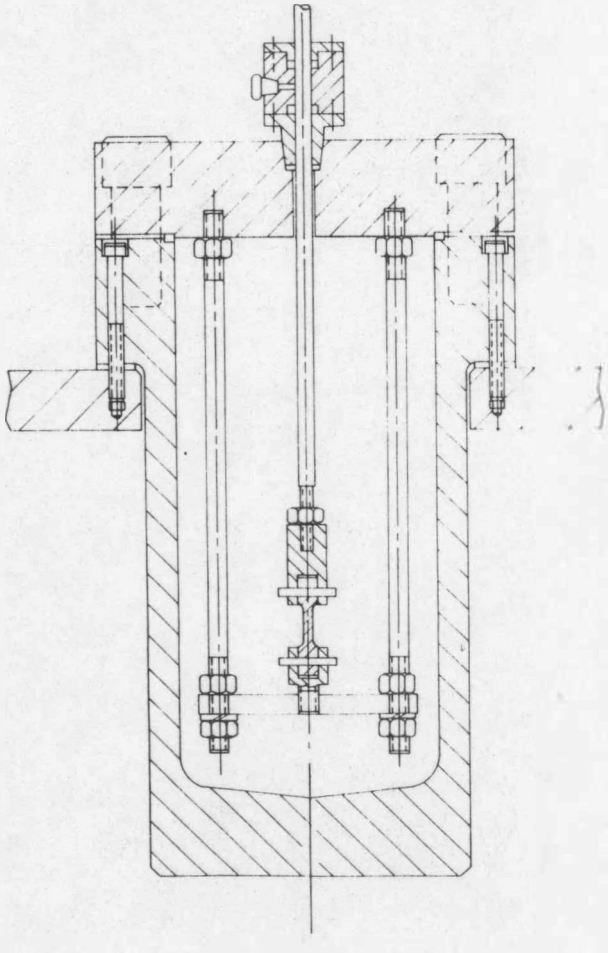

ONE SPECIMEN ARRANGEMENT

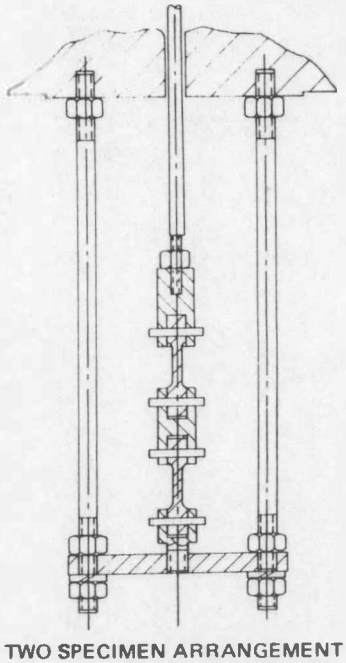

TWO SPECIMEN ARRANGEMENT

Figure 4.5. Specimen Arrangement

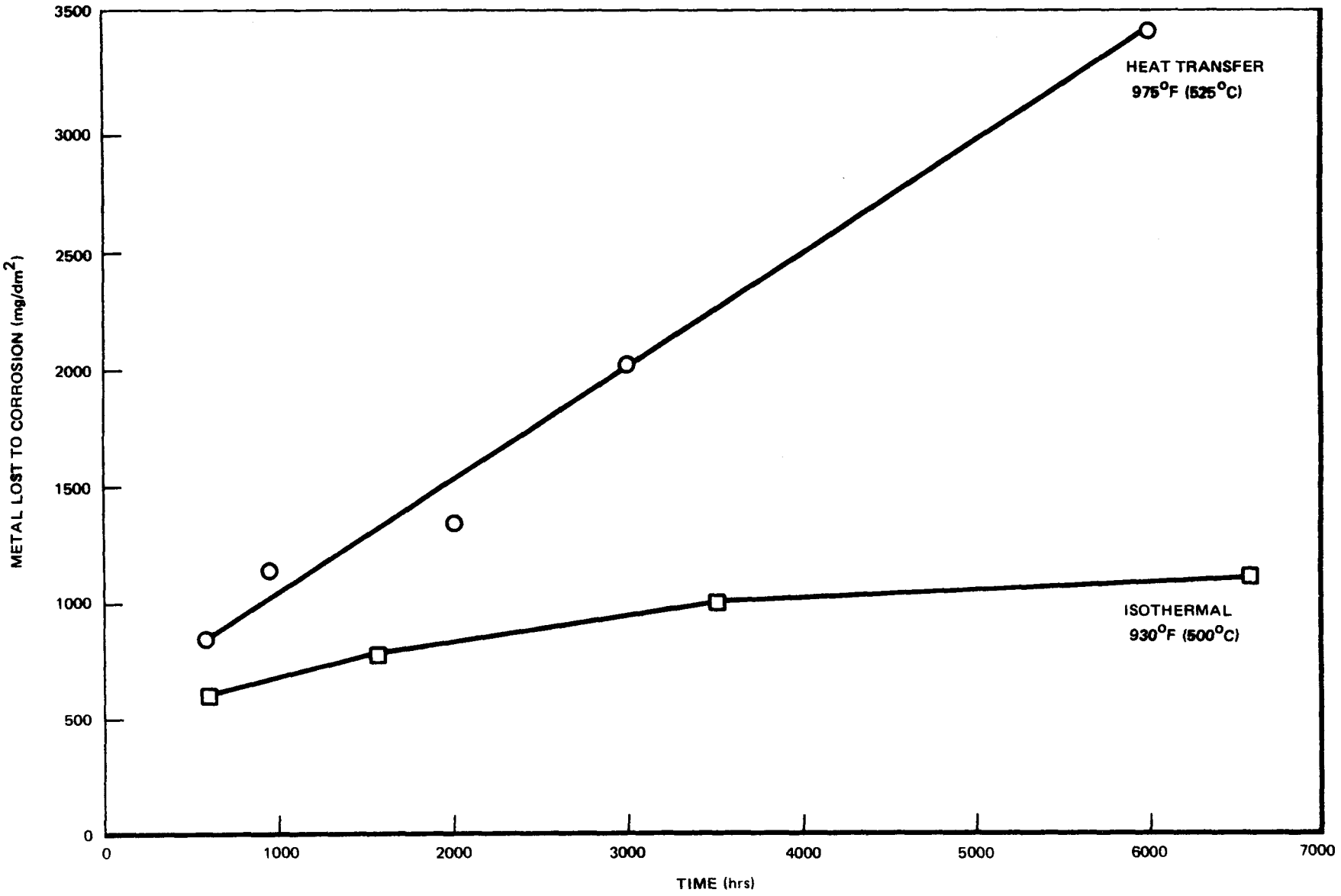

Figure 4.6. Heat Transfer Corrosion Results

5. MECHANICAL PROPERTIES OF STAINLESS STEEL IN CARBURIZING SODIUM (SUBTASK C)

5.1 FATIGUE CRACK GROWTH STUDIES - J. F. Copeland/G. R. Dodson

The objective of this program is to determine the environmental influence of liquid sodium on the fatigue crack propagation rates for annealed Type 316 stainless steel. To be prototypic of expected LMFBR Intermediate Heat Transport System (IHTS) piping conditions, this testing is being done at low frequency (0.5 cycles per minute (cpm) and at 510°C(950°F). Additionally, the existence of a high carburizing potential in the liquid sodium environment is a distinct possibility[1]. Since the exact carburizing potential of the IHTS sodium has not been determined, this experiment is being run under the most severe conditions, of carbon-saturated sodium. The use of carbon-saturated sodium also allows the acceleration of carburization in order to represent design life conditions with a relatively short-term test. Control tests in air are also being performed under the same loading conditions, in order to truly discern environmental effects. These results will show whether or not penalties or allowances for crack growth in secondary system sodium are required or warranted.

ASTM E399, 12.7 mm. (0.5 in.) thick, 3-point bend specimens were machined from annealed 15.9 mm. (5/8 in.) Type 316 plate[1] and fatigue precracked. Specimens to be tested in air were aged at 510°C(950°F) for 1000 hrs. in air. Those to be fatigued in high carbon sodium were pre-exposed in Loop A sodium with a Grade 1050 carbon steel source at 510°C(950°F) for 1000 hrs. The carburization incurred by these specimens during sodium pre-exposure is shown in Figure 5.1, and is typical of that anticipated[1] for a 30-year LMFBR design life with a 2¼Cr-1Mo steel carbon source.

Fatigue crack growth tests were performed in air and flowing, high carbon sodium in two specially designed fatigue test facilities[1]. Three tests could be run concurrently in each facility. After loading for an estimated number of cycles, the specimens were withdrawn and examined for crack growth. When the crack growth approximated 0.76 mm. (30 mils) the specimen was fractured to accurately measure crack growth. A crack growth rate was then computed from the ratio of crack extension to cycles. The stress intensity factor range (ΔK) was calculated at half the crack extension. Preliminary results for tests in air and sodium are shown in Figure 5.2, and compared to other data[2,3,4,5]. The control data (air) is in excellent agreement with previous results[2,3]. Several more tests will be run to more exactly determine this crack growth line. The sodium results fall below the air test values (slower crack growth in sodium) for the low ΔK values, where crack growth is slower and environment is expected to have more influence. These results fall slightly above the lower carbon sodium results at 427°C(800°F) and 600°C(1112°F) of HEDL and CEGB. This may indicate a slight environmental effect. At higher ΔK levels there appears to be little environmental influence on crack propagation rates. It should be noted that reference foil monitors indicate a fairly low carburizing potential of the sodium during these six tests. This will be verified and corrected. Further testing is being pursued to verify these preliminary trends. Also, future testing will include slower cycle rates and the influence of hold-times under load. Additional specimens, including some from GTA weldments, are being prepared.

In analyzing the results shown in Figure 5.2, an assessment of fatigue crack growth rate versus carburization rate was performed. Special attention was given to future test planning with hold-times, where carburization could

occur during the hold-time period between cycles. Hold-time must be adjusted to allow the diffusion of carbon into the sample to affect crack growth. The carbon must diffuse through the fatigue pre-crack to the surface of the growing crack tip and into the metal. Simple estimates of the time required for carbon diffusion to influence crack growth have been made and hold-times of approximately 1 hour are indicated. The diffusion coefficient for carbon in sodium lies between 10^{-3} and 10^{-5} $\frac{cm^2}{sec}$ at the testing temperatures. The fatigue pre-crack length of the specimen is approximately 1.4 mm (55 mils). During a time interval of 1 minute, carbon can effectively diffuse from 0.2 to 2.5 mm (7.9 to 98 mils), depending upon the value of the diffusivity of carbon in sodium. In 1 hour this distance is approximately 2 to 20 mm (.079 to .79 in.). Since carbon must diffuse through the sodium in the fatigue crack before it reaches the crack tip, hold-times of approximately 1 hour are required. The effective distance of carbon diffusion into the stainless steel crack tip, provided the sodium can freely supply carbon, is approximately $2X10^{-4}$ mm (7.9×10^{-6} in.) for a hold-time of 1 minute and 1.6×10^{-3} mm (6.3×10^{-5} in.) for a hold-time of 1 hour. The value of 10^{-3} mm (3.9×10^{-5} in.) is approximately the crack growth distance per fatigue cycle. If hold-times of less than 1 minute are employed, the crack extension should outstrip the diffusion length of the metal and no significant effect of carburization or crack extension will occur. For 1 hour hold-time, the effective diffusion distance of carbon through the fatigue pre-crack and into the stainless steel is theoretically large enough for the effect of carburization on crack growth to appear. For crack growth rates on the order of 10^{-4} or 10^{-5} mm/cycle (3.9×10^{-6} or 3.9×10^{-7} in./cycle), as at lower ΔK values, even the one or two minute hold-time could reveal the influence of carburization on crack growth rates. Several longer hold-time tests will be run in the near future.

5.2 CREEP/FATIGUE STUDIES - P. P. Pizzo

The objective of this program is to evaluate the tension creep properties of Type 316H stainless steel in a carburizing sodium environment. Particular attention has been given creep behavior under both sustained and cyclic load conditions. Analysis of the preliminary data results has been presented elsewhere.[6] In the following discussion, recently acquired data is presented. Also, previously reported data has been modified to incorporate temperature/stress corrections based on data obtained on instrumented test specimens. The data presented in this discussion supersede data reported in previous GE(FBRD) documents.

Table 5.1 lists the test parameters applicable to the creep-fatigue program. A tubular sample configuration is used to provide a continuously carburizing environment during testing. Specimens are filled with either high purity sodium and a Grade 1095 steel (wire) carbon source, or with Argon for control testing. Tensile test data characterizing the 316H stainless steel test material are included in Table 5.2.

Table 5.3 is a comprehensive tabulation of creep data obtained at 502°C(935°F). The stress rupture data from this table are graphically presented in Figure 5.3. No definite trend exists for this data. Data representing the main experimental parameters (mode of loading and environment) fall within a common scatter band. All data fall above the minimum expected value for stress rupture approximated from ASME Code Case 1592 data.

Figure 5.4 is a logarithmic plot of the minimum creep rate as a function of the applied stress. Again, no definite trend exists in distinguishing the

data as a function of test parameter. It is to be noted that limited control data is available for comparison. Major effort in the current phase of testing is focused on obtaining control test (Argon filled) data.

The data of Table 5.3 indicate that a large plastic strain is incurred upon specimen loading. This loading strain is equivalent to that obtained in a standard tensile test, $\dot{\varepsilon} \cong 10^{-3}s^{-1}$, at the test temperature, 510°C(950°F). That is, for the stress conditions of this test program (365 to 565 MPa/53 to 82 ksi), the applied stress is greater than the yield stress at the test temperature (173 MPa/25 ksi). Thus upon loading, the sample deforms (strains), until sufficient work hardening takes place to resist further time independent deformation. Subsequent to this initial strain, time dependent flow (or creep) occurs. These events are illustrated in the strain/time curves of Figure 5.5. Creep strains less than 3% are nominally observed for existing data.

The strain upon loading for control test specimens is plotted in Figure 5.5. Control specimens are found to undergo a larger instantaneous strain than Na/C exposed samples under equivalent test conditions. This information will be used in subsequent testing to isolate potential environmental influences.

REFERENCES

1) "Program for the Development of Design Data - LMFBR Steam Generator Materials" prepared for the ERDA under contract at (04-3)-893 Task 10-G and Task 18, July 16 & 17, 1975

2) L. A. James, "Effect of Thermal Aging Upon the Fatigue-Crack Propagation of Austenitic Stainless Steels", Met. Trans., Vol. 5, Apr. 1974, pp. 831-838

3) P. Shahinian et al, "Fatigue Crack Growth in Type 316 Stainless Steel at High Temperature", Trans. ASME, Nov. 1971, pp. 976-980

4) P. Marshall, "The Fatigue Behaviour of Annealed AISI 316 Stainless Steel in Air and High Temperature Sodium: Review and Preliminary Results", Central Electricity Generating Board, Report RD/B/N 3236, Nov. 1974

5) L. A. James and R. L. Knecht, "Fatigue-Crack Propagation Behavior of Type 304 Stainless Steel in a Liquid Sodium Environment", Met. Trans., Vol. 6A, Jan. 1975, pp. 109-116.

6) Fifth Quarterly Report, Steam Generator Materials Engineering, July - September 1975, GEAP-14029-5, U.S. ERDA Contract E (04-3)-893 Task 18, Oct. 1975

Table 5.1 Creep-Fatigue Test Parameters
Tubular Tension Samples

Environment	- Carbon saturated Na or argon (inside diameter) - Air (outside diameter)
Test Temperature	- 502°C (935°F)
Material	- Annealed Type 316H stainless steel
Loading Modes	- Constant load for creep Periodic load increase of approximately 69MPa (10ksi) for creep-fatigue
Load Increase Frequency	- 1 cycle per hr.
Hold-Time at Peak Load	- 15s and 1800s

Table 5.2 Test Material Characterization-
Tensile Tests

316H Stainless Steel	0.2% Y.S., MPa	(Ksi)	U.T.S., MPa	(Ksi)	% El.	% R.A.
1/4 Sched. 80 Pipe Tests*						
Room Temp.	272	(39.4)	623	(90.4)	50.0	55.3
	300	(435)	612	(88.7)	44.0	48.5
510°C (950°F)	173	(25.1)	479	(69.4)	28.5	36.3
	166	(24.0)	491	(71.2)	32.5	36.6

* 8.9 mm (0.35 in.) O.D. X 0.46 mm (0.018 in.) wall X 50.8 mm (2 in.) reduced section

Table 5.3 Creep Data at 502°C(935°F) for Annealed Type 316H Stainless Steel

Specimen	Stress (Ksi)	Stress (MPa)	Peak Stress Hold-Time (Hr)	Pre-exposure/Test Environment(a)	Rupture Time (Hr)	Strain Upon Load Application (%)	Creep Strain (%)	Creep Rate (%/Hr)
C10	57	393	-	Na/C	2430	4.3	1.1	$3.6X10^{-4}$
C6	63	434	-	Na/C	680	7.2	0.7	$7.0X10^{-4}$
C9	69	476	-	Na/C	917	9.5	0.9	$8.0X10^{-4}$
C7	76	524	-	Na/C	428	13.4	0.7	$1.3X10^{-3}$
C1	48/59	331/407	0	Ar	(b)	7.4	(b)	$2.5X10^{-4}$
C22	61/71	421/490	0	Ar	2584	22.0	3.2	$4.7X10^{-5}$
C11	54/66	372/455	0	Na/C	2108	9.8	0.7	$3.1X10^{-4}$
C15	62/75	428/517	0	Na/C	842	10.9	3.3	$9.2X10^{-4}$
C18	62/75	428/517	0	Na/C	1860	12.0	-	-
C16	63/76	434/524	0	Na/C	4.6	15.5	<.1	-
C13	70/82	483/565	0	Na/C	1585	21.2	4.9	$4.6X10^{-3}$
C12	53/64	365/441	.5	Na/C	904	12.3	1.0	$8.8X10^{-4}$
C19	60/72	414/496	.5	Na/C	2322	-	-	-
C14	60/72	414/496	.5	Na/C	423	12.3	0.9	$1.3X10^{-3}$

(a) All samples pre-exposed to 510C(950F) for 1000 hr, air
(b) Test discontinued prior to failure

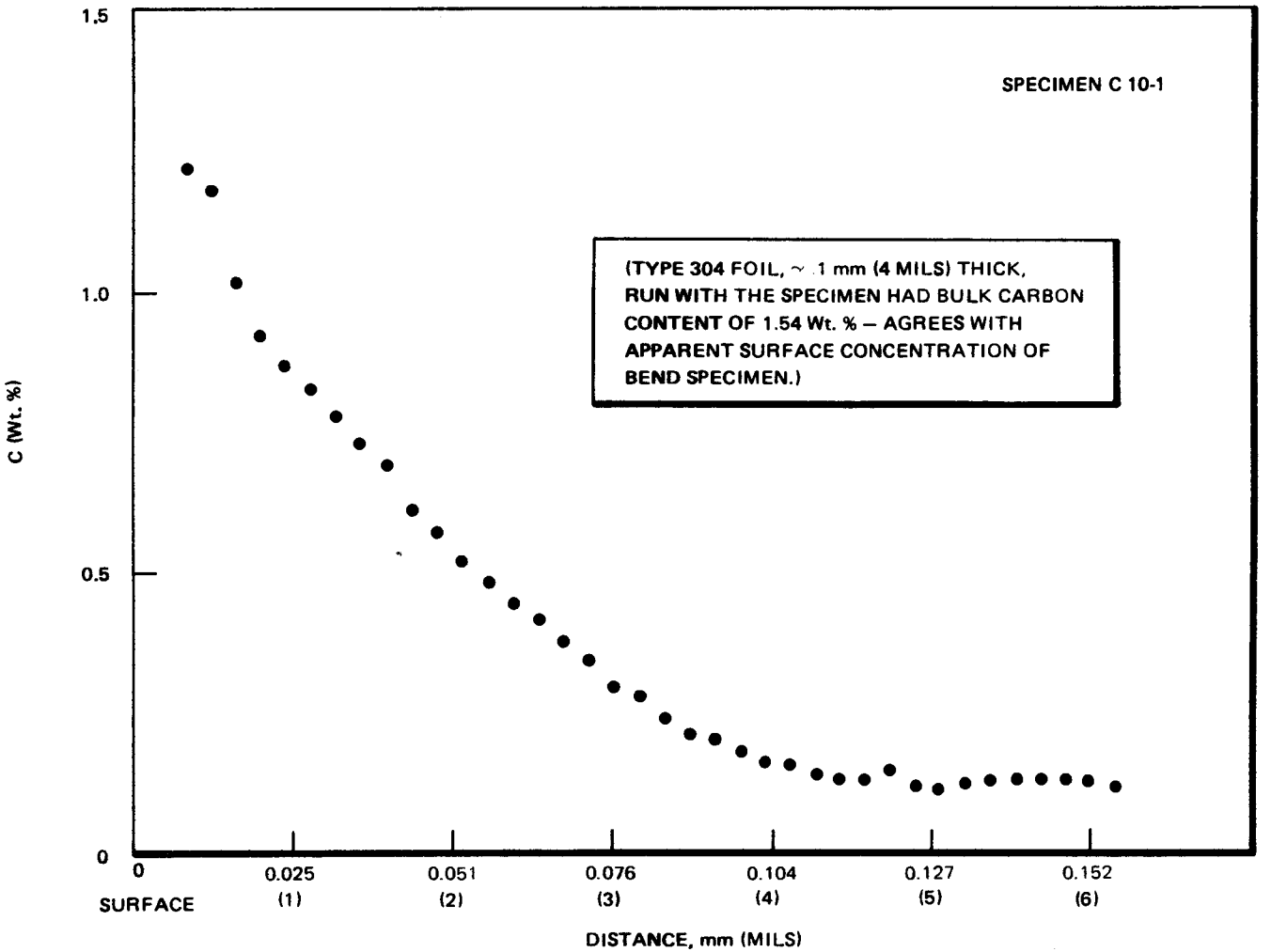

Figure 5.1. Carbon Profile (Electron Microprobe) on Annealed Type 316 12.7 mm (0.5 in.) Bend Specimen Aged in Loop A for 1000 Hr at 510°C (950° F). 1050 Carbon Steel Source (Carbon – Saturated Sodium)

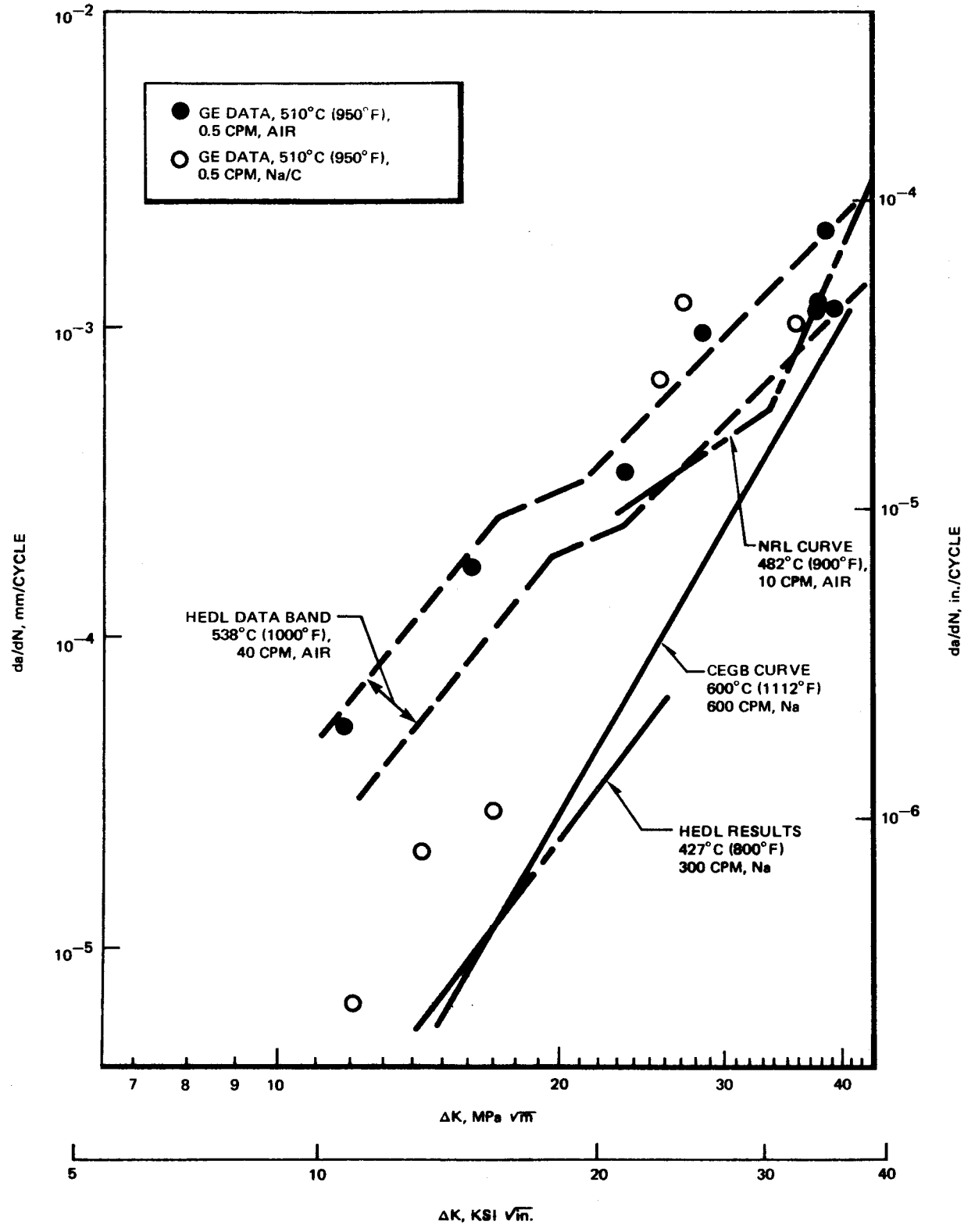

Figure 5.2. Comparison of Fatigue Crack Propagation Rate Results for Annealed Type 316 Stainless Steel in Air and Sodium at Elevated Temperatures.

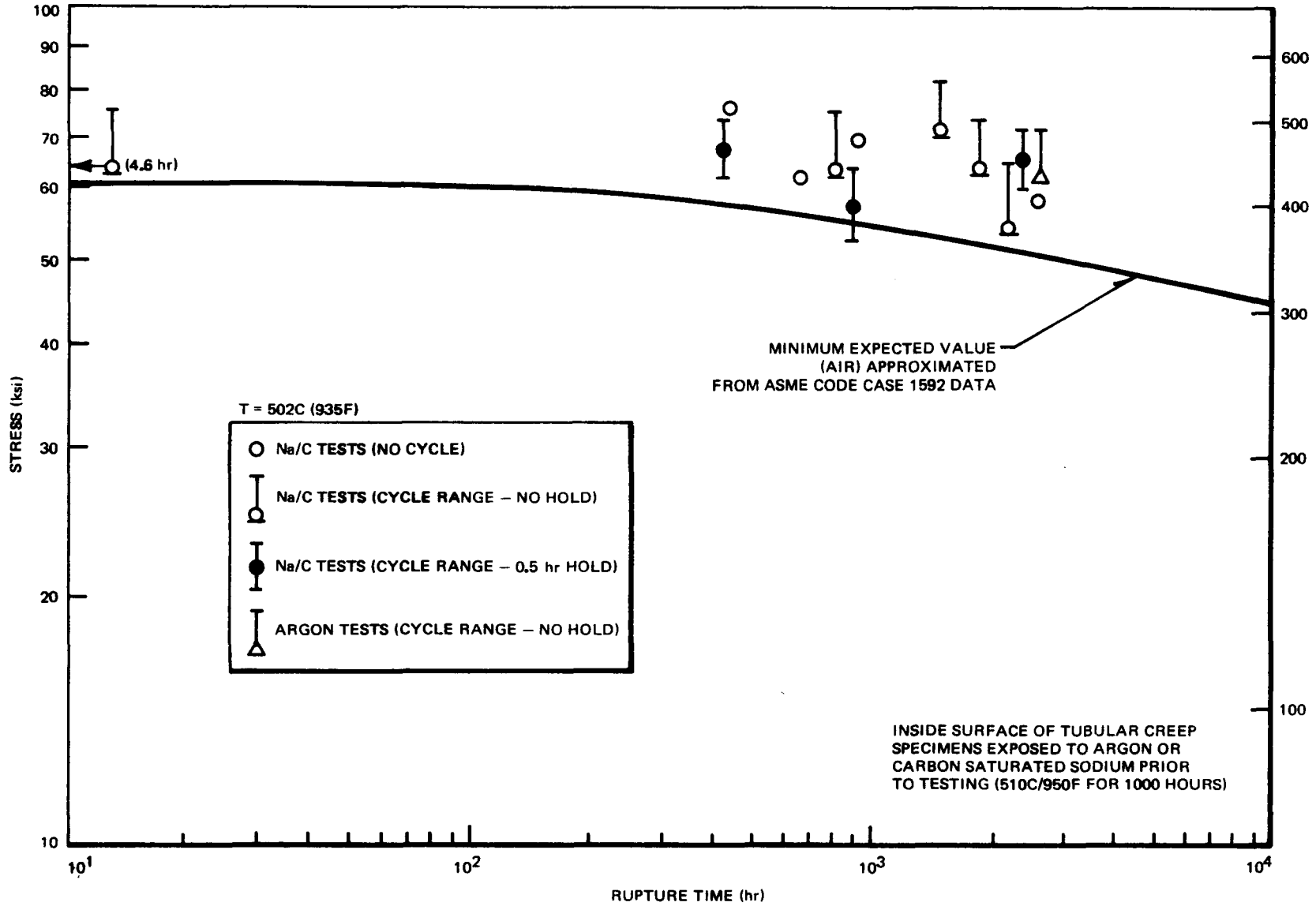

Figure 5-3. Stress Rupture Results for Annealed 316H Stainless Steel Tubular Creep Specimens

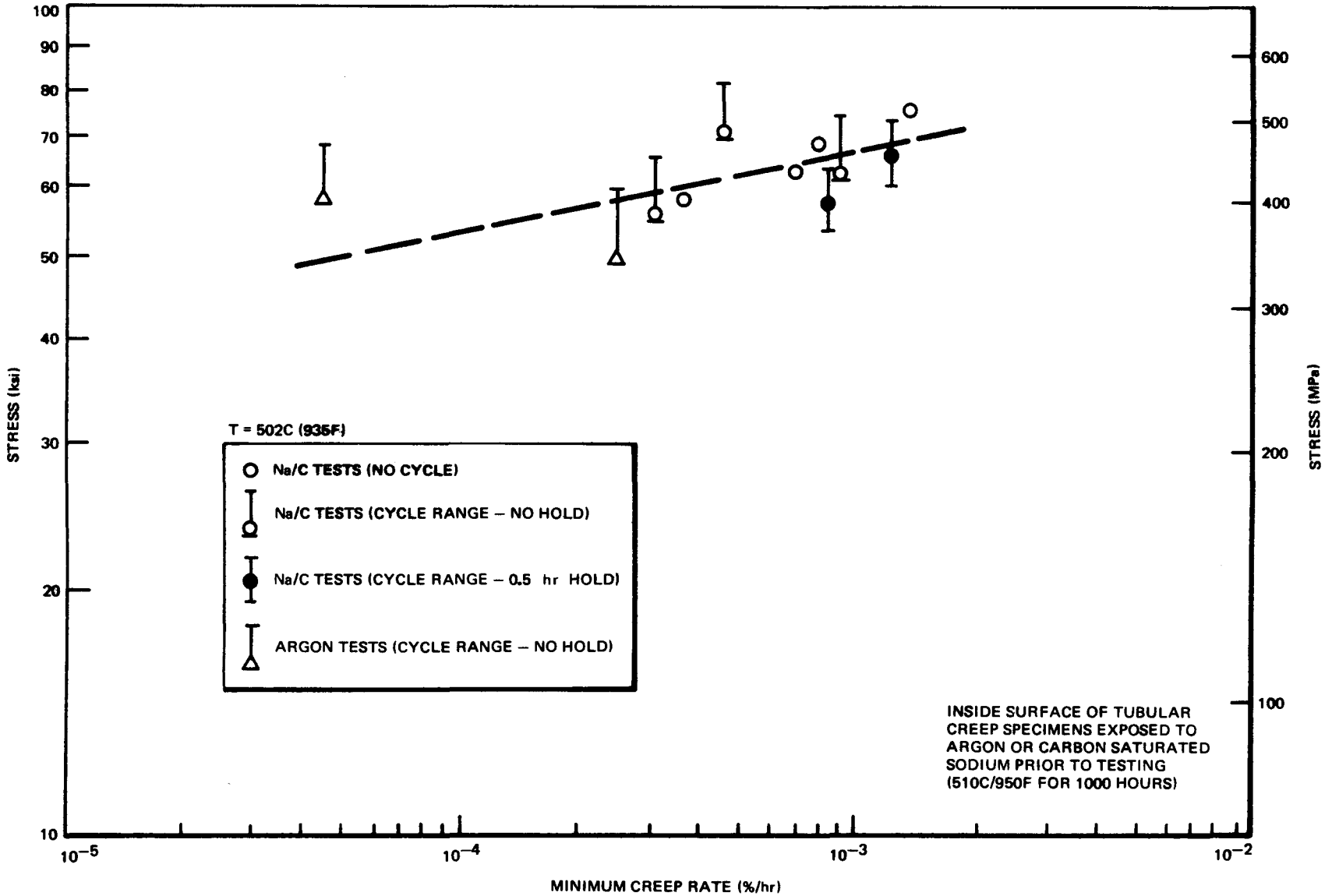

Figure 5-4. Minimum Creep Rate Results for Annealed 316H Stainless Steel Tubular Creep Specimens

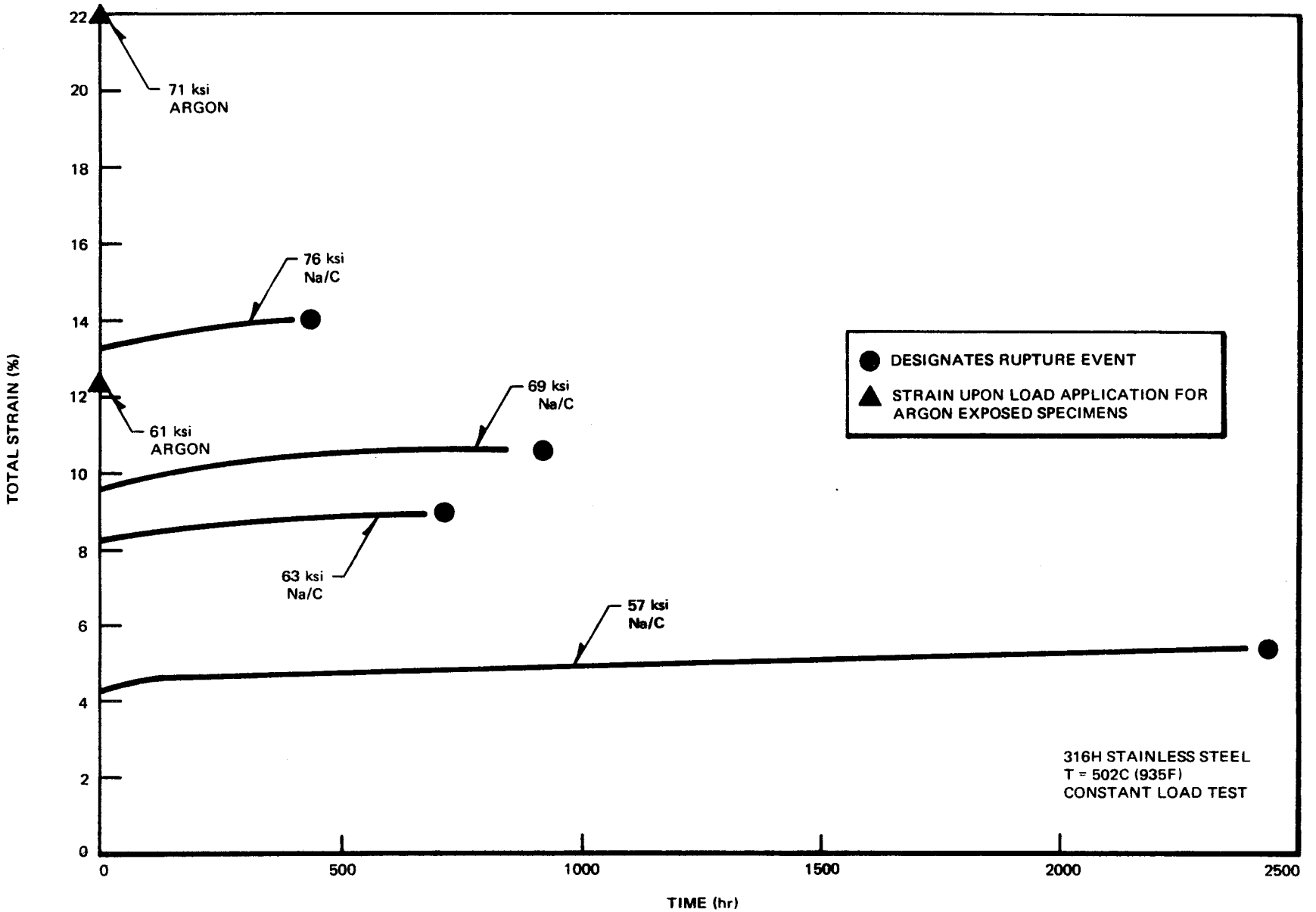

Figure 5.5. Total Strain As A Function of Time. Uniaxial Creep Test

6. SIMULATION OF THE INTERMEDIATE HEAT TRANSPORT SYSTEM - ISML (SUBTASK D)

J. L. Krankota

6.1 OBJECTIVE

The objective of simulating the IHTS with the ISML (Intermediate System Mockup Loop) is to confirm the predicted carburization and decarburization rates of stainless steel and 2¼Cr-1Mo in non-isothermal, flowing sodium. In addition, the anticipated pattern of carbon transport in sodium throughout a bimetallic piping system at prototypical temperatures can be verified. This information, when coupled with mechanical properties data on carburized stainless steels and decarburized 2¼Cr-1Mo, will permit the designers to account for possible degradation of the pressure boundary integrity.

6.2 CURRENT PROGRESS

Run B-2

The second test run (Run B-2) was completed after 912 hours at test conditions. The loop performed without significant incident at operating temperatures which varied not more than ±3°C (±5.4°F) during the run. The samples removed from the loop included some with 912 hours and some with 1503 hours (the cumulative exposure during Runs B-1 and B-2.)

The majority of the samples are still being analyzed for carbon and prepared for metallographic examination.

During this run the heating and cooling capability of the Specimen Equilibration System was checked out with no specimens in the sample holder. The temperature of the sodium passing through the sample holder was maintained at 750 ± 5°C (1382 ± 9°F) for four hours as required in RDT F3-40 (June 1975 draft). The sodium

flow rate of 0.00126 liter/sec (0.2 gpm) was greater than the minimum required in the standard (0.00063 liter/sec, 0.01 gpm) for the length of 0.25 mm diameter vanadium wire to be used. The specimen holder is designed to hold 18Cr-8Ni steel foils and electrochemical meters and can be emptied by means of an inert cover gas pressure. Vanadium wire and 18Cr-8Ni steel (supplied by R. McCowen, HEDL) will be included in the Specimen Equilibration System during the next run (B-3).

Run B-1

Results of carbon and metallographic analyses from samples from the first run (B-1, 591 hours) indicate that the trends observed in the shakedown run were repeated. As shown in Figure 6.1, the thin (0.025 cm, 0.010 inch) samples of Type 304SS carburized slightly (50-130 ppm carbon), in general, throughout the loop. The test results are tabulated in Table 6.1. Similar samples of 2¼Cr-1Mo with a stable microstructure (20% tempered pearlite, 80% ferrite) decarburized to 900 ppm C in the isothermal hot leg, which simulates the entrance region of the steam generator. (Samples are characterized with respect to microstructure because conventional heat treatment terms do not always convey the state of the microstructure in 2¼Cr-1Mo.) The microstructures of these two heats of material in the as-received condition are shown in Figure 6.2. Samples located further downstream at the entrance to the first heat exchanger (which simulates the superheater tubing region) decarburized to 1100 ppm C. Samples of 2¼Cr-1Mo with the same stable microstructure located further downstream in the cooler regions of the two heat exchangers (which simulate the length of the steam generator tubing) experienced only minor decarburization from the original carbon content of 1350 ppm C. Samples of 2¼Cr-1Mo with a microstructure of 15% Bainite, 85% Ferrite, located in the second 2¼Cr-1Mo heat exchanger (HX-4), decarburized from 1100 ppm C to 800 ppm C. This rate of carbon loss was larger than that for samples with a relatively stable microstructure. The decarburization rate constants calculated for each heat of 2¼Cr-1Mo are shown in

Figure 6.3. The rate constants for the two samples in HX-3 and the one in SH-2 with stable microstructures fall within the band of data from all other investigations. The two samples of less stable microstructure in HX-2 gave rate constants about one order of magnitude above the scatterband of data from all other investigations. The difference in the rate of decarburization between the unstable and stable 2¼Cr-1Mo will be determined more accurately during the course of the next few runs; the unusually high rate for the unstable 2¼Cr-1Mo will probably decrease as the alloy ages.

The microstructures of exposed samples of the two heats of 2¼Cr-1Mo are shown in Figure 6.4 and those of exposed samples of the two heats of 304SS are shown in Figure 6.5. The samples of the stable microstructure 2¼Cr-1Mo exhibited a lower density of carbide particles with no discernible gradient from the surface inward. The electron microprobe which had been modified for detection of low levels of carbon (1000 ppm) was not used to determine carbon concentration profiles because it proved to be insensitive below 1000 ppm carbon. The third photomicrograph in Figure 6.4 illustrates the rapid decomposition of the bainite during decarburization. The decomposition apparently precedes decarbruziation because very few decomposition products (pearlite or agglomerated carbides) are evident. The tempering of the bainite was not expected to proceed at a significant rate at this low temperature (406°C [767°F]). The microstructures of the austenitic stainless steel samples reveal little evidence of carburization; some decoration of slip lines in cold worked regions was the only indication that carbon ingress had occurred. The amount of carbon picked up by the first sample in Figure 6.5 and by a thinner (0.076mm, 0.003 in.) sample during the shakedown run (175 hours) is compared with other data in Figure 6.6. The rates are similar to those for stainless steel in other bimetallic (2¼Cr-1Mo/stainless steel) systems at similar temperatures.

Weight changes measured during the first two runs are shown in Figure 6.7. No significant changes were noticed between the first and second runs in the stainless steel heat exchangers and in the cold leg piping section. In the hot leg piping section and the 2¼Cr-1Mo heat exchangers the weight losses increased with increase in exposure. The primary cause of the weight changes is from change in carbon content. This is shown in Figure 6.8 where the weight changes calculated from the change in bulk carbon content of the thin (0.25 mm, 0.010 in.) samples are compared with the total weight changes measured on samples before and after exposure. The weight changes calculated from carbon content changes are from 50 to 80% of the total measured weight change.

The use of the low carbon 2¼Cr-1Mo piping in the construction of the ISML referred to in the last quarterly has been thoroughly reviewed and modifications to the loop initiated. A report discussing this work is attached to this report as Appendix A.

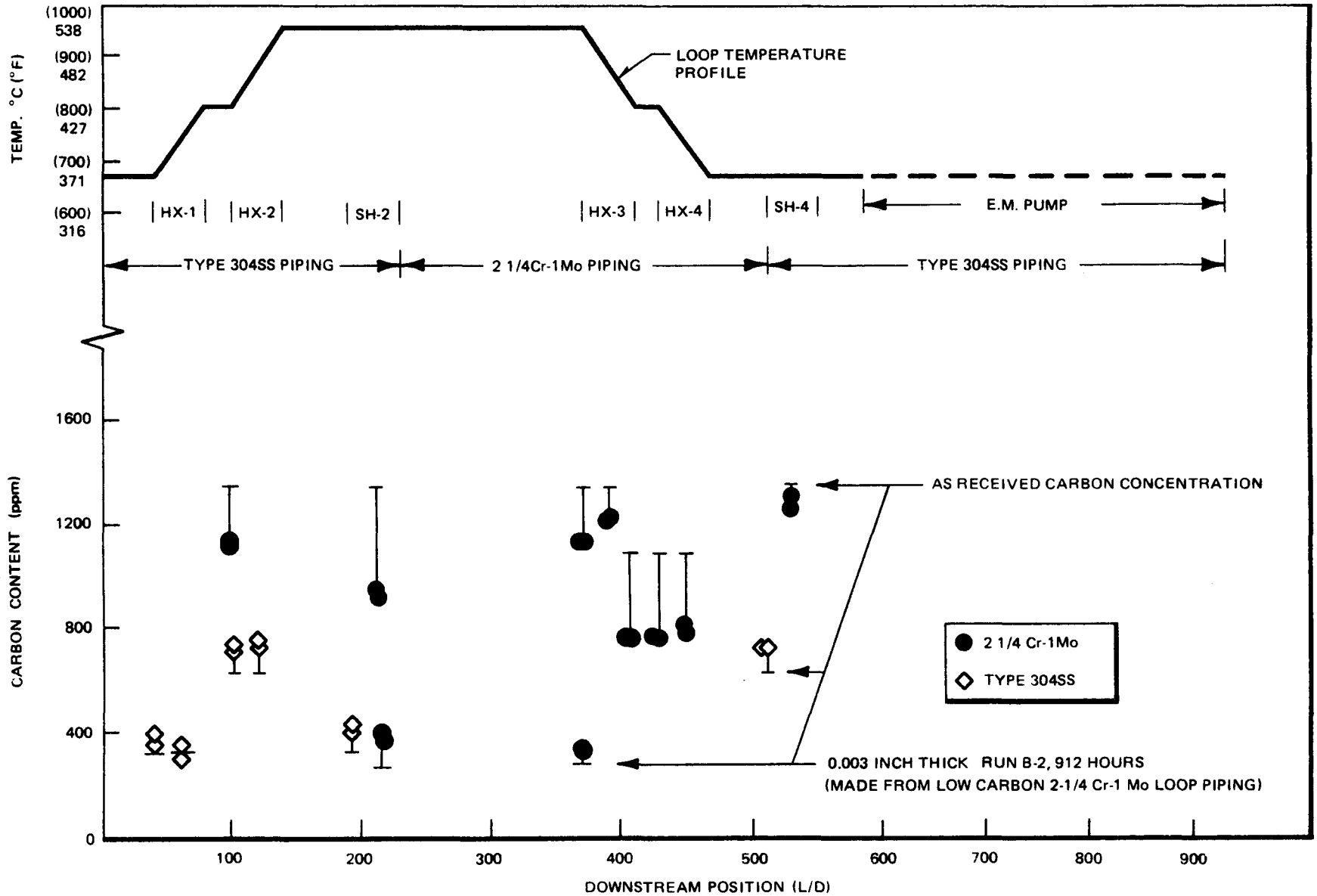

Figure 6.1. Carbon Concentration Profile in ISML After First Test Run (Run B-1, 591 Hours)
Note: All Samples are 0.025 cm (0.010 in.) Thick unless Otherwise Designated

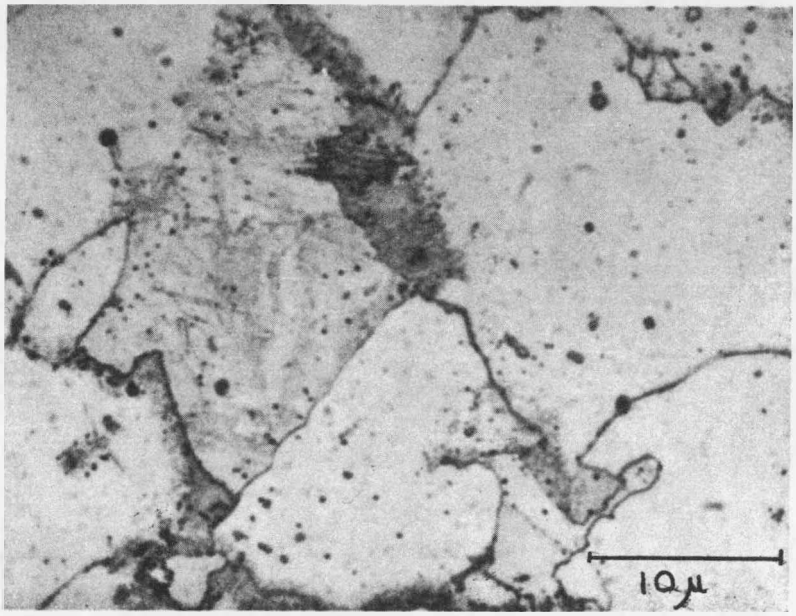

HEAT NO. 8T0326 (BAINITIC)

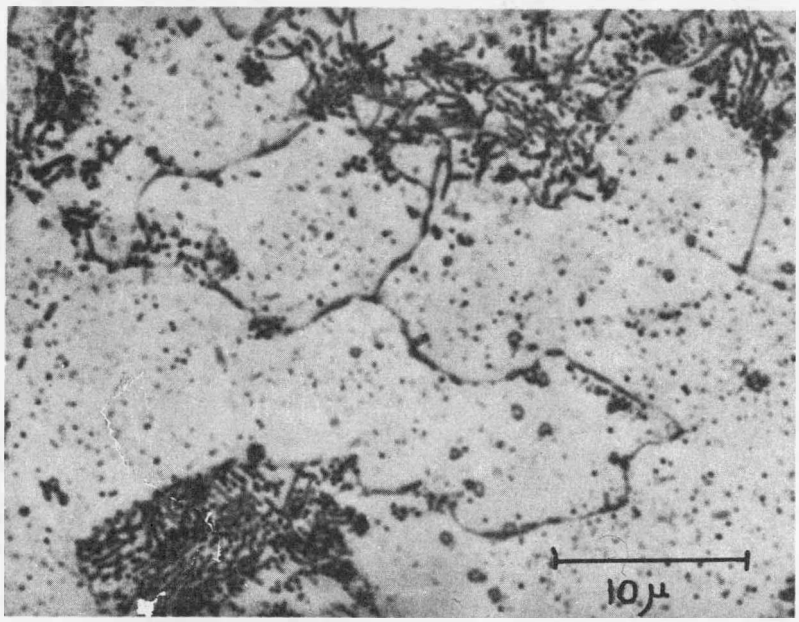

HEAT NO. 25443 (TEMPERED PEARLITE)
NOTE: IN BOTH PHOTOS THE MARK DENOTES 10 μm (0.4 mil)

Figure 6.2. Microstructure of as Received 2 1/4 Cr-1 Mo

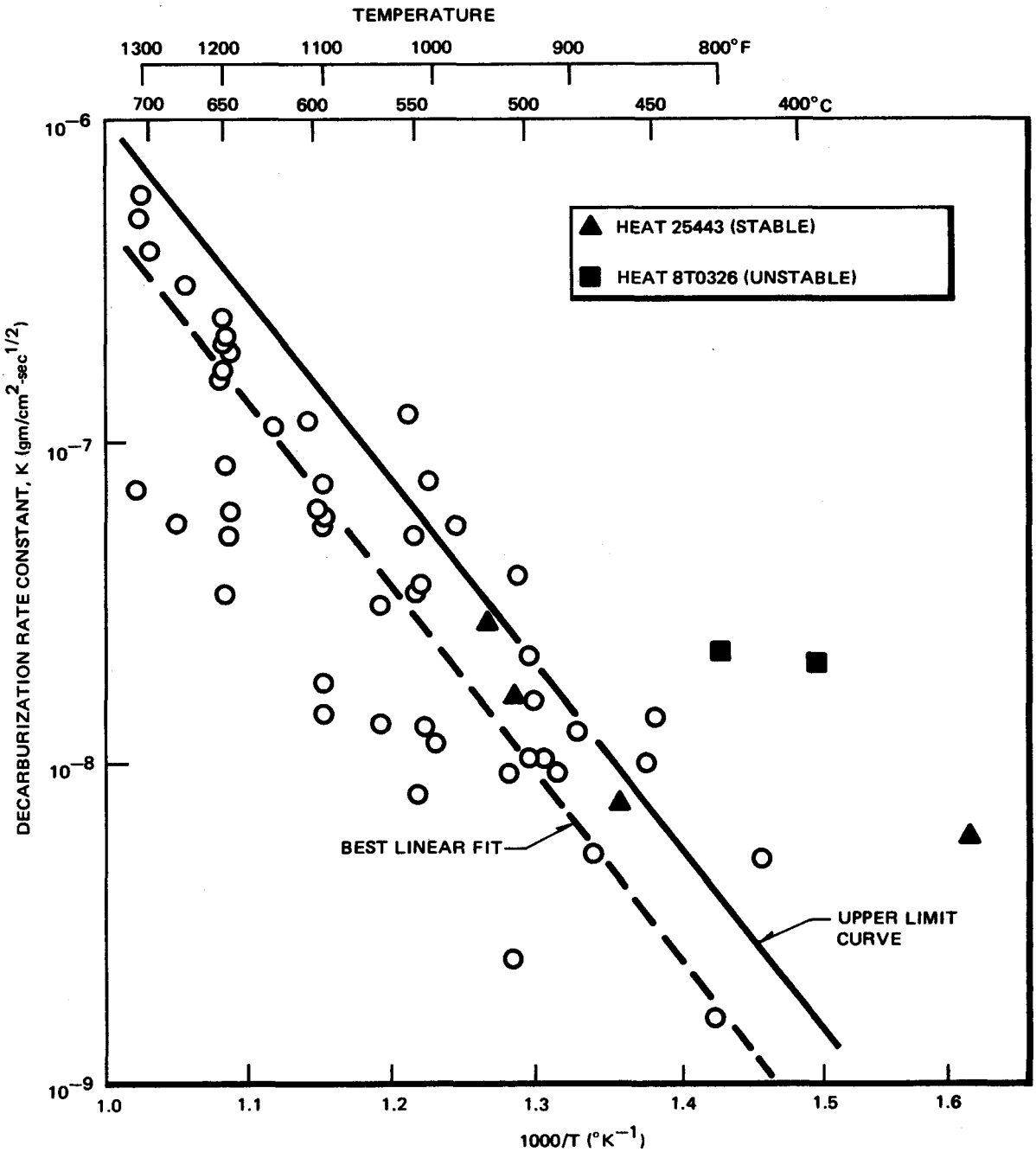

Figure 6.3. Decarburization Rate Constants for 2 1/4 Cr-1 Mo in Sodium: Data From ISML Compared with All Other Investigations (Run B-1).

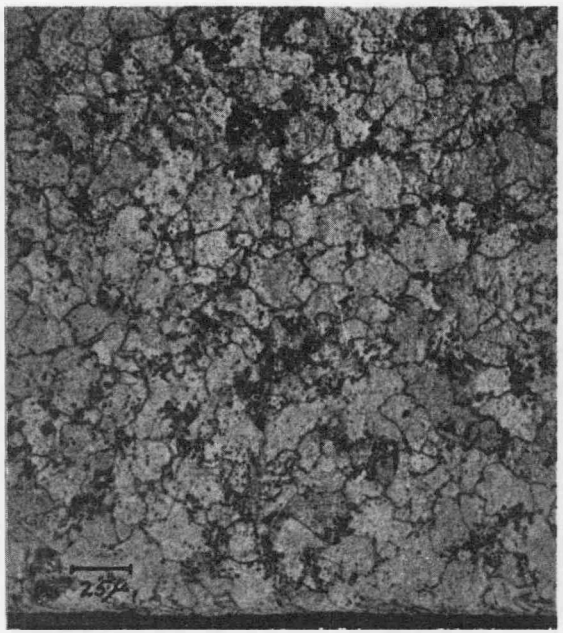

SAMPLE: H601
HEAT NO.: 25443
TEMPERATURE: 413°C (776°F)
CARBON: 1130 ppm

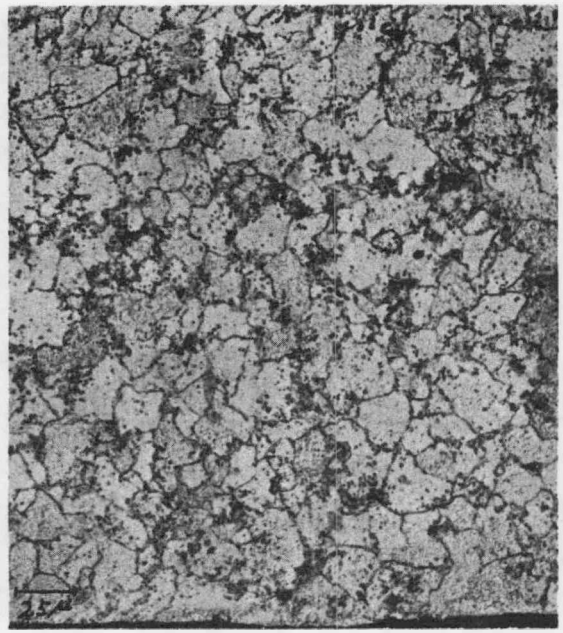

SAMPLE: S421
HEAT NO.: 25443
TEMPERATURE: 520°C (967°F)
CARBON: 930 ppm

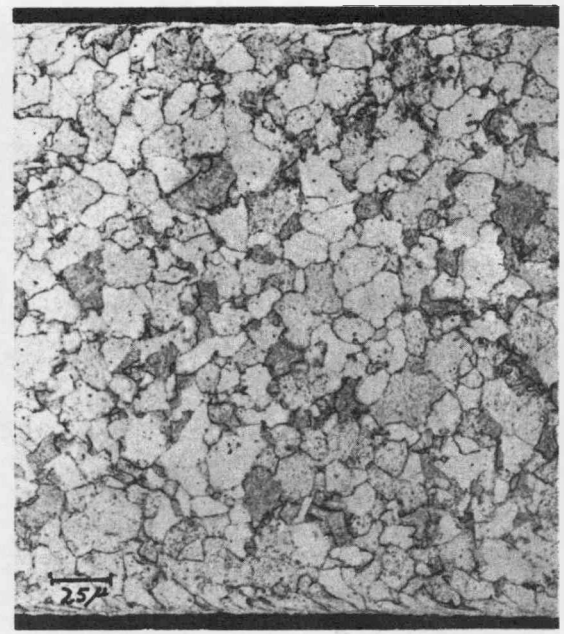

SAMPLE: H821
HEAT NO.: 8T0326
TEMPERATURE: 406°C (762°F)
CARBON: 795 ppm

Figure 6.4. Microstructures of 2 1/4 Cr-1 Mo Decarburized in Sodium in the ISML During Run B-1 (591 Hours)
Note: As received carbon contents = 1345 ppm (No. 25443)
1083 ppm (No. 8T0326)

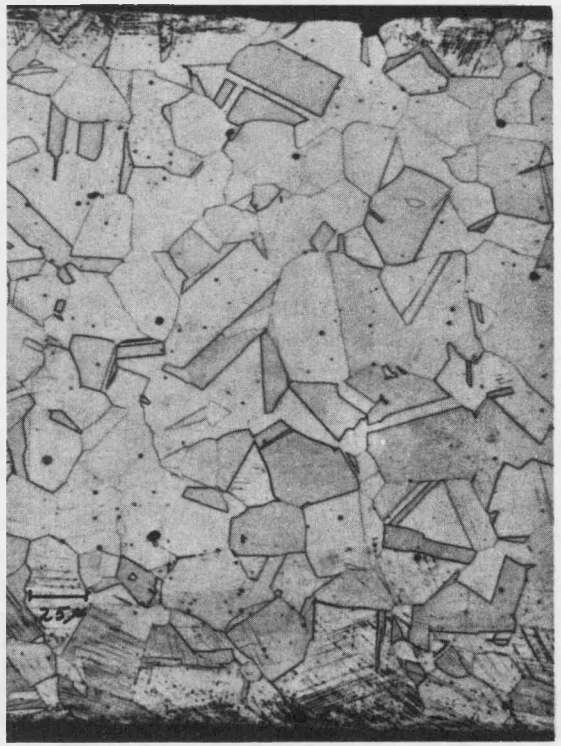

SAMPLE: H421
HEAT NO.: 89023
TEMPERATURE: 458°C (857°F)
CARBON: 741 ppm

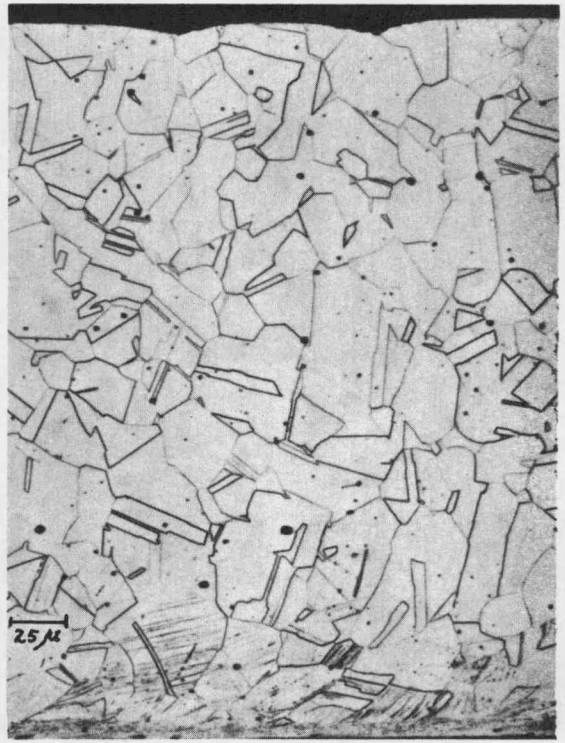

SAMPLE: S201
HEAT NO.: 89023
TEMPERATURE: 352°C (666°F)
CARBON: 632 ppm

SAMPLE: S401
HEAT NO.: 127824
TEMPERATURE: 520°C (967°F)
CARBON: 417 ppm

Figure 6.5. Microstructures of Type 304 SS Carburized in Sodium in the ISML During Run B-1 (591 hours)
Note: As received carbon contents = 623 ppm (No. 89023)
325 ppm (No. 127824)

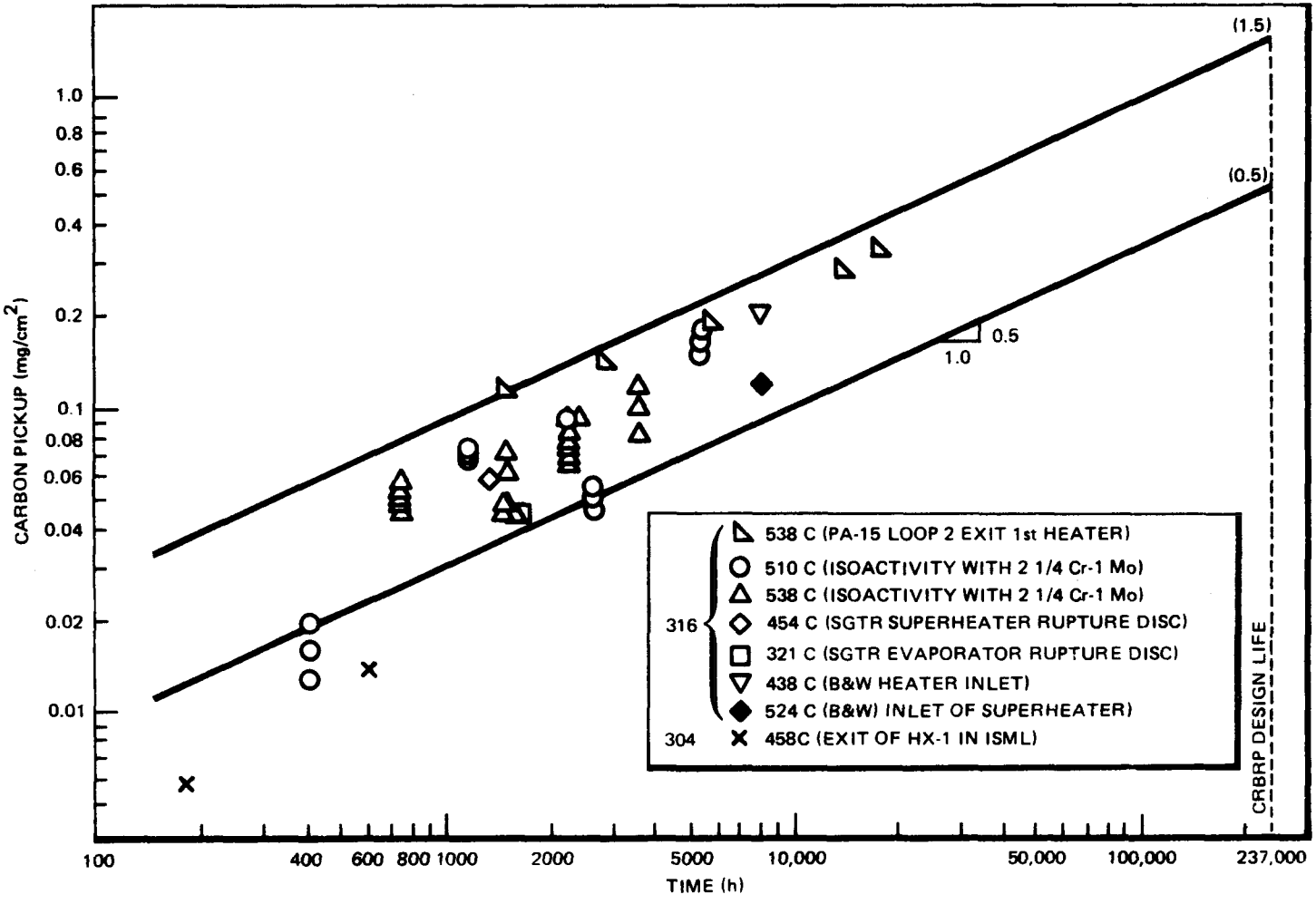

Figure 6.6. Carburization of Stainless Steels in Sodium in Bimetallic (2 1/4 Cr-1 Mo/Stainless Steel) Loops

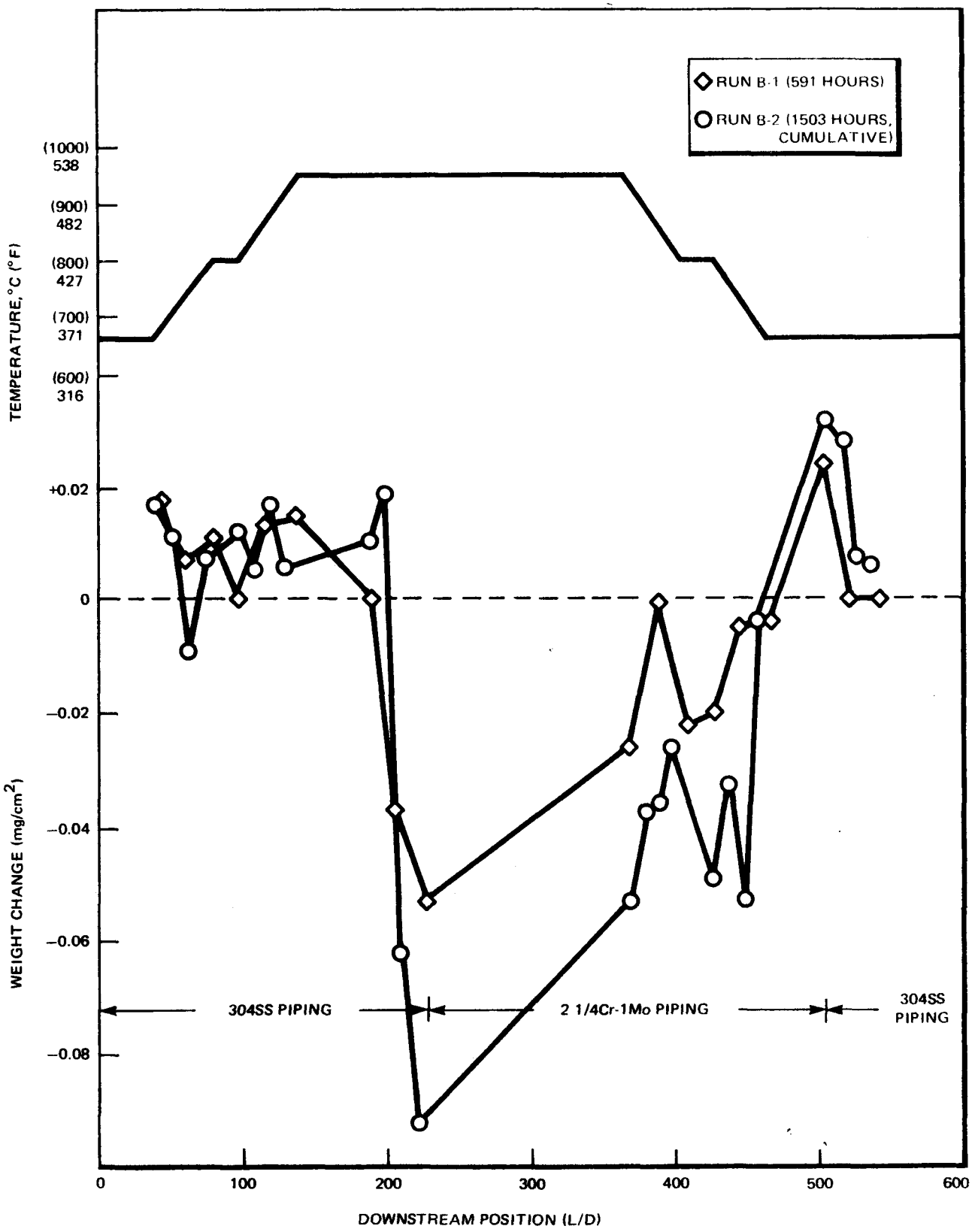

Figure 6.7. Weight Changes During the First Two Runs in the ISML

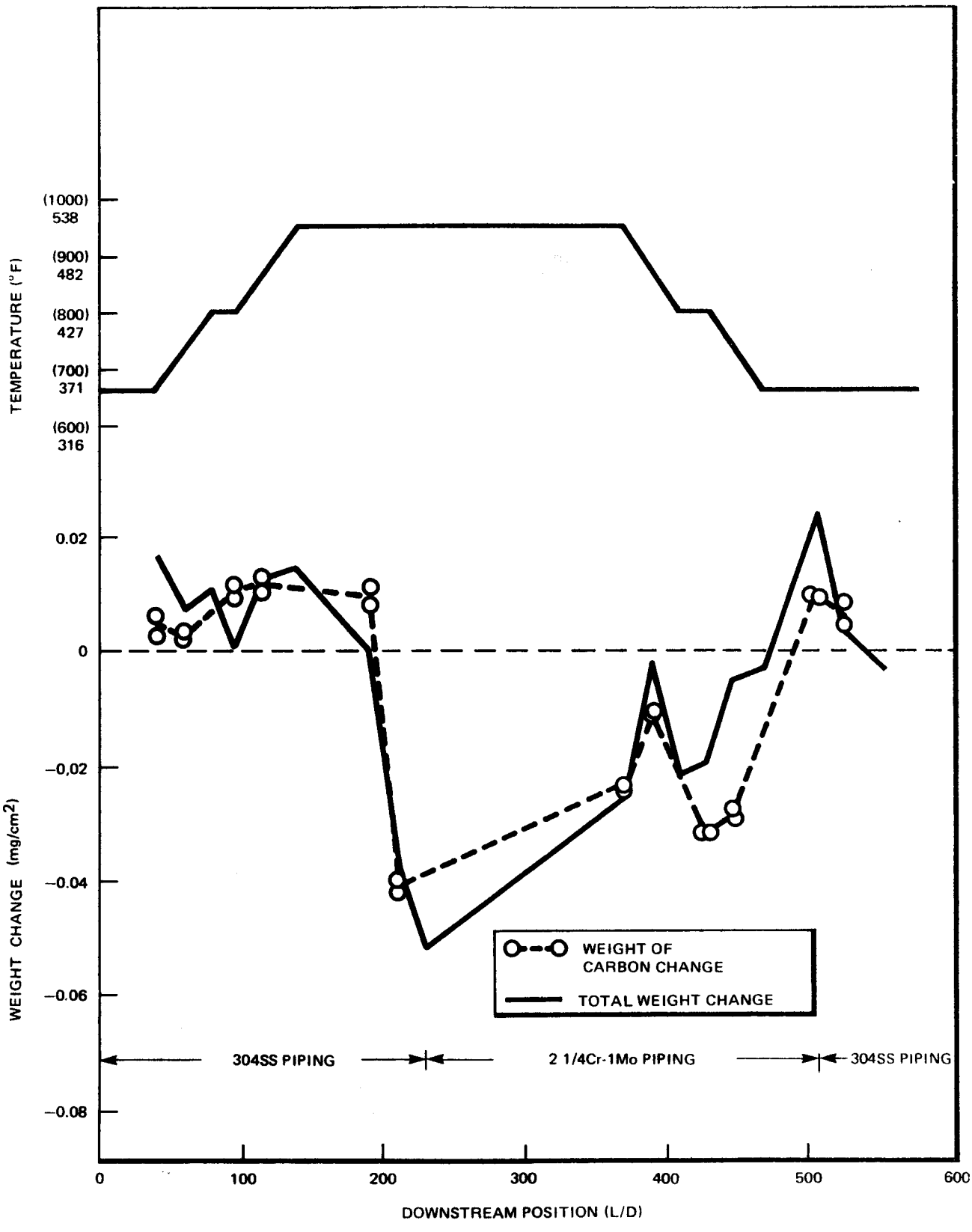

Figure 6.8. Comparison of Total Weight Change with Weight Change Due to Carbon Loss or Gain During Run B-1

7. NUCLEAR SYSTEM MATERIAL HANDBOOK (SUBTASK E)

J. F. Copeland

During the first quarter (July-September 1975) extensive review and reanalysis of 2¼Cr-1Mo stress rupture and time-to-start tertiary creep correlations for the NSMH (Nuclear Systems Materials Handbook) was achieved at ORNL and GE. A joint meeting was held to exchange viewpoints and to solidify a position. This work was continued during the second quarter, and these correlations appear to be nearing completion. The results of this important work were presented by ORNL and GE to pertinent groups of the ASME Boiler and Pressure Vessel Code for their consideration in reevaluating present Code methods of analysis. There are three basic differences between the NSMH analysis and the Code analysis:

a) NSMH uses time as the dependent variable, instead of stress, in regression,

b) the models used for analysis are slightly different, and

c) the statistical methods used in setting a lower limit for prediction (extrapolation to long times) are different

Although these differences in analysis may cause a slight discrepancy, in some cases, between NSMH and Code values, it is imperative to remember that the Code is involved with the development of design values, whereas the NSMH goal is to compile statistical evaluations of expected and predicted values.

During the first quarter, ORNL delivered 2¼Cr-1Mo total-life fatigue curves in a submittal to the Handbook. These curves take on special importance in view of their application to an evaluation of Departure from Nucleate Boiling (DNB) fatigue damage in LMFBR steam generator evaporators. It was concluded that the fatigue data set is relatively good. Several minor revisions, such as the

elimination of design curves, are currently ongoing at ORNL, and a resubmittal in the near future is expected.

A meeting of the NSMH Advisory Group was hosted at GE in October 1975. One result of this meeting was the reevaluation of NSMH submittal requirements and priorities. A current listing of Priority 1 property requirements[1] for the Working Group on Low Alloy Steels is given in Table 7.1. Completion dates will be set for these items by January 12, 1976, and these target dates will be submitted to HEDL. Note that three of these thirteen requirements were recently received at GE, from ORNL[2], and are currently undergoing review by the Working Group.

During the past quarter, the NSMH submittals on proportional limit and on true fracture stress were approved for issue in Volumes I and II of the NSMH.

Review of an outline for Volume III of the NSMH was performed, and comments were submitted to HEDL.

As mentioned, a sizeable submittal was received from ORNL in December 1975. The content of this submittal is listed in Table 7.2. Review by the Working Group is proceeding. Emphasis will also be placed on obtaining resubmittals from ORNL on the creep and fatigue properties listed in Table 7.1, during the next quarter.

REFERENCES

1) J. E. Irvin, Chairman NSM Handbook Advisory Group, "NSM Handbook Data Requirements", Letter/Package to NSM Handbook Working Group Chairmen, HEDC-MA-JEI-75-174, Nov. 26, 1975

2) P. Patriarca, "ORNL Submittal to NSM Handbook", Letter/Package to J. F. Copeland, Chairman, WG on Low Alloy Steels, CRB LTR No: 1218-202-75, Dec. 18, 1975

Table 7.1 LISTING OF PRIORITY 1 MATERIALS DATA REQUIREMENTS FOR WORKING GROUP ON LOW ALLOY STEELS (A.2)

(Reference 1)

Material	Property Code	Property Title
2 1/4 Cr-1Mo Steel	2108	Eng. Stress-Strain
2 1/4 Cr-1Mo Steel	2205	Time to Tertiary Creep
2 1/4 Cr-1Mo Steel	2206	Creep
2 1/4 Cr-1Mo Steel	2302	Impact Strength
2 1/4 Cr-1Mo Steel	2401	Strain-Controlled Fatigue
2 1/4 Cr-1Mo Steel	2411	Stress-Controlled Fatigue
2 1/4 Cr-1Mo Steel	2421*	Equiv. Bilinear YS vs. Max Strain
2 1/4 Cr-1Mo Steel	2422*	Parameters K and K_i
2 1/4 Cr-1Mo Steel	2423*	Parameters C and C_m
2 1/4 Cr-1Mo Steel	2424	Cyclic Stress-Strain Curves
2 1/4 Cr-1Mo Steel	2431	Fracture Mechanics Parameters (K_{Ic} & J_{Ic})
2 1/4 Cr-1Mo Steel	2432	Fracture Mechanics Parameters ($da/_{dN}$)
2 1/4 Cr-1Mo Steel	4103	Reactions with Aqueous Media

* Items submitted for review by ORNL on Dec. 18, 1975 (Reference 2).

Table 7.2 ORNL Submittal of Dec. 18, 1975 to NSM Handbook

(Reference 2)

Title	Property Code No.
Total Elongation - Tensile, Vols. I and II	2105
Total Elongation - Creep, Vol. II	2208
Reduction of Area - Creep, Vol. II	2208
Reduction of Area - Tensile, Vols. I and II	2106
Young's Modulus, Vol. I and II	2111
Shear Modulus, Vols. I and II	2112
Poisson's Ratio, Vol. I and II	2110
Toughness for Tensile Instability, Vols. I and II	2306
True Stress-Strain Curves/Equations, Vols. I and II	2107
σ/ε Curve Cyclic and Saturated, Vols I and II	
Equivalent Bilinear Yield Strength vs. Maximum Strain	2421*
Stress-Strain for Cyclically Hardened Material - Parameters K_0, K_1, K_2, K_3	2422*
Stress-Strain for Cylically Hardened Materials - Parameters C, E_m	2423*

* Priority 1 items per Reference 1.

8. PARTICULATE DEPOSITION (SUBTASK F)

P. Roy/R. Akbari-Kenari

8.1 OBJECTIVE

The objective of Subtask F is to study the effect of particulate deposition in a non-isothermal sodium loop on the performance of sodium heat exchangers. Previous investigations at W-ARD[1] have shown that particulate deposition can produce a significant reduction in the overall heat transfer coefficient of a heat exchanger. Subtask F is designed to simulate the deposition that will occur in full-scale LMFBR heat exchangers and anticipate resulting changes in the heat transfer efficiency of these heat exchangers.

8.2 EFFECT OF PARTICULATE DEPOSITION ON THE HEAT TRANSFER COEFFICIENT

Heat transfer tests are performed in loop 1R which is equipped with an instrumented heat exchanger and a hot leg containing weighable corrosion samples. The test heat exchanger is a helical, single pass, sodium-to-sodium heat exchanger with counter current flow. A schematic of loop 1R and the test heat exchanger appears in Reference 2.

The first heat transfer test performed in this loop accumulated 2600 test hours. The parameters of the test appear in Table 8.1. At the outset of the first test, the overall heat transfer coefficient of the heat exchanger was 53.35 watts/m^2 - °K. (9.4 Btu/hr-ft^2 - °F) after 580 hours the heat transfer coefficient had increased 8.7% to a value of 57.9 W/m^2 - °K (10.3 Btu/hr-ft^2 - °F). At that time a small sodium leak occurred in the loop, and the test was temporarily halted for repair. After repairs and start up, the test continued for an accumulated period of 2600 hours. At the end of this time the heat transfer coefficient had dropped to the original value of 53.4 W/m^2 - °K (9.4 Btu/$_{hr}$-ft^2 - °F). The first

heat transfer test was terminated at this point in order to instrument loop 1 for more accurate temperature and heat transfer coefficient measurements. Existing type K (chromel-alumel) thermocouples were augmented with newly installed, and higher output, type E (chromel-constentan) thermocouples. This increased the number of thermocouples monitoring the test heat exchanger temperatures from 4 to 12 (3 thermocouples per heat exchanger inlet/outlet). A digital voltmeter was also included with the loop instrumentation for faster and more accurate thermocouple readings.

The second heat transfer test was initiated in July, 1975. Table 8.1 includes the parameters for the second test. To date, 4000 hours have been accumulated and no change in the heat transfer coefficient of the heat exchanger has been detected. These results are considered reliable and do not confirm the results of the first test. Figure 8.1 shows a plot of the overall heat transfer coefficient during the second test. The heat transfer coefficient has remained constant at 60.4 W/m^2 - °K (10.7 $Btu/_{hr-ft^2}$ - °F) during the entire test. The second test, as the first, employs a cold trap temperature of 121°C(250°F). This corresponds to an oxygen concentration in the sodium of approximately 1 ppm. Vanadium wire equilibration tests have confirmed this oxygen concentration during loop operations. W-ARD experience indicates that at high oxygen concentrations the fouling effect due to particulate deposition is quite significant. Therefore, this test will be terminated shortly and the loop will be prepared for tests with higher cold trap temperatures and oxygen concentrations.

REFERENCES

1) W. E. Ray, R. L. Miller, S. L. Schrock, and G. A. Whitlow, Nucl. Tech., Vol. 16, pp. 249-262, October 1972

2) General Electric Report Titled, "Program for the Development of Design Data, LMFBR Steam Generator Materials", presented at the ORNL Review Meeting on July 16-17, 1975 at Oak Ridge, Tenn.

Table 8.1 First and Second Test Run Parameters

	First Test	Second Test
Duration	3000 hrs	4000 hrs
Flow Rate	0.22ℓ/sec (3.5 gpm)	0.22ℓ/sec (3.5 gpm)
Maximum Temperature	705°C(1300°F)	650°C(1200°F)
Minimum Temperature	~300°C(~700°F)	~300°C(~700°F)
Cold Trap Temperature	121°C(250°F)(<1 ppm O_2)	121°C(250°F)(<1 ppm O_2)

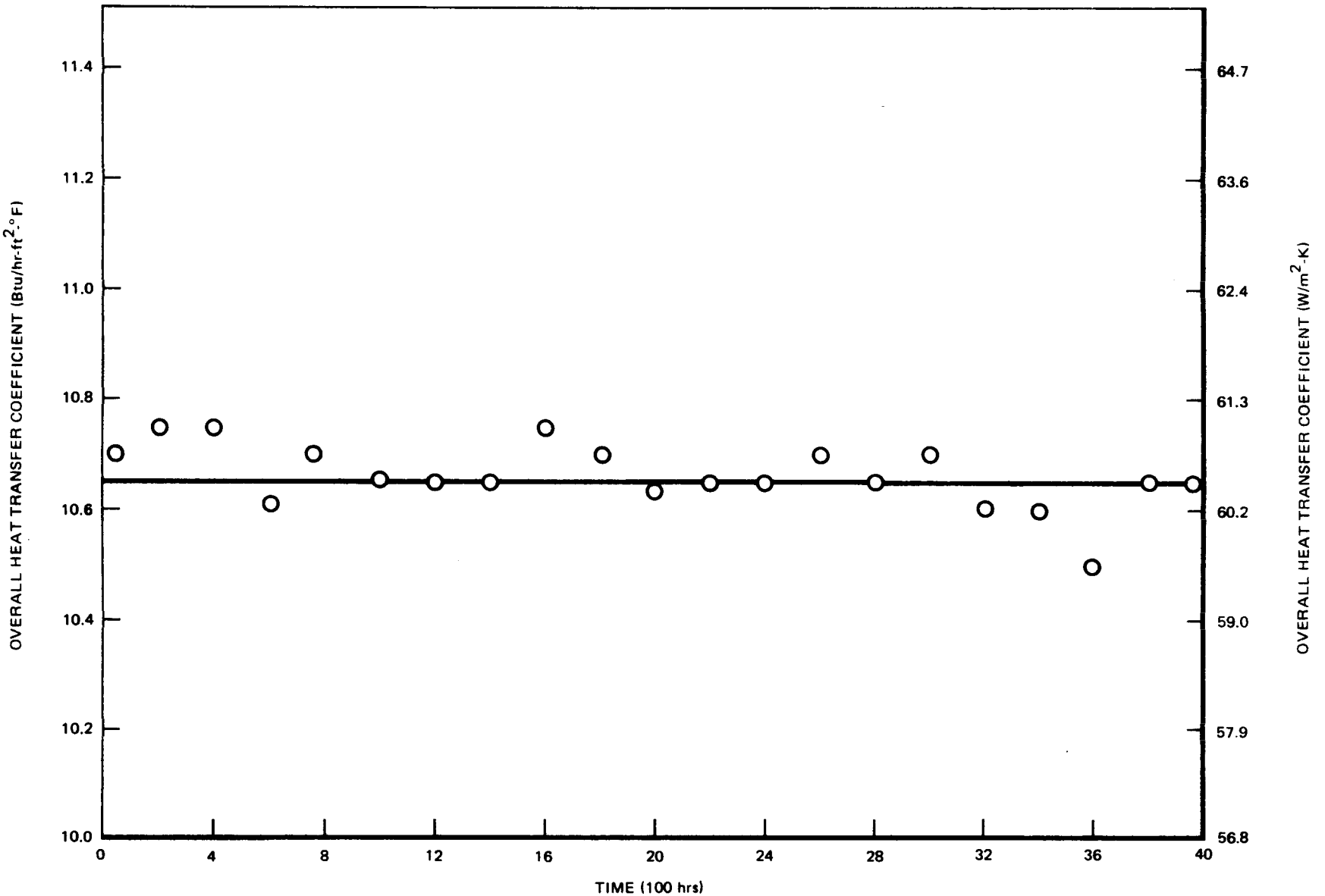

Figure 8.1. Effect of Particulate Deposition (Fouling) on the Performance of Loop 1R Heat Exchanger

9. FRACTURE TOUGHNESS OF LMFBR STEAM GENERATOR MATERIALS (SUBTASK G)

J. F. Copeland/G. R. Dodson

The objective of this program is to determine fracture toughness values (K_{Ic} at 24°C[75°F]) and higher temperatures, for potential LMFBR Steam Generator shell and tubesheet materials. These results will be combined with Charpy V-notch and drop-weight test values (RT_{NDT} determinations) and tensile test results to evaluate resistance to fracture. The essence of this approach to prevent fracture is set forth in the K_{IR} curve of Appendix G to Section III of the ASME Boiler and Pressure Vessel Code. No toughness data on 2¼Cr-1Mo steel was included in the derivation of the Code K_{IR} curve. Therefore, testing is required at hydrostatic test and at service temperatures to assure that the present K_{IR} curve approach is adequate for this material. In order to evaluate the fracture toughness of 2¼Cr-1Mo above the Nil Ductility Transition Temperature (NDTT), it is necessary to employ elastic-plastic fracture toughness testing methods, such as the J-Integral approach.

Thick section 2¼Cr-1Mo steel plates were procured for this program and heat treated to represent potential LMFBR material conditions. The emphasis is on air-melted material, although some testing was done on Vacuum Arc Remelted (VAR) steel, and these results are presented for comparison. The chemical compositions and heat treatments are given in Tables 9.1 and 9.2. Sulfide inclusion characterization is shown in Figure 9.1 and verifies a lack of directionality (longitudinal versus transverse) for the air-melted plates. Also, as shown in Figure 9.2, there is no significant influence of heat treatment on the microstructural phases present at the quarter thickness (¼ T) location of this 89 mm. (3.5 in.) thick plate.

Table 9.3 gives room temperature tensile test results which, as predicted by the microstructures, reveal no significant effect of heat treatment. One exception is that aging for 1000 hr. at 510°C(950°F) does decrease the room temperature yield strength. Charpy V-notch (CVN) impact test results are tabulated in Table 9.4, and the transition curves for the air-melted steel are given in Figures 9.3-9.6. The significant CVN criteria, along with drop-weight test NDTTs are summarized in Table 9.5. The RT_{NDT} values are limited in all cases by the drop-weight NDTTs which are approximately equivalent, at -1°C(30°F), for all five material conditions. Condition B (annealed and tempered air-melt) has the greatest Charpy upper shelf energy.

The CTS design used in the J-Integral fracture toughness tests is illustrated in Figure 9.7. After fatigue precracking, this specimen was loaded monotonically at 24°C(75°F) under constant stroke rate control until rapid, brittle, crack extension (pop-in) occurred or until appreciable deformation resulted in stable, ductile crack extension. The extent of crack extension was determined after the test by examination of the fracture surface, as shown in Figure 9.8. Load versus load-point displacement curves were recorded for each specimen and used to compute J-Integral values at the point of specimen unloading. The results of these tests are given in Table 9.6 and plotted in Figure 9.9 for the determination of J_{Ic} at the onset of real crack extension. K_{Ic} values were then computed from these values of J_{Ic} and are also given in Table 9.6.

The K_{Ic} results of Table 9.6 fall in essentially two groups: The air-melt results which are all at or above 206 MPa $\sqrt{m}$(187 Ksi$\sqrt{in.}$) and are approximately equal, and the VAR results which are at or above 121 MPa $\sqrt{m}$(110 Ksi $\sqrt{in.}$). Scanning Electron Microscopy (SEM) was performed on fracture surfaces to attempt explaining the following phenomena: (a) why the VAR K_{Ic} results were lower than the air-melt results, and (b) why brittle pop-in, as noted in Table 9.6, occurred in some specimens. For heat treatment B, specimens G7 and G6 (which did not and which did, respectively) have brittle pop-in were examined. The results are shown in Figures 9.10a and b. The pop-in region is characterized by quasi-cleavage, which differs from true cleavage in that: (a) some ductility is seen, as with microvoid coalescence, (b) river patterns tend to radiate from the center of the cleavage facets, and (c) fracture is not confined to strictly cleavage planes. Large sulfide inclusions were found in the ductile crack extension regions of both specimens. No reason for the difference in behavior of the two specimens was apparent, except that the test temperature was very close to the CVN 50% Fracture Appearance Transition Temperatures (Table 9.6), and statistical scatter in the fracture mode would be expected. Figures 9.10c and d illustrate similar behavior for a condition E specimen which had pop-in. Figure 9.10e shows a CVN fracture for condition D, a potential temper embrittlement treatment. Although the CVN values are lower for D than for B, no intergranular fracture (characteristic of temper embrittlement) is observed. These CVN values are being rechecked. Figure 9.10f, representing the VAR material, shows no stable crack extension on the microscopic scale, but illustrates the immediate initiation of cleavage fracture. CVN specimens will be run from this plate (broken CTS piece) to determine the transition temperatures.

The K_{Ic} results of this study are shown in comparison to the Code K_{IR} curve in Figure 9.11. The values all fall above the curve for this temperature, and indicate safe performance when Appendix G and the K_{IR} curve, design, loading and inspection approaches are followed. This must also be verified at the higher service temperatures. Also, further statistical confidence (especially heat-to-heat variation) is desired at the hydrotest temperature of approximately room temperature. Figure 9.12 illustrates the effect of fracture toughness and applied stress on the maximum crack size allowed to prevent fast fracture. For applied stresses above 138 MPa(20 Ksi), inspection for flaws becomes critical, especially for the lower fracture toughness.

Further specimens are currently being machined for elevated temperature J-Integral tests of air-melt material. SMAW weldments are also being prepared for weld metal and HAZ testing.

Table 9.1 Chemical Compositions of 2¼Cr-1Mo Steel Plates for Fracture Toughness Testing (wt. %)

Melting Process	Heat No.		C	Mn	P	S	Si	Cr	Ni	Mo	Al	As	Sb	Sn
AM	86693	Melt	0.11	0.45	0.009	0.028	0.20	2.01	--	1.04	--	--	--	--
		Check	0.11	0.41	0.014	0.026	0.19	2.00	0.12	1.00	<0.005	0.013	0.007	0.012
VAR	55262	Melt	0.09	0.52	0.016	0.014	0.08	2.22	--	0.01	--	--	--	--
		Check	0.10	0.50	0.013	0.016	0.07	2.26	0.15	1.00	<0.005	0.008	<0.002	0.004

Table 9.2 Heat Treatment of 2¼Cr-1Mo Steel Plates for Fracture Toughness Testing

A. Anneal (AM)

927°C (1700°F) for 3 hr., furnace cool at max. rate of 55.5°C (100°F) per hr. to room temperature

B. Anneal + Temper (AM)

927°C (1700°F) for 3 hr., furnace cool at max. rate of 55.5°C (100°F) per hr. to room temperature
+727°C (1340°F) for 4 hrs., air cool

C. Anneal + Temper (VAR)

927°C (1700°F) for 3 hr., furnace cool at max. rate of 55.5°C (100°F) per hr. to room temperature

+

727°C (1340°F) for 4 hr., air cool

D. Anneal + Temper + Embrittlement Treatment (AM)

927°C (1700°F) for 3 hr., furnace cool at max. rate of 55.5°C (100°F) per hr. to room temperature

+

727°C (1340°F) for 4 hr., air cool

+

510°C (950°F) for 1000 hr., air cool

E. Normalize + Temper (AM)

927°C (1700°F) for 3 hr., air cool

+

727°C (1340°F) for 4 hr., air cool

Table 9.3 Tensile Test Properties at 24°C(75°F) for 2¼Cr-1Mo Heat 86693. Air-Melt 89 mm. (3.5 in.) Thick Plate, Properties at ¼ T Location. Strain Rate = 0.04 $min.^{-1}$. Also, results for VAR Heat 55262.

Heat Treatment	Yield Point MPa (Ksi)	0.2% Y.S. MPa (Ksi)	U.T.S. MPa (Ksi)	%El (25.4 mm)	% R.A.
A (Anneal)	270 (39.2)	243 (35.2)	472 (68.5)	39.6	65.3
	262 (38.0)	243 (35.2)	466 (67.6)	38.2	66.1
B (Ann. + Temp.)	295 (42.8)	261 (37.9)	466 (67.6)	33.3	65.9
	297 (43.1)	267 (38.7)	467 (67.7)	34.6	65.1
C, VAR* (Ann. + Temp.)	--	275 (39.9)	439 (63.7)	36.1	51.6
D (Ann. + Temp. + 510°C, 1000 hr.)	234 (33.9)	221 (32.1)	459 (66.6)	34.8	64.4
	223 (32.4)	220 (31.9)	465 (67.4)	38.1	67.2
E (Norm. + Temp.)	298 (43.2)	285 (41.4)	462 (67.0)	38.4	68.7
	285 (41.4)	264 (38.3)	460 (66.7)	40.0	68.8

* Results by H. P. Offer (GE) on same VAR Heat No. (55262) - different plate, funded under 189a-SG029.

Table 9.4 Charpy V-Notch Impact Test Properties for 2¼Cr-1Mo Heat 86693. Air-Melt 89 mm.(3.5 in.) Thick Plate, Properties at ¼ T Location. Rolling Ratio of 1.0.

Heat Treatment A

(Anneal)

Spec. No.	Test Temp. °C (°F)	Fracture Energy J. (ft-lb)	Lateral Expan. mm. (mils)	Fracture Appearance, % Ductile
G3-1	-12 (10)	8 (6)	0.20 (8)	8
-2	-12 (10)	30 (22)	0.61 (24)	12
-3	24 (75)	73 (54)	1.40 (55)	42
-4	24 (75)	52 (38)	1.09 (43)	43
-7	24 (75)	64 (47)	1.24 (49)	35
-8	43 (110)	58 (43)	1.17 (46)	38
-9	43 (110)	95 (70)	1.70 (67)	54
-10	43 (110)	77 (57)	1.47 (58)	68
-5	66 (150)	87 (64)	1.60 (63)	85
-6	66 (150)	130 (96)	2.14 (84)	95
-11	66 (150)	109 (80)	1.73 (68)	83
-12	93 (200)	103 (76)	1.83 (72)	93
-13	93 (200)	127 (94)	2.06 (81)	99

Table 9.4 (continued)

Heat Treatment B

(Anneal + Temper)

Spec. No.	Test Temp. °C (°F)	Fracture Energy J. (ft-lb)	Lateral Expans. mm. (mils)	Fracture Appearance, % Ductile
G5-1	-12 (10)	39 (29)	0.69 (27)	13
-2	-12 (10)	76 (56)	1.22 (48)	20
-3	24 (75)	22 (163)	2.11 (83)	91
-4	24 (75)	107 (79)	1.75 (69)	53
-8	43 (110)	172 (127)	2.16 (85)	97
-9	43 (110)	153 (113)	2.31 (91)	97
-5	66 (150)	175 (129)	2.26 (89)	96
-6	66 (150)	195 (144)	2.34 (92)	99
-11	93 (200)	195 (144)	2.08 (82)	98

Table 9.4 (continued)

Heat Treatment D

(Anneal + Temper + 510°C, 1000 hr.)

Spec. No.	Test Temp °C (°F)	Fracture Energy J. (ft-lb)	Lateral Expan. mm. (mils)	Fracture Appearance, % Ductile
G12-13	-12 (10)	11 (8)	0.25 (10)	5
-14	-12 (10)	11 (8)	0.15 (6)	5
-1	24 (75)	61 (45)	1.17 (46)	30
-2	24 (75)	56 (41)	1.07 (42)	30
-8	24 (75)	46 (34)	0.89 (35)	30
-10	43 (110)	71 (52)	1.27 (50)	40
-11	43 (110)	75 (55)	1.40 (55)	40
-3	66 (150)	79 (58)	1.52 (60)	75
-4	66 (150)	87 (64)	1.52 (60)	70
-12	66 (150)	88 (65)	1.57 (62)	80
-5	93 (200)	107 (79)	1.78 (70)	99
-6	93 (200)	98 (72)	1.63 (64)	99
-7	93 (200)	107 (79)	1.73 (68)	95

Table 9.4 (continued)

Heat Treatment E

(Normalize + Temper)

Spec. No.	Test Temp °C (°F)	Fracture Energy J. (ft-lb)	Lateral Expans. mm. (mils)	Fracture Appearance, % Ductile
G13-1	-12 (10)	11 (8)	0.23 (9)	10
-2	-12 (10)	14 (10)	0.36 (14)	11
-3	24 (75)	131 (97)	1.96 (77)	98
-4	24 (75)	69 (51)	1.22 (48)	32
-7	24 (75)	77 (57)	1.40 (55)	37
-8	43 (110)	88 (65)	1.55 (61)	53
-9	43 (110)	117 (86)	1.91 (75)	82
-5	66 (150)	121 (89)	1.78 (70)	90
-6	66 (150)	127 (94)	1.93 (76)	89
-10	66 (150)	126 (93)	1.98 (78)	99
-11	93 (200)	123 (91)	2.01 (79)	99
-12	93 (200)	130 (96)	1.98 (78)	99

Table 9.5 Charpy V-Notch Toughness Criteria and P-3 Drop-Weight Nil Ductility Transition (NDT) Results for 2¼Cr-1Mo Heat 86693. Air-Melt (3.5 in.) Thick Plate, Properties at ¼ T Location. Rolling Ratio of 1.0. Also, Transverse Results for VAR Heat 55262.

Heat Treatment	68 J. (50 ft-lb) Transition Temp °C	(°F)	0.89 mm, (35 mils) Lateral Expans. Transition Temp. °C	(°F)	50% Fract. Appear. Transition Temp. °C	(°F)	NDT °C (°F)	Reference NDT (RT, NDT)*	Upper Shelf CVN Fracture Energy (93°C (200°F)) J.	(ft-lb)
A	29	(84)	11	(52)	32	(90)	(30)	(30)	118	(87)
B	-10	(14)	-13	(8)	22	(72)	(30)	(30)	203	(150)
C (VAR)**	2	(35)	-4	(25)	29	(85)	(20)	(20)	125	(92)
D	36	(96)	14	(58)	46	(114)	(20)	(20)	102	(75)
E	13	(56)	7	(45)	19	(66)	(30)	(30)	129	(95)

* Determined according to ASME B&PV Code, Section III, NB-2300.

** Results by H. P. Offer (GE) on same VAR Heat No. (55262) - different plate. Funded under 189a-SG029.

Table 9.6 Compact Tension Specimen (50.8 mm. (2 in.) Thick) Fracture Toughness Results for 2¼Cr-1Mo Heat 86693. Air-Melt 89 mm. (3.5 in.) Thick Plate with Rolling Ratio of 1.0. Also, Transverse Results for VAR Heat 55262, 50.8 mm. (2 in.) Thick Plate. Specimen Load Point Displacement Rate of 1.52 mm/min. (0.06 in./min.). All tests at 24°C (75°F).

Spec. No.	Heat Treatment	Stable Crack Extension, Δa, at Unload. mm.	(in.)	Remarks	J at Unload J./mm^2	(in-lb/in.^{2})	J at COS*, J_{Ic} J./mm^2	(in-lb/in.^{2})	K_{Ic} MPa $\sqrt{m}$.	(Ksi $\sqrt{in}$.)
G1		0.25	(0.0099)	COS* only.	18.4	(1050)				
G2	A	3.00	(0.1180)	Stable Δa.	22.6	(1290)	18.4	(1050)	206	(187)
G3		0.76	(0.030)	Δa, Pop-in.	24.9	(1425)				
G6		0.70	(0.0276)	Δa, Pop-in.	20.3	(1160)				
G7	B	3.00	(0.1180)	Stable Δa.	44.5	(2540)	20.3	(1160)	216	(196)
G8		2.90	(0.1140)	Stable Δa.	60.2	(3440)				
GV1		———		Pop-in.	9.3	(530)	9.3	(530)	145	(132)
GV2	C (VAR)	———		Pop-in.	11.7	(670)	11.7	(670)	164	(149)
GV3		———		Pop-in.	6.5	(370)	6.5	(370)	121	(110)
G10		0.30	(0.0118)	Δa, Pop-in.	23.1	(1320)				
G11	D	0.90	(0.0355)	Δa, Pop-in.	38.8	(2220)	24.5	(1400)	236	(215)
G12		2.00	(0.0790)	Stable Δa.	42.8	(2450)				
G14		0.30	(0.0118)	Δa, Pop-in.	22.6	(1290)				
G15	E	1.00	(0.0394)	Stable Δa.	37.6	(2150)	22.9	(1310)	229	(208)
G16		3.50	(0.1380)	Stable Δa.	54.9	(3140)				

* Crack Opening Stretch - No Real Crack Extension

100X

A. VIEW FROM PLATE EDGE

100X

B. VIEW FROM PLATE EDGE AT 90° TO A

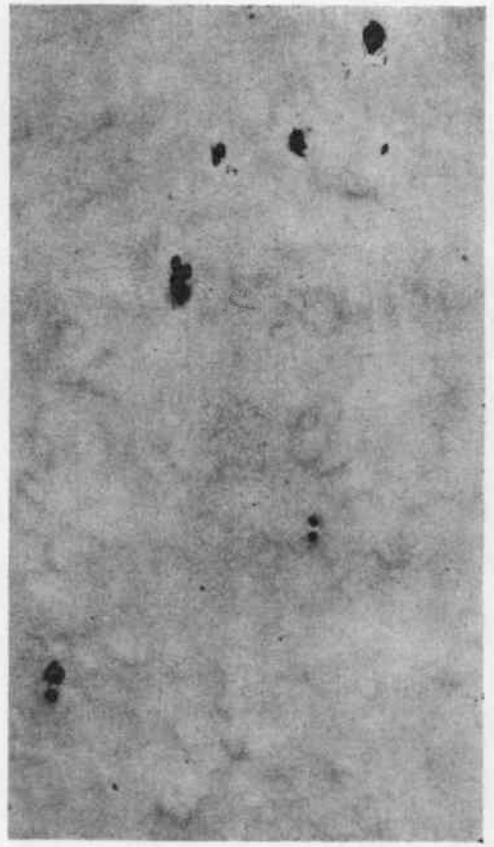

100X

C. VIEW FROM PLATE ROLLED SURFACE

Figure 9.1. Sulfide Inclusion Size and Shape as Related to Plate Orientation, Illustrating Lack of Longitudinal-transverse Directionality Resulting from a Cross-rolling Ratio of 1.0. Heat 86693, 89 mm (3.5 in.) Thick Air Melt Plate at 1/4 T Location. As-polished Specimens

500X

A. HEAT TREATMENT A.

500X

B. HEAT TREATMENT B.

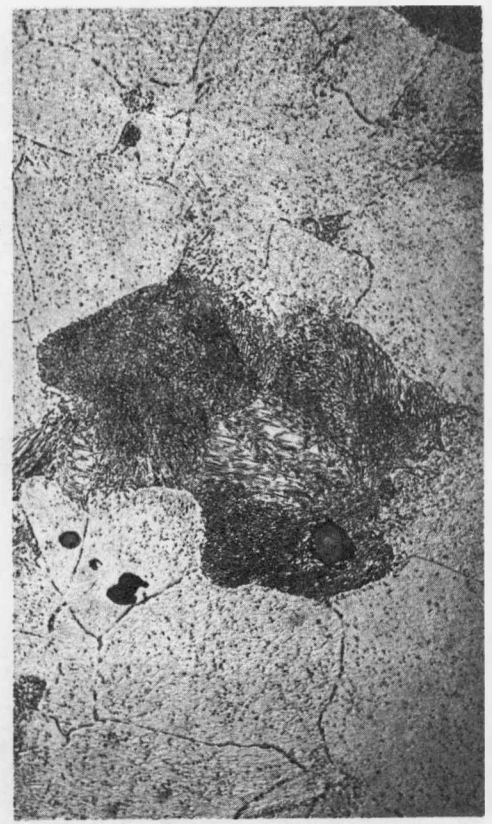

500X

C. HEAT TREATMENT E.

Figure 9.2. Microstructure as Related to Heat Treatment for Heat 86693, 89 mm (3.5 in.) Thick Air Melt Plate at 1/4 T Location. Nital-picral Etch

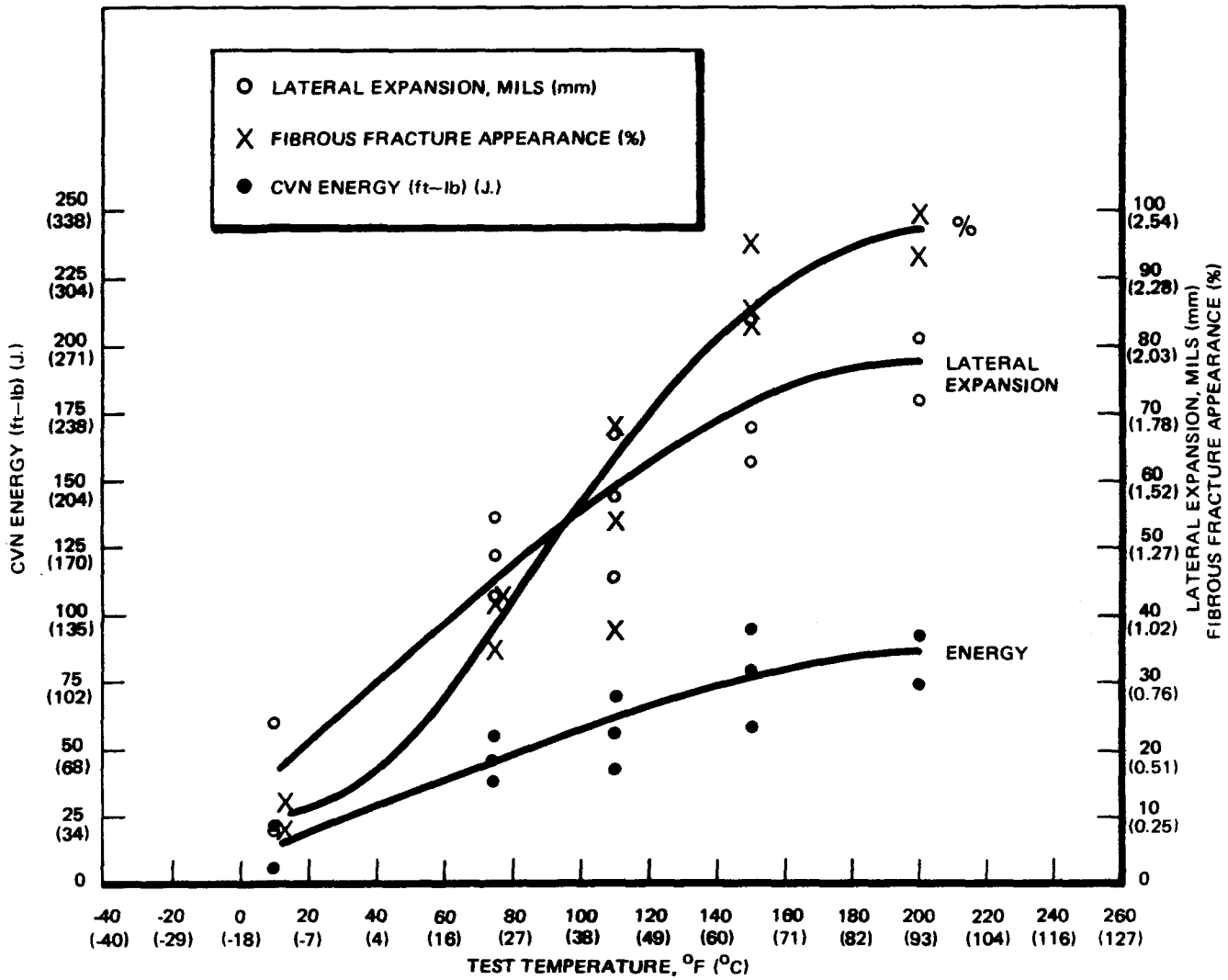

Figure 9.3. Charpy V-Notch Transition Curves for 2¼ Cr-1 Mo Heat 86693, Air Melt 89mm (3.5 in.) Thick Plate, Properties at Quarter Thickness, Rolling Ratio = 1.0, Heat Treatment A.

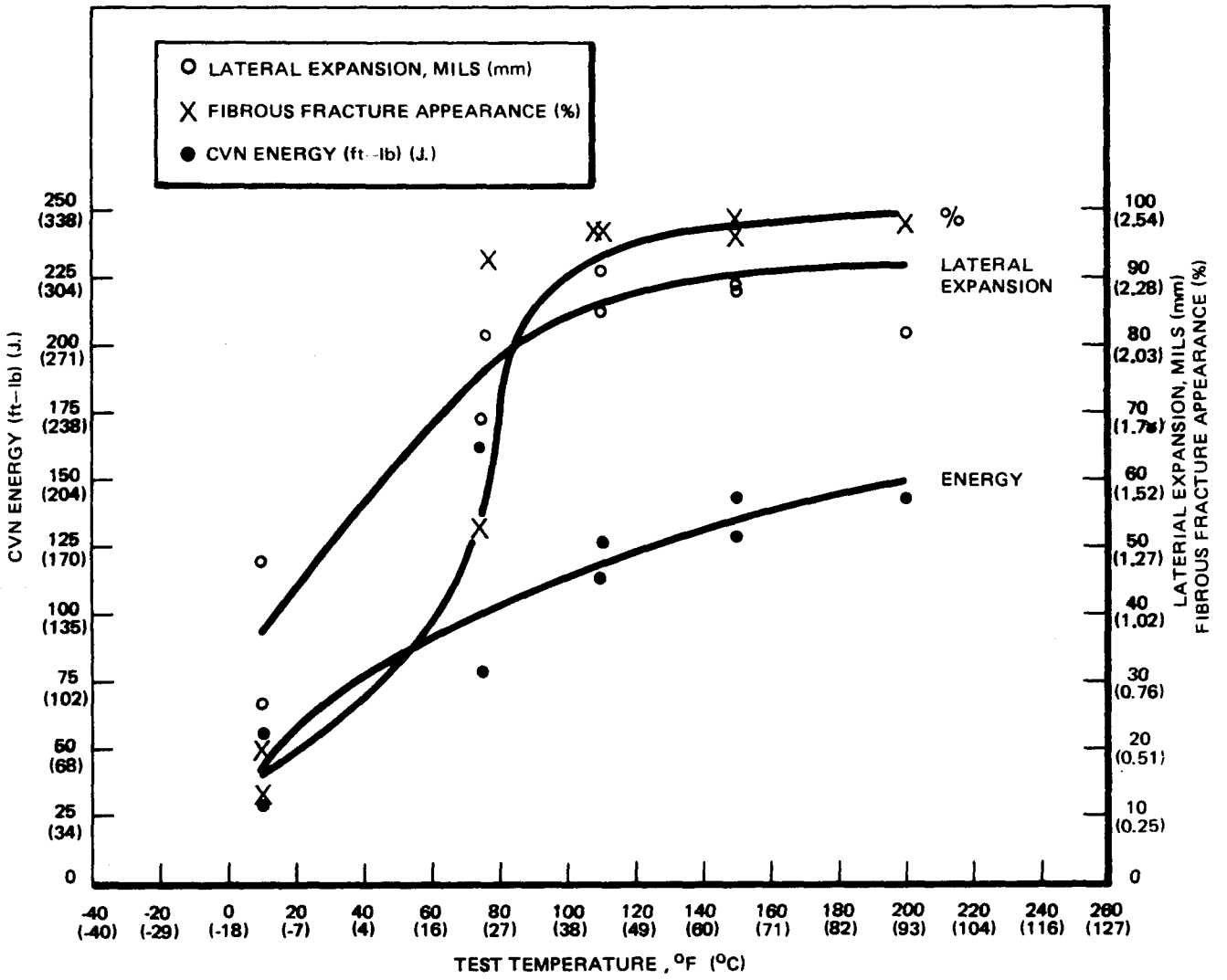

Figure 9.4. Charpy V-Notch Transition Curves for 2¼ Cr-1 Mo Heat 86693, Air Melt, (89 mm) 3.5 in. Thick Plate, Properties at Quarter Thickness, Rolling Ratio = 1.0, Heat Treatment B.

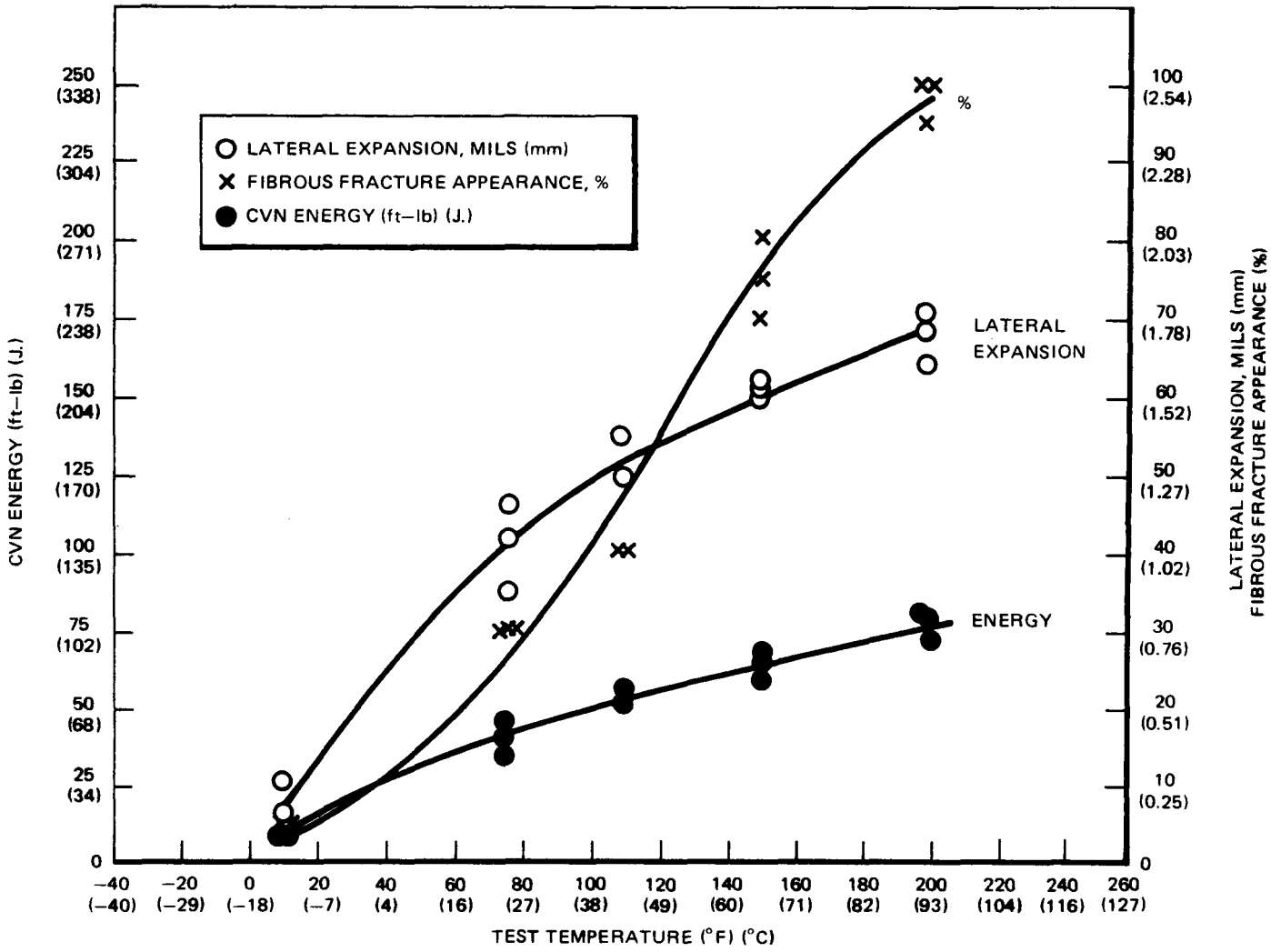

Figure 9.5. Charpy V-Notch Transition Curves for 2 1/4 Cr-1 Mo Heat 86693, Air Melt, 89 mm (3.5 in.) Thick Plate, Properties at Quarter Thickness, Rolling Ratio = 1.0, Heat Treatment D

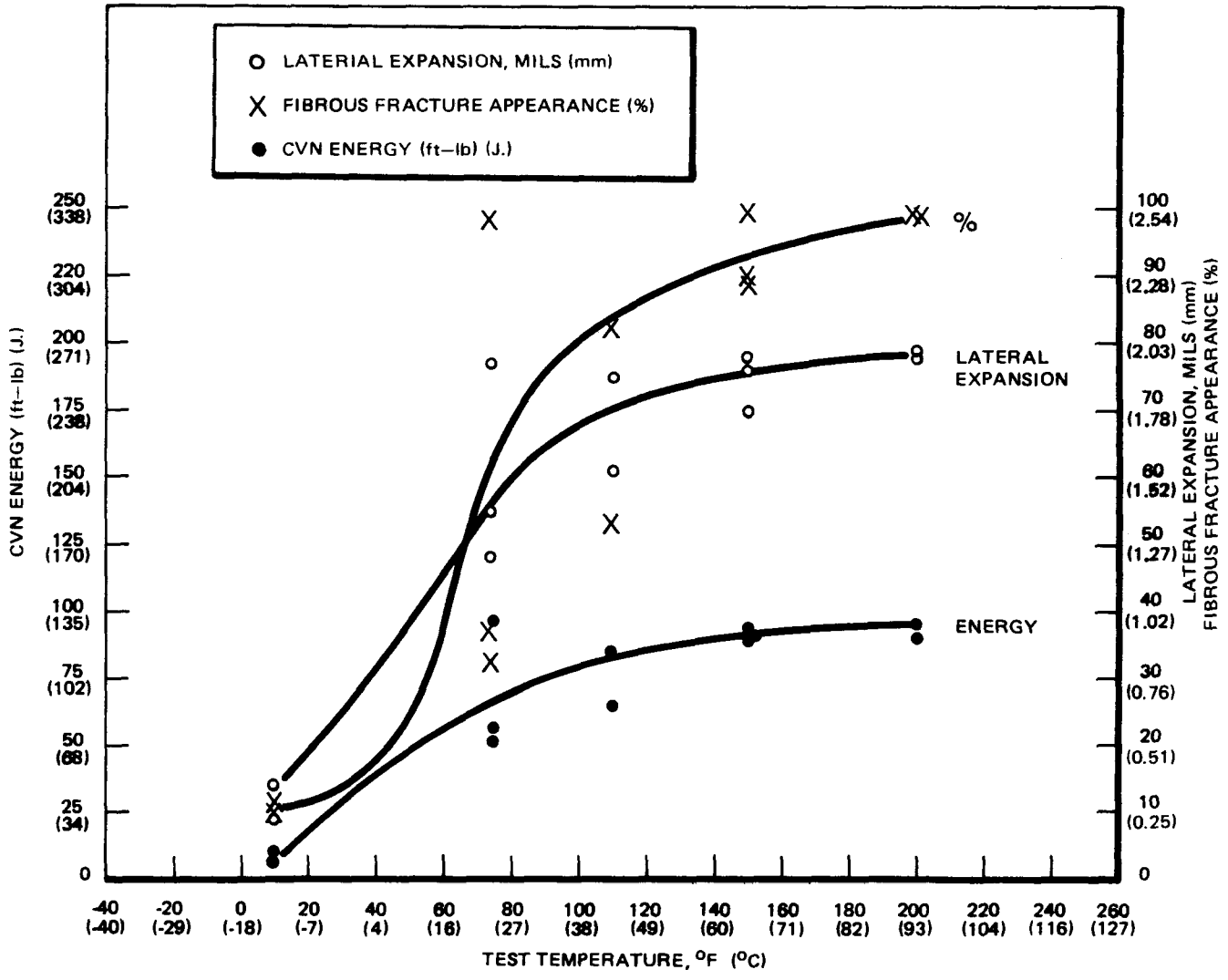

Figure 9.6. Charpy V-Notch Transition Curves for 2¼ Cr-1 Mo Heat 86693, Air Melt, 3.5 in. (89 mm.) Thick Plate, Properties at Quarter Thickness, Rolling Ratio = 1.0, Heat Treatment E

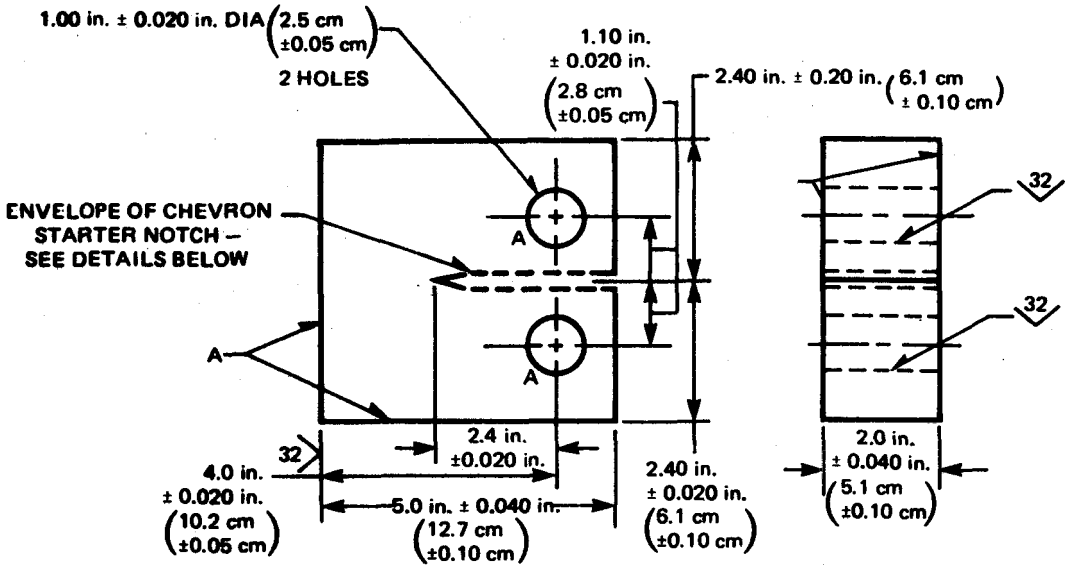

NOTE 1 – A SURFACES SHALL BE PERPENDICULAR AND PARALLEL WITHIN 0.001 in. (0.0025 cm) TIR

NOTE 2 – CRACK STARTER PERPENDICULAR TO SPECIMEN LENGTH AND THICKNESS TO WITHIN ± 2 DEG

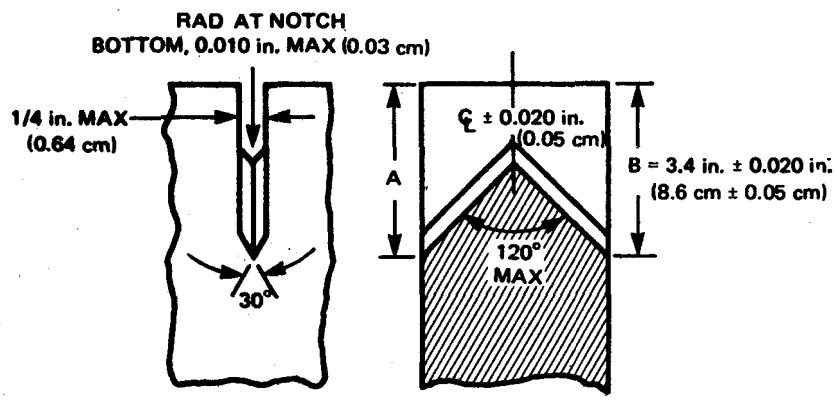

CHEVRON NOTCH CRACK STARTER DETAILS

NOTE 1 – A = B TO WITHIN 0.040 in. (0.10 cm)

Figure 9.7. 50.8 mm (2 in.) Thick Compact Tension Specimen for Fracture Toughness. Drawing Dimensions in Inches (mm).

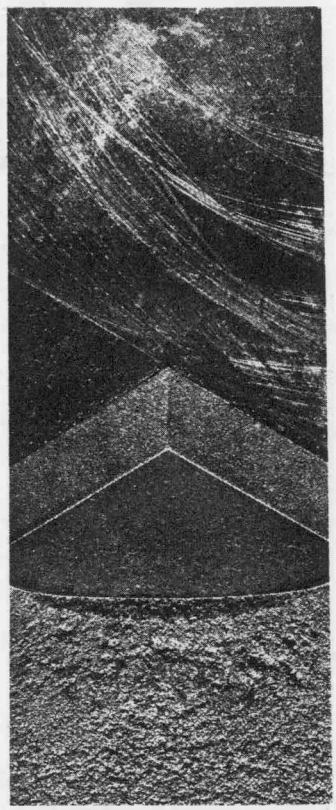

Figure 9.8. Typical 50.8 mm (2 in.) Thick Compact Tension Specimen Fracture Surface After J_{Ic} Test, Heat Treatment A, 24°C (75°F). Shows (From Top) Machined Chevron Notch, Fatigue Precrack, Crack Extension During Test (Dark Cresent), and Brittle Separation Fracture (−196°C [−320°F] for Convenience).

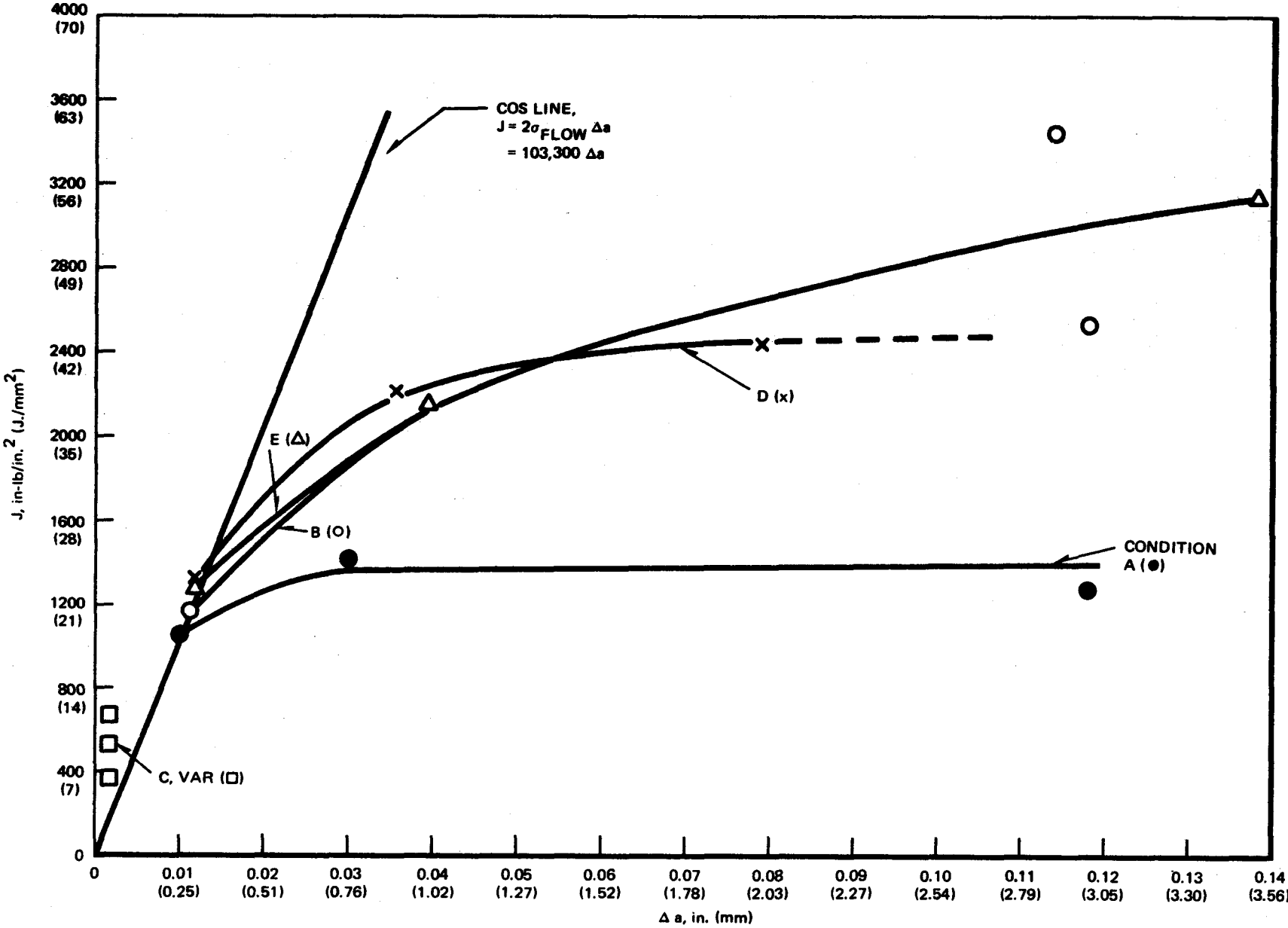

Figure 9.9. J-Integral Resistance Curves for 2 1/4 Cr-1 Mo Material Conditions at 24°C (75°F) Showing J-Integral Values (J) Versus Crack Extension (Δa) at Specimen Unloading.

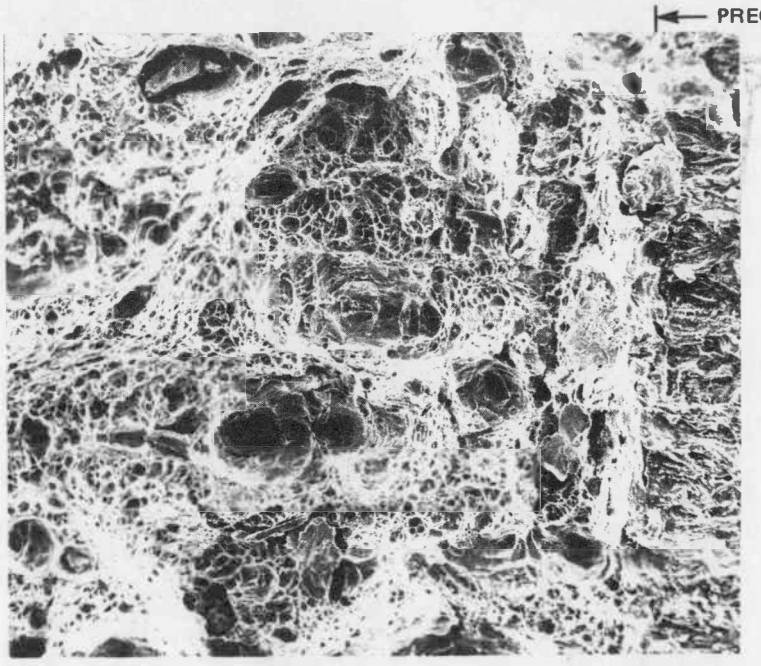

100X

A. SPECIMEN G7 (TREATMENT B), CTS, SHOWING FATIGUE PRECRACK (RIGHT) AND DUCTILE, STABLE CRACK EXTENSION ZONE

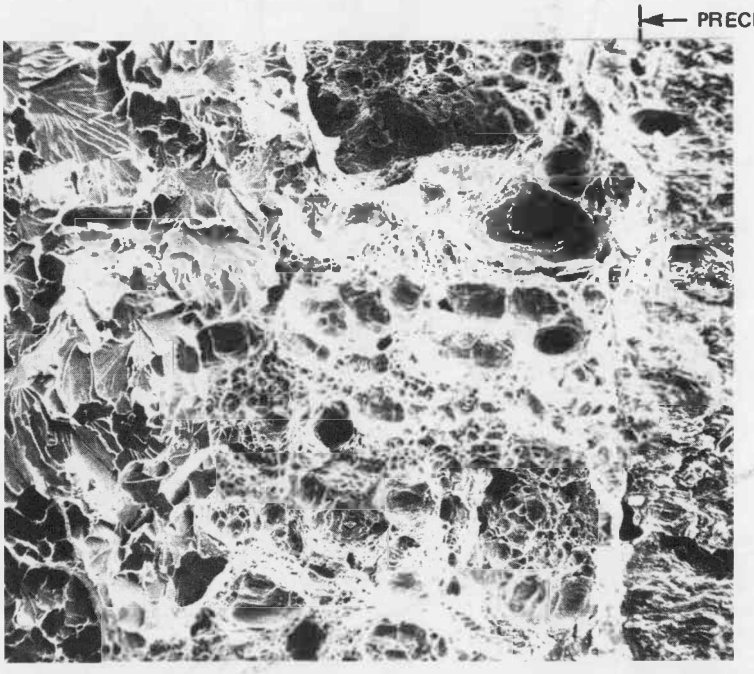

100X

B. SPECIMEN G6 (TREATMENT B), CTS, SHOWING PRECRACK (RIGHT), DUCTILE, STABLE CRACK EXTENSION AND QUASI-CLEAVAGE (LEFT) WHICH CHARACTERIZES BRITTLE POP-IN.

Figure 9.10. Scanning Electron Micrographs Characterizing Specimens for Various Material Conditions Which Did and Did Not Experience Brittle Pop-in

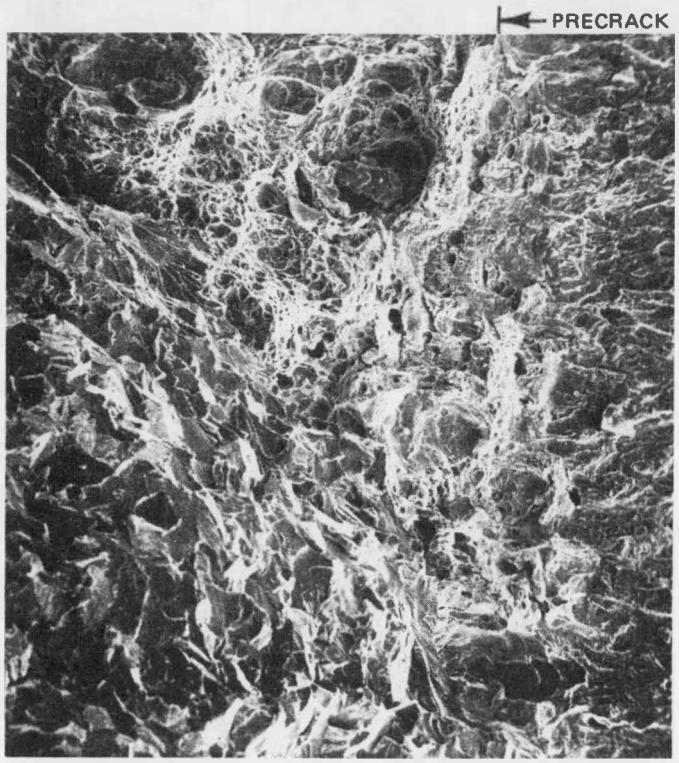

100X

C. SPECIMEN G14 (TREATMENT E), CTS, SHOWING FATIGUE PRECRACK (RIGHT), SMALL REGION OF DUCTILE, STABLE CRACK EXTENSION (TOP, LEFT), AND QUASI-CLEAVAGE (BOTTOM, LEFT) CHARACTERIZING POP-IN.

300X

D. SPECIMEN G14 (TREATMENT E), CTS, SHOWING FATIGUE PRECRACK (RIGHT) AND QUASI-CLEAVAGE (LEFT) CHARACTERIZING BRITTLE POP-IN. DIFFERENCE IN ELEVATION BETWEEN PRECRACK AND QUASI-CLEAVAGE ZONES INDICATES CRACK OPENING STRETCH PRIOR TO CRACK GROWTH.

Figure 9.10. Scanning Electron Micrographs Characterizing Specimens for Various Material Conditions Which Did and Did Not Experience Brittle Pop-in. (Continued)

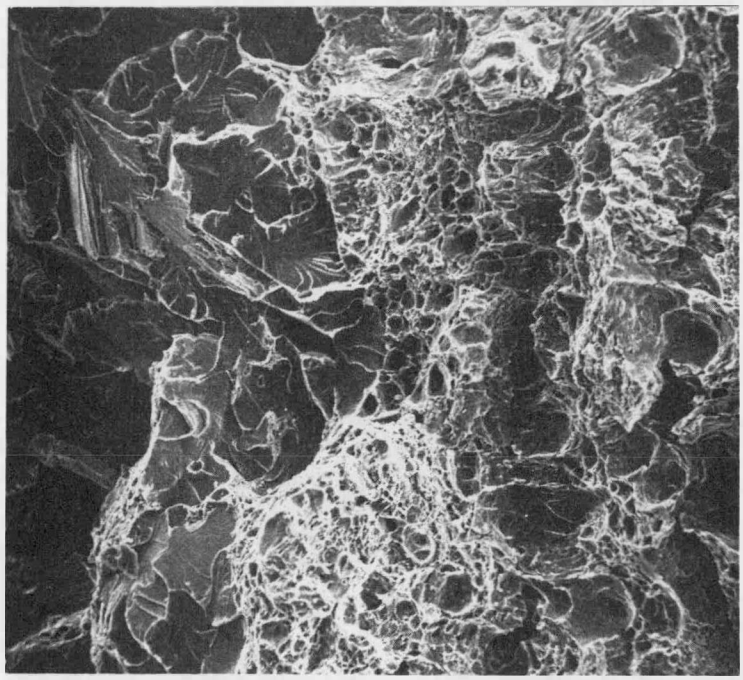

250X

E. CHARPY SPECIMEN (TREATMENT D) FRACTURED AT 43°C (110°F), SHOWING DUCTILE ZONE (MICROVOID COALESCENCE) AT EDGE OF SPECIMEN (RIGHT) AND QUASI-CLEAVAGE (LEFT)

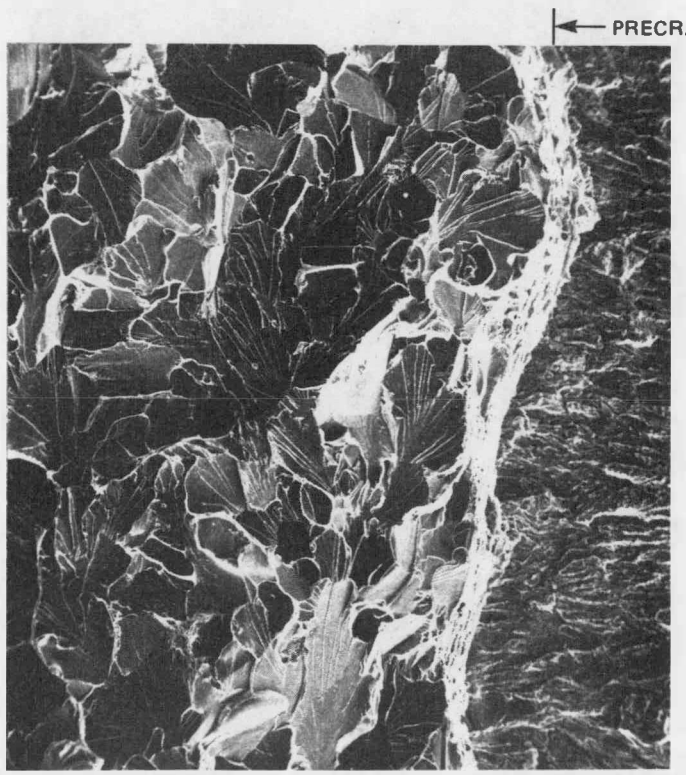

100x

F. SPECIMEN GV1 (TREATMENT C), CTS, SHOWING FATIGUE PRECRACK (RIGHT) AND CLEAVAGE ZONE (LEFT) CHARACTERISTIC OF BRITTLE POP-IN

Figure 9.10. Scanning Electron Micrographs Characterizing Specimens for Various Material Conditions Which Did and Did Not Experience Brittle Pop-in (Continued)

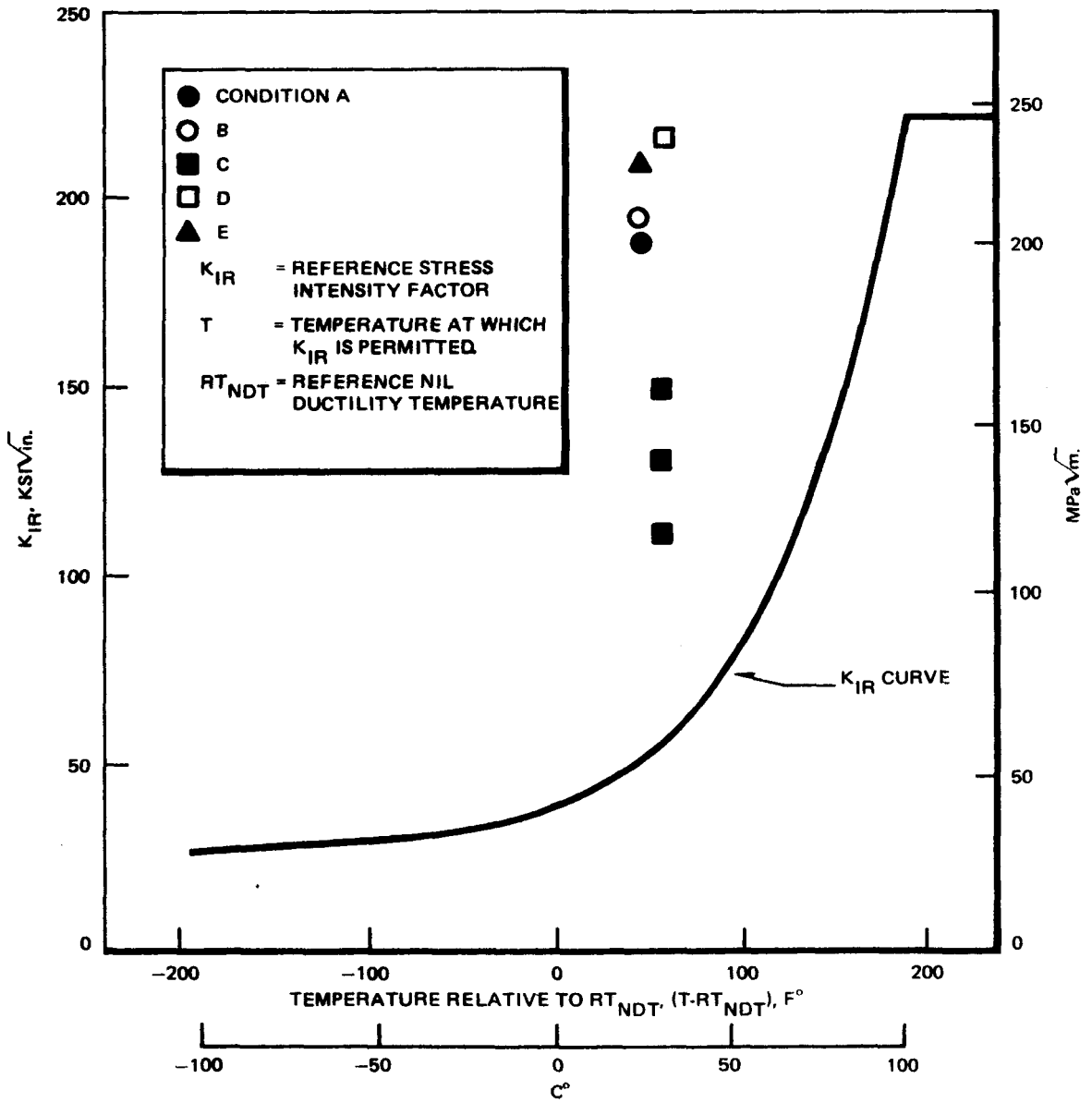

Figure 9.11. Comparison of Fracture Toughness Data with ASME Code Section III K_{IR} Curve.

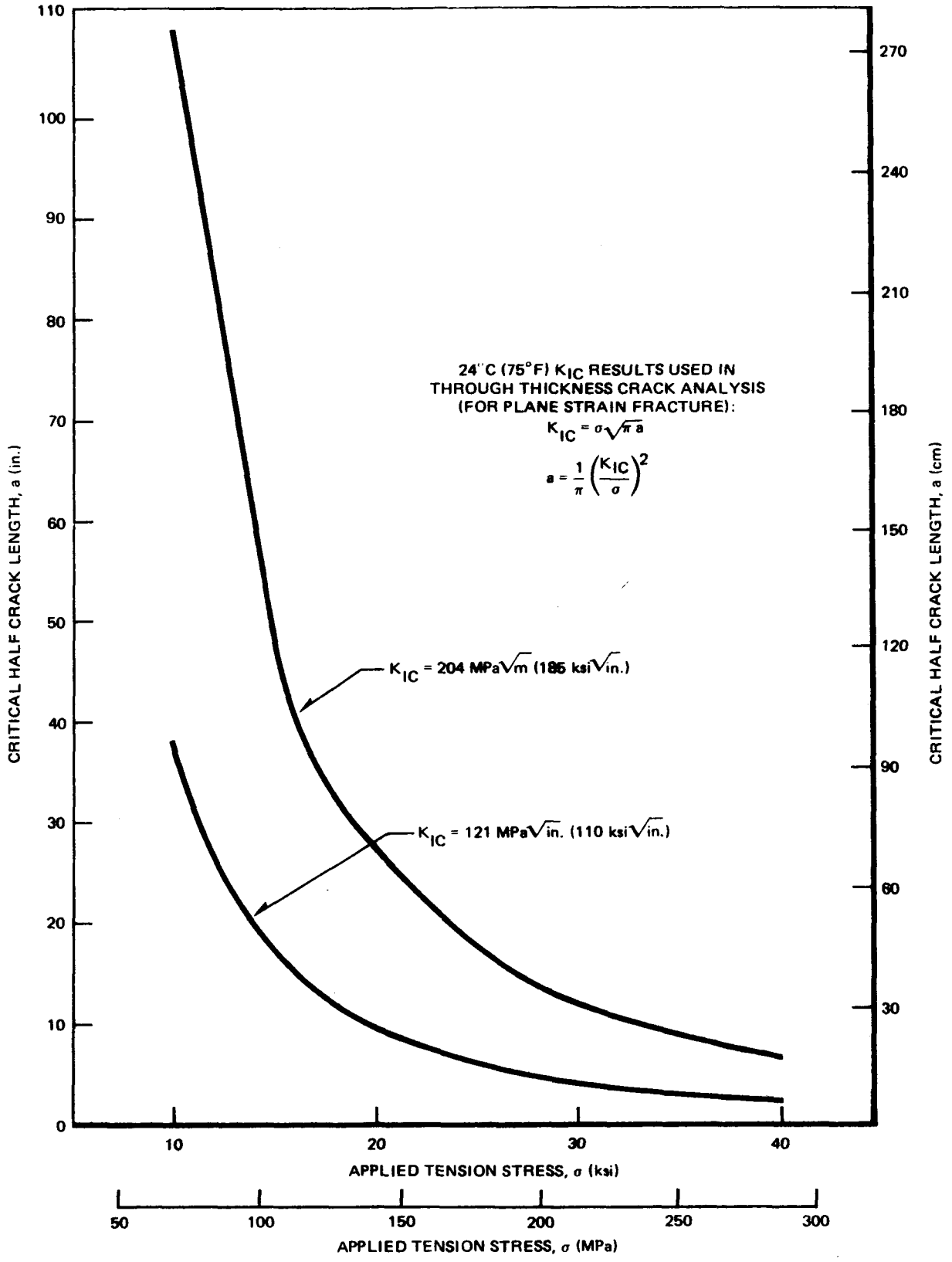

Figure 9.12. Half Critical Flaw Length (for Through Thickness Crack in Tension) as Related to 24°C (75°F) Fracture Toughness and Applied Stress.

CONTRACT NO. AT(04-3) 893-10 TASK G

189-SG029 FY 76

STEAM GENERATOR MATERIALS QUALIFICATION

FY 76 HIGHLIGHTS

- Negotiations have led to the placement of a purchase order with Pacific Tube Company (Patco) for the CRBRP prototype and plant steam generator tubing
- Tensile test results indicate that post weld heat treatments considered for CRBRP steam generator tubing produce a stable short term microstructure, as shown by almost constant tensile strength values between one and twenty hours of PWHT at 727°C (1340°F)
- Above 454°C (850°F) the yield strength for VAR and ESR material generally fell below the ASME Code Case 1592 expected minimum value
- Charpy v-notch tests indicate that the full anneal plus post weld heat treatment provides the best resistance to brittle fracture. The ESR material was found to be superior to the VAR material in this respect
- The remelted steel creep-rupture data, for the few heat treatments and two remelted techniques considered, falls within the tolerance limits of the NSMH and above the minimum values established by the ASME Code
- Fracture toughness testing of compact tension specimens indicates safe behavior with respect to fracture for components of VAR material designed in accordance with the K_{IR} curve of Appendix G to Section III of the ASME Code
- Friction and wear testing in sodium of a tube-to-tube support model has been initiated
- Results of Phase I of the friction and wear model tests indicate some wear of 2 1/4 Cr - 1 Mo but testing is incomplete

- A position paper describing the nondestructive examination needs of the Clinch River Breeder Reactor IHTS and steam generators has been completed, and reviewed by CRBR project personnel
- An ultrasonic examination specification for CRBRP steam generator tubing has been issued and included in the ordering data
- Weld porosity standards have been set for examination of tube-to-tubesheet welds using a rod anode x-ray machine
- Neuces Bay testing of feedwater chemistry has shown feasibility of 0.1 ppb maximum Na ion concentration in polisher effluent. A report summarizing this result will be issued in January 1976 (NEDG-14086)
- Design of a test section for the Bull Run evaporator corrosion study has been completed
- A hot-wire GTA weld system has been purchased, installed and made operational
- Low dilution, defect free welds have been made between Type 316 SS and Incoloy 800

CONTRACT NO. AT(04-3) 893-10 TASK G

189-SG029 FY 76

STEAM GENERATOR MATERIALS QUALIFICATION

I. INTRODUCTION

The Steam Generator Materials Qualification Task was initiated July 1974 in support of the development of materials and processes used in Clinch River Breeder Reactor (CRBR) steam generators. The objective of this Task is to (1) develop and qualify material specifications, (2) develop fabrication procedures and processes, (3) purchase tubing and tubesheet material for development programs, (4) application and development of nondestructive examination techniques for the Intermediate Heat Transport System (IHTS) of the CRBRP, (5) guide and coordinate the design of the steam generators in the area of water chemistry, (6) provide technical management to wear and friction testing of IHTS material, and (7) develop the design and fabrication procedures for the austenitic stainless to ferritic steel transition joints of the CRBR.

The topics discussed are:

II LMFBR Steam Generator Tubing
III LMFBR Steam Generator Tubesheet Forgings (Characterization of VAR/ESR Melted 2 1/4 Cr - 1 Mo)
IV Friction, Wear and Self-Welding
V Nondestructive Examination Development
VI Water Chemistry Studies
VII Transition Joint Development

The description of each subject includes a statement of its objective and the results to date. The program is keyed to the design and fabrication schedule of the CRBR and associated development programs.

II. LMFBR STEAM GENERATOR TUBING

The objective of this activity is to provide the technical support necessary for the procurement of prototype and plant tubing for the CRBRP steam generators.

Concentrated technical negotiations have been carried out with five tubing mills (three domestic and 2 foreign) that have shown interest in this program. These negotiations have led to the placement of a purchase order with Pacific Tube Company (Patco) for the CRBRP prototype and plant steam generator tubing.

During preprocurement activities for steam tubing for the SG's, it became apparent that tubing meeting the requirements of the RDT Standard would be very expensive. Discussions with various vendors were undertaken to see whether substantial economies would result from modifications of the Standard.

It was determined that substantial savings and an increased number of bids would result with small changes in the Standard. Final proposed changes that GE believes are acceptable were made as a result of the recommended tubing vendor's bid. The changes are summarized below.

1. Increase maximum carbon on the product analysis from 0.11 to 0.12%; increase silicon range on the product analysis from "0.20 to 0.40%" to "0.10 to 0.50%". This change was required by Patco's tube hollow supplier (B & W) to reflect the fact that the electro-slag remelt process results in a wider silicon range.
2. Permit the removal of local surface defects that the recommended tubing vendor stated will be found by liquid penetrant examination. GE has the choice of accepting the defects and relax the requirements of an "indication free surface", or to permit defect removal. GE recommends the latter because the defects could be cracks; there is sufficient excess material to permit removal of most defects.
3. Permit use of the red dye liquid penetrant method to reflect the recommended vendor's present capability, which GE believes will result in technically acceptable tubing.

4. Permit more latitude in selecting a packaging procedure to reflect the experience of the tubing vendor and the steam generator manufacturers.

5. Change the metallurgical cleanliness requirement from the finished tube to the tube hollow to reflect the fact that the tubing vendor has no control over this requirement.

An alternate heat treatment was also selected primarily due to furnace limitations at Pacific Tube Company. The Patco furnace can only provide a maximum isothermal heat treatment of 90 minutes assuming the tubing enters the last two zones of the three zone furnace at 704°C (1300°F). To add assurance that the tubing will be heat treated as specified, the austenitizing temperature will be decreased from 927 to 916°C (1700 to 1680°F) and furnace adjustments will be made to minimize the time required to decrease temperature from 916 to 704°C (1680 to 1300°F). The alternate heat treatment shown below will be qualified using traveling thermocouples inside representative steam generator tubing.

1. Anneal at 916°C ± 14°C (1680°F ± 25°F) [Zone 1 of furnace] for 15 to 30 minutes maximum.

2. Cool directly to 704°C ± 14°C (1300°F ± 25°F) [Zones 2 & 3 of furnace] for approximately 90 minutes.

3. Follow final anneal with a furnace treatment of 727°C ± 14°C (1340°F ± 25°F) for one hour.

4. The furnace atmosphere shall be commercial grade DX gas.

GE-FBRD data on isothermal transformation (Figure 7 of last semiannual report) show that for three heats of ESR and VAR 2 1/4 Cr - 1 Mo alloy steel investigated, 90 minutes is sufficient to reduce hardness to minimum values. This adds confidence that the maximum practical ferrite transformation can be attained in 90 minutes.

DEVELOPMENT TUBING FOR LMFBR STEAM GENERATORS

The objective of this activity is to quickly provide steam generator tubing as close to RDT M3-33 as possible. This tubing is required for specific development programs including tube-to-tubesheet welding programs, mechanical testing, and Few Tube Test Model program.

Two procurements were initiated: one for short tubes (2.1 m; 7 ft.) produced by CarTech and the other for long tubes (21 m; 69 ft.) produced by Southwest Tube (SWT). The CarTech tubes have been received and characterization of these tubes has been initiated. The SWT tubes have been manufactured and heat treated. However, a measurable decrease in UTS was observed in both tubing heats because of the required post weld heat treatment of tensile test specimens. This indicates that a stable microstructure was not attained after the isothermal heat treatment and temper heat treatment of these tubes. Extensive testing at GE of CIW heat #55262 has shown that both yield strength and ultimate tensile strength should remain relatively constant after the temper heat treatment for isothermally heat treated material. This difference in post weld heat treatment response can be interpreted as indicating that the isothermal heat treatment given the long tubing did not produce the desired microstructure. Therefore, negotiation with the vendor has been initiated to have the tubing reheat treated. The following paragraph discusses a short study made of the microstructural stability of isothermally annealed 2 1/4 Cr - 1 Mo.

MICROSTRUCTURAL STABILITY OF ISOTHERMALLY HEAT TREATED 2 1/4 Cr - 1 Mo ALLOY

A program was initiated to establish the microstructural stability of VAR 2 1/4 Cr - 1 Mo alloy tubing given the isothermal heat treatment specified in RDT M3-33. Short term tensile tests were performed on this material after it had been given a specific temper treatment and varied post weld heat treatments. This approach is based on the premise that a stable microstructure should result in a relatively constant set of tensile properties.

A Cameron Iron Work (CIW) heat (#55262) was selected for this program. Tubing was manufactured to 15.9 mm O.D. X 2.8 mm minimum wall (0.625" X 0.109") and given the isothermal heat treatment (see Table I) specified in RDT M3-33 in a batch type vacuum furnace. The tubing was then cut to shorter lengths and heat treated at 727°C (1340°F) for specific lengths of time and tested as described below.

Fifteen inch (38.1 cm) long sections of isothermally heat treated tubing were sealed in a retort filled with high purity argon at room temperature. Calibrated thermocouples traceable to the National Bureau of Standards were mounted inside the sealed retort at the center and one end of the specimen to

determine the hot zone gradient; this was found to be negligible. The specimens were heat treated in a tube furnace according to Table I with continuous temperature recording. All specimens receiving the same treatment were heated as one batch. The retort was not opened to the atmosphere until the tubing was at approximately room temperature. This procedure produced a bright surface with negligible oxidation and decarburization.

The tubing was then tensile tested according to ASTM Standard E8-69 without a reduced diameter gage section. An LVDT-type extensometer was used to generate a stress-strain curve up to about 5% strain, from which the 0.2% offset yield strength was determined. The tensile properties resulting from the various heat treatments are given in Table II. The yield and ultimate tensile strengths are plotted in Figure 1.

Figure 1 shows that very little, if any, change occurs in the yield stress of isothermally heat treated material due to further exposure to 21 hours at 727°C (1340°F). A slight drop (~8%) in ultimate tensile strength (UTS) does occur however, during the initial hour at 727°C, but the UTS remains relatively stable thereafter.

The results indicate that both post weld heat treatments considered produce a stable short-term microstructure, as shown by almost constant strength values between one and twenty hours of PWHT at 727°C (1340°F).

MECHANICAL TEST PROGRAM FOR STEAM GENERATOR TUBING

This section describes the test plans for the mechanical test program for steam generator tubing. The test plan is designed to provide a description of the response of prototypic steam generator tubing to both short term and long term stress applications. The program should provide an estimate of the degree of conservatism used in current steam generator creep design criteria based on actual test data from prototypic (remelted) steam generator tubing.

The initial plan is based on three materials. Additional materials shall be added as they become available.

Material

Presently, there are three heats of ASME SA-213, Grade T22 tubing available

for testing: two VAR heats, #55262 and #91506 and one ESR heat, #91505. The chemical analysis for each heat is shown in Table III. All tubing was manufactured by CarTech and given the isothermal heat treatment specified in RDT M3-33. This heat treatment was performed in a batch type vacuum furnace.

Biaxial specimens will be fabricated in accordance with Figure 2 for both short term burst testing and longer term creep testing. All specimens will be given a temper and post weld heat treatment similar to the CRBRP steam generator tubing. All heat treatments are shown in Table II.

Test Methods

Biaxial burst testing will be conducted in the two rigs: 1. Hydrostatic burst rig and 2. Pneumatic burst rig. The hydrostatic burst test will be for ambient testing only and can test full sized tube samples having a 2.8 mm (0.109 in.) minimum wall. The pneumatic burst rig will test specimens as shown in Figure 2. Both rigs will be equipped to measure and record internal pressure and outside diameter.

To insure that similar data are obtained by both testing rigs, ambient test results for tube samples having three different wall thicknesses will be compared. These results will be taken into account in the method used for stress calculations.

Each tube lot will be burst tested as described in Table IV. Duplicate tests will be performed where applicable.

Biaxial stress rupture tests will be conducted in the SR-III rig at 510°C (950°F). The stress levels and estimated times to rupture are shown in Table V. Specific samples will be removed at 1, 10, 100, 1000, and 10,000 hours to measure strain. These samples may or may not be returned to test conditions based on earlier strain measurements.

TABLE I

EFFECT OF HEAT TREATMENT ON TENSILE PROPERTIES
OF 2 1/4 Cr - 1 Mo ALLOY TUBING AT ROOM TEMPERATURE

HEAT TREATMENT(1)	0.2% YIELD STRENGTH MPa (ksi)	ULTIMATE TENSILE STRENGTH MPa (ksi)	TOTAL ELONGATION IN 51mm (2")
1(2)	264 (38.3)	481 (69.8)	35%
1	264 (38.3)	485 (70.4)	36%
1	264 (38.3)	490 (71.1)	34%
2	268 (38.81)	444 (64.34)	42%
2	265 (38.42)	441 (63.89)	41%
2	268 (38.88)	444 (64.41)	37%
3	270 (39.13)	437 (63.41)	39%
3	260 (37.65)	430 (62.40)	37%
3	260 (37.71)	434 (62.92)	37%
4	261 (37.84)	428 (62.01)	40%
4	257 (37.25)	425 (61.65)	39%
4	258 (37.45)	422 (61.23)	42%

(1) Heat Treatment

1. Isothermal anneal in vacuum at 927°C (1700°F) for 1/2 hr.
   Cool to 704°C (1300°F) in 1 1/2 hrs. and hold 704°C for 2 hrs.
   Cool to room temperature in 1 hr. with argon purge.

2. Same as 1.
   Temper at 727°C (1340°F) for 1 hr. in argon.
   Air cool to room temperature.

3. Same as 2.
   Post weld heat treat (PWHT) at 727°C (1340°F) for 4 hrs. in argon.
   Air cool to room temperature.

4. Same as 2.
   Post weld heat treat (PWHT) at 727°C (1340°F) for 20 hrs. in argon.
   Air cool to room temperature.

(2) Heat treatment #1 and tensile tests were performed by an outside vendor.

TABLE II

HEAT TREATMENT OF BIAXIAL TEST SPECIMENS

1. Isothermal Heat Treatment

927°C ± 14°C (1700°F ± 25°F), hold for 1/2 hr. minimum
Cool to 704°C (1300°F), hold for 2 hrs. minimum
Cool to room temperature.

2. Temper Heat Treatment

727°C ± 19°C (1340°F ± 35°F), hold for 1 hr. minimum
Cool to room temperature.

3. Post Weld Heat Treatment

727°C ± 19°C (1340°F ± 35°F), hold for 20 hrs. minimum
Heating rate not to exceed 83°C/hr. (150°F/hr.)
Cooling rate not to exceed 111°C/hr. (200°F/hr.)

TABLE III

CHEMICAL ANALYSIS OF STEAM GENERATOR TUBING (wt%)

GE LOT NO.	1	2	3
Heat Number	55262	91505	91506
Remelt	VAR	ESR	VAR
Manufacturer	CIW	CarTech	CarTech
C	0.09	0.09	0.09
Mn	0.52	0.45	0.44
Cr	2.22	2.27	2.29
Mo	1.01	1.02	1.02
Si	0.08	0.25	0.32
P	0.016	0.011	0.011
S	0.014	0.004	0.005
Ni	0.05	0.05	0.06
Cu	0.12	0.05	0.05
Ti	0.02	0.01	0.03
V	0.01	0.01	0.01

TABLE IV

BURST TESTS FOR STEAM GENERATOR TUBE SAMPLES

TEST TEMPERATURE °C (°F)	TEST RIG
Ambient	Hydrostatic
Ambient	Pneumatic
200 (392)	Pneumatic
300 (572)	Pneumatic
400 (752)	Pneumatic
500 (932)	Pneumatic
510 (950)	Pneumatic
600 (1112)	Pneumatic

TABLE V

CREEP RUPTURE TEST FOR STEAM GENERATOR TUBING

SAMPLE IDENTITY	TEST[1] PRESSURE MPa (psi)	ESTIMATED STRESS MPa (ksi)	ESTIMATED[2] TIME OF TEST (hrs)
A-15	59.7 (8,658)	276 (40)	10
A-16, A-17	52.2 (7,576)	241 (35)	100
A-18, A-19	44.8 (6,494)	207 (30)	500
A-20, A-21, A-22	37.3 (5,411)	172 (25)	1000
A-23, A-24, A-25	29.8 (4,329)	138 (20)	5000
A-26, A-27, A-28	22.4 (3,247)	103 (15)	>10000
LATER	14.9 (2,165)	68.9 (10)	>10000
B-15	59.7 (8,658)	276 (40)	10
B-16, B-17	52.2 (7,576)	241 (35)	100
B-18, B-19	44.8 (6,494)	207 (30)	500
B-20, B-21, B-22	37.3 (5,411)	172 (25)	1000
B-23, B-24, B-25	29.8 (4,329)	138 (20)	5000
B-26, B-27, B-28	22.4 (3,247)	103 (15)	>10000
LATER	14.9 (2,165)	68.9 (10)	>10000
C-15	59.7 (8,658)	276 (40)	10
C-16, C-17	52.2 (7,576)	241 (35)	100
C-18, C-19	44.8 (6,494)	207 (30)	500
C-20, C-21, C-22	37.3 (5,411)	172 (25)	1000
C-23, C-24, C-25	29.8 (4,329)	138 (20)	5000
C-26, C-27, C-28	22.4 (3,247)	103 (15)	>10000
LATER	14.9 (2,165)	68.9 (10)	>10000

(1) Based on outside fiber stress calculated using: stress = 4.6198 pressure

(2) Estimated for temperature at 510°C (950°F)

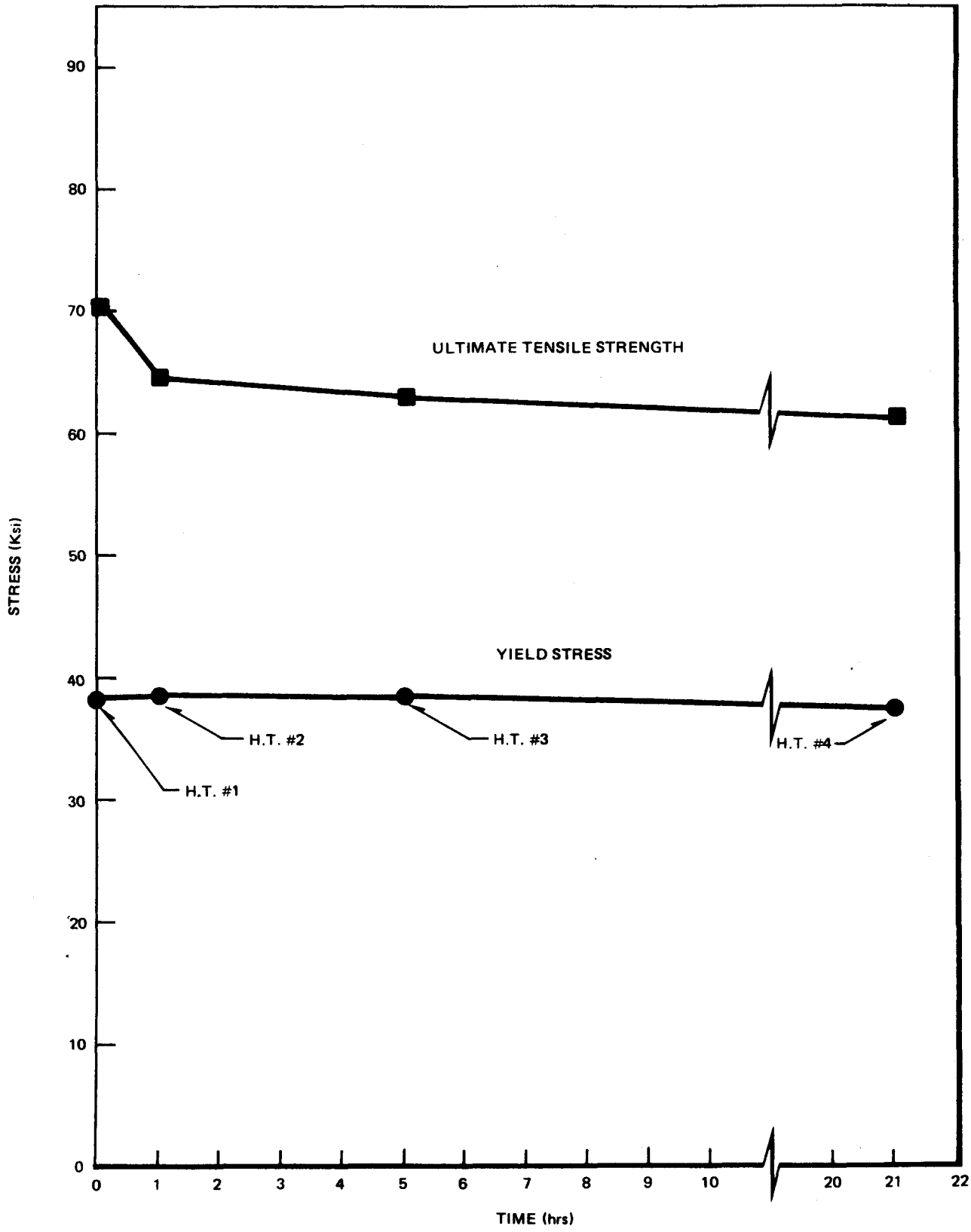

Figure 1. Effect of Time at 1340°F on the Tensile Properties of Isothermally Heat Treated ASME SA-213, Grade T22 Tubing Heat No. 55262)

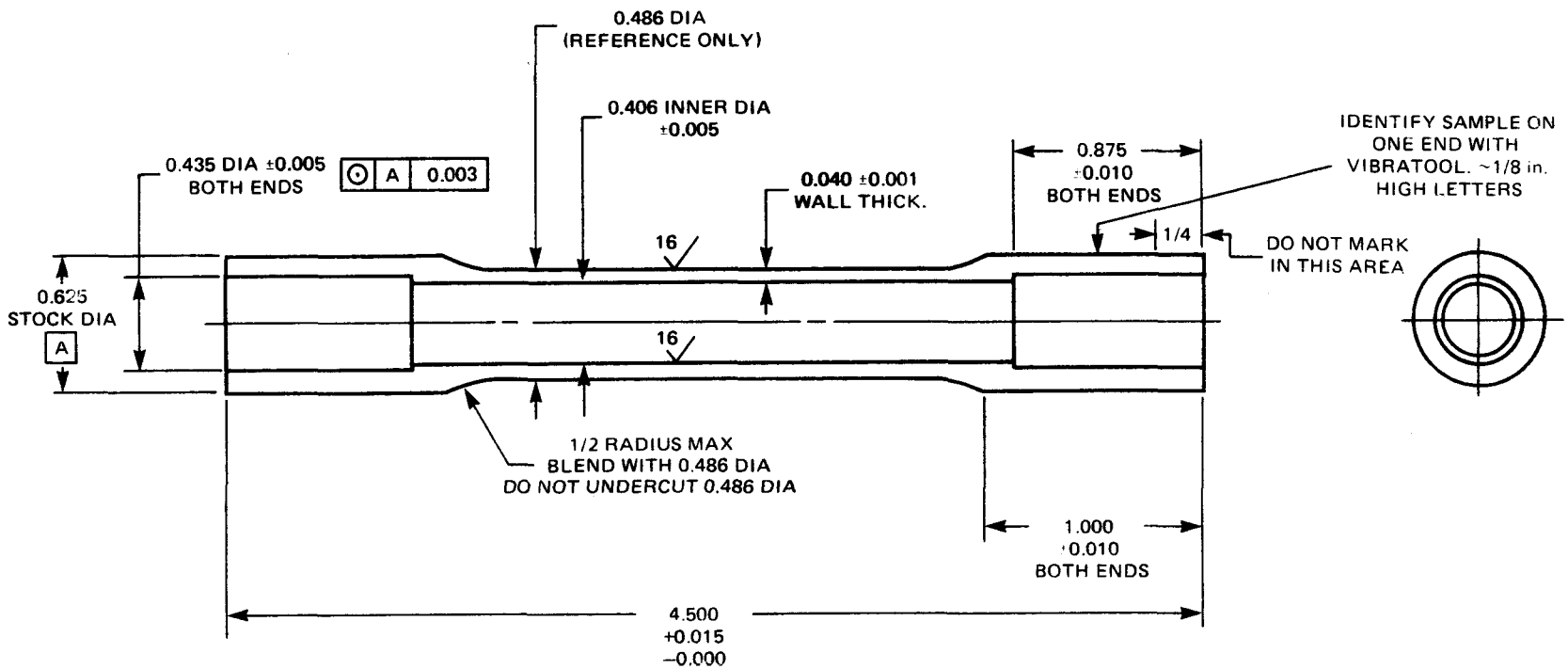

Figure 2. Biaxial Test Specimen

III. LMFBR STEAM GENERATOR TUBESHEET FORGINGS

METALLURGICAL CHARACTERIZATION OF VAR AND ESR 2 1/4 Cr - 1 Mo ALLOY STEEL

The objective of this activity is to generate preliminary mechanical property and microstructural characterization data for consumable remelted 2 1/4 Cr - 1 Mo alloy steel. Vacuum arc remelting (VAR) and electroslag remelting (ESR) will provide high purity material for the critical tube-tubesheet weld region. The mechanical properties resulting from these processing techniques must be shown to meet the applicable ASME Code and RDT Standards, which are based on non-remelted material. Testing and examination conducted and reported earlier[1] include room temperature tensile tests, drop-weight tests, creep-rupture tests, chemical composition*, microcleanliness, grain size and hardness, and isothermal transformation data.

HEAT TREATMENT

The heat treatments used in this study closely simulate the various possible heat treatments applicable to the tubesheet forging and tubing. These heat treatments include an isothermal anneal and a full anneal both with and without a post weld heat treatment. Also included is a normalize and temper with post weld heat treatment. The heat treatment parameters are listed in Table I.

TENSILE TESTS

Tensile tests were conducted for VAR heat #55262 and ESR heat #R0110 at 21, 204, 371, 454, 510, and 566°C (70, 400, 700, 850, 950, and 1050°F). The yield and ultimate strength, elongation, and reduction in area values are reported in Tables II and III. The yield and ultimate strengths are plotted as a function of temperature in Figures 1, 2, 3, and 4, along with the Nuclear Systems Materials Handbook (NSMH) expected value and the 0.95 upper and lower tolerance limits. The expected value of yield strength as a function of temperature given in ASME Code Case 1592 is also shown in Figures 1 and 2. The yield and ultimate strength for both the VAR and ESR material generally

* Please see the end of this section for a corrected analysis.

(with the exception of ESR at room temperature) lie between the NSMH expected value and lower tolerance limit at all temperatures tested. The yield strength at 454°C (850°F) and above is generally below the Code Case 1592 expected value for all conditions tested for the ESR material. For the VAR material, only the isothermal anneal produced yield strengths below this expected value above 454°C.

CHARPY V-NOTCH TESTS

A brief summary of the results of charpy v-notch impact testing was reported earlier[1]. A complete summary of tests to date is given in Table IV for VAR heat #55262, VAR heat #56067, and ESR heat #R0110. The absorbed energy, lateral expansion, and percent shear fracture are plotted as a function of test temperature in Figures 6 to 15. Of the four heat treatments considered, the full anneal plus post weld heat treatment (PWHT) gives the best assurance of nonductile fracture based on the temperature for 67.8 J (50 ft.-lb.) impact energy and 889 μm (35 mils) lateral expansion. These values are required simultaneously by ASME Code Section III - Division I, Article NB-2300, at the nil-ductility transition temperature (NDT) + 33.3°C (60°F). As previously reported, NDT ranged from -45.6 to -40.0°C (-50 to -40°F) for the ESR material and from -28.9 to -3.9°C (-20 to 25°F) for the VAR material. For full anneal plus PWHT of ESR and VAR material the minimum values are met at -42.8°C (-45°F) and 1.7°C (35°F), respectively. This makes the minimum hydrostatic test temperatures approximately -6.7°C (20°F) for ESR forgings and 29.4°C (85°F) for VAR forgings.

The upper shelf energy of ESR material was observed to be much higher than VAR material. This difference in absorbed energy is attributed primarily to the morphology and distribution of non-metallic inclusions (primarily the sulfide type). The inclusion distributions are different for the ESR and VAR processes. Large cylindrical (~15 μm long, ~1 μm diameter) and spherical (~1 - 2 μm diameter) inclusions were typically observed in the VAR material by scanning electron microscopy. No non-metallic inclusions were visible on the fracture surface of the ESR material. Micrographs of VAR and ESR specimens that were fully annealed with PWHT and fractured in the temperature range of the upper shelf are shown in Figure 5.

The effect of the difference in ferrite and prior austenite grain size reported earlier[1] for these two remelting methods is being determined. Grain size has been increased in ESR specimens to match that of the VAR specimens. These will be tested as a function of temperature to verify the effect of grain size on the absorbed energy and fracture appearance transition temperatures.

CREEP-RUPTURE TESTS

Log stress-log minimum creep rate plots at 454, 510, and 566°C (850, 950, and 1050°F) were reported previously[1] for VAR heat #55262 and ESR heat #R0110. These plots are reproduced in Figures 16 to 18 with additional data points, along with log stress-log time to tertiary creep and log stress-log rupture time plots in Figures 19 to 21 and 22 to 24, respectively. The data are listed in Table V. On the above figures, comparisons are made of remelted steel to air melted steel. The air melt data is in the form of curves of minimum or expected values developed for the ASME Code Case 1592-4 or the Nuclear Systems Materials Handbook. In all cases, the remelted steel data falls within the tolerance limits of the NSMH and above the minimum values established by the Code. That is, the creep-rupture behavior of VAR and ESR is within the variability observed for air melted steels.

ISOTHERMAL TRANSFORMATION STUDY

Four heats of 2 1/4 Cr - 1 Mo steel were isothermally annealed at 704°C (1300°F) for various times from 30 to 180 minutes after austenitizing at 927°C (1700°F) for 1/2 hour. The resulting hardness values were reported previously[1]. The purpose of this study is to determine the ferrite + carbide phase boundary of the isothermal transformation diagram. The same study has been repeated at 691, 704, and 718°C (1275, 1300, and 1325°F) for 12 heats of 2 1/4 Cr - 1 Mo steel including air melted, VAR, and ESR material. The resulting hardness values are given in Table VI. A chemical analysis for all of these heats is listed in Table VII. The carbon content ranged from 0.09 to 0.16%. This exceeds the RDT Standard M3-33 maximum of 0.110%, but it was considered useful to observe the effect of carbon content on transformation time.

The formation of ferrite + carbide as pearlite at 704°C (1300°F) takes approximately 120 minutes. The time for transformation is longer at 691°C (1275°F) than at 718°C (1325°F). This indicates that the nose of the ferrite + carbide phase region on the isothermal transformation diagram for 2 1/4 Cr - 1 Mo steel is above 704°C (1300°F), the presently accepted temperature for air melted material[2]. This result will be verified by additional isothermal annealing of the same heats at 732°C (1350°F). The microstructures resulting from various hold times at 704°C (1300°F) and water quenching were reported earlier[1]. At approximately 120 minutes hold time, the phases present after water quenching are proeutectoid ferrite, bainite, martensite, discontinuous precipitation, general precipitation, and fine pearlite. All of these phases can be seen in Figure 25. It should be noted that the fine pearlite shown is typical in morphology, but occurs only in isolated areas.

FRACTURE TOUGHNESS TESTING OF VAR MATERIAL

The objective of this program is to determine fracture toughness values (K_{Ic}) at 24°C (75°F) for steam generator tubesheet materials. These results are then used along with charpy v-notch and drop-weight test values (RT_{NDT} determinations) and tensile test results to evaluate the resistance to fracture. The philosophy of this approach to fracture prevention is set forth in the K_{IR} curve of Appendix G to Section III of the ASME Boiler and Pressure Vessel Code. No toughness data on 2 1/4 Cr - 1 Mo steel was included in the derivation of this Code K_{IR} curve. Therefore, an important application of these results is to verify the conservatism of the K_{IR} curve for 2 1/4 Cr - 1 Mo steel.

A vacuum arc remelted (VAR) 50.8 mm (2 in.) thick plate (heat #55262) was procured. The chemical composition, tensile test, charpy v-notch, and drop-weight test results have been previously reported for this heat[1]. An RT_{NDT} value of 7°C (20°F) was reported. This plate was heat treated as follows: 927°C (1700°F) for 3 hours, furnace cool to room temperature, plus 727°C (1340°F) for 4 hours, air cool to room temperature. Three 50.8 mm (2 in.) thick ASTM E399 Compact Tension Specimens (CTS) were machined from this plate in the transverse (WR) orientation. The crack lengths were extended by fatigue precracking to a crack length to specimen width ratio (a/w) of approximately 0.65.

These CTS's were tested at 24°C (75°F) under constant stroke control of 1.52 mm/min. (0.06 in./min.). Load versus load-point displacement curves were generated and used to compute J_{Ic} values. These J_{Ic} values, and the K_{Ic} results computed from them, are shown in Table VIII. The values of J_{Ic} were determined from the points on the load-displacement curves where a brittle pop-in (rapid crack extension) occurred. The brittle pop-in has been shown by Scanning Electron Microscopy (SEM) to be related to cleavage fracture of these specimens. Even with this brittle behavior, the minimum K_{Ic} value of 121 MPa $\sqrt{m}$ (110 ksi $\sqrt{in}$) is above the corresponding K_{IR} curve value of approximately 60 MPa $\sqrt{m}$ (55 ksi $\sqrt{in}$). Further testing would be necessary to determine if this remains the case at higher temperatures relative to the RT_{NDT}. Therefore, safe behavior with respect to fracture, for components designed in accordance with the Code K_{IR} curve and Appendix G, is indicated for this material. However, it is recommended that more testing of this type be done to gain statistical confidence in this conclusion, especially in view of the brittle fracture mode. Testing at elevated temperatures is also required to verify that the material toughness is above the K_{IR} curve at service temperatures, and that stable crack extension (ductile) can be achieved.

CRBRP PROTOTYPE AND PLANT TUBESHEET FORGINGS

The objective of this activity is to provide the technical support to the procurement of the CRBR prototype, plant, and development tubesheet forgings. These items will be purchased to RDT M2-19.

The order for VAR 2 1/4 Cr - 1 Mo forgings placed earlier this year for the various CRBRP programs is being processed. Vacuum arc remelting and hot working of remelted ingots has been completed.

Two (2) air melt heats of 2 1/4 Cr - 1 Mo alloy were made for the GE program. Each air melted heat was for ~45.4 metric tons (50 tons) with a yield of ~38555 kg (85,000 lbs.) per heat. Each air melted heat was conditioned and vacuum arc remelted into 5 VAR ingots. The yield again was ~38555 kg (85,000 lbs.) per heat or 77111 kg (170,000 lbs.) total. The VAR ingots were conditioned and extruded an bars of ~74 cm (29 in.) and 36 cm (14 in.) in diameter. The larger diameter material will be made into the LLTI and prototype forgings;

the smaller diameter material will be used for the FTTM and weld development forgings. Therefore, two lots of material were shipped to ORNL from two heats: Lot #1 (~4536 kg; 10,000 lbs.) contained two (2) pieces of 74 cm diameter bar from heat #56448 and Lot #2 (~4536 kg; 10,000 lbs.) contained one (1) piece of 74 cm diameter bar from the other heat. The chemical analysis of heat #56448 met all requirements of RDT M2-19 as shown below:

CHEMICAL ANALYSIS

Heat No.	C	Mn	P	S	Si	Cr	Ni	Mo	Ti	V	Cu	Co
56448	.10	.56	.010	.006	.26	2.15	.15	1.01	.01	.01	.09	.01

The purchase orders have been placed with Cameron Iron Works to forge the 74 cm (29 in.) and 36 cm (14 in.) bars to thicknesses and diameters required for the various tubesheets. The entire order for the prototype, LLTI, FTTM, and weld development forgings is expected to be completed by the end of February 1976. A complete summary of the status of tubesheet purchases is given in Table IX.

CORRECTION TO THE PREVIOUSLY REPORTED CHEMICAL ANALYSIS

The mechanical properties determined in this study indicated that the composition for some of the elements as reported by the chemical analysis vendor were in error. A second product analysis verified this indication. The second chemical analysis is shown below:

CHEMICAL ANALYSIS

Heat No.	Al	Si	S
VAR 56067	0.005	0.28*	0.007*
ESR R0110	0.027	0.18	0.006

* Same value as reported in first analysis.

REFERENCES

1. LMFBR Steam Generator Materials - Program for the Development of Design Data, July 16 - 17, 1975, prepared for ERDA under Contract AT(04-3)-893 Task 10-G and 18.

2. Copeland, J. F., "Factors Influencing the Notch Toughness and Transition Temperature of ASTM A542 Steel", PhD Dissertation, Department of Metallurgy and Materials Science, Lehigh University, 1973.

TABLE I

HEAT TREATMENTS* FOR 2 1/4 Cr - 1 Mo STEEL

A.	Isothermal Anneal:	954°C (1750°F) for 1/2 hr. Furnace cool to 710°C (1310°F) for 2 1/2 hr. Air cool to room temperature.
	Postweld:	727°C (1340°F) for 4 hr. Air cool to room temperature.
B.	Anneal:	916°C (1680°F) for 1 1/4 hr. Furnace cool [@ 27.7 to 55.6°C/hr. (@ 50 - 100°F/hr.) to 316°C (600°F)] Air cool to room temperature.
	Postweld:	727°C (1340°F) for 4 hr. Air cool to room temperature.
C.	Normalize and Temper:	954°C (1750°F) for 1 hr. Air cool to room temperature. 727°C (1340°F) for 1 3/4 hr. Air cool to room temperature.
	Postweld:	727°C (1340°F) for 4 hr. Air cool to room temperature.
D.	(Same as B without Postweld)	
E.	(Same as A without Postweld)	

* Monitored according to specimen surface temperature.

TABLE II

TENSILE PROPERTIES OF VAR 2 1/4 Cr - 1 Mo STEEL*

Temperature °C	Temperature (°F)	Strength, MPa (ksi) Yield 0.2% Offset	Strength, MPa (ksi) Ultimate	Total Elongation, (%)	Reduction in Area, (%)
Heat Treatment A - Isothermal Anneal with PWHT**. Longitudinal Orientation					
21	(70)	221 (32.0)	465 (67.5)	29.5	72.9
204	(400)	216 (31.3)	406 (58.9)	27.6	65.2
371	(700)	190 (27.6)	491 (71.2)	26.0	64.2
454	(850)	165 (24.0)	405 (58.8)	26.2	62.4
510	(950)	165 (23.9)	379 (54.9)	26.6	73.0
566	(1050)	157 (22.8)	317 (46.0)	32.2	81.6
Heat Treatment B - Full Anneal with PWHT. Longitudinal Orientation					
21	(70)	241 (34.9)	441 (63.9)	32.1	65.4
204	(400)	216 (31.3)	384 (55.7)	30.1	65.2
371	(700)	208 (30.2)	444 (64.4)	23.7	60.7
454	(850)	179 (25.9)	423 (61.4)	27.1	68.3
510	(950)	187 (27.1)	396 (57.4)	27.2	75.2
566	(1050)	168 (24.4)	352 (51.1)	33.2	74.7
Heat Treatment D - Full Anneal without PWHT. Longitudinal Orientation					
21	(70)	243 (35.2)	472 (68.5)	33.1	66.4
204	(400)	213 (30.9)	410 (59.5)	29.7	66.4
371	(700)	215 (31.2)	452 (65.6)	22.9	60.7
454	(850)	214 (31.0)	449 (65.2)	26.1	61.9
510	(950)	204 (29.6)	429 (62.2)	24.6	64.8
566	(1050)	200 (29.0)	372 (54.0)	30.0	72.4

* Strain Rate - 6.67×10^{-4}/sec

** PWHT - Post Weld Heat Treatment

TABLE III

TENSILE PROPERTIES OF ESR 2 1/4 Cr - 1 Mo STEEL*

Temperature °C	Temperature (°F)	Strength, MPa (ksi) Yield 0.2% Offset	Strength, MPa (ksi) Ultimate	Total Elongation, (%)	Reduction in Area, (%)
Heat Treatment B - Full Anneal with PWHT. Longitudinal Orientation					
21	(70)	225 (37.0)	480 (69.6)	36.1	74.4
204	(400)	- -	- -	-	-
371	(700)	192 (27.9)	421 (61.0)	29.4	66.4
454	(850)	146 (21.2)	378 (54.8)	24.8	71.9
510	(950)	149 (21.6)	360 (52.2)	39.3	73.3
566	(1050)	144 (20.9)	301 (43.7)	42.1	80.8
Heat Treatment B - Full Anneal with PWHT. Transverse Orientation					
21	(70)	296 (43.0)	483 (70.0)	37.5	73.4
204	(400)	242 (35.1)	405 (58.7)	33.7	72.5
371	(700)	209 (30.3)	402 (58.3)	27.1	68.1
454	(850)	177 (25.7)	399 (57.8)	30.2	68.9
510	(950)	174 (25.3)	370 (53.7)	33.4	69.2
566	(1050)	145 (21.1)	305 (44.2)	40.3	79.9
Heat Treatment D - Full Anneal without PWHT. Longitudinal Orientation					
21	(70)	268 (38.9)	472 (68.5)	40.6	72.8
204	(400)	226 (32.8)	403 (58.4)	27.6	74.2
371	(700)	192 (27.9)	413 (59.9)	28.3	67.7
454	(850)	160 (23.2)	399 (57.9)	28.9	68.0
510	(950)	148 (21.4)	360 (52.2)	34.5	73.9
566	(1050)	150 (21.7)	314 (45.5)	38.3	77.5

* Strain rate - 6.67×10^{-4}/sec

TABLE III, Continued

TENSILE PROPERTIES OF ESR 2 1/4 Cr - 1 Mo STEEL*

Temperature °C	Temperature (°F)	Strength, MPa (ksi) Yield 0.2% Offset	Strength, MPa (ksi) Ultimate	Total Elongation, (%)	Reduction in Area, (%)
Heat Treatment D - Full Anneal without PWHT. Transverse Orientation					
21	(70)	299 (43.4)	487 (70.6)	37.5	72.1
204	(400)	226 (32.8)	401 (58.2)	34.0	67.7
371	(700)	195 (28.3)	459 (66.5)	25.1	65.3
454	(850)	168 (24.3)	403 (58.5)	27.6	65.6
510	(950)	154 (22.4)	378 (54.8)	31.8	70.1
566	(1050)	155 (22.5)	321 (46.5)	37.8	75.8
Requirements of RDT M3-33 (Tubing)					
21	(70)	206 (30)min.	414 (60) to 586 (85)	30 min.	--
Requirements of RDT M2-19 (Tubesheet Forging)					
21	(70)	206 (30)min.	414 (60) to 586 (85)	20 min.	--

* Strain Rate - 6.67×10^{-4}/sec

TABLE IV

CHARPY V-NOTCH RESULTS FOR 2 1/4 Cr - 1 Mo STEEL

Specimen No.	CVN J (ft.-lb.)	Temp. °C (°F)	Lateral Expansion μm (mils)	Shear Fracture (%) Observation				Heat**	Heat Treatment	Orientation***
				#1	#2	#3	Avg.			
V-10	3.5 (2.6)	-45.6 (-50)	25 (1)	0	1	2	1	V-1	B	L
V-3	11.5 (8.5)	-40 (-40)	203 (8)	2	2	4	3	V-1	B	L
V-5	22.4 (16.5)	-34.4 (-30)	432 (17)	8	4	2	5	V-1	B	L
V-7	14.9 (11.0)	-34.4 (-30)	279 (11)	5	3	2	3	V-1	B	L
V-6	324.3 (239.2)	-31.7 (-25)	2390 (94)	100	100	100	100	V-1	B	L
V-8	6.2 (4.6)	-31.7 (-25)	0 (0)	2	2	2	2	V-1	B	L
V-9	4.3 (3.2)	-31.7 (-25)	25 (1)	1	1	2	1	V-1	B	L
V-4	>324.6 (>239.4)	-28.9 (-20)	2310 (91)	100	100	100	100	V-1	B	L
V-2	>315.6 (>232.8*)	-17.8 (0)	2460 (97)	100	100	100	100	V-1	B	L
V-1	>317.8 (>234.4*)	23.9 (75)	2260 (89)	100	100	100	100	V-1	B	L
V-12	4.2 (3.1)	-17.8 (0)	0 (0)	2	5	4	4	V-1	A	T
V-13	5.2 (3.8)	-6.67 (20)	76 (3)	2	4	4	3	V-1	A	T
V-14	14.9 (11.0)	15.6 (60)	356 (14)	12	15	5	11	V-1	A	T
V-18	12.8 (9.5)	18.3 (65)	305 (12)	8	10	5	8	V-1	A	T
V-19	15.2 (11.2)	21.1 (70)	279 (11)	10	14	5	10	V-1	A	T
V-11	90.8 (67.0)	23.9 (75)	1520 (60)	30	20	10	20	V-1	A	T
V-15	76.7 (56.6)	37.8 (100)	1380 (55)	35	25	15	25	V-1	A	T
V-17	116.6 (86.0)	65.6 (150)	1910 (75)	65	65	60	63	V-1	A	T
V-16	137.8 (101.6)	98.9 (210)	1980 (78)	85	80	75	80	V-1	A	T
V-20	139.6 (103.0)	176.7 (350)	1930 (76)	100	99	98	99	V-1	A	T

* Hammer stopped
** V-1 = VAR 55262, V-2 = VAR 56067, E = ESR R0110
*** L = Longitudinal, T = Transverse

TABLE IV, Continued

CHARPY V-NOTCH RESULTS FOR 2 1/4 Cr - 1 Mo STEEL

Specimen No.	CVN J (ft.-lb.)	Temp. °C (°F)	Lateral Expansion µm (mils)	Shear Fracture (%) Observation				Heat**	Heat Treatment	Orientation***
				#1	#2	#3	Avg.			
V-24	15.2 (11.2)	-28.9 (-20)	254 (10)	5	10	5	7	V-1	B	T
V-22	14.9 (11.0)	-17.8 (0)	330 (13)	5	9	1	5	V-1	B	T
V-23	46.4 (34.2)	-6.67 (20)	838 (33)	10	22	3	12	V-1	B	T
V-29	73.8 (54.4)	4.44 (40)	1300 (51)	20	20	10	17	V-1	B	T
V-25	84.3 (62.2)	15.6 (60)	1400 (55)	25	40	15	27	V-1	B	T
V-21	86.2 (63.6)	23.9 (75)	1400 (55)	35	25	10	23	V-1	B	T
V-26	113.2 (83.5)	37.8 (100)	1800 (71)	80	70	40	63	V-1	B	T
V-28	126.4 (93.2)	65.6 (150)	1910 (75)	95	98	90	94	V-1	B	T
V-27	126.1 (93.0)	98.9 (210)	1980 (78)	100	99	90	96	V-1	B	T
V-30	125.0 (92.2)	176.7 (350)	1960 (77)	100	99	90	96	V-1	B	T
V-34	10.8 (8.0)	-28.9 (-20)	203 (8)	2	8	2	4	V-1	C	T
V-32	8.1 (6.0)	-17.8 (0)	76 (3)	5	10	8	8	V-1	C	T
V-33	46.8 (34.5)	-6.67 (20)	787 (31)	10	17	10	12	V-1	C	T
V-38	50.4 (37.2)	4.44 (40)	914 (36)	15	15	15	15	V-1	C	T
V-40	62.3 (47.4)	10. (50)	1120 (44)	20	20	15	18	V-1	C	T
V-35	81.9 (60.4)	15.6 (60)	1420 (56)	35	40	20	32	V-1	C	T
V-31	90.6 (66.8)	23.9 (75)	1470 (58)	35	35	20	30	V-1	C	T
V-36	100.3 (74.0)	37.8 (100)	1570 (62)	40	40	25	35	V-1	C	T
V-39	108.5 (80.0)	65.6 (150)	1650 (65)	80	80	75	78	V-1	C	T
V-37	118.2 (87.2)	98.9 (210)	1780 (70)	100	99	95	98	V-1	C	T

TABLE IV, Continued

CHARPY V-NOTCH RESULTS FOR 2 1/4 Cr - 1 Mo STEEL

Specimen No.	CVN J (ft.-lb.)	Temp. °C (°F)	Lateral Expansion µm (mils)	Shear Fracture (%) Observation				Heat**	Heat Treatment	Orientation***
				#1	#2	#3	Avg.			
V-44	4.7 (3.5)	-28.9 (-20)	25 (1)	0	1	1	1	V-1	D	T
V-42	9.8 (7.2)	-17.8 (0)	203 (8)	5	9	5	6	V-1	D	T
V-43	35.9 (26.5)	-6.67 (20)	711 (28)	10	15	5	10	V-1	D	T
V-48	53.1 (39.2)	4.44 (40)	991 (39)	15	18	15	16	V-1	D	T
V-50	66.7 (49.2)	10. (50)	1220 (48)	20	20	15	18	V-1	D	T
V-45	75.1 (55.4)	15.6 (60)	1300 (51)	22	25	15	21	V-1	D	T
V-41	65.6 (48.4)	23.9 (75)	1190 (47)	20	25	15	20	V-1	D	T
V-46	98.3 (72.5)	37.8 (100)	1600 (63)	50	50	25	42	V-1	D	T
V-49	116.6 (86.0)	65.6 (150)	1830 (72)	95	95	90	93	V-1	D	T
V-47	118.0 (87.0)	98.9 (210)	1850 (73)	98	98	95	97	V-1	D	T
V-52	4.7 (3.5)	-17.8 (0)	51 (2)	2	8	2	4	V-1	E	T
V-53	9.8 (7.2)	4.44 (40)	203 (8)	5	8	5	6	V-1	E	T
V-51	28.2 (20.8)	23.9 (75)	610 (24)	15	17	20	17	V-1	E	T
V-54	51.5 (38.0)	37.8 (100)	1040 (41)	35	25	15	25	V-1	E	T
V-57	59.4 (43.8)	48.9 (120)	991 (39)	38	45	40	41	V-1	E	T
V-58	66.2 (48.8)	54.4 (130)	1270 (50)	18	20	15	18	V-1	E	T
V-56	103.2 (76.1)	60. (140)	1750 (69)	65	75	70	70	V-1	E	T
V-60	91.1 (67.2)	65.6 (150)	1600 (63)	45	55	30	43	V-1	E	T
V-55	113.2 (83.5)	98.9 (210)	1880 (74)	85	90	90	88	V-1	E	T
V-59	116.9 (86.2)	176.7 (350)	1910 (75)	100	99	95	98	V-1	E	T

TABLE IV, Continued

CHARPY V-NOTCH RESULTS FOR 2 1/4 Cr - 1 Mo STEEL

Specimen No.	CVN J (ft.-lb.)	Temp. °C (°F)	Lateral Expansion µm (mils)	Shear Fracture (%) Observation				Heat**	Heat Treatment	Orientation***
				#1	#2	#3	Avg.			
V-62	7.6 (5.6)	-17.8 (0)	203 (8)	2	5	2	3	V-2	B	T
V-63	12.2 (9.0)	4.44 (40)	305 (12)	5	5	5	5	V-2	B	T
V-71	24.4 (18.0)	23.9 (75)	559 (22)	10	13	8	10	V-2	B	T
V-64	33.9 (25.0)	37.8 (100)	737 (29)	15	15	20	17	V-2	B	T
V-67	44.5 (32.8)	48.9 (120)	914 (36)	20	23	30	24	V-2	B	T
V-65	54.5 (40.2)	60. (140)	1090 (43)	22	22	30	25	V-2	B	T
V-66	62.6 (46.2)	71.1 (160)	1270 (50)	30	40	50	40	V-2	B	T
V-68	74.6 (55.0)	82.2 (180)	1370 (54)	70	75	60	68	V-2	B	T
V-69	85.6 (63.4)	93.3 (200)	1600 (63)	80	85	60	75	V-2	B	T
V-61	100.3 (74.0)	98.9 (210)	1780 (70)	85	90	80	85	V-2	B	T
V-72	115.0 (84.8)	121.1 (250)	1880 (74)	98	98	95	96	V-2	B	T
V-70	117.7 (86.8)	176.7 (350)	2030 (80)	100	99	95	98	V-2	B	T
V-73	114.4 (84.4)	176.7 (350)	2010 (79)	100	99	95	98	V-2	B	T
V-75	7.6 (5.6)	-17.8 (0)	152 (6)	2	5	5	4	V-2	D	T
V-76	14.1 (10.4)	4.44 (40)	305 (12)	5	10	5	7	V-2	D	T
V-74	21.8 (16.1)	23.9 (75)	508 (20)	10	13	15	13	V-2	D	T
V-77	28.5 (21.0)	37.8 (100)	711 (28)	20	15	18	18	V-2	D	T
V-81	41.2 (30.4)	48.9 (120)	914 (36)	25	20	25	23	V-2	D	T
V-79	55.9 (41.2)	60. (140)	1090 (43)	28	30	25	28	V-2	D	T
V-80	62.4 (46.0)	71.1 (160)	1270 (50)	35	45	30	37	V-2	D	T
V-83	70.5 (52.0)	76.7 (170)	1300 (51)	60	70	50	60	V-2	D	T
V-82	79.3 (58.5)	82.2 (180)	1450 (57)	65	70	50	62	V-2	D	T
V-85	78.6 (58.0)	93.3 (200)	1520 (60)	68	70	50	63	V-2	D	T
V-78	103.0 (76.0)	98.9 (210)	1780 (70)	90	90	80	87	V-2	D	T
V-86	112.8 (83.2)	121.1 (250)	2010 (79)	98	97	95	97	V-2	D	T
V-84	116.6 (86.0)	176.7 (350)	1980 (78)	100	99	95	98	V-2	D	T

TABLE IV, Continued

CHARPY V-NOTCH RESULTS FOR 2 1/4 Cr - 1 Mo STEEL

Specimen No.	CVN J (ft.-lb.)	Temp. °C (°F)	Lateral Expansion μm (mils)	Shear Fracture (%) Observation				Heat**	Heat Treatment	Orientation***
				#1	#2	#3	Avg.			
V-94	10.6 (7.8)	-56.7 (-70)	178 (7)	1	3	5	3	E	B	L
V-90	10.6 (7.8)	-51.1 (-60)	254 (10)	2	8	5	5	E	B	L
V-96	12.9 (9.5)	-48.3 (-55)	279 (11)	2	8	8	6	E	B	L
V-91	28.5 (21.0)	-45.6 (-50)	584 (23)	5	10	5	7	E	B	L
V-93	155.6 (114.8)	-42.8 (-45)	2490 (98)	40	45	35	40	E	B	L
V-88	129.1 (95.2)	-40. (-40)	2130 (84)	30	33	35	33	E	B	L
V-97	311.6 (229.8)	-37.2 (-35)	2210 (87)	100	100	100	100	E	B	L
V-95	>323.4 (>238.5)	-34.4 (-30)	2160 (85)	100	100	100	100	E	B	L
V-92	>324.0 (>239.0)	-28.9 (-20)	2130 (84)	100	100	100	100	E	B	L
V-89	>319.4 (>235.6)	-17.8 (0)	2360 (93)	100	100	100	100	E	B	L
V-87	>324.7 (>239.5*)	23.9 (75)	2210 (87)	100	100	95	98	E	B	L
V-101	11.5 (8.5)	-51.1 (-60)	279 (11)	2	5	5	4	E	B	T
V-100	123.7 (91.2)	-45.6 (-50)	1980 (78)	25	30	20	25	E	B	T
V-98	>323.9 (>238.9*)	-17.8 (0)	2210 (87)	100	100	100	100	E	B	T
V-99	>317.3 (>234.0)	10. (50)	2360 (93)	100	100	100	100	E	B	T
V-110	7.5 (5.5)	-51.1 (-60)	152 (6)	0	3	3	2	E	D	L
V-103	9.5 (7.0)	-40. (-40)	203 (8)	8	8	5	7	E	D	L
V-107	63.0 (46.5)	-34.4 (-30)	1120 (44)	10	20	5	12	E	D	L
V-108	20.6 (15.2)	-34.4 (-30)	457 (18)	5	8	3	5	E	D	L
V-106	103.3 (76.2)	-28.9 (-20)	1700 (67)	20	30	15	22	E	D	L
V-105	189.8 (140.0)	-17.8 (0)	2590(102)	45	50	45	47	E	D	L
V-109	122.6 (90.4)	-12.2 (10)	1930 (76)	30	30	20	27	E	D	L
V-111	>324.6 (>239.4)	-12.2 (10)	1910 (75)	100	100	100	100	E	D	L
V-104	>323.4 (>238.5*)	-6.67 (20)	2210 (87)	100	100	100	100	E	D	L
V-102	>323.8 (>238.8*)	23.9 (75)	2260 (89)	100	100	100	100	E	D	L
V-114	60.2 (44.4)	-40 (-40)	1090 (43)	5	21	20	15	E	D	T
V-112	119.3 (88.0)	-28.9 (-20)	1850 (73)	20	30	20	23	E	D	T
V-113	>323.4 (>238.5*)	10. (50)	2180 (86)	100	100	100	100	E	D	T

TABLE V

CREEP-RUPTURE DATA FOR 2 1/4 Cr - 1 Mo STEEL

SPECIMEN NUMBER	HEAT TREATMENT	STRESS KSI (MPa)	RUPTURE TIME (hr.)	TIME TO THIRD* STAGE (hr.)	STRAIN TO THIRD* STAGE (%)	MINIMUM CREEP* RATE (%/hr.)	ELONGATION (%)	REDUCTION IN AREA (%)	PLASTIC ON LOADING (%)
Heat VAR 55262					850°F (454°C)				
C25	C	60 (413.7)	**	--	--	--	23.4	74.4	6.9
C1	A	55 (379.2)	6.3	3.3	2.25	0.515	24.3	71.1	3.2
T8	B	55 (379.2)	167.4	101.0	5.10	0.0386	27.1	71.2	4.6
T35**	C	55 (379.2)	0.4	--	--	--	28.9	71.0	10.0+
C4	A	52 (358.5)	61.0	46.1	3.78	0.0629	24.7	73.3	5.0
C16	B	52 (358.5)	494.1	293.0	4.83	0.0122	28.2	73.8	3.1
C28	C	52 (358.5)	21.8	13.7	3.30	0.195	26.0	77.2	4.2
C7	A	48 (330.9)	968.4	664.0	3.40	0.0034	25.2	75.0	3.2
C19	B	48 (330.9)	2035.1	1175.0	4.28	0.0025	29.1	74.5	2.3
C31	C	48 (330.9)	119.6	57.8	2.41	0.0318	27.9	79.0	3.0
C10	A	40 (275.8)	2864.8††	2450;2200	3.23;2.24	0.00100;0.000263	29.2	79.7	1.8
C34	C	40 (275.8)	1359.9	~810.	~2.85	0.0029†	31.3	82.5	1.2
Heat ESR R0110									
C51	B	52 (358.5)	2.5	1.74	8.00	3.678	31.9	73.7	6.2
C54	D	52 (358.5)	80.6	66.7	11.00	0.144	32.9	71.2	5.0
T22	B	40 (275.8)	298.4	1325.0	6.78	0.0038	36.0	75.0	0.4
T42***	D	40 (275.8)							

* Determined by 0.2% strain offset
** Specimen failed on loading
*** Specimen on test
† Average for discontinuous behavior
†† Strain discontinuity at 1010 hours

TABLE V, Continued

CREEP-RUPTURE DATA FOR 2 1/4 Cr - 1 Mo STEEL

SPECIMEN NUMBER	HEAT TREATMENT	STRESS KSI (MPa)	RUPTURE TIME (hr.)	TIME TO THIRD* STAGE (hr.)	STRAIN TO THIRD* STAGE (%)	MINIMUM CREEP* RATE (%/hr.)	ELONGATION (%)	REDUCTION IN AREA (%)	PLASTIC ON LOADING (%)
Heat VAR 55262					950°F (510°C)				
C26	C	40 (275.8)	20.3	5.4	1.47	0.200	34.1	81.9	1.6
C2	A	35 (241.3)	90.0	29.9	1.75	0.0408	41.6	80.6	1.6
C14	B	35 (241.3)	430.3	166.0	3.28	0.0133	39.4	83.3	1.5
T17	C	35 (241.3)	51.2	13.2	1.69	0.0871	42.2	83.9	0.8
C5	A	30 (206.8)	245.9	82.0	1.25	0.0104	50.2	83.6	1.5
C17	B	30 (206.8)	1398.4	427.0	2.35	0.0041	46.6	85.5	0.6
C29	C	30 (206.8)	226.1	55.6	1.44	0.0201	45.9	84.2	0.3
C8	A	25 (172.4)	721.2	198.0	0.83	0.0032	57.5	87.3	0.3
C20	B	25 (172.4)	2842.8	580.0	1.46	0.0019	54.6	87.3	0.2
C32	C	25 (172.4)	853.3	134.0	0.41	0.0014	51.6	86.2	0.08
C11	A	22 (151.7)	763.6	150.0	0.76	0.0032	51.1	87.6	1.1
C35	C	22 (151.7)	2184.2	298.0	0.50	0.0010	55.1	88.4	0.07
Heat ESR R0110									
C52	B	30 (206.8)	387.0	172.0	9.50	0.0466	51.2	76.2	1.3
C55	D	30 (206.8)	895.6	274.0	5.33	0.0150	45.5	68.8	0.8
T23	B	22 (151.7)	3325.4	1065.0	6.75	0.0058	48.7	61.5	0.2
T43***	D	22 (151.7)							

TABLE V, Continued

CREEP-RUPTURE DATA FOR 2 1/4 Cr - 1 Mo STEEL

SPECIMEN NUMBER	HEAT TREATMENT	STRESS KSI (MPa)	RUPTURE TIME (hr.)	TIME TO THIRD* STAGE (hr.)	STRAIN TO THIRD* STAGE (%)	MINIMUM CREEP* RATE (%/hr.)	ELONGATION (%)	REDUCTION IN AREA (%)	PLASTIC ON LOADING (%)
Heat VAR 55262					1050°F (566°C)				
C3	A	27.5 (189.6)	9.1	2.1	2.75	1.071	24.5	70.5	12.1
C13	B	27.5 (189.6)	**	--	--	--	52.6	87.2	1.1
C15	B	27.5 (189.6)	89.2	29.2	1.78	0.0459	43.5	85.4	0.4
T12	B	27.5 (189.6)	50.1	15.0	4.23	0.235	64.1	87.5	0.6
C27	C	27.5 (189.6)	10.1	2.0	3.00	1.000	55.2	87.2	0.4
C6	A	25 (172.4)	17.3	3.9	2.28	0.456	52.7	85.7	0.3
C18	B	25 (172.4)	76.0	16.7	2.58	0.125	61.5	87.9	0.2
C30	C	25 (172.4)	21.0	5.9	3.32	0.503	54.0	90.4	0.2
C9	A	22 (151.7)	44.6	11.6	5.10	0.422	68.0	88.3	0.4
C21	B	22 (151.7)	168.9	24.6	1.64	0.0483	72.5	89.2	0.06
C33	C	22 (151.7)	73.5	9.3	1.47	0.132	62.3	89.9	0.1
C12	A	18 (124.1)	210.2	12.6	0.44	0.0349	68.0	90.6	0.05
C24	B	18 (124.1)	749.7	70.5	1.02	0.0113	68.0	90.9	0.3
C36	C	18 (124.1)	353.3	126.0	5.43	0.0413	63.5	90.8	0.02
T6	A	14 (96.53)	1259.2	475.0	7.61	0.0152	60.8	91.3	0.01
T18	C	14 (96.53)	2788.5	952.0	5.35	0.0054	56.5	92.0	0.0
Heat ESR R0110									
C53	B	22 (151.7)	89.9	37.2	11.90	0.282	74.2	76.8	0.6
C56	D	22 (151.7)	142.5	21.0	3.80	0.138	57.4	74.4	0.2
T24	B	14 (96.5)	1489.3	530.0	7.90	0.0141	56.8	65.5	0.02
T44	D	14 (96.5)	1879.7	690.0	5.70	0.0078	46.9	62.3	0.02

TABLE VI

BRINELL HARDNESS VALUES OF 2 1/4 Cr - 1 Mo SPECIMENS
FOR ISOTHERMAL TRANSFORMATION STUDY

			ISOTHERMAL HOLD TIME (minutes)						
HEAT #	CARBON	TEMP °C	30	45	60	90	120	180	300
VAR 56067	0.11	704	195	195;185	150	165;150	150;147	144	
Air Melt 113632	0.15	704	270	265;270	210	228;200	210;234	169	
ESR R0110	0.10	704	185	159;159	144	141;139	141;144	141	
VAR 55262	0.09	704	190	151;190	162	162;139	150;150	150	
VAR B9783	0.165	690	237	305	276;276	222;255	197	180	170
		704	294	250	225;222	165;167	156	162	156
		718	210	163	159;159	148;142	140	141	147
VAR B9784	0.153	690	263	248	235;234	210;228	190	172	170
		704	245	213	182;178	162;165	159	159	153
		718	213	182	154;159	144;148	151	147	147
VAR 91506	0.10	690	305	273	235;250	259;228	222	205	185
		704	293	260	225;222	195;216	195	167	154
		718	222	197	178;178	148;174	165	160	142
ESR 9796	0.153	690	362	352	352;322	342;342	301	219	192
		704	347	305	268;283	235;240	205	165	163
		718	309	265	234;235	185;185	159	153	151
ESR 9797	0.155	690	265	235	228;228	250;245	234	195	176
		704	313	290	262;257	228;228	182	169	160
		718	276	235	213;216	172;163	157	150	153
ESR 91505	0.088	690	228	234	222;216	203;200	187	185	163
		704	205	195	185;190	185;185	160	157	151
		718	200	165	176;157	137;157	147	153	139
Air Melt 113632	0.147	690	322	313	287;283	260;255	237	195	174
		704	273	237	210;219	180;180	165	159	154
		718	228	200	169;172	156;151	150	147	147
Air Melt 279251	0.09	690	205	197	185;190	178;172	165	160	156
		704	182	169	159;156	160;162	157	151	144
		718	163	153	147;151	147;147	147	144	137
Air Melt 5P4430	0.09	690	187	174	162;167	151;157	154	148	140
		704	163	156	153;150	153;150	150	142	141
		718	144	140	138;141	144;141	137	139	135

M3-33 Specification: Maximum Brinell 165 (R_B 85)

690°C = 1275°F; 704°C = 1300°F; 718°C = 1325°F

TABLE VII

CHEMICAL ANALYSIS OF 2 1/4 Cr - 1 Mo STEEL FOR ISOTHERMAL TRANSFORMATION STUDY

HEAT NUMBER		Al%	Sb%	As%	C%	Cr%	Co%	Cu%	H%	Mn%	Mo%	Ni%	N%	O%	P%	Si%	S%	Sn%	Ti%	V%
VAR 56067		0.005	<0.002	0.006	0.098	2.31	<0.002	0.08	0.0007	0.42	0.99	0.17	0.006	<0.001	0.010	0.28	0.015	<0.002	0.002	0.006
Air Melt 113632					0.15	2.39				0.45	1.10				0.011	0.23	0.021			
ESR R0110		0.027	<0.002	0.010	0.100	2.26	<0.002	0.10	0.0005	0.50	0.99	0.15	0.008	<0.001	0.013	0.09	0.007	<0.002	<0.002	0.013
VAR 55262		<0.005	<0.002	0.008	0.099	2.26	<0.002	0.09	0.0006	0.50	1.00	0.15	0.008	<0.001	0.013	0.07	0.016	0.004	<0.002	0.013
VAR B9783					0.165*	2.40				0.39	1.10			0.014	0.009	0.20	0.034*			
VAR B9784					0.153*	2.39				0.34	1.08			<0.005	0.013	0.21	0.025*			
VAR 91506					0.10	2.32		0.05		0.39	1.02	0.06			0.011	0.39	0.005			
ESR 9796					0.153*	2.44				0.47	1.09			0.008	0.009	0.14	0.016			
ESR 9797					0.155*	2.42				0.46	1.08			0.008	0.007	0.19	0.017			
ESR 91505					0.088	2.25		0.06		0.46	1.02	0.05			0.011	0.30	0.004			
Air Melt 279251					0.09	2.32				0.52	0.93				0.12	0.36	0.009			
Air Melt 5P4430					0.09	2.35				0.40	1.00				0.006	0.23	0.012			
RDT M2-19	Minimum				0.070	1.90				0.30	0.87					0.20				
RDT M3-33	Maximum				0.110	2.60		0.35		0.60	1.13	0.25			0.015	0.40	0.015		0.03	0.03

* Average Values

TABLE VIII

COMPACT TENSION SPECIMEN [50.8 mm (2 in) Thick]

FRACTURE TOUGHNESS RESULTS FOR 2 1/4 Cr - 1 Mo VAR HEAT 55262 50.8 mm (2 in) THICK PLATE

TESTS FOR TRANSVERSE ORIENTATION AT 24°C (75°F)

WITH SPECIMEN LOAD POINT DISPLACEMENT RATE OF 1.52 mm/min (0.06 in/min)

Spec. No.	Stable Crack Extension, Δa, at Unload mm (in)	Remarks	J at Unload J/mm^2 (in-lb/in^2)	J at COS, J_{Ic} J/mm^2 (in-lb/in^2)	K_{Ic} MPa $\sqrt{m}$ (ksi $\sqrt{in}$)
GV1	--	Pop-in	9.3 (530)	9.3 (530)	145 (132)
GV2	--	Pop-in	11.7 (670)	11.7 (670)	164 (149)
GV3	--	Pop-in	6.5 (370)	6.5 (370)	121 (110)

TABLE IX
FORGING MATERIAL STATUS

ITEM	MELT PROCESS	SUPPLIER MELTER	SUPPLIER FABRICATOR	NO.	SIZE	SPEC	ANALYSIS % C, Si, P, Other*	DELIVERY STATUS	P/O
LLTI Upper Tubesheet	VAR	CIW	AI	2	58 1/2" Dia. X 16 1/2" Tk. 12,500 lbs.	RDT M2-19	Meets Spec.	12/1/75	C8V09G Item 1 33.5K each
Weld Qualification Lower Tubesheet	VAR	CIW	AI	1	48 1/2" Dia. X 13 1/4" Tk. 5,900 lbs.	RDT M2-19	Meets Spec.	2/1/76	C8V10G Item 1 $18,000 each
FTTM Tubesheet	VAR	CIW	AI	6	12" Dia. X 8" Tk. 260 lbs.	RDT M2-19	Meets Spec.	12/1/75	C8V09G Item 2 $7,000 each
Prototype Upper Tubesheets	VAR	CIW	AI	2	48 1/2" Dia. X 15 3/4" Tk. 7,230 lbs.	RDT M2-19	Meets Spec.	4/1/76	C8V11G Item 1 $21,500 each
Prototype Lower Tubesheets	VAR	CIW	AI	2	48 1/2" Dia. X 13 1/4" Tk. 5,900 lbs.	RDT M2-19	Meets Spec.	4/1/76	C8V11G Item 2 $18,000 each
Task 10G-2 Tubesheet	VAR	CIW	GE	1	48 1/2" Dia. X 13 1/4" Tk. 5,900 lbs.	RDT M2-19	Meets Spec.	2/1/76	C8V10G Item 1 $18,000 each
Weld Development Forging (In process control)	VAR	CIW	AI	6	22" Dia. X 5" Tk. 535 lbs.	RDT M2-19	Meets Spec.	2/1/76	C8V10G Item 2 $2,000 each
Weld Development Forging (Weld Qualification)	VAR	CIW	AI	14	8" Dia. X 5" Tk. 70 lbs.	RDT M2-19	Meets Spec.	2/1/76	C8V10G Item 3 $1,000 each
Mechanical Property Forging Billets	VAR	CIW	ORNL	LOT	20,000 lbs.	RDT M2-19	Meets Spec.	10/75 Delivered	C8V10G Item 4 $19,700 each

CHEMICAL ANALYSIS OF 2 1/4 Cr - 1 Mo STEEL

	VAR 55262 Check Chemical Analysis (Anamet)	VAR 56067 Check Chemical Analysis (Anamet)	ESR R0110 Check Chemical Analysis (Anamet)	RDT M2-19 RDT M3-33 Minimum	Maximum
Aluminum	<0.005%	0.005%	0.027%		
Antimony	<0.002%	<0.002%	<0.002%		
Arsenic	0.008%	0.006%	0.010%		
Carbon	0.099%*	0.098%**	0.100%***	0.070%	0.110%
Chromium	2.26%	2.31%	2.26%	1.90%	2.60%
Cobalt	<0.002%	<0.002%	<0.002%		
Copper	0.09%	0.08%	0.10%		0.35%
Hydrogen	0.0006%	0.0007%	0.0005%		
Manganese	0.50%	0.42%	0.50%	0.30%	0.60%
Molybdenum	1.00%	0.99%	0.99%	0.87%	1.13%
Nickel	0.15%	0.17%	0.15%		0.25%
Nitrogen	0.008%	0.006%	0.008%		
Oxygen	<0.001%	<0.001%	<0.001%		
Phosphorus	0.013%	0.010%	0.013%		0.015%
Silicon	0.07%	0.28%	0.018%	0.20%	0.40%
Sulfur	0.016%	0.007%	0.006%		0.015%
Tin	0.004%	<0.002%	<0.002%		
Titanium	<0.002%	0.002%	<0.002%		0.03%
Vanadium	0.013%	0.006%	0.013%		0.03%

* Average of 0.093%, 0.090%, 0.115%
** Average of 0.095%, 0.105%, 0.095%
*** Average of 0.113%, 0.103%, 0.086%

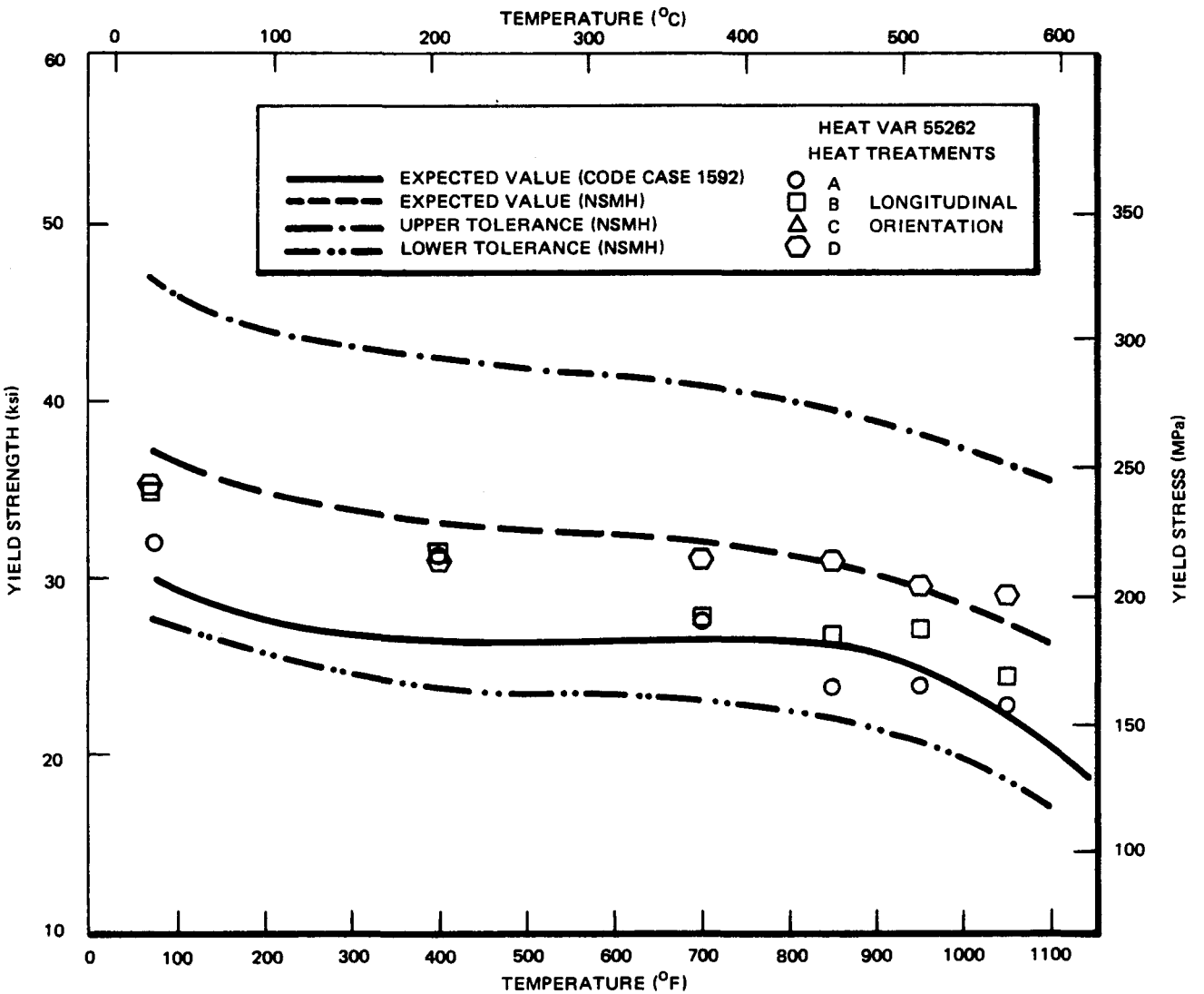

Figure 1. Relationship Between Yield Strength and Temperature for 0.10%C, VAR 2¼ Cr- 1 Mo Steel

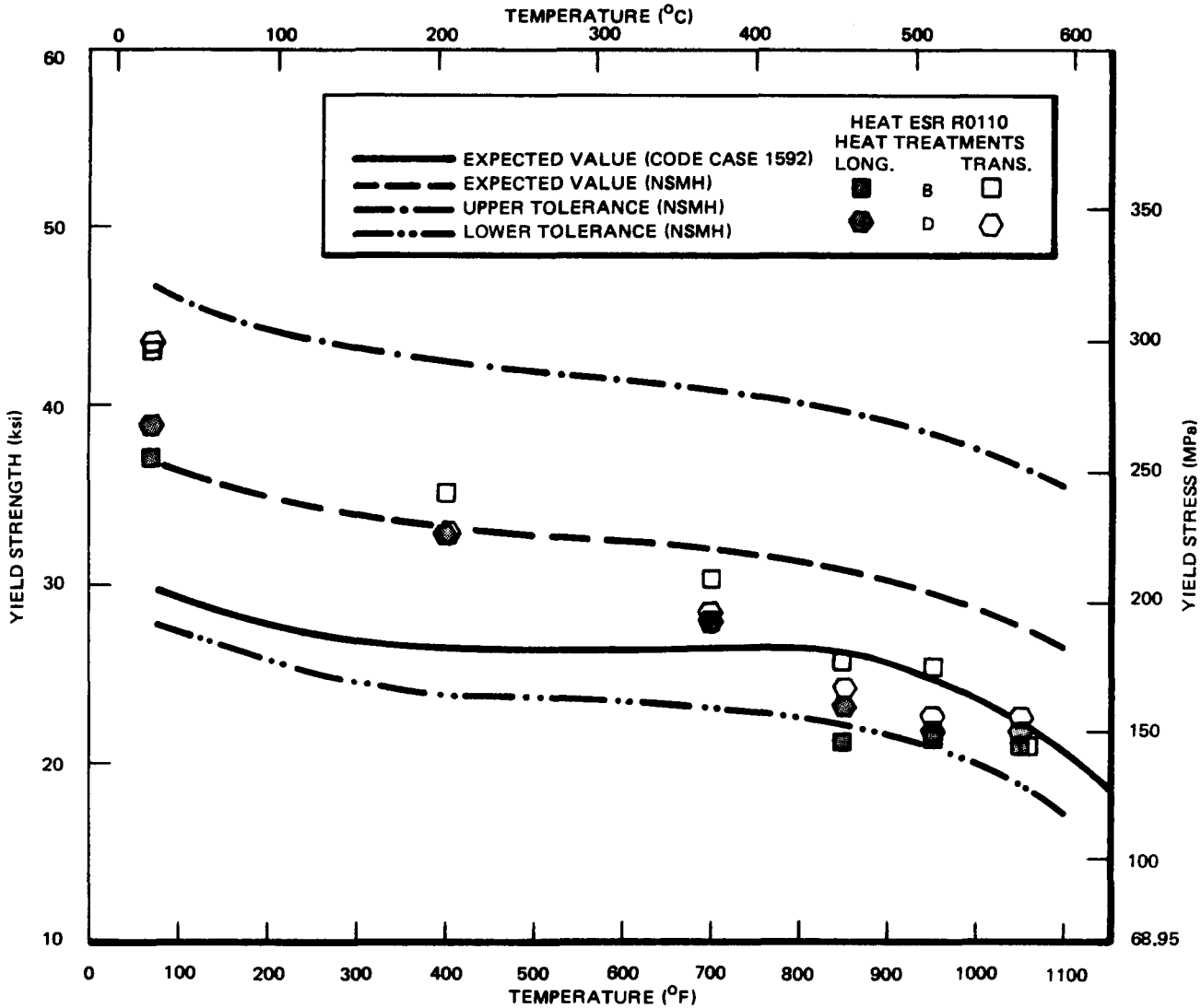

Figure 2. Relationship Between Yield Strength and Temperature for 0.10%C, ESR 2¼ Cr – 1 Mo Steel

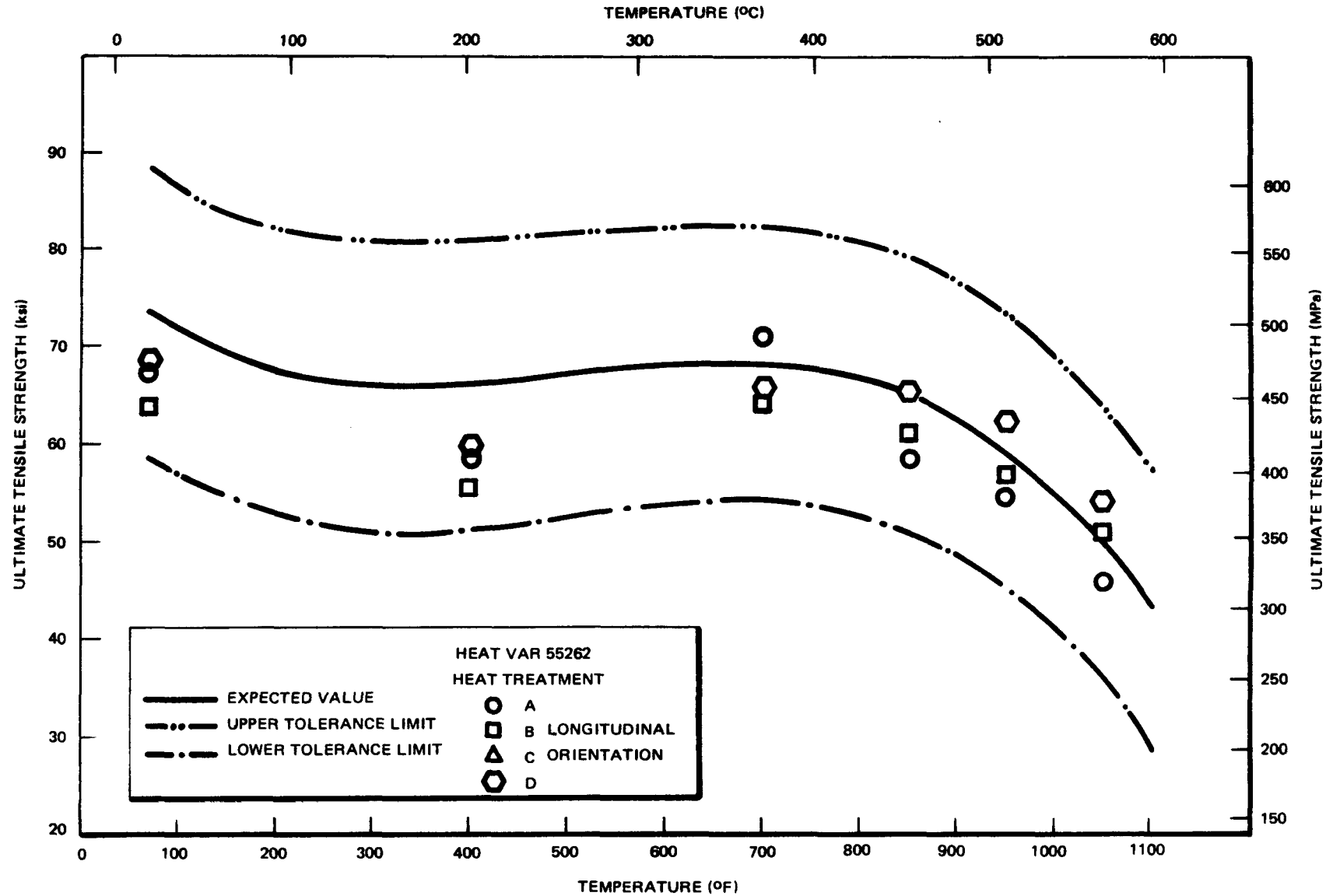

Figure 3. Relationship Between Ultimate Tensile Strength and Temperature for 0.10%C, VAR 2¼ Cr – 1 Mo Steel

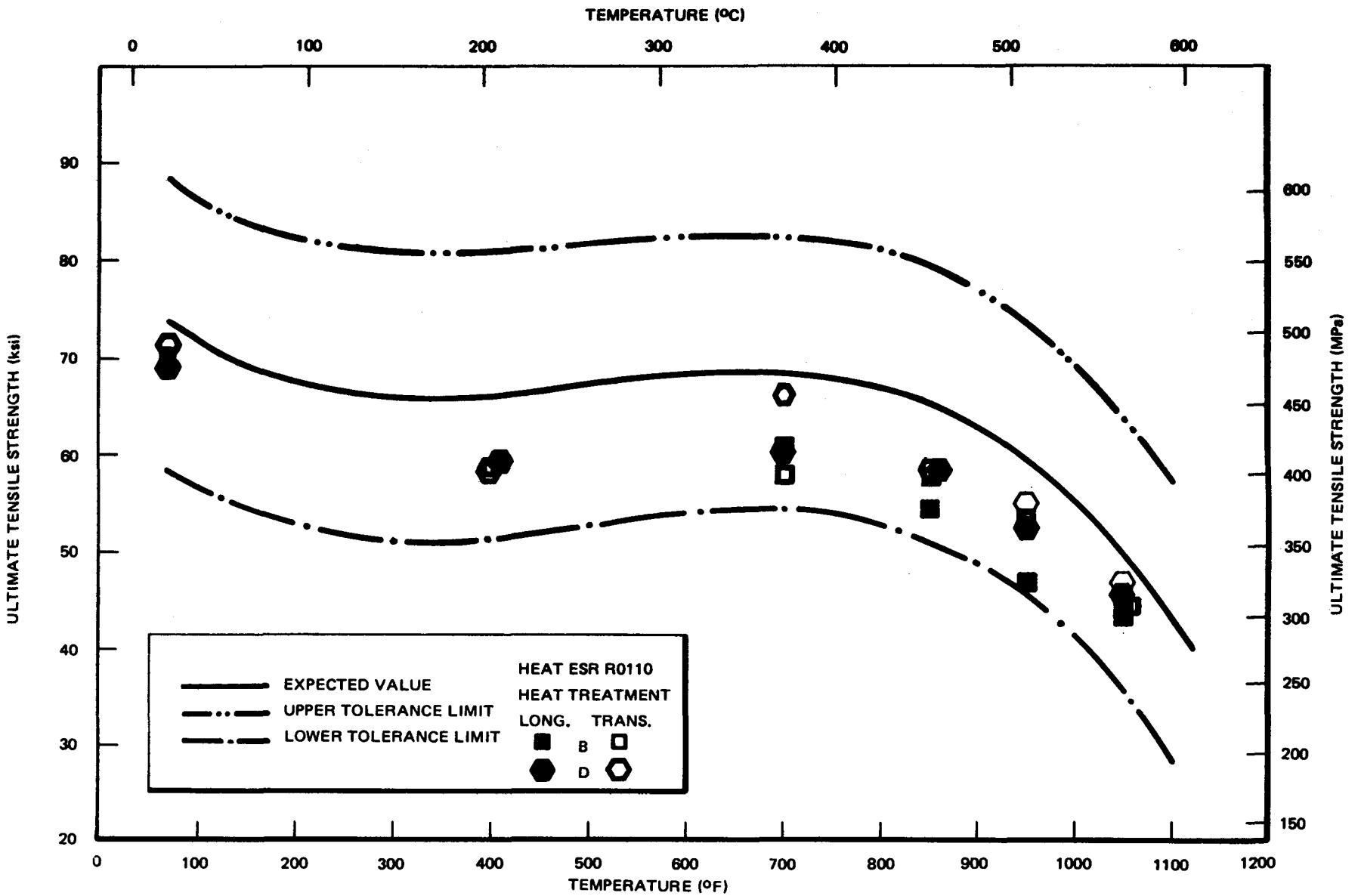

Figure 4. Relationship Between Ultimate Tensile Strength and Temperature for 0.10%C, ESR 2¼ Cr – 1 Mo Steel

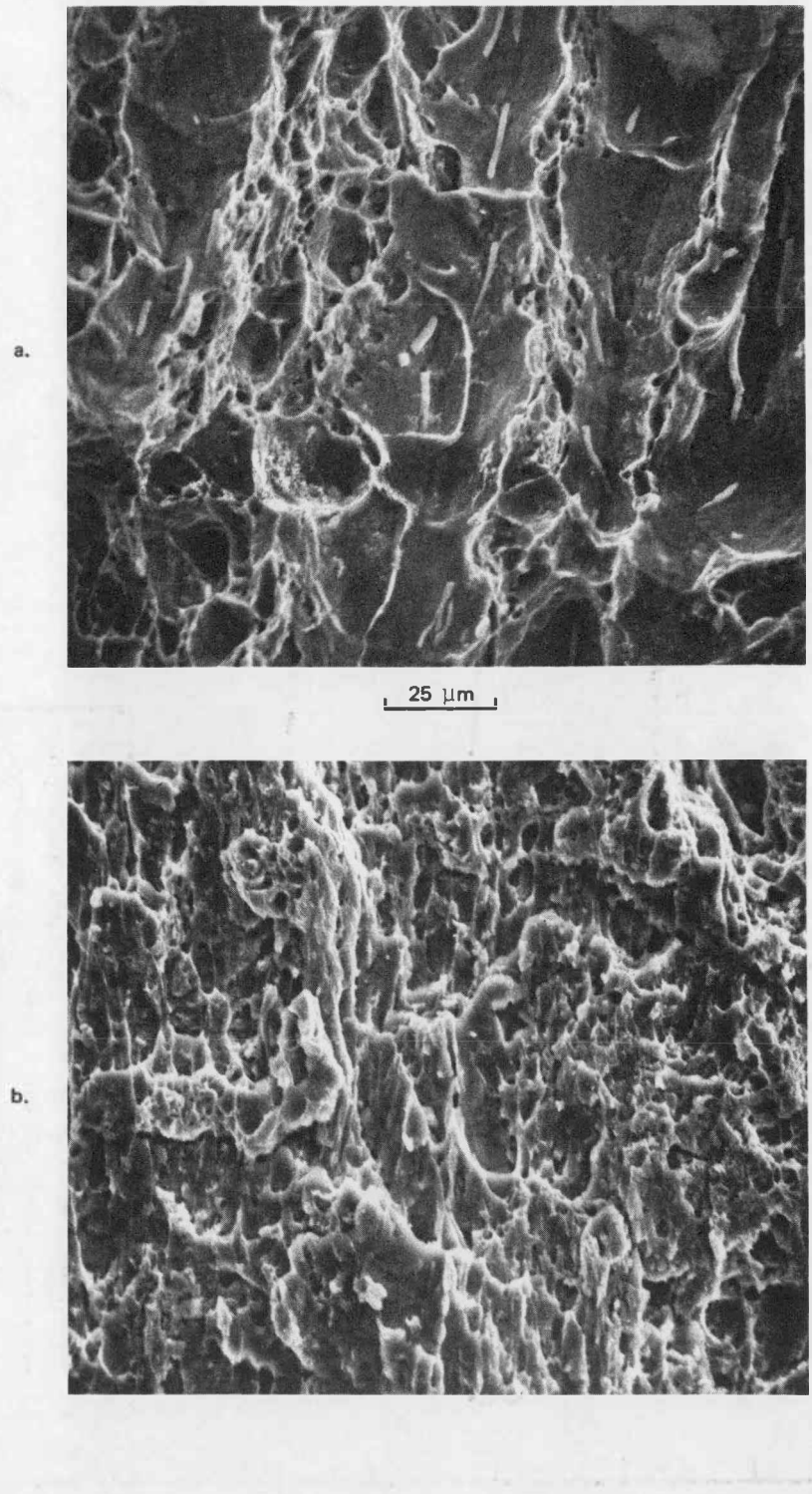

Figure 5. Typical area of fracture surface of Charpy V-Notch specimen broken – the upper shelf temperature range (a) VAR heat 55262 specimen broken at 65.6°C (150°F), (b) ESR heat RO110 Specimen broken at – 17.8°C (0°F)

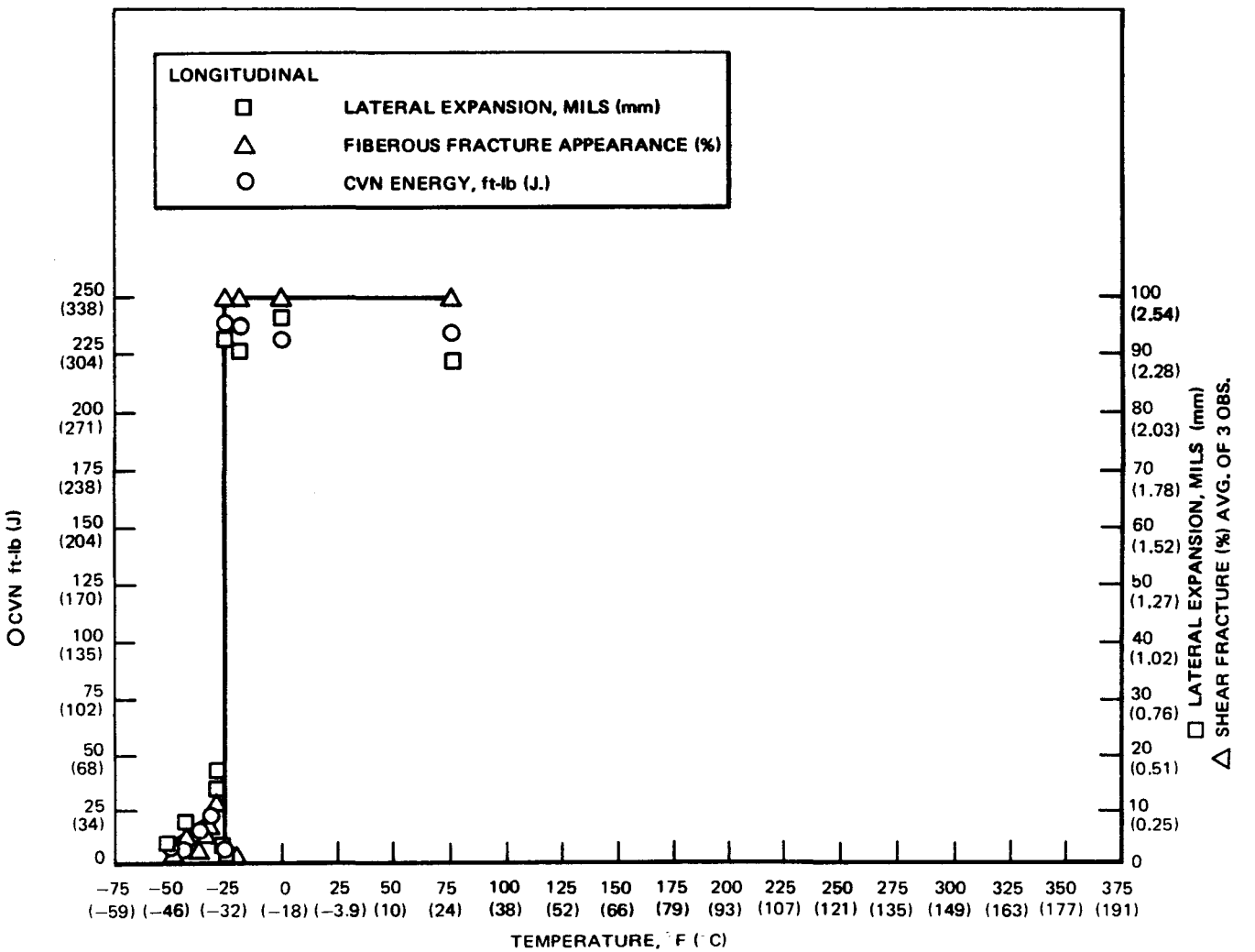

Figure 6. VAR Heat 55262 Longitudinal "B" Heat Treat. V1 to V10

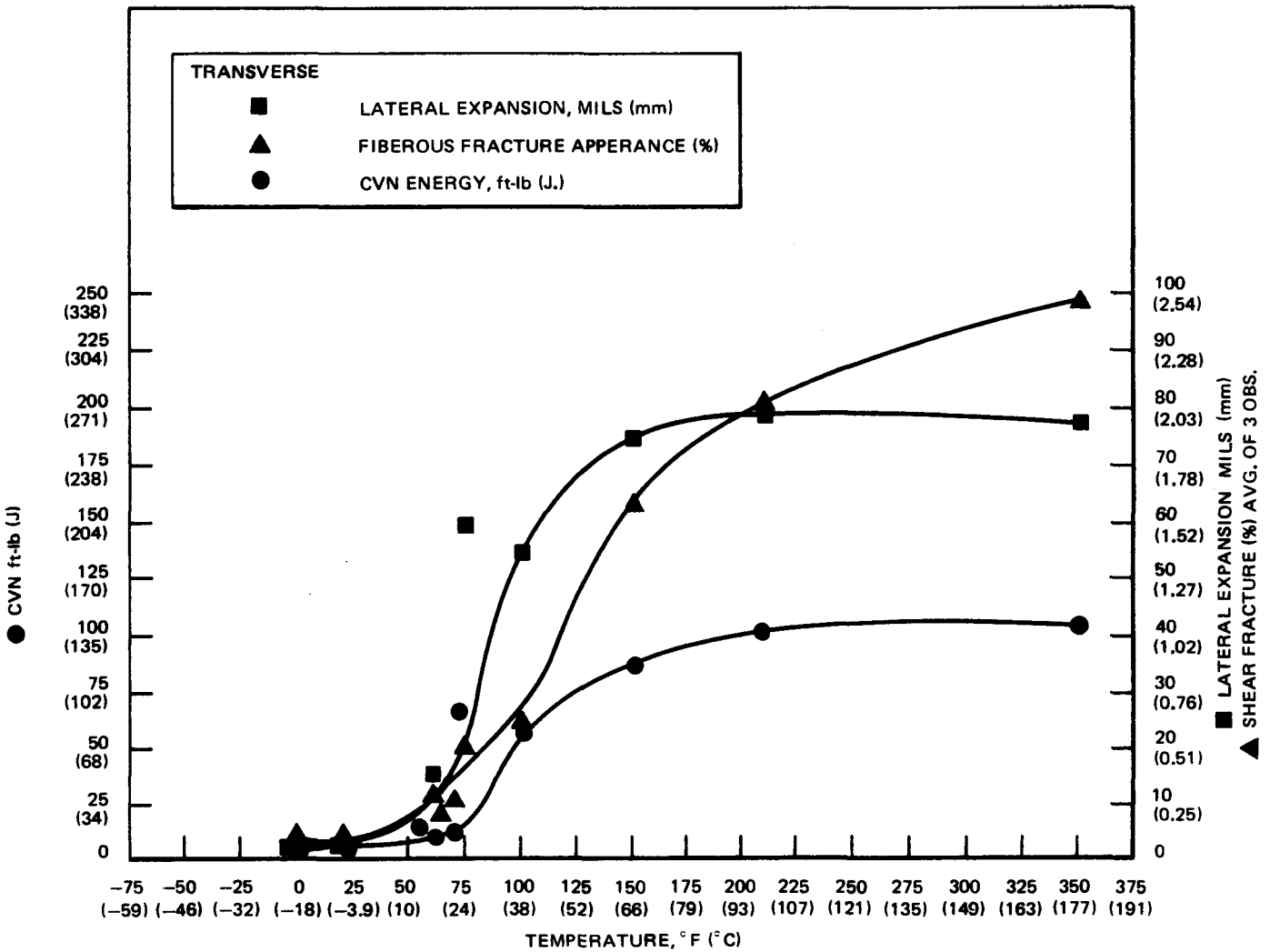

Figure 7. VAR Heat 55262 Transverse "A" Heat Treat. V11 to V20

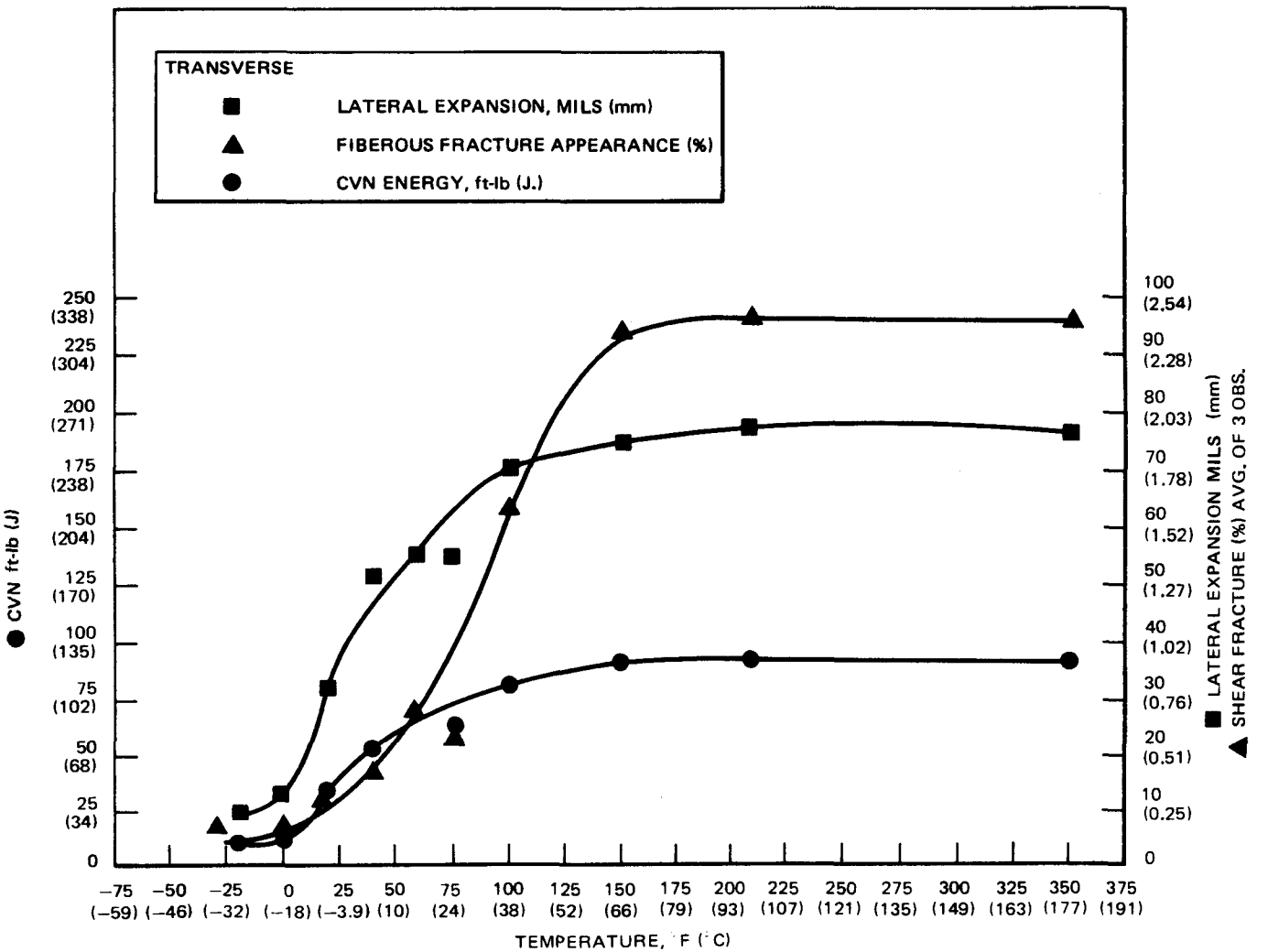

Figure 8. VAR Heat 55262 Transverse "B" Heat Treat. V21 to V30

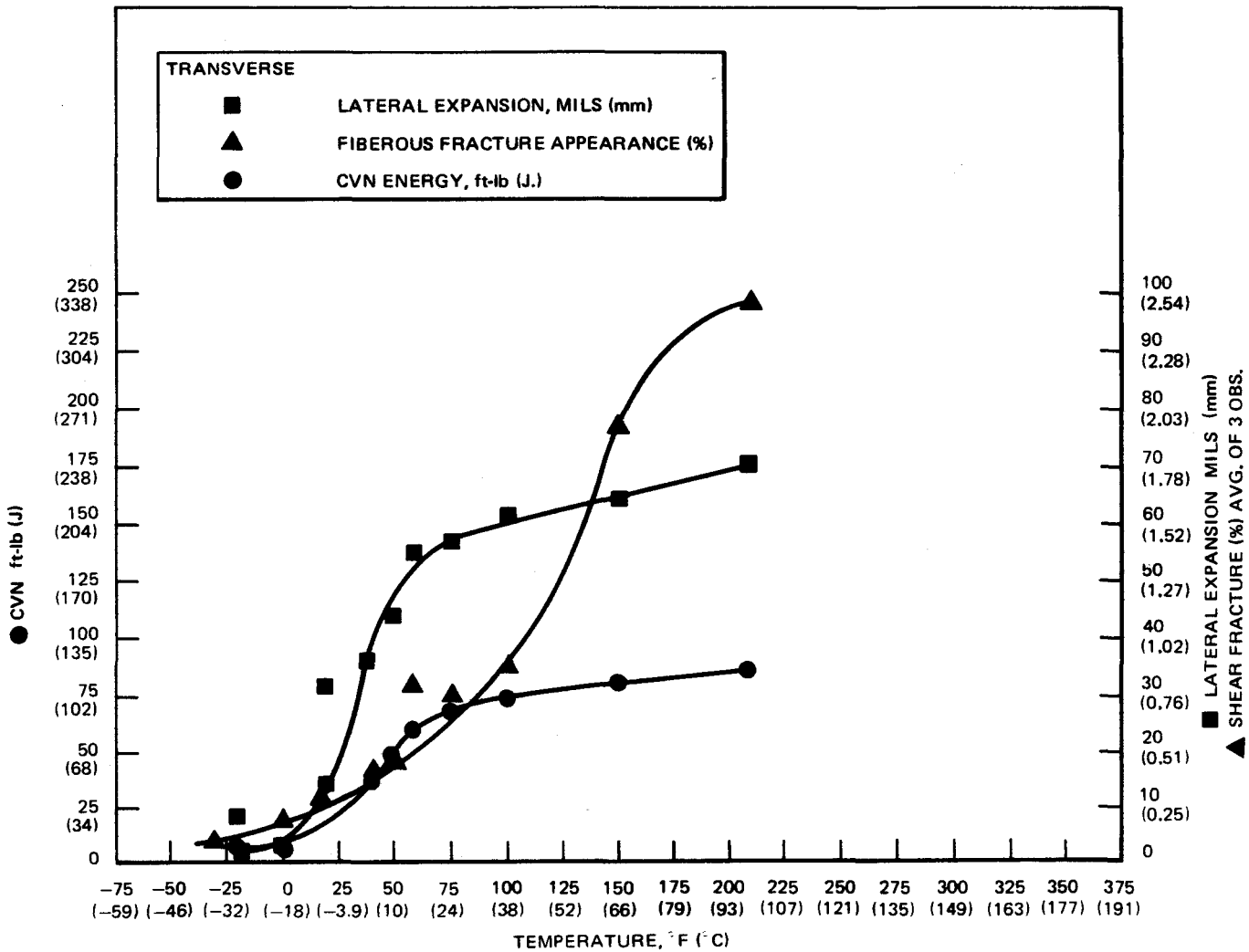

Figure 9. VAR Heat 55262 Transverse "C" Heat Treat. V31 to V40

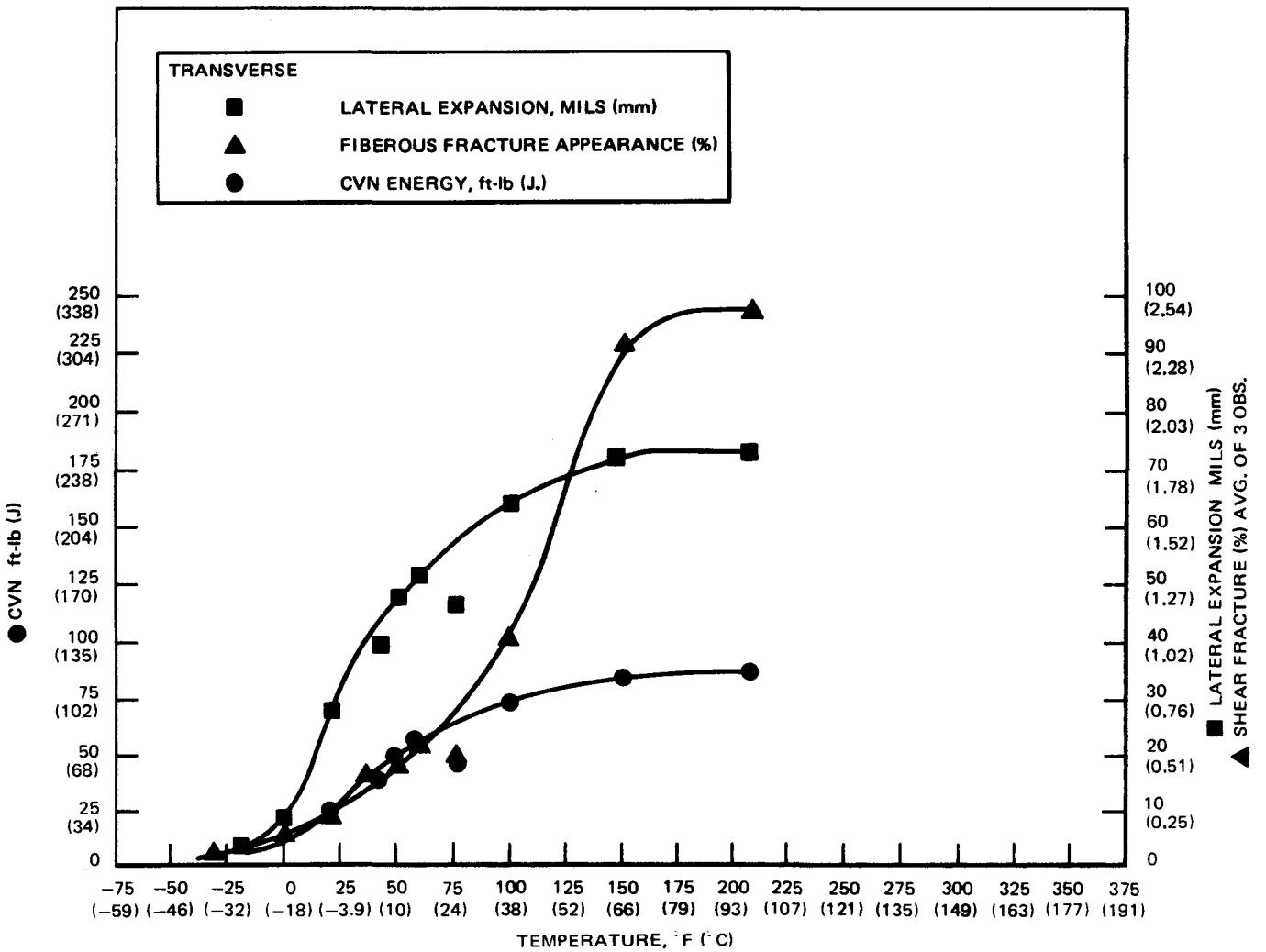

Figure 10. VAR Heat 55262 Transverse "D" Heat Treat. V41 to V50

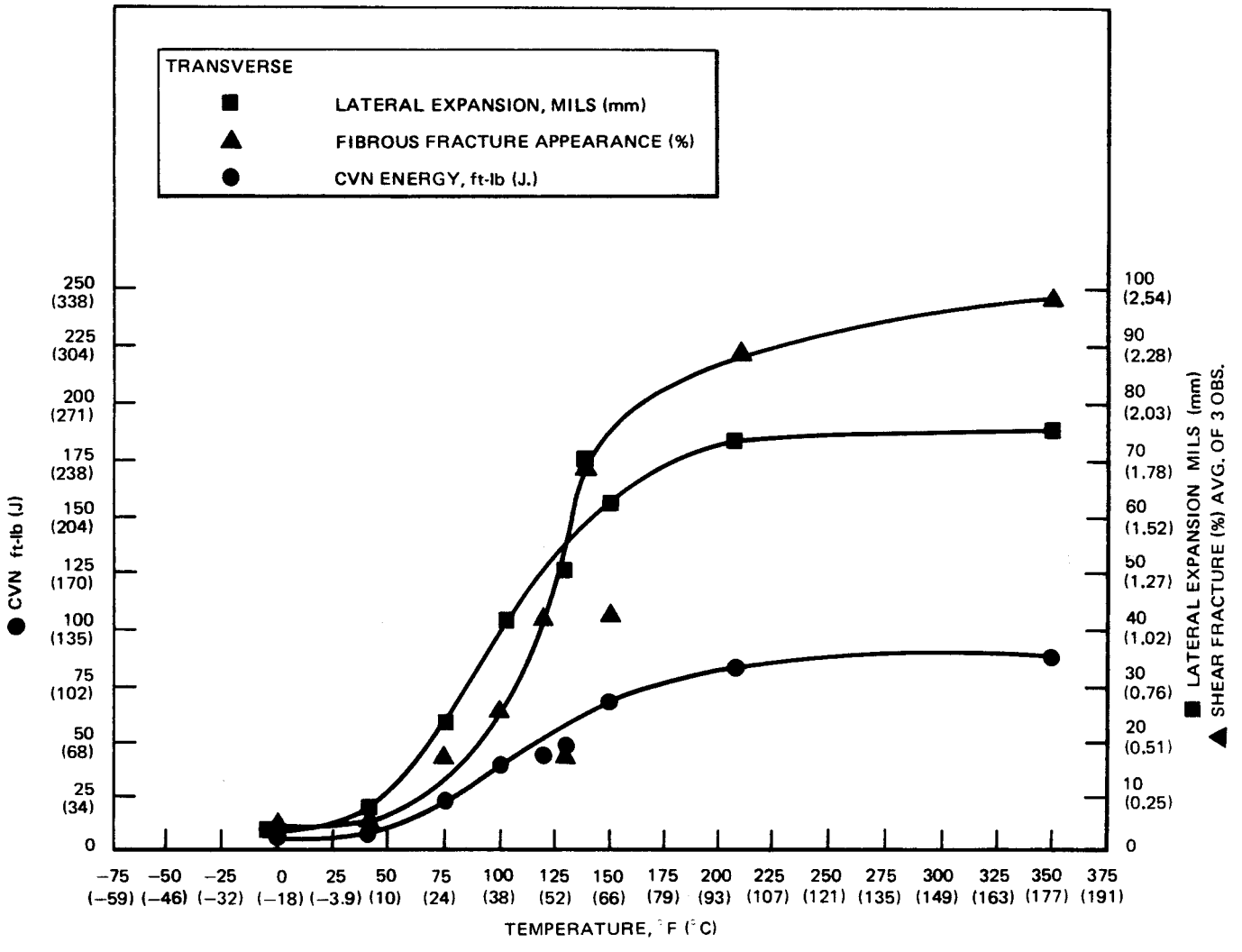

Figure 11. VAR Heat 55262 Transverse "E" Heat Treat. V51 to V60

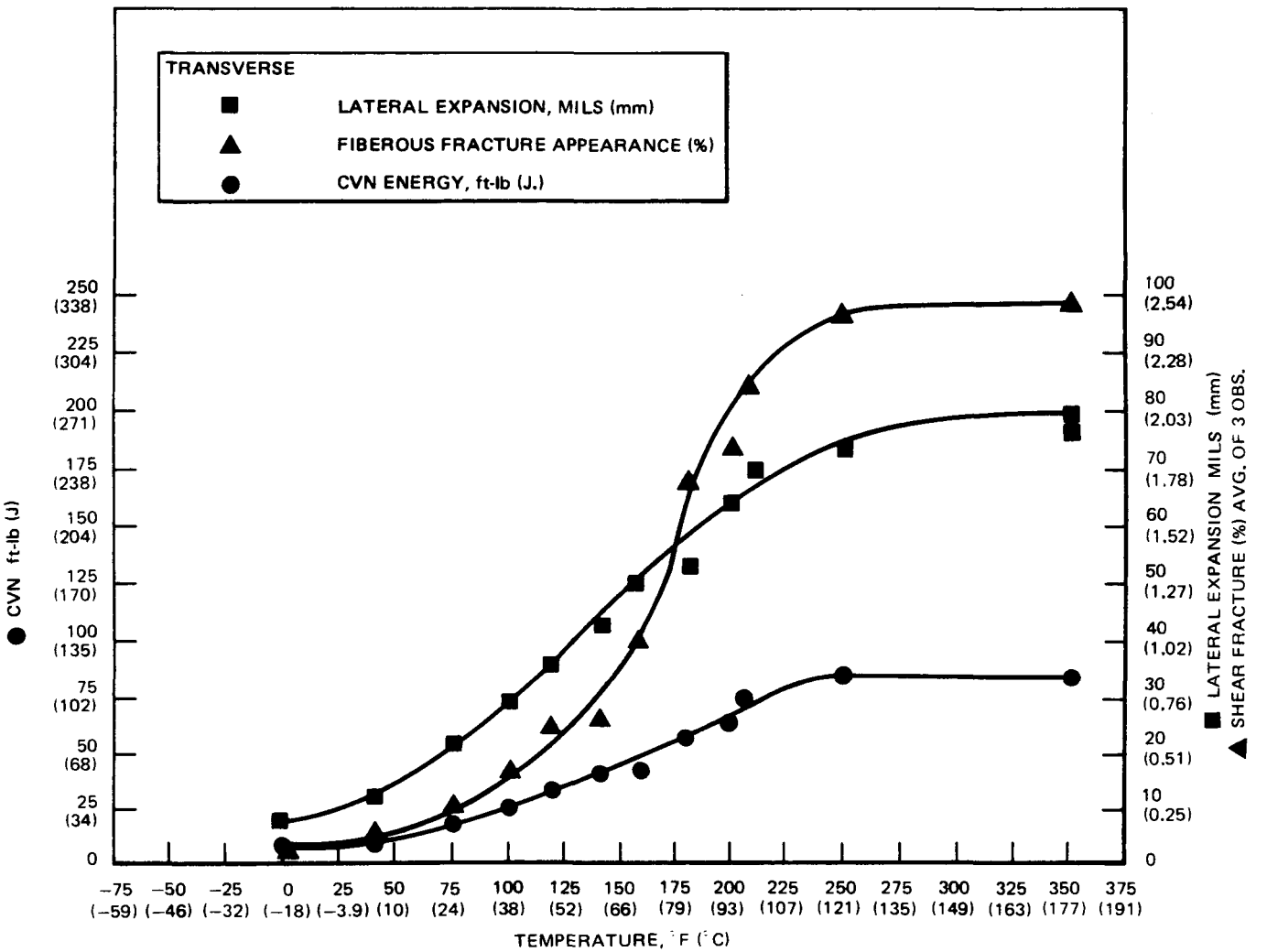

Figure 12. VAR Heat 56067 *Transverse "B" Heat Treat. V61 to V73.*

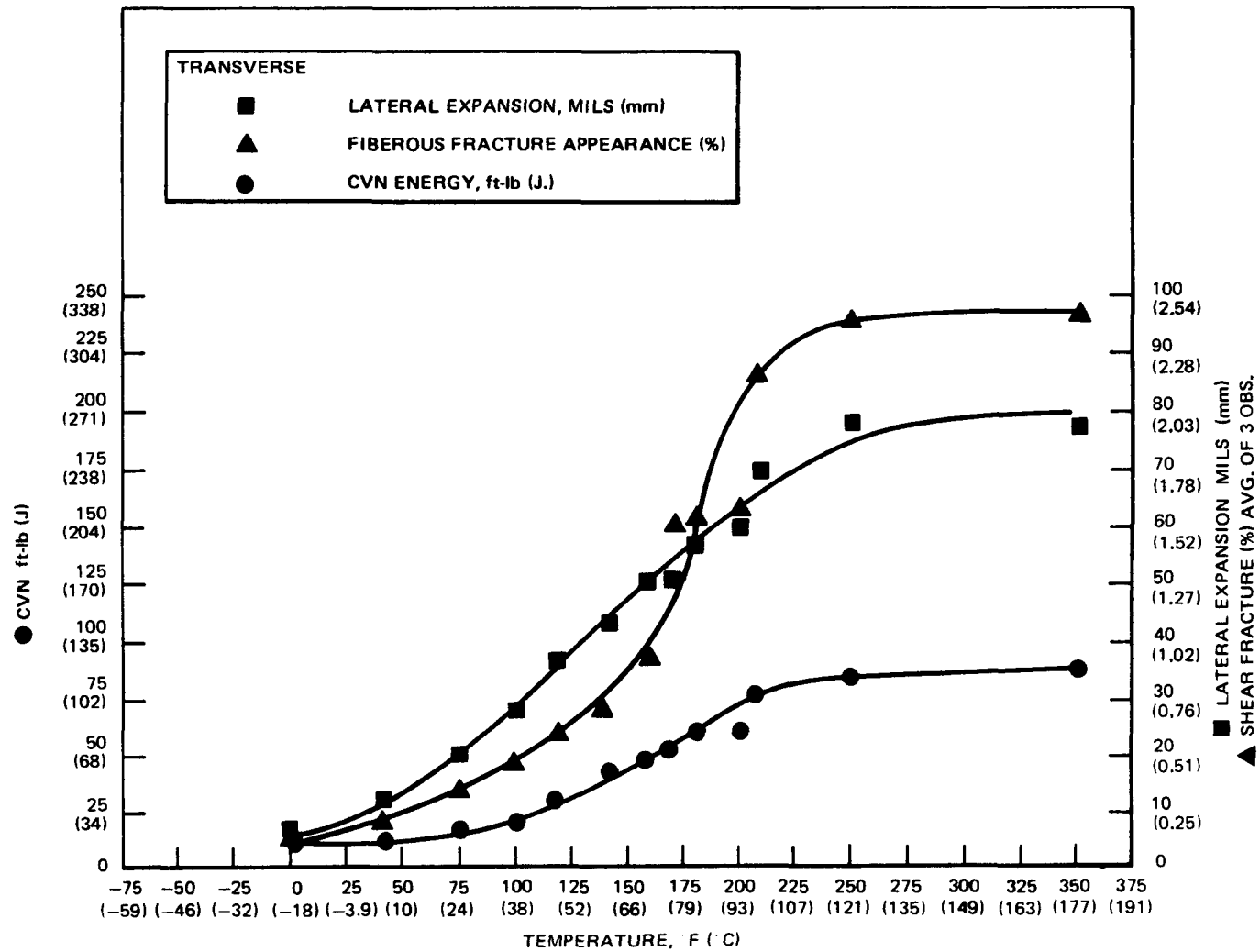

Figure 13. VAR Heat 56067 Transverse "D" Heat Treat. V74 to V86

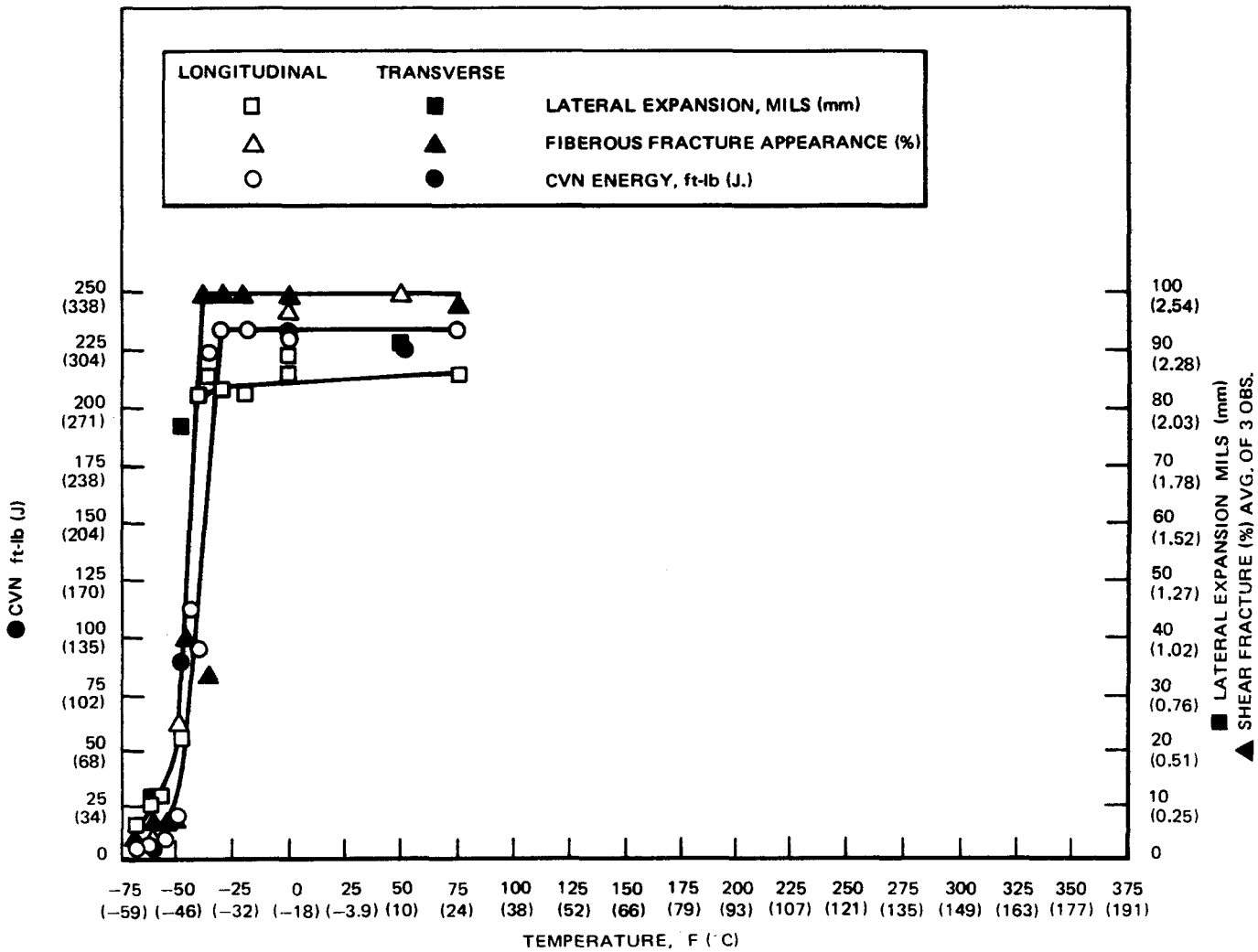

Figure 14. ESR Heat R0110 Longitudinal○ Transverse● "B" Heat Treat. V87 to V97 Longitudinal, V98 to V101 Transverse

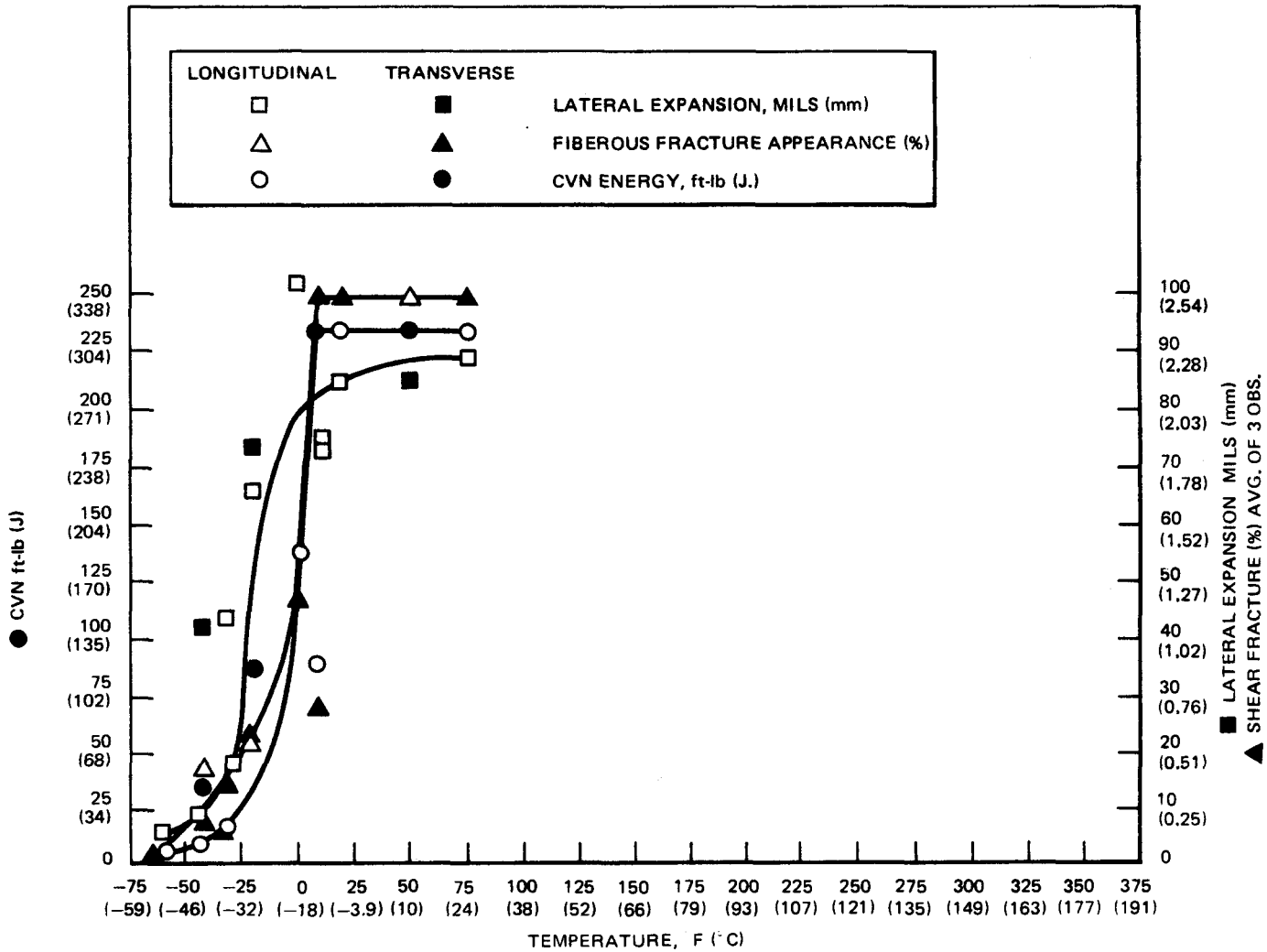

Figure 15. ESR Heat R0110 Longitudinal ○ Transverse ● "D" Heat Treat. V102 to V111 Longitudinal, V112 to V114 Transverse

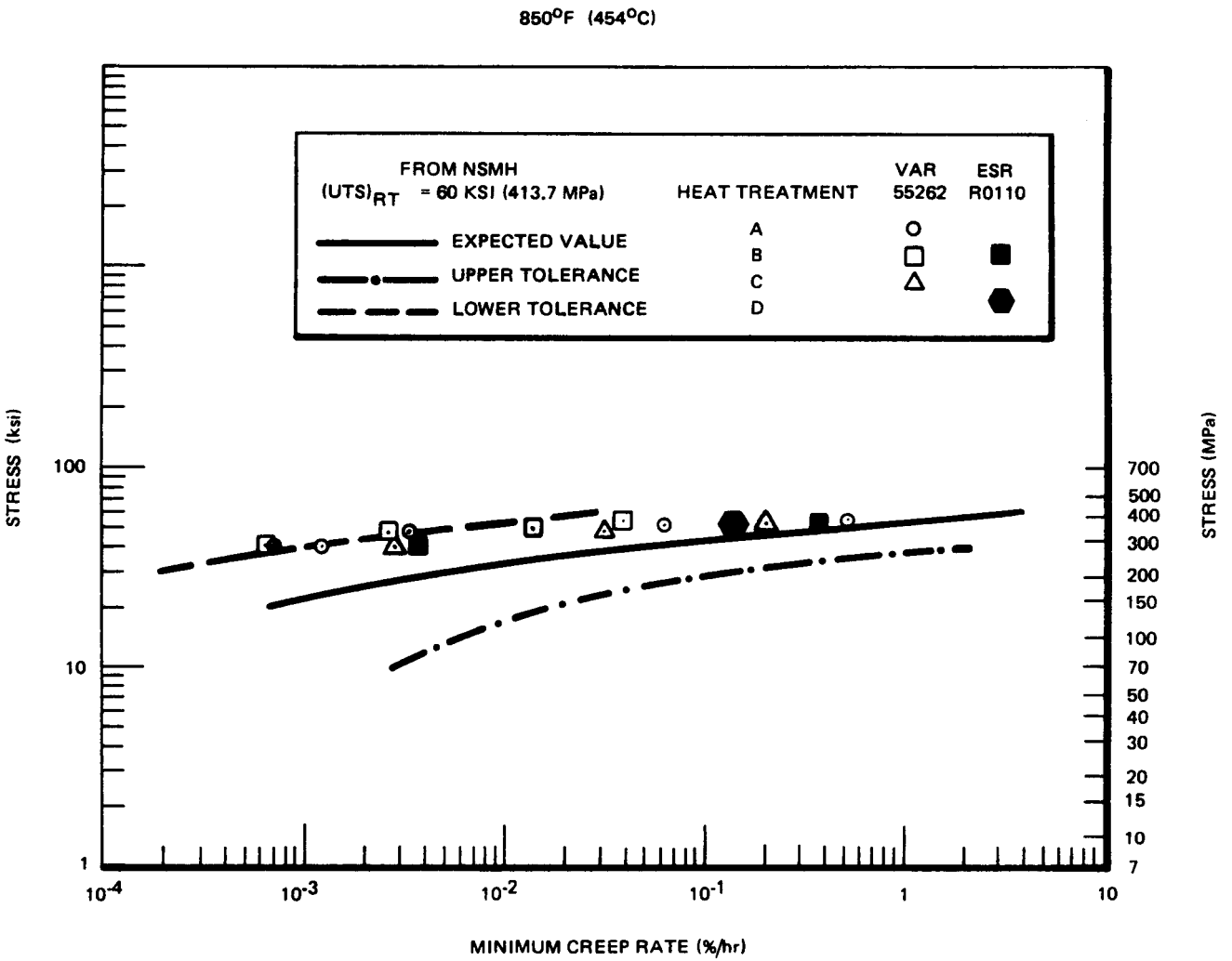

Figure 16. Relationship Between Stress and Minimum Creep Rate for 0.10%C, 2¼ Cr – 1 Mo Steel at 850°F (454°C)

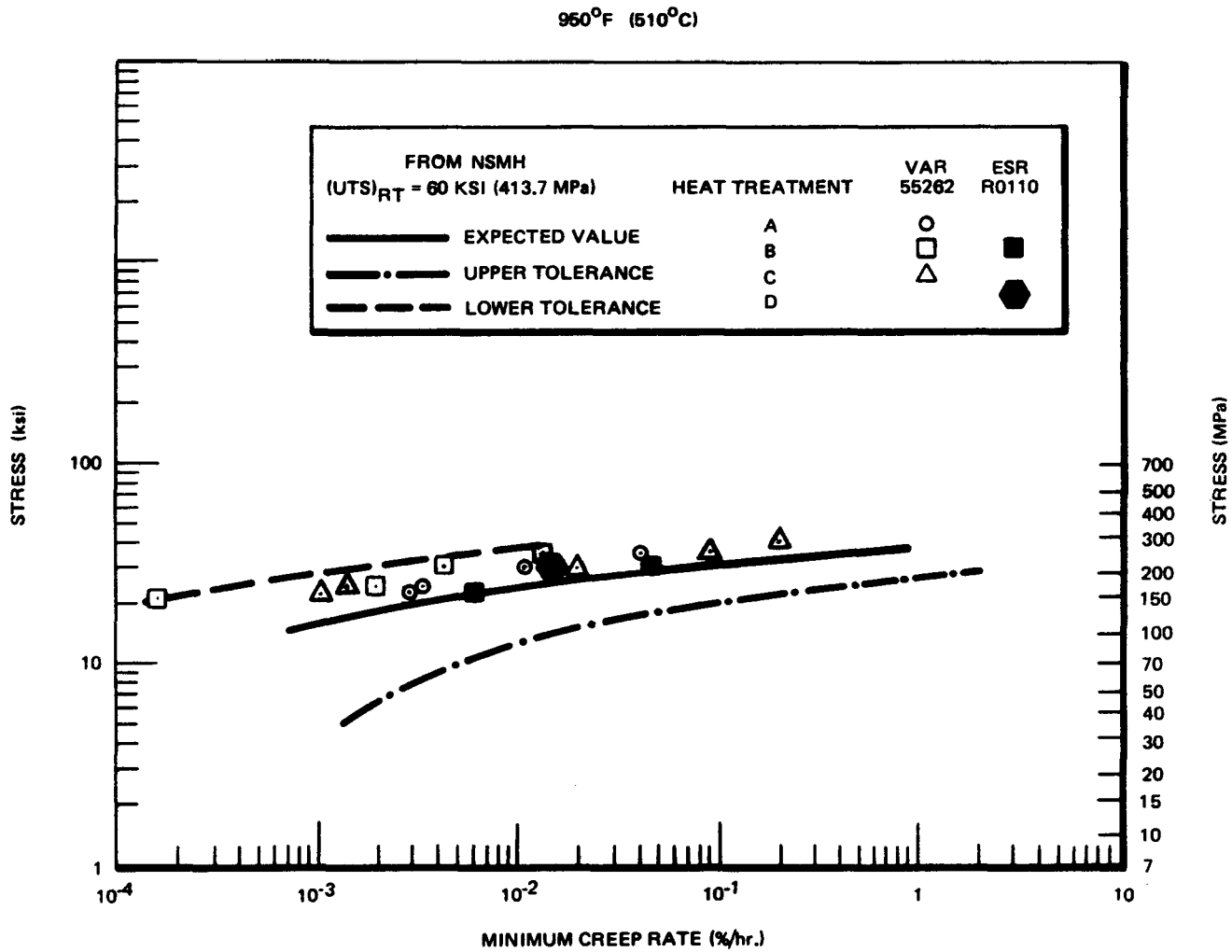

Figure 17. Relationship Between Stress and Minimum Creep Rate for 0.10%C, 2¼ Cr-1 Mo Steel at 950°F (510°C)

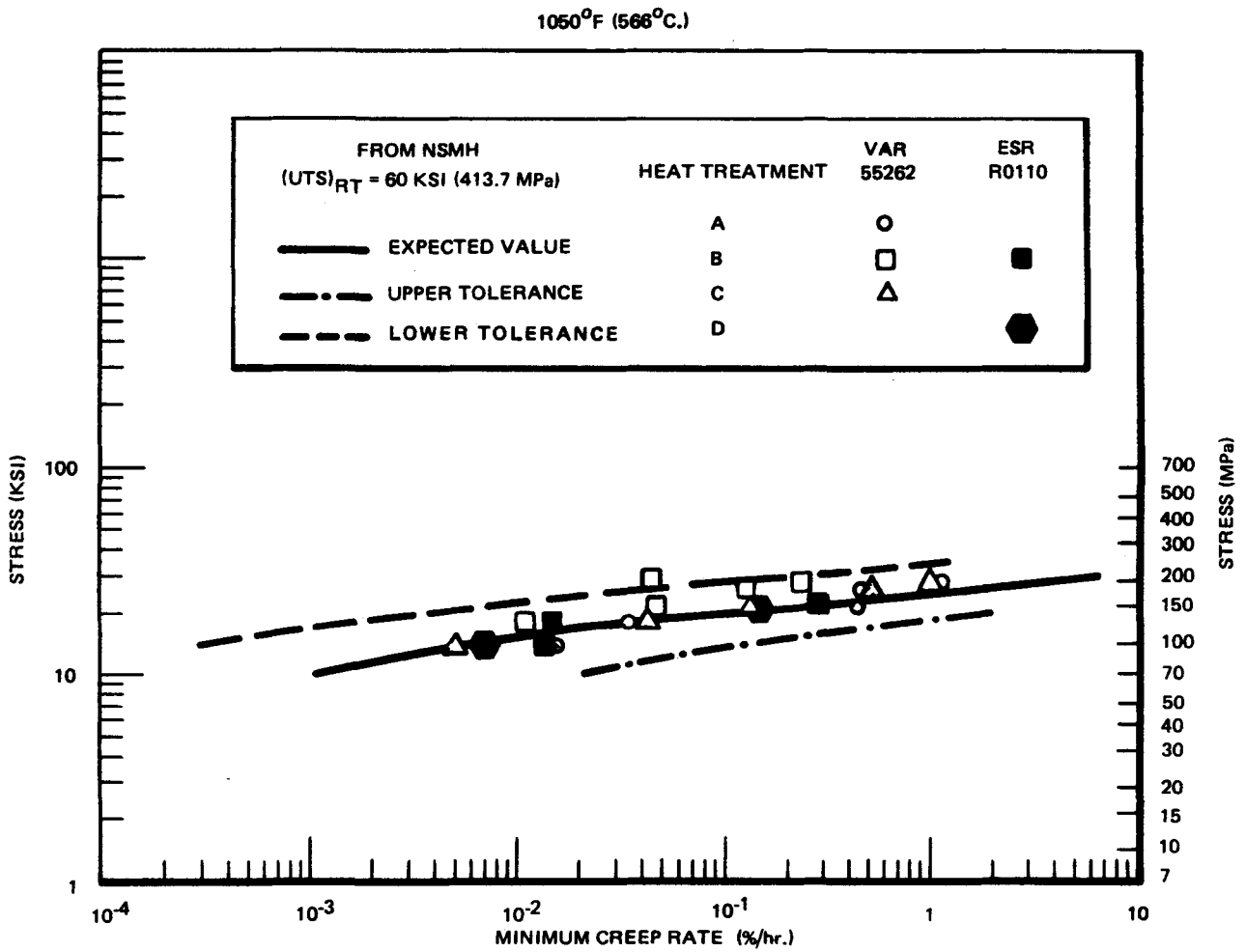

Figure 18. Relationship Between Stress and Minimum Creep Rate for 0.10%C, 2¼ Cr-1 Mo Steel at 1050°F (566°C)

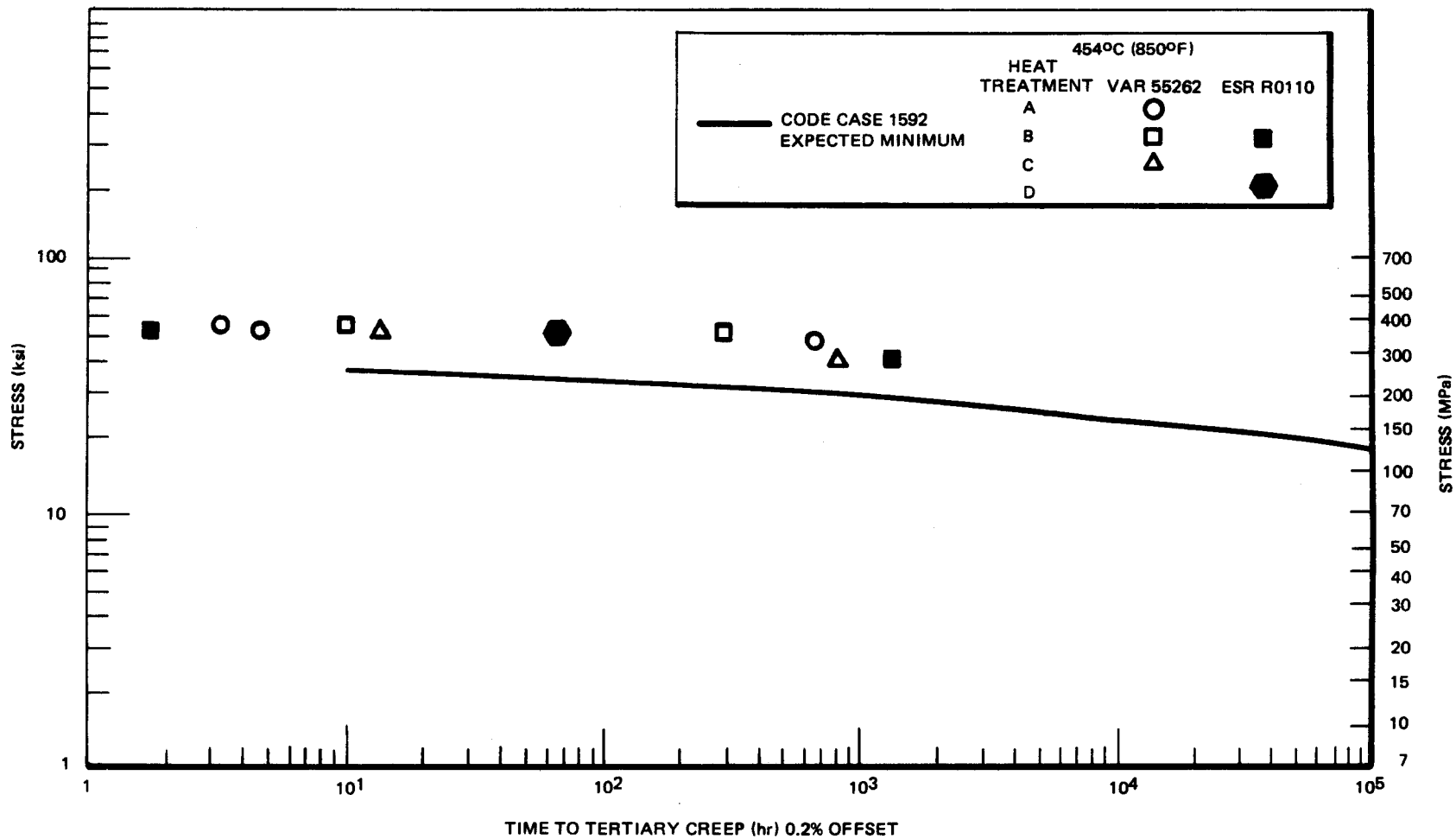

Figure 19. Relationship Between Stress and Time to Tertiary Creep for 0.10%C, 2¼ Cr – 1 Mo Steel at 850°F (454°C)

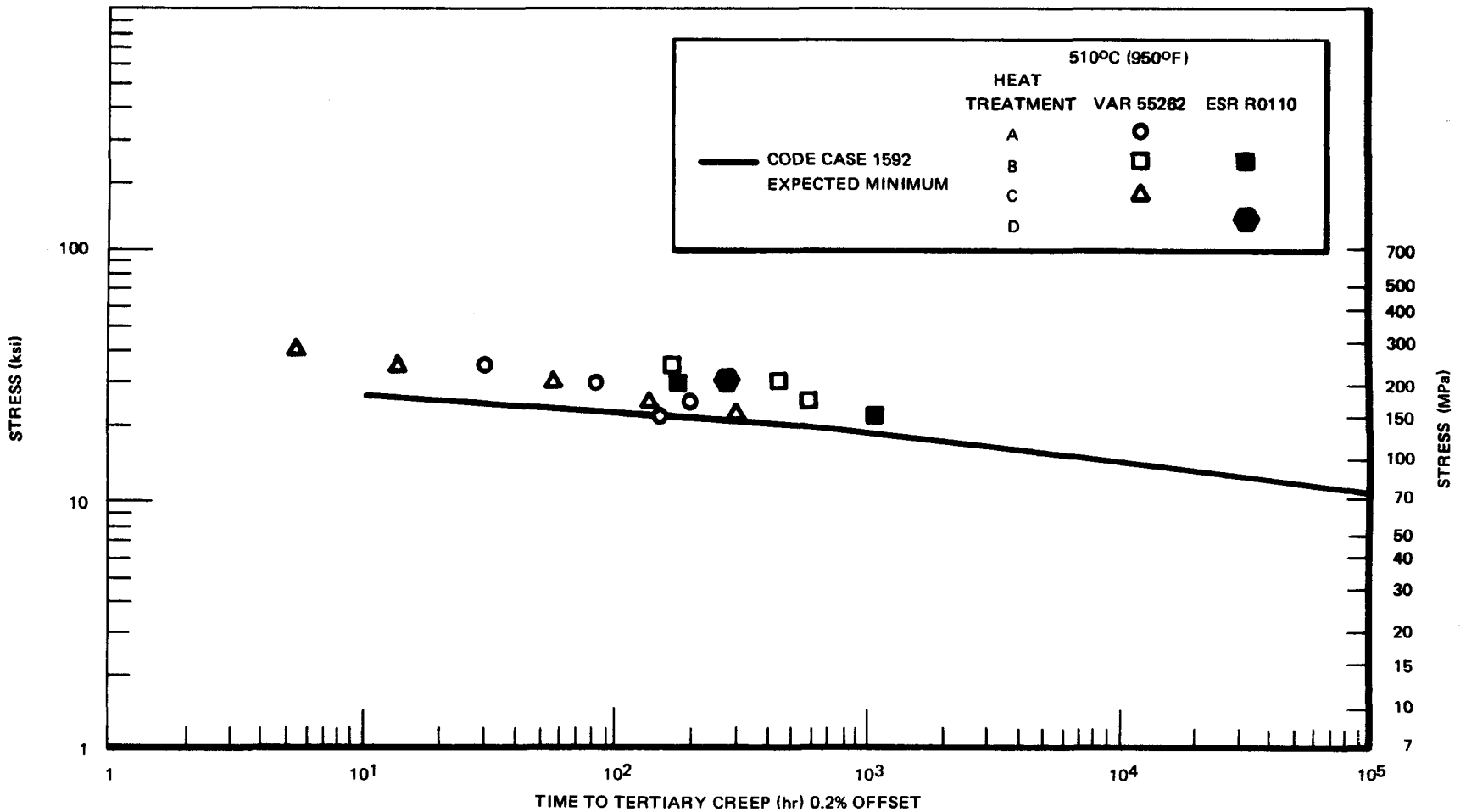

Figure 20. Relationship Between Stress and Time to Tertiary Creep for 0.10%C, 2¼ Cr – 1 Mo Steel at 950°F (510°C)

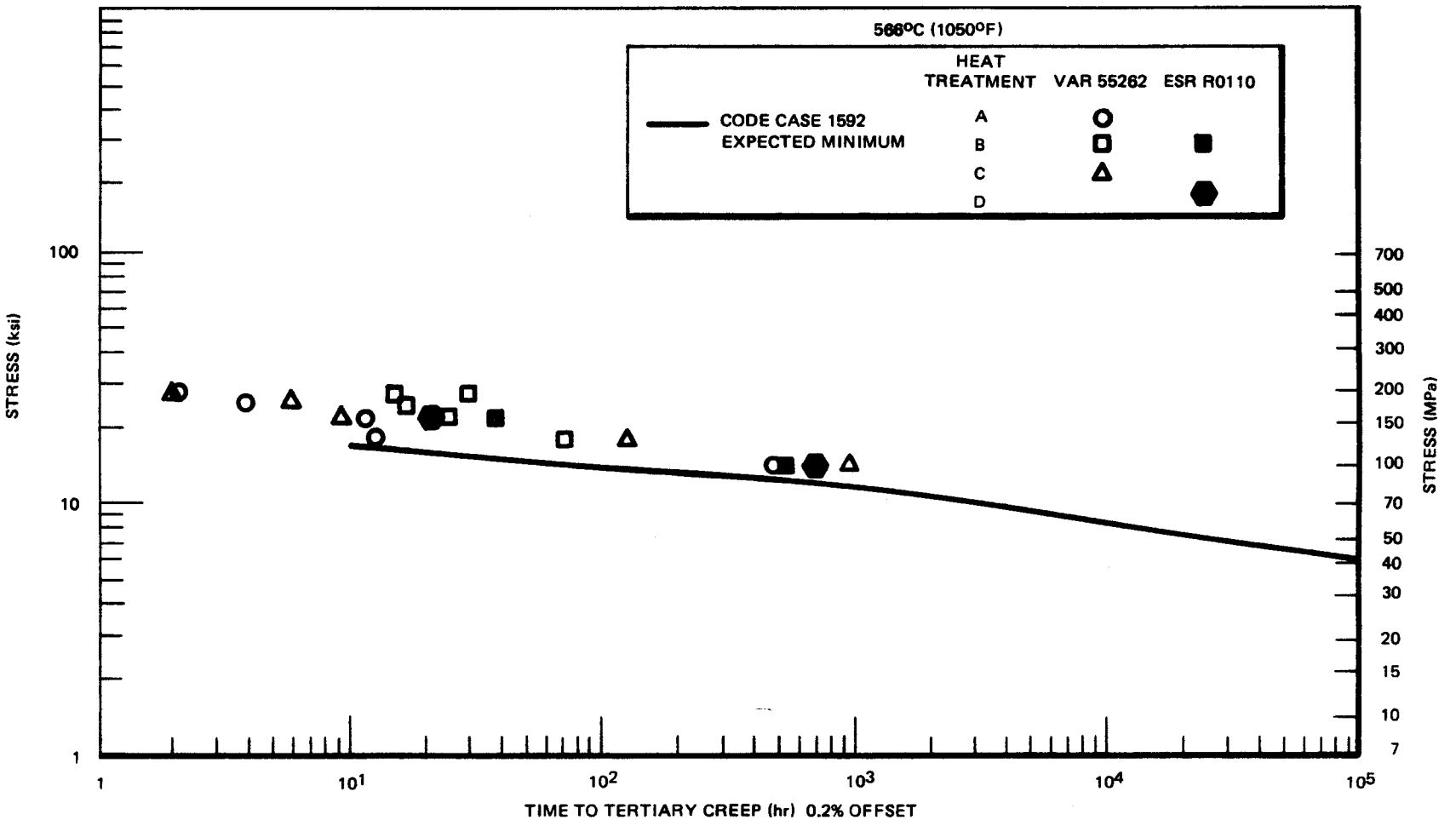

Figure 21. Relationship Between Stress and Time to Tertiary Creep for 0.10%C, 2¼ Cr – 1 Mo Steel at 1050°F (566°C)

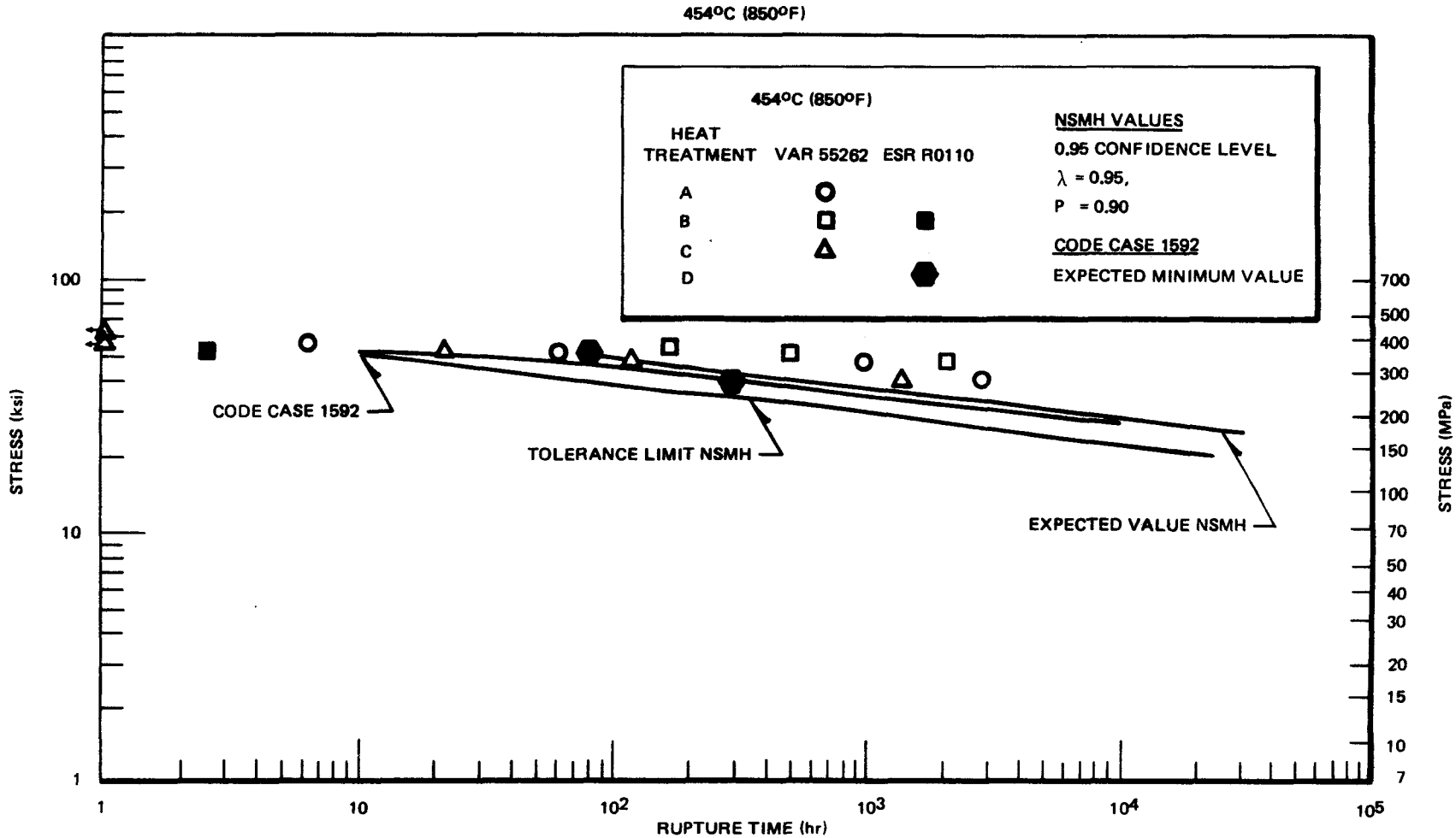

Figure 22. Relationship Between Stress and Rupture Time for 0.10 %C, 2¼ Cr – 1 Mo Steel at 850°F (454°C)

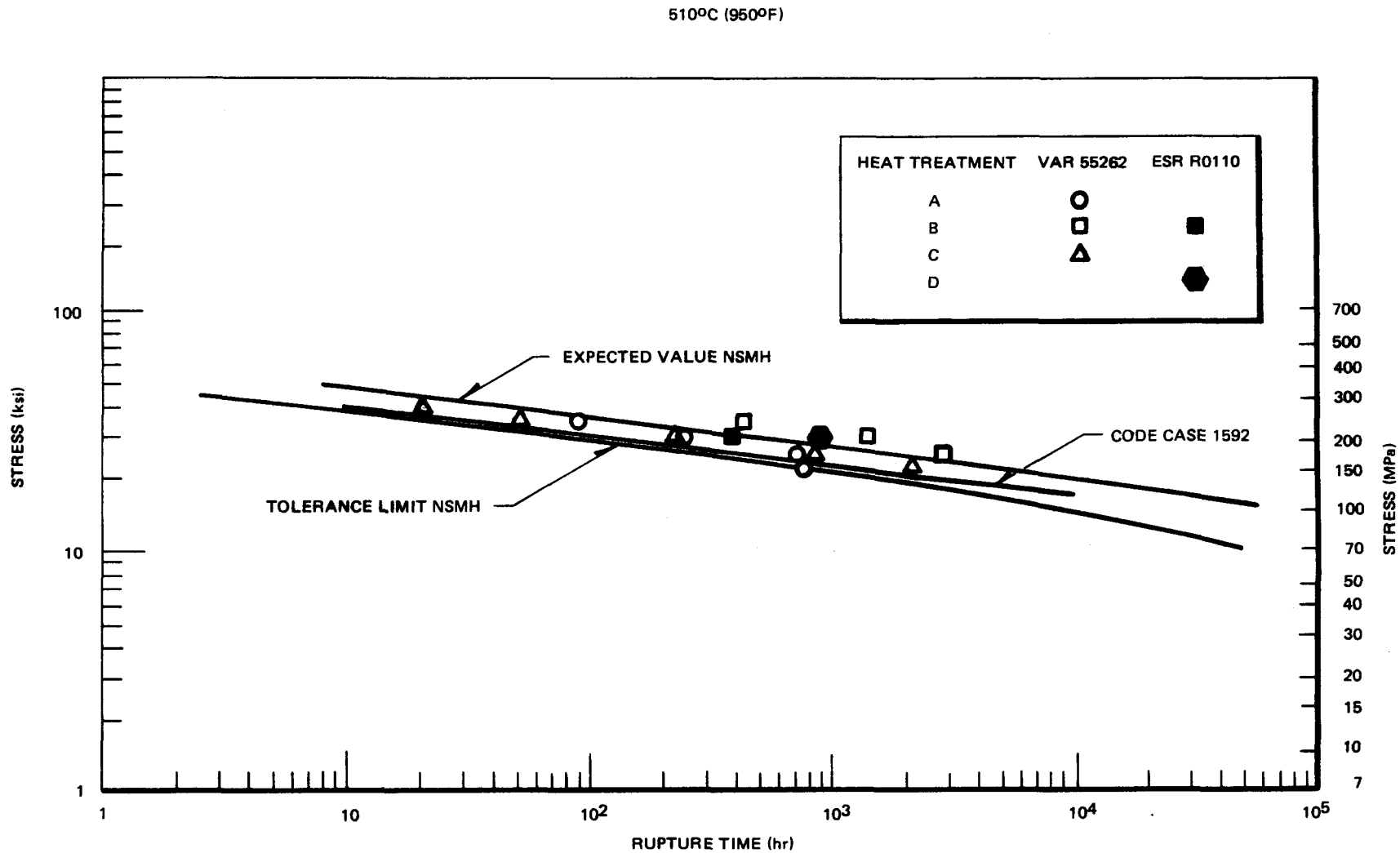

Figure 23. Relationship Between Stress and Rupture Time for 0.10%C, 2¼ Cr – 1 Mo Steel at 950°F (510°C)

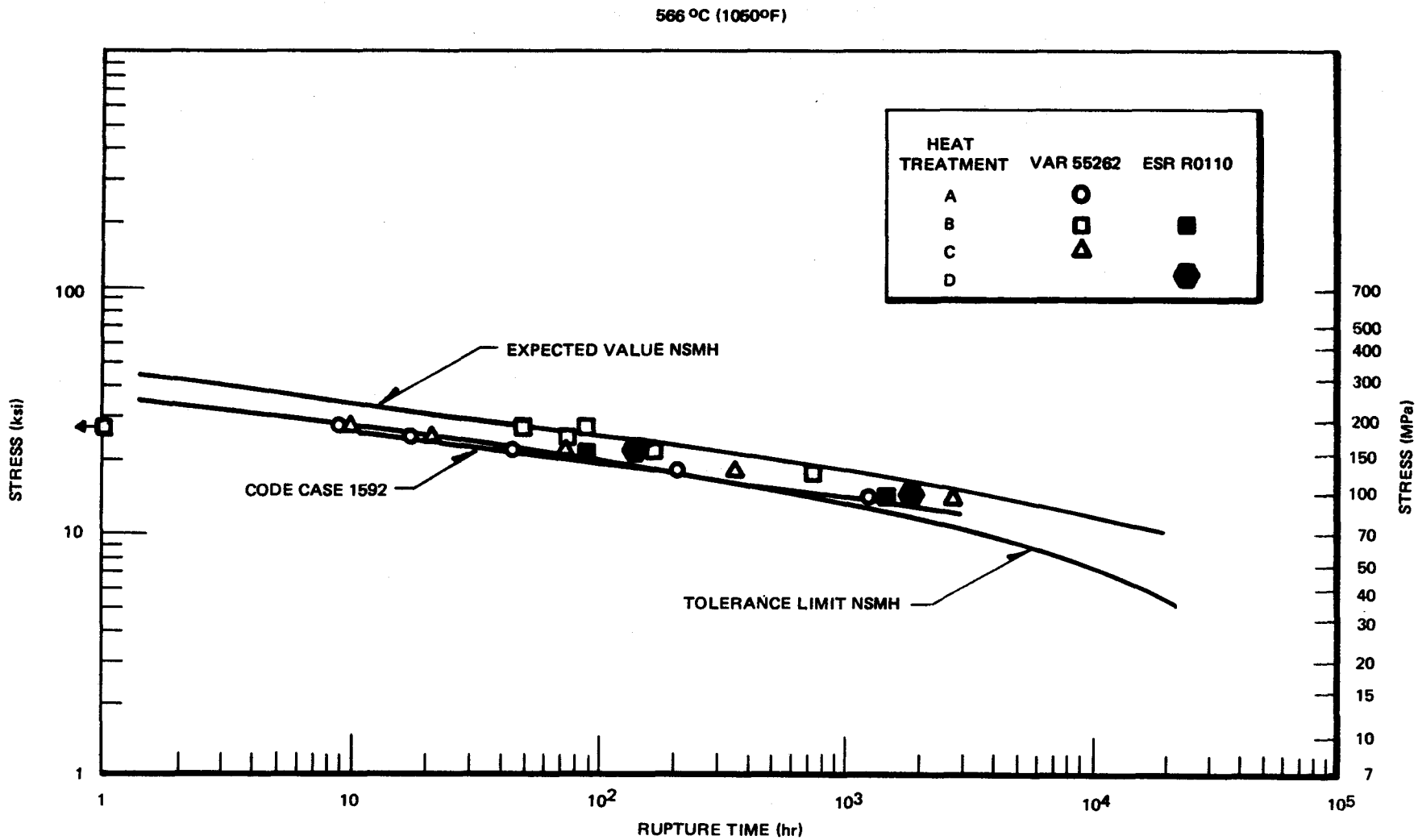

Figure 24. Relationship Between Stress and Rupture Time for 0.10%C, 2¼ Cr – 1 Mo Steel at 1050°F (566°C)

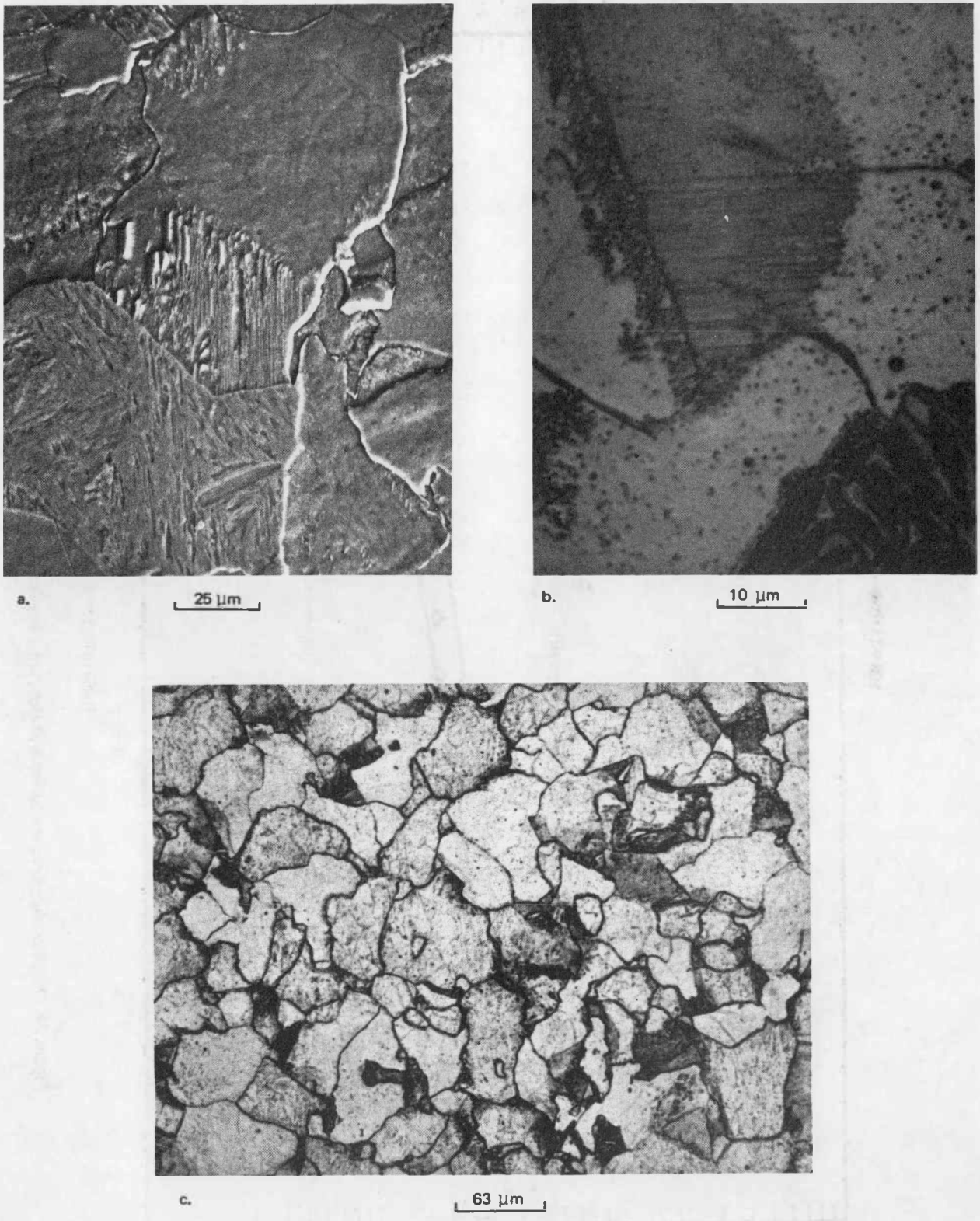

Figure 25. Typical micrographs of VAR heat 55262 isothermally transformed at 704°C (1300°F) for 120 minutes and water quenched (a) scanning electron micrograph, (b) and (c) optical micrographs

IV. FRICTION, WEAR AND SELF-WELDING

The purpose of this testing is to provide characterization of the friction, wear, and self-welding properties of steam generator materials planned for use in the CRBRP. The testing is performed under prototypic conditions of loading and sodium environment. To assure that in-service performance is not impaired by excessive galling and seizure or high rates of tube wall thinning, these tests will be run on model tube-to-tube support configurations. Tailoring of materials and/or special fabrication processes and treatments may become necessary for use in CRBRP.

PIN-ON-PLATE TESTS ON 2 1/4 Cr - 1 Mo

To date, screening tests (pin-on-plate) on air melted 2 1/4 Cr - 1 Mo steel in flowing sodium have been performed at Atomics International. The data are presented in Figure 1 which shows the test temperature profile along with the corresponding average static and dynamic coefficients of friction. Data on 316 stainless steel are shown for comparison. Supplementary base line data have been generated (W-ARD) utilizing a similar pin-on-plate geometry. The temperature profile and average maximum coefficient of dynamic friction at 2.1 and 6.9 MPa (300 and 1000 psi) are shown in Figure 2. A summary of the parameters used in these two tests and comparative results are presented in Table I. In general, the static and dynamic coefficients measured by AI and W-ARD are very similar, even though there were great differences in velocity and total distance traveled.

The W-ARD testing included breakaway friction studies at 538, 427, and 317°C (1000, 800, and 600°F) as noted on Figure 2 (solid circles). These tests consisted of 63.5 cm (25 inches) of rubbing followed by a load/dwell period for various time intervals. The data are plotted in Figure 3 showing a linear relationship between the breakaway coefficient ($\Delta\mu$) and the square root of time. This generally indicates behavior corresponding to Fick's second law. This suggests that a diffusion process controls the value of breakaway coefficients.

Post test evaluation of the wear specimens (W-ARD test 5-507) revealed a loss of material on both the pin and plate. The dimensional and volumetric changes are shown on Table II. Material build-up was found on both plate specimens at the end of the weld scar, indicating that galling had occurred.

STEAM GENERATOR TESTS

Long term performance data on VAR tubing against an air melted tube support plate are required to assure sodium-water boundary integrity. GE has supplied all the required testing conditions to W-ARD. These tests should satisfy the above data needs[1]. Testing priorities have been revised, incorporating this request into a plan, DAD/DRS 31.1.27 plus Addendum I, (pending approval). The specific test parameters are outlined in Table III. Stage I consists of three short scoping tests utilizing the test fixture shown in Figure 4. These tests will yield prototypic results for the worst wear conditions, namely 529°C (985°F) and 445 N (100 lb.) contact loads. At the same time, this will establish the dependence of wear on stroke travel and velocity. These scoping tests were started mid-October and will be complete by the end of December. At this point, depending on the scoping test results, one of two options for further testing will be exercised:

Option 1: If the Stage I testing demonstrates acceptable wear, then testing of the back-up material would not be initiated and testing of the reference alloy would be discontinued after Stage IIa. The Stage IIa tests are intended to permit a more realistic determination of wear, self-welding, and galling as a function of dwell time. These tests would also confirm the results from Stage I and establish a relationship between load and wear by utilizing the multiple loading fixture, Figure 5. It is anticipated that for this option, testing would be carried out in Vessel 2 on the reference material (2 1/4 Cr - 1 Mo) only; testing of the alternate materials would be eliminated.

Option 2: If the Stage I scoping tests demonstrate unacceptably heavy wear, then testing must proceed through Stage IIb, including the alternate materials matrix. Utilization of the dormant vessel (1)

would be required for the alternate materials. Testing would parallel the conditions imposed on the reference material, see Matrix Table III. Continuation of the reference material testing is required to establish the extent to which heavy wear persists under less severe loading conditions. Although some redesign may be required for heavy loading conditions, it may be reasonable to continue to use 2 1/4 Cr - 1 Mo for less severe steam generator conditions. The inclusion of the alternate materials at this point will allow selection of preferable material for the worst steam generator wear conditions. The test fixture configuration for the alternate materials is shown in Figure 6.

To date, Test 6-538a (Table III) has been completed, with 6-538b in progress. No data analysis has been performed, but visual examination shows galling type wear. Measurements made during the test show an increase in the friction coefficient at the end of each stroke, indicating material build-up. No problems were encountered with the hardware used in these tests.

Completion of the steam generator tests is tentatively planned for June 1976. The need date for this data is July 1976. The scheduling of the pump materials portions of the test matrix has not been finalized.

PUMP TESTS

Sodium pump materials are another area requiring wear and self-welding characterization. Proposed testing of selected materials (i.e., stellites and colmonoys) have been submitted in GE's input to DAD 51.27B[1]. The original test scope has been limited to materials testing (pin-on-plate) rather than model tests because of funding and facilities limitations. Current pump design is not finalized at this time and test parameters reflect the best estimates available.

Cyclic run/dwell tests to simulate 100 start-up and shut-down sequences are planned for sodium pump bearing materials, Table IVa. The long term periods of inactivity, up to 6 months, will be investigated under the test matrix in Table IVb. These tests simulate the self-welding environment present

on pump material surfaces (nozzle outlet) under a 82.7 MPa (12,000 psi) preload. They will determine "breakaway" coefficients, wear, and galling. Effects of wear and self-welding will be assessed visually.

REFERENCES

1. Letter, R. J. Michalak (GE) to H. S. McCreary (W-ARD), "Task 10, LMFBR Steam Generator Systems Development Program, Subtask G-3", GE-W-10-GE-1110, Encl. (input to DAD 51.27B).

TABLE I

TESTING TO DATE: PIN-ON-PLATE

TESTING LABORATORY	TEMPERATURE RANGE °C (°F)	LOADS MPa (psi)	PIN DIAMETER cm (in)	STROKE (cm) (in)	VELOCITY (cm/sec) (in/sec)	TOTAL TRAVEL cm (in)	FRICTION COEFFICIENTS		
							BREAKAWAY	STATIC	DYNAMIC
ATOMICS INTERNATIONAL	626/232 (1160/450)	5.5 (800)	12.7 (.5)	.635 (.25)	.178 (.07)	297 (117.5)	>2.0	.84	1.15
WESTINGHOUSE ARD	530/204 (1000/400)	6.89/2.06 (1000/300)	2.54 (1.0)	.761 (.31)	152 (60)	6970 (2750)	.71	.87	1.49

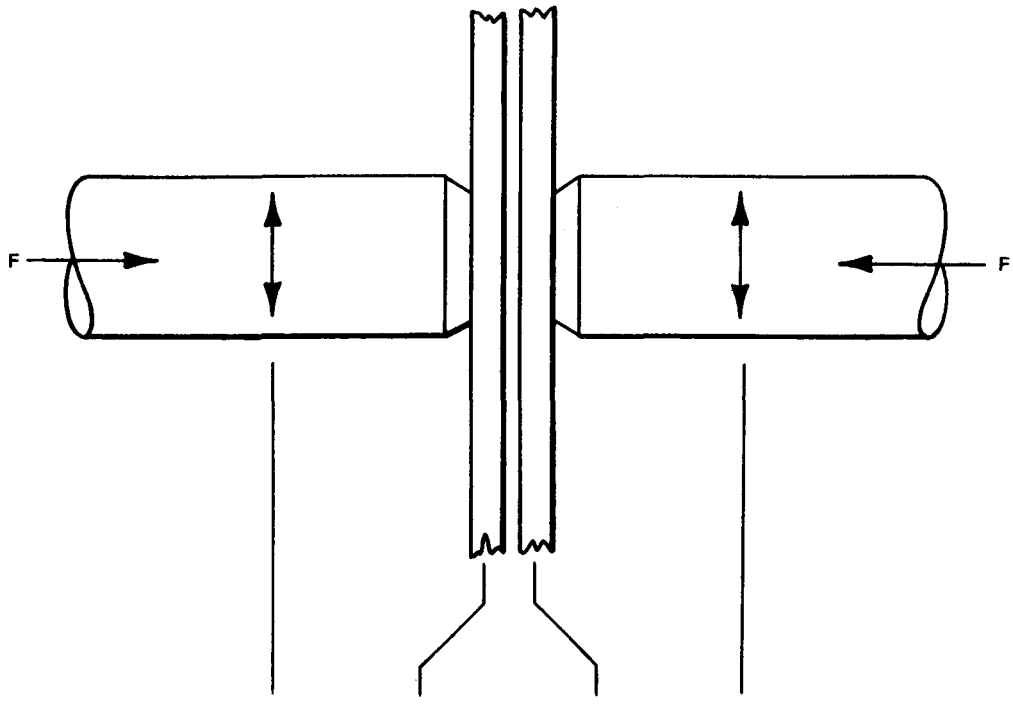

MAXIMUM WEAR DIMENSIONAL CHANGE	-.0049	(+.0070) -.0055	(+.0057) -.0056	-.0049	in
	-0.012	(+.0178) -.0140	(+.0145) -.0142	-0.012	cm
VOLUMETRIC CHANGE	-101.93	-20.74	-17.37	-97.17	(cc x 10^4)

\+ GAIN (MATERIAL BUILDUP)
\- LOSS

TABLE II POST-TEST SPECIMEN EXAMINATION, 6970 cm (2750 in) OF ACCUMULATIVE TRAVEL (WARD TEST 5-507).

TABLE III

PLANNED TEST MATRIX - "Primary" and "Back-up" Steam Generator Tube-to-Tube Support Materials
(To Be Conducted in W-ARD's Sweater 1 Facility)

		Vessel 2 "Primary" Matrix - 2 1/4 Cr - 1 Mo VS. Self						Vessel 1 "Back-up" Matrix - 2 1/4 Cr - 1 Mo VS. Inconel 718 / Ingot Iron						
	Test No.	Temperature °C (°F)	Contact[1] Load kg (lbs)	Dwell[2] Time (hrs/day)	Stroke[3] Travel cm (in)	Stroke[3] Velocity (in/min)	Total Travel cm (in)	Temp °C (°F)	Contact[1] Load kg (lbs)	Dwell[2] Time (hrs/day)	Stroke[3] Travel cm (in)	Stroke[3] Velocity (in/min)	Total Travel cm (in)	Vessel[5] Residence Time (hrs)
STAGE I	6-538a	542 (935)	45.4 (100)	---	.25 (.10)	1.5 (.6)	1002 (4000)	--	--	---	--	--	--	134
	6-538b	542 (935)	45.4 (100)	---	.025 (.01)	1.5 (.6)	1002 (4000)	--	--	---	--	--	--	134
Scoping Tests	6-539	542 (935)	45.4 (100)	---	.25 (.10)	1.5 (.6)	254 (1000)	--	--	---	--	--	--	278
STAGE IIa	6-540a	542 (935)	9.1/13.6/ 22.9/45.4 (20/30/50/100)	16	.25 (.10)	1.5 (.6)	1002 (4000)[4]	*	9.1/22.9	*	*	*	*	471
	6-540b	487 (835)	↓	16	.25 (.10)	1.5 (.6)	1002 (4000)[4]	*	9.1/22.9	*	*	*	*	471
	6-540c	342 (650)		16	.25 (.10)	1.5 (.6)	1002 (4000)[4]	*	9.1/22.9	*	*	*	*	471
STAGE IIb	6-541a	542 (935)		---	.25 (.10)	1.5 (.6)	1002 (4000)[4]	*	9.1/22.9	*	*	*	*	134
	6-541b	487 (835)		---	.25 (.10)	1.5 (.6)	1002 (4000)[4]	*	9.1/22.9	*	*	*	*	134
	6-541c	342 (650)		---	.25 (.10)	1.5 (.6)	1002 (4000)[4]	*	9.1/22.9	*	*	*	*	134

(1) Load calibrated over a 1 1/2 in. support plate contact. Multiple loads accomplished with special test fixture, Figure 2.
(2) Dwell periods during overnight and weekend shutdowns throughout tests (loaded condition).
(3) Maximum rate of stroke travel and velocity pending auxiliary testing during STAGE I.
(4) Interim shutdown and surface inspection measurement after 254 cm (1000 in.) travel.
(5) 471 hrs. < 3 wks., 168 hrs/wk.

* Identical parameter to that used in Vessel 2 on primary matrix.

TABLE IV

OVERALL FRICTION, WEAR, AND SELF-WELDING TEST MATRIX

	Material	Temperature °C (°F)	Load MPa (psi)	Stroke: Velocity SMPM (SFPM)	Stroke: Length m (ft)	Total Travel m (ft)		Dwell
A.	SODIUM PUMP BEARINGS*							
I	Stellite 6 (316 SS)	538 (1000)	.394/6.89 (500/1000) (Hertzian)	38 (125) (unidirectional)	228 (750)	22800 (75,000)		3 - 4 hrs
		316 (600)	↓	↓	↓	↓		↓
		427 (800)						
II	Colmonoy 5	538 (1000)						
		316 (600)						
		427 (800)	↓	↓	↓	↓		↓
B.	SODIUM PUMP INTERNALS			(Reciprocating)				
I	316	538 (1000)	82.5 (12000)** (Hertzian)	0 cps	0	0		1 MTH @ 204°C + 1 MTH @ 316°C (1 MTH @ 400°F + 1 MTH @ 600°F)
		↓	↓	.1	.317 (.125)	4.58×10^5	(1.8×10^5)	↓
				.2	.076 (.03)	3.66×10^4	(1.4×10^4)	
				16.0	.032 (.012)	1.16×10^5	(4.6×10^4)	
II	Stellite			0	0	0		
				.1	.317 (.125)	4.58×10^5	(1.8×10^5)	
				2.0	.076 (.03)	3.66×10^4	(1.4×10^4)	
		↓	↓	16.0	.032 (.012)	1.16×10^4	(4.6×10^4)	↓

* Includes 100 intermittent dwell periods

** Unloaded to 5,000 psi Hertzian during dwell periods

NOTE: Materials and test conditions represent the best estimates available and will be updated as design progresses.

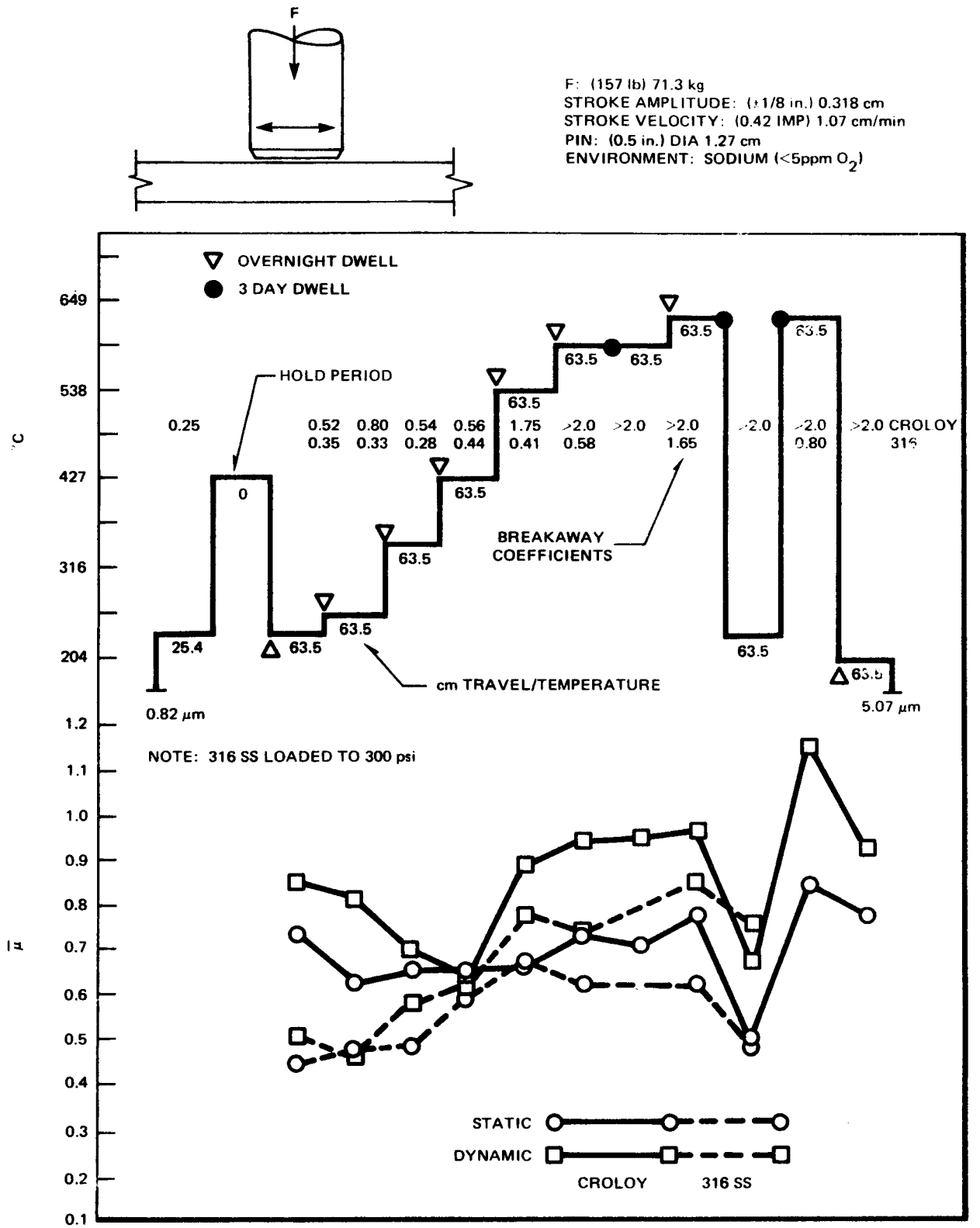

Figure 1. Pin-on-Plate Friction Data 2 1/4 Cr – 1 Mo Steel (A.I. Test Matrix 11)

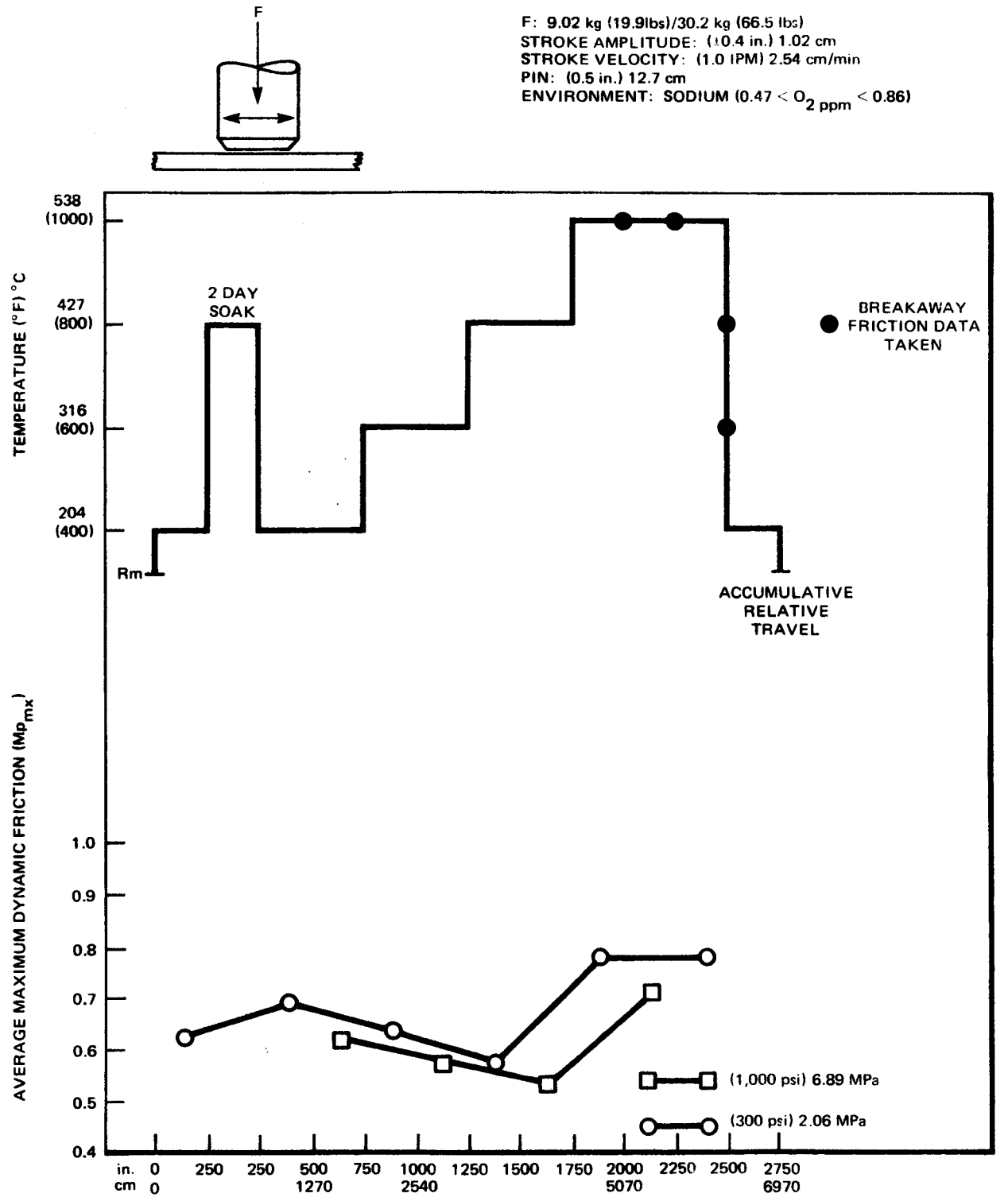

Figure 2. Pin-on-Plate Friction Data 2 1/4 Cr-1Mo Steel (Ward Test 5-507)

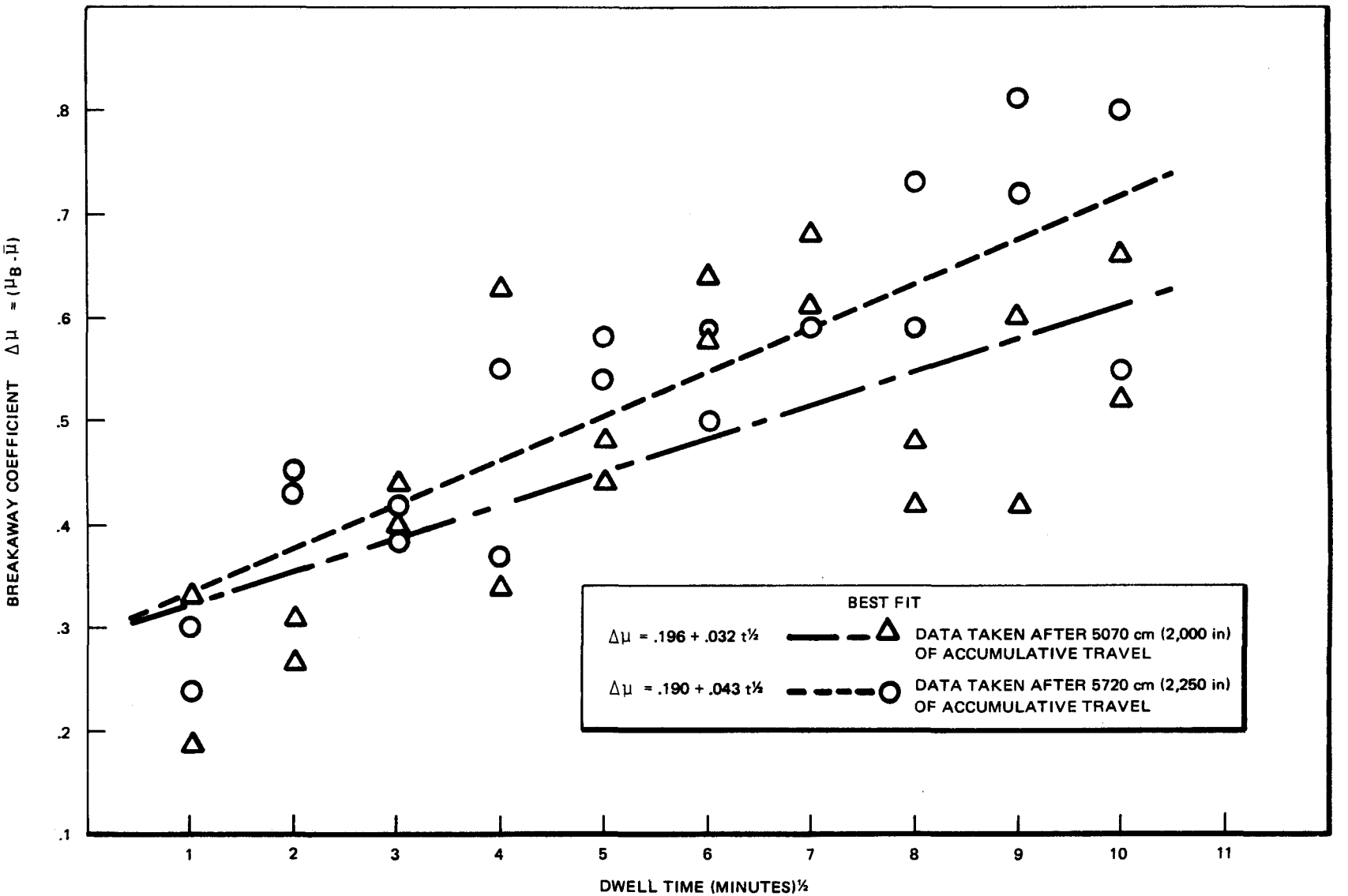

Figure 3. Behavior of 2¼ Cr - 1 Mo at 538°C (1000°F) from a 2.07 MPa (300 psi) LOAD/DWELL — Breakaway (Ward Test 5-507)

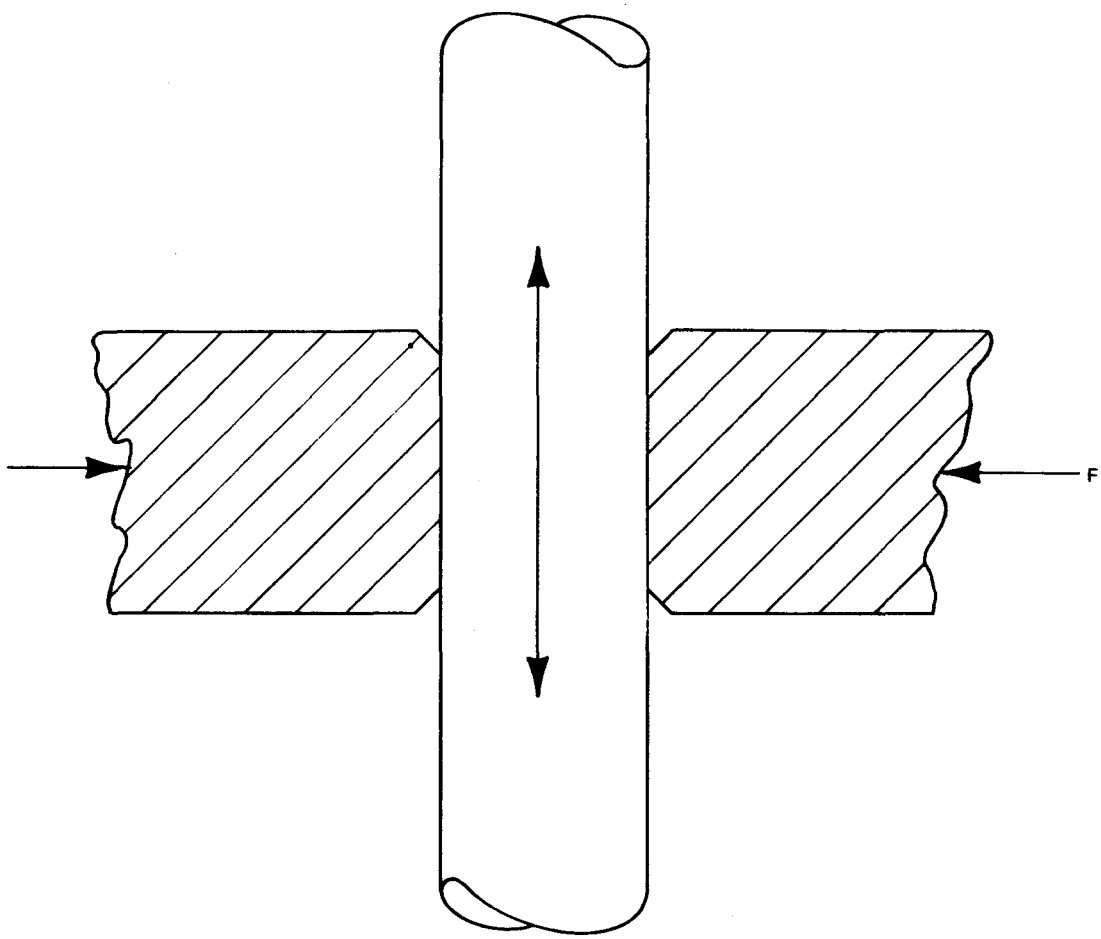

ITEM:	2¼ Cr – 1 Mo STEEL TUBE		SUPPORT PLATE .030 cm (.012 in) CLEARANCE
	15.9 cm O.D. NOM, 1.60 μm (0.625 in O.D. NOM, 63 μin)	VERSUS	3.18 μm (125 μin)
TEMPERATURES:	343°C, 487°C, AND 542°C (650°, 835°, AND 935°F (Na))		
MOTION:	RECIPROCATING, 10160 cm AND 2540 cm (4000 in AND 1000 in)		
SIDE LOAD (F):	45,360 g (100 lb)		

Figure 4. Tube-to-Tube Support Tests/2¼ Cr – 1 Mo Steel, Single Tube Model Configuration

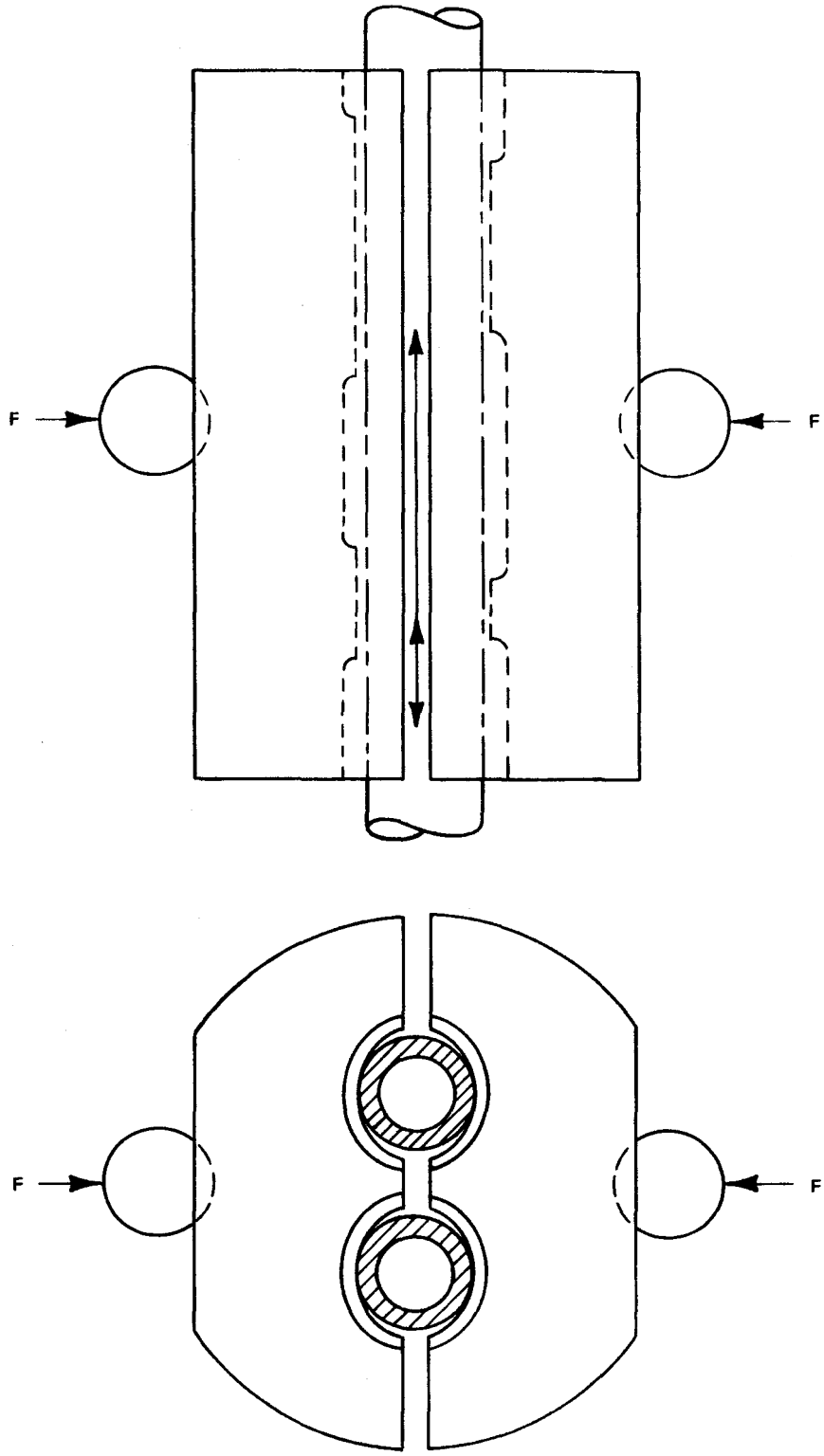

Figure 5. Multiple Point Steam Generator Model Friction and Wear Test

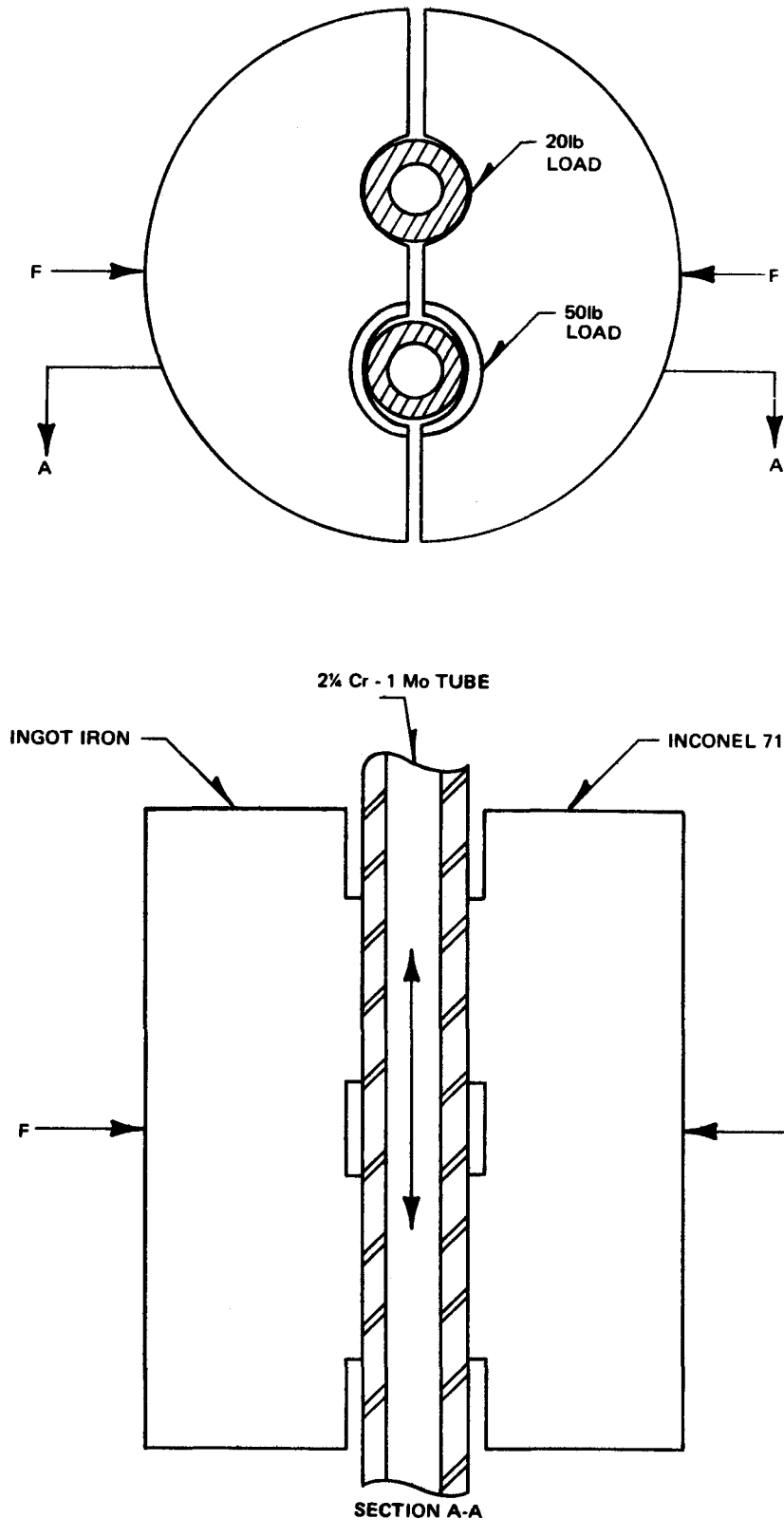

Figure 6. Saddle Block Test Components Utilizing Back-Up Materials

V. NONDESTRUCTIVE EXAMINATION DEVELOPMENT

The objectives of this task are to identify and develop, if necessary, NDE methods which are to be applied to meet the requirements for the CRBRP intermediate heat transfer system. The current work scope and status for this effort is summarized in Table I.

NDE NEEDS OF CRBRP IHTS AND STEAM GENERATOR SYSTEMS

A position paper describing the nondestructive examination needs of the CRBRP IHTS and Steam Generator Systems has been released to the Project.

The paper describes the existing state-of-the-art and needed development for these systems. Existing specifications were described relative to the CRBRP needs and a plan of action and schedule were presented.

Review comments have been received from CRBR Project and RRD personnel; these comments are being integrated into the final document.

DEPARTURE FROM NUCLEATE BOILING (DNB) TEST SECTION - INSITU MONITORING

The DNB test section is an accelerated corrosion test using worst case CRBRP water chemistry. A single tube sodium-heated evaporator is used with a water-side DNB zone, monitored by thermocouples and other sensors. The DNB region is of greatest interest from a water-side corrosion point of view. Monitoring of corrosion at periodic intervals requires that changes of less than 12.7 μm (0.0005 in.) be detected in the inside diameter of the tube. Pretest ultrasonic wall thickness measurements of the test section have been performed in place, using the fixture shown in Figure 1. The measurements were reproducible to 12.7 μm (0.0005 in.). A study of the error sources indicates that the most significant errors are in: (1) the velocity difference between the calibration standard and the tube, and (2) the geometrical errors introduced by "play" at right angles to the sound beam. The calculated errors are shown in Figure 2. Improvements in the probe shown in Figure 1 are being pursued.

Air-gage measurements of the inside diameter of the test section tube have also been completed with a precision of approximately 1.8 μm (0.000070 in.). The air-gage is not satisfactory for plant in-service examination but is ideal for the DNB test. Alternate methods that would be usable in the plant are also being explored. Linear Variable Differential Transformers (LVDT), eddy currents, and optical gages are under investigation.

Because water is used as an ultrasonic couplant in the wall thickness measurements, concern has been expressed on the possible occurrence of pitting corrosion. Tests conducted on samples of ESR and air-melted 2 1/4 Cr - 1 Mo with weld metal show no pitting after seven weeks exposure to water doped with hydrazine and ammonia. (Proposed wet lay-up water chemistry for CRBRP.) The samples were contained in beakers such that 194 cm^2 (30 square inches) of water surface was exposed to air. Exposure to air is considerably less for the DNB test section and can be held to zero if necessary using inert cover gases.

Techniques, jigs, and equipment developed to examine the DNB test sections are, in part, applicable to in-service inspection for steam generators.

ULTRASONIC EXAMINATION SPECIFICATION FOR TUBING

The ultrasonic examination specification for plant tubing, GE specification 22A3634, has been issued and it is now a part of ordering data for the CRBRP steam generator tubing. A twelve-notch standard is used along with sophisticated statistical calibration and control. The statistical techniques, developed by HEDL parallel to those of RDT F3-33, have been adapted for the specific geometries and materials relevant to CRBRP. The nominal reject criterion is a defect > 3% of the tube wall thickness.

TUBING EXAMINATION

Selected tubing from prospective vendors was examined by FBRD and some rejects have been found. Most rejects are caused by drawing marks along with some transverse flaws due to metallurgical or handling problems. The oxide surface of the tubing can interfere with liquid penetrant examination and this should be considered in processing the tubing. A typical example of a reject piece of tubing with longitudinal defects is shown in Figure 3. The transverse

channel shows typical "noise" signals from surface roughness and/or coatings.

Surface finish (oxide) scale may require special production practice if liquid penetrant examination is to be applied effectively.

TUBE-TO-TUBESHEET WELD EXAMINATION

The tube-to-tubesheet joint requires very high quality welds. Radiography with ytterbium sources and with the ORNL rod anode x-ray machine has demonstrated the ability of these two methods to detect pores. The frequency of smaller pores is unknown, but Figures 4(a) and (b) show ytterbium and rod anode laboratory radiographs taken by ORNL. The part examined was a steam generator weld from GE's Steam Generator Test Rig that was suspected of leaking. The rod anode machine can detect pores of approximately 25 microns while the ytterbium source can only detect pores 375 microns and larger. Specification for pore acceptance criteria have been established recently and will exclude all pores larger than 375 microns. In addition, the criteria will restrict pore spacing and the number of smaller pores allowed in each weld.

IN-SERVICE INSPECTION (ISI)

Two deliberately flawed tube samples were received from Carpenter Technology. The tubes had small holes drilled prior to the final reduction. The two samples are shown in Figure 5. The tubing is 2 1/4 Cr - 1 Mo having the same dimensions as the reference steam generator design. An examination, using equipment and technique to be used in-service, was performed on these two samples. A 15-MHz transducer was used with a 0.63 cm (0.25 in.) diameter element and a 2.54 cm (1 in.) focal length in water. The defects were readily detectable as shown in Figures 6 (a) and (b).

TRANSITION WELDS EXAMINATION

The transition joint will be used to join the 2 1/4 Cr - 1 Mo steam generator inlet and outlet nozzles to the stainless steel piping of the Intermediate Heat Transport System. These joints will consist of at least three materials and possibly more. One candidate joint consists of 2 1/4 Cr - 1 Mo joined directly to Type 316 stainless steel with Inco 82 weld metal. Ultrasonic examination of Inco 82 weld metal in a prototypical

weld has been accomplished using various methods. The most successful method used so far has been immersion ultrasonics. Figure 7 shows results obtained from one Inco 82 weld. The high attenuation of the weld metal (approximately 16 Db greater than the 2 1/4 Cr - 1 Mo metal of the same thickness) prevents the detection of the same type of flaws at different depths. The flaws near the surface saturate the instrument causing the signal to be "flat topped" as shown in Figure 7. This difficulty can be solved with distance amplitude correction or rescanning the weld at a different gain. The flaw sizes shown in Figure 7 are not necessarily the detection limit for the immersion method. Further studies will establish the detection limit, effects of welding parameters, and the detection limit for other types of flaws.

TABLE I

SUMMARY OF GE-FBRD NDE DEVELOPMENT

Project	Scope	Present Status
Steam Generator Tubing	Provide specifications, procedures, and expertise	Specification 22A3634 is complete and issued.
Tubesheet Forging	Provide specifications, procedures, and expertise	Specifications complete and issued; procedures complete and approved; examination to begin in early 1976.
Tube-to-Tubesheet Welds	Provide specifications and develop needed methods	Radiographic development complete; ultrasonic development ongoing; preliminary radiographic specifications are complete.
Tubesheet After Final Machining	Specifications, procedures and expertise	Preliminary specifications complete.
Shell	Specifications, procedures and expertise	Specifications complete and issued for plate steel.
Tube-Plug Welds	Specifications and develop needed methods	Development ongoing.
Transition Welds	Specifications and develop needed methods	Ultrasonic development in progress; radiographic qualification test in progress.
Large Leak Damage Assessment	Specifications and needed development	Preliminary radiographic and ultrasonic development in progress.
Rupture Discs	Development of methods and specifications	Development proposal and schedule complete - to begin in mid-1976.
In-service Inspection		
A. Small Leak	Develop method and equipment, and write specifications	Ultrasonic and eddy current development are ongoing; leak testing development is proceeding; acoustic emission methods also being investigated.
B. DNB	Develop methods and equipment, and write specifications	Ultrasonic wall thickness methods under development and successfully applied in GE DNB test; eddy current methods under development are also applicable here.

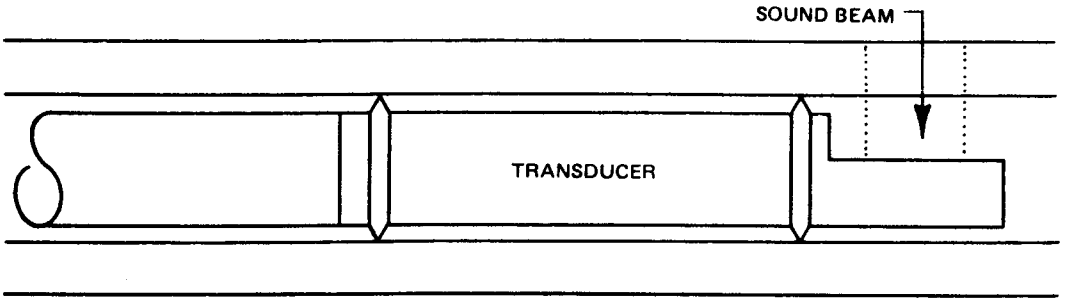

Figure 1. Fitted Transducer Used for DNB Measurements. A rigid coupling is used for the DNB for positional reproducibility. A flexible coupling would be used for full-length plant tubing.

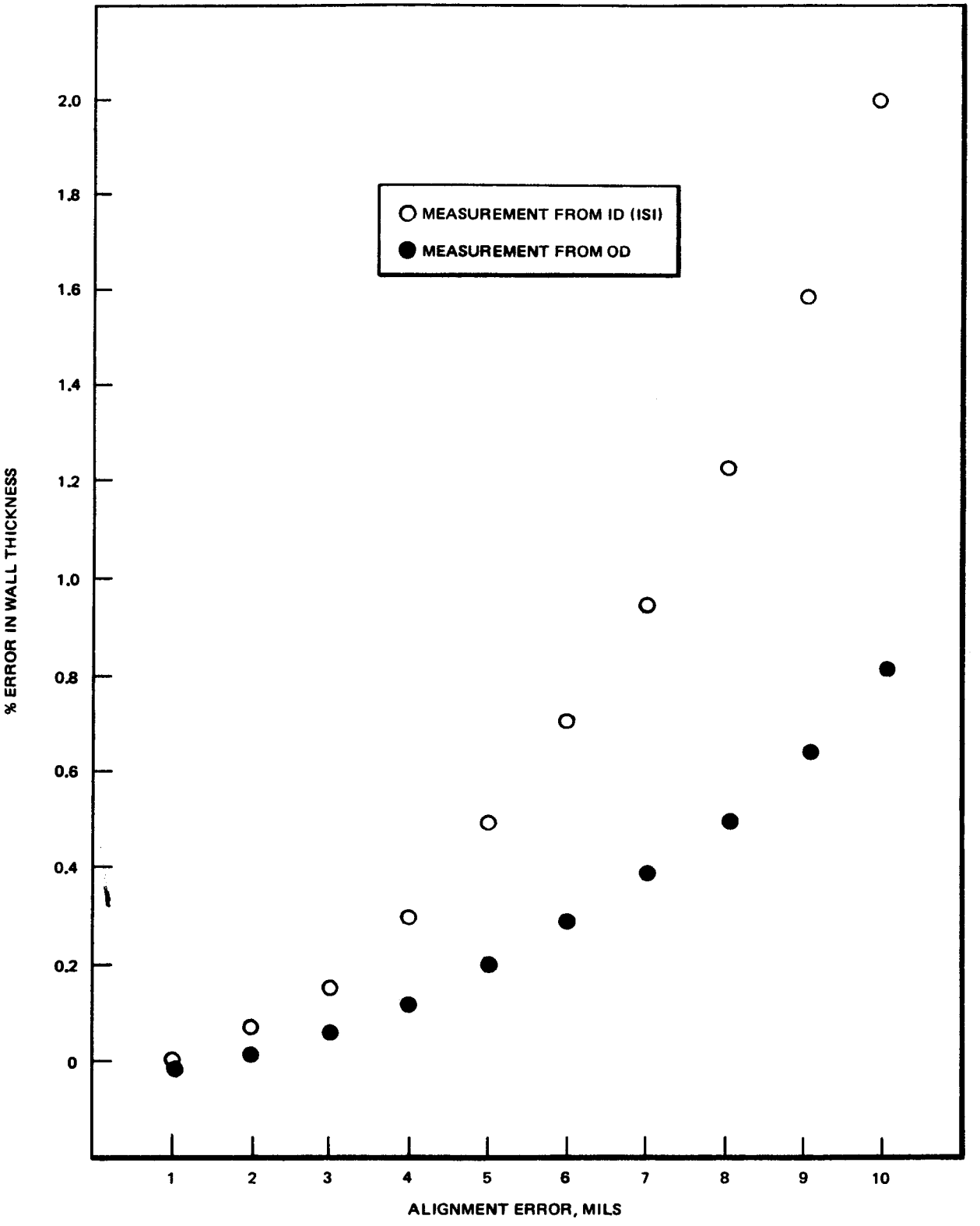

Figure 2. Calculated Errors for a Small Axial Displacement for Measuring Wall Thickness of Tubing for Two Diameters Corresponding to Inspection from the outside and inside surface, respectively, of reference design steam generator tubing.

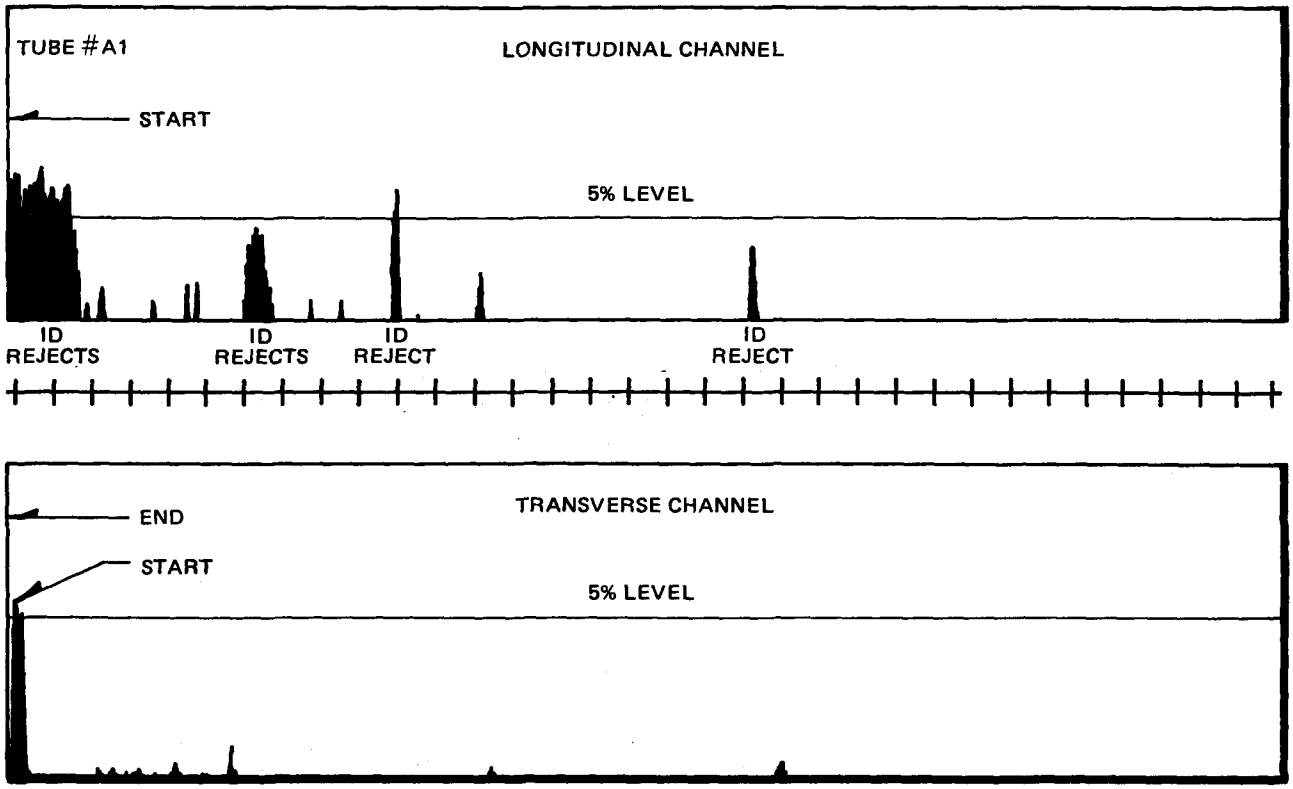

Figure 3. Typical Ultrasonic Examination of a 2-1/4 Cr-1 Mo Tube with Rejectable Longitudinal Defects

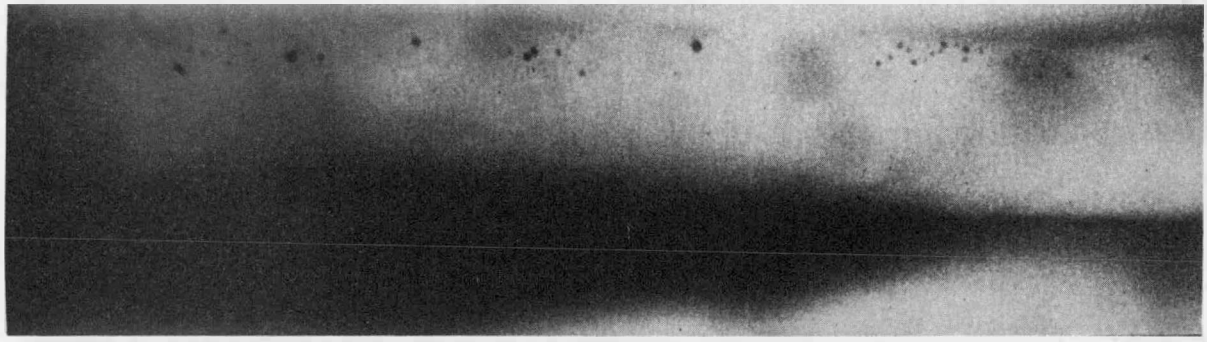

a) ORNL ROD ANODE X-RAY MACHINE THE LARGEST PORE IS 0.63 mm

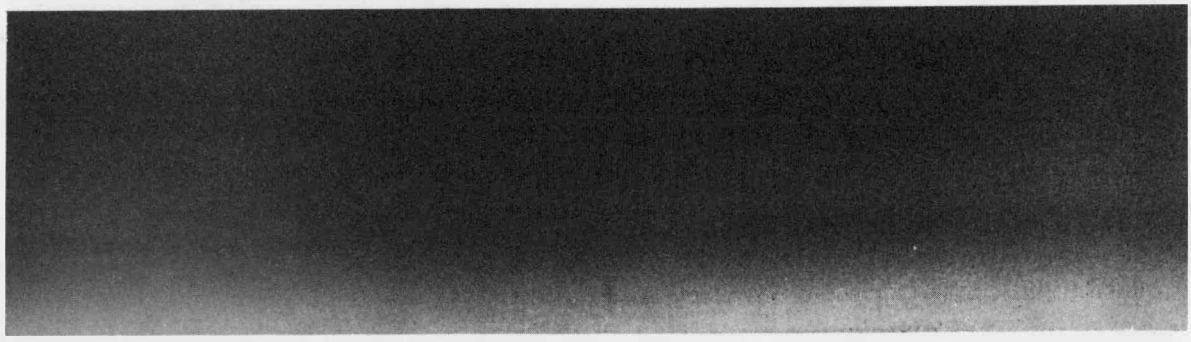

b) ORNL YTTERBIUM SOURCE, THE TWO FILMS WERE INADVERTENTLY MIRROR IMAGED DURING THE PHOTOCOPYING PROCESS

Figure 4. Photocopies of Tube-To-Tubesheet Weld Suspected of Leaking. a) ORNL rod anode x-ray machine, b) ORNL ytterbium isotope.

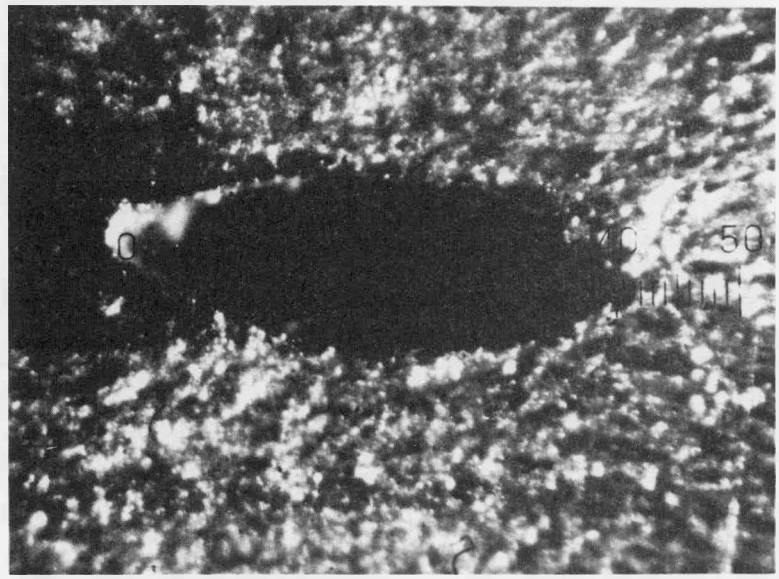

(a)

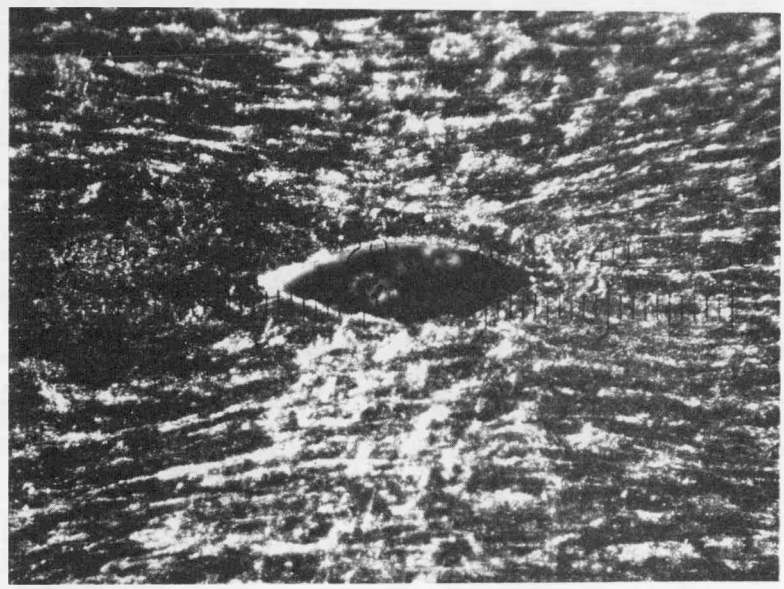

(b)

Figure 5. Photomicrographs of Flaws Induced by Drilling Small Through-Wall Holes Prior to Final Reduction. (a) Initially 0.026-in hole (after reduction 0.0121 by 0.0341 in). (b) Initially 0.013-in hole (after reduction 0.0060 by 0.0186 in).

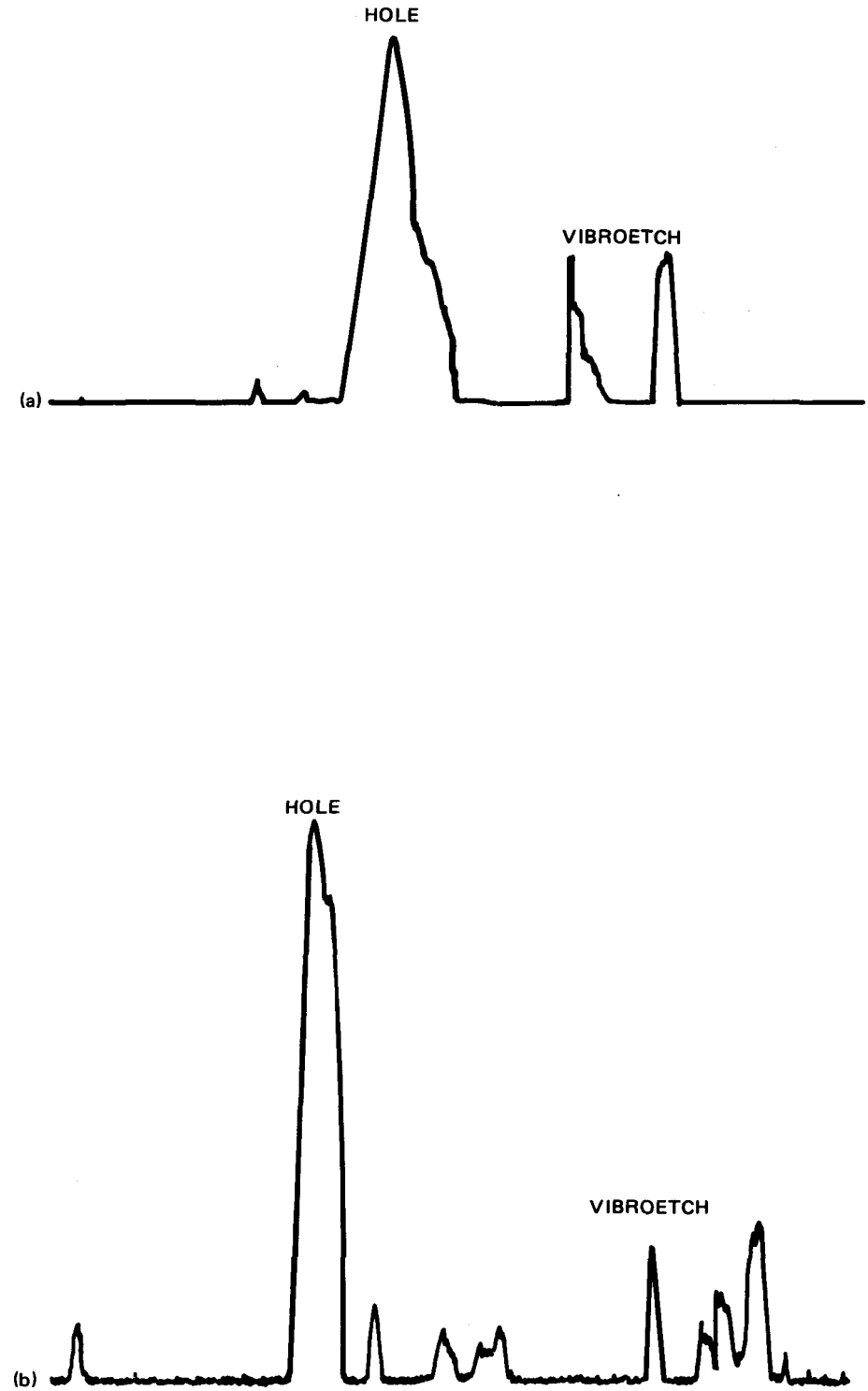

Figure 6 Ultrasonic Examination of Artificial Flaw Samples of Reference Design Tubing. The signals seen next to hole signal are from a Vibroetch mark used to locate the hole. (a) 0.013-in initial hole size. (b) 0.026-in initial hole size.

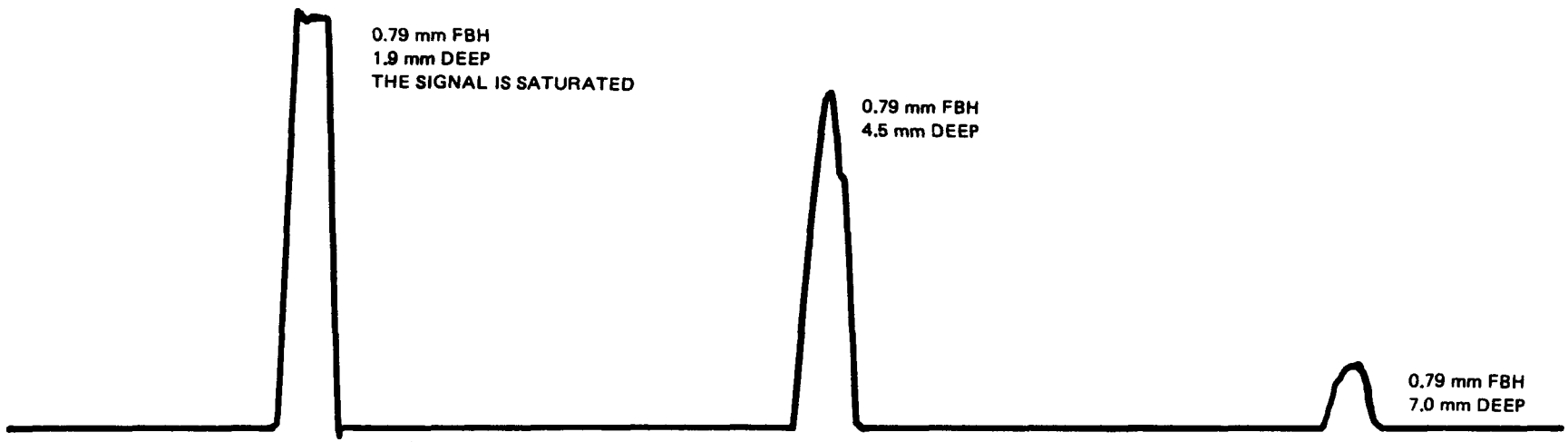

Figure 7. Scan Along Transition Weld in the Weld Metal. The three flaws are "flat bottom" holes (FBH) with different depths in the weld metal.

VI. WATER CHEMISTRY STUDIES

The objective of this subtask is to apply current information and practice of water technology to LMFBR steam generators to assure the integrity of the system; to coordinate and standardize chemical information and specifications for the CRBRP and supporting steam generator tests; and to carry out or support experimental programs in fouling, cleaning, and corrosion of steam generators with particular emphasis on the problems associated with departure from nucleate boiling.

The application of modern boiler water practice to the CRBR plant has been described[1]. During the present reporting period a summary[2] of the potential damage mechanisms associated with the critical heat flux (DNB) situation was prepared. The paper describes the steps taken to reduce the problem, alternatives in plant operation, and confirmatory and supporting developmental tests in progress.

COORDINATION/STANDARDIZATION ACTIVITIES

The Neuces Bay testing program, described in the previous report in this series, was completed. The data shown in Table I indicates that in routine operation, the sodium level was less than 1 ppb for nearly the entire testing period. No special precautions were taken to achieve this level and the plant does not have any of the specialized equipment currently available to reduce caustic throw from the demineralizers. Further, there was condenser leakage (saline water) throughout the test period. This data was used as a basis for CRBR insistence to Burns & Roe (the plant architect engineer) that the polisher for the plant be specified to meet the 1 ppb sodium (maximum) believed necessary.

Table II shows the results of attempts to determine the anionic content of the demineralizer effluent. While the data is somewhat inconsistent, it suggests that chloride, not caustic, is the major constituent. However, elevation of the pH in two instances does retain some concern about caustic

throw. A complete report of this work will be issued in January (NEDG-14086).

Both EBR-II and T.V.A. were asked to examine the sodium content of their feedwater. EBR-II reports < 1 ppb during the fairly short period of testing. This work continues. T.V.A. data, obtained by workers from Graver Water Division of Ecodyne Corporation, shows < 0.5 ppb for water at the Bull Run Plant.

In part, as a result of our interest (predominantly because of concern about turbine damage) the ASME Research Committee on Water for Thermal Steam Plants is addressing the question of polisher effluent composition. Hopefully, definitive answers should result rapidly. In any event, our participation can now be limited to auditing and application rather than experimentation in this area.

Impact on on-going programs has included setting the specification for water chemistry for the Few Tube steam generator tests and continuing surveillance of the Westinghouse and General Electric single tube DNB effects rigs. There has been particular emphasis placed on the formulation of follow-up work, Phase II, of the GE DNB test. It has been recommended that the test extension examine long term corrosion effects as compounded by fouling.

FOULING, CLEANING, CORROSION EXPERIMENTS

Evaporator Corrosion

Design was completed of a test section to be installed at the Bull Run Station of T.V.A. for the purpose of studying evaporator corrosion. The topic is covered in detail as follows*.

Test Facilities

The proposed evaporator corrosion study will be conducted at the Bull Run Steam Plant operated by T.V.A. Superheated steam bled from the plant will be used as the heating fluid while the plant feedwater will be used as the fluid to be heated. Feedwater specifications for the Bull Run Steam Plant are quite similar to those to be specified for CRBR[1] and are listed in Table III. All volatile water treatment is used in this plant with pH adjustments by

---

* This work was partially funded by Task 18B.

ammonia additions. The propensity for fouling product accumulation should be much greater at this plant than CRBR because carbon steel is used in the feedwater train at Bull Run rather than the stainless steel proposed for CRBR[4]. However, the overall heat flux for the proposed test is significantly less than that of CRBR (Table IV) which will tend to decrease the deposition rates.

Test Description

A schematic diagram of the corrosion test is shown in Figure 1. As shown, the evaporator is simulated by three individual heat exchanger sections. The heat exchanger sections will be fabricated from prototypic tubing materials (ESR, 1.59 cm O.D., 0.25 cm wall). The diagram shows that 328°C (622°F) saturated feedwater enters the 2.6 m (8.6 ft.) nucleate boiling heat exchanger and exits as 328°C (622°F), 21% quality steam. From here, the steam enters the DNB test section where its quality is increased to 35%. Finally the steam goes through the film boiling heat exchanger exiting at 45% quality. Each evaporator boiling stage is achieved in the separate heat exchanger sections.

The heating fluid is 538°C (1000°F) superheated steam flowing countercurrent to the feedwater and transferring heat through the outside diameter of the test sections. This fluid establishes axial metal wall temperature variations along each test section. Actual test conditions are listed in Table IV.

The table indicates a $\Delta(\Delta T)$ at the DNB zone of 27°C (80°F) for the test making it conservative relative to actual plant conditions. Figure 1 shows that metal wall temperatures of the DNB test section will be monitored by thermocouples included in the tube wall and arranged at different axial locations. The arrangement is illustrated in Figure 2. Here it is shown that grooves are cut into the test section wall to accommodate the thermocouples. The thermocouple bead is held in intimate contact with the tube wall by a silver fill compound. Axial temperature monitoring will therefore aid in identifying the exact location of the DNB zone.

Corrosion on the inside of the tube will be measured by weight loss. To eliminate the corrosion effects of the superheated steam on the heat exchanger

tube outside diameter, a sacrificial 0.045 cm (0.018 in.) thick shell tube will be shrunk-fit over each test section. This shell will corrode instead of the test section outside diameter. Tolerances on this outer shell will be such that on heat-up, a metallurgical bond will form between the inner diameter of the shell and the outer diameter of the test section. After exposure, the shell will be removed from the test section with an hydraulic extractor[5].

Test sections will be exposed for long times (~10,000 hrs.) in order to evaluate the effects of steady state corrosion behavior on the 2 1/4 Cr - 1 Mo tubing material.

Magnetite Formation

The distribution of the corrosion product hydrogen in the evaporator scale has a significant influence on the type of scale formed and therefore on the corrosion rate. Experimental results[6,7,8] indicate that in the absence of hydrogen gradient, a thin, tightly adherent oxide film is formed whose thickness does not increase appreciably with time (Bloom-type scale). However, when a gradient does exist in the scale, the non-protective Potter-Mann scale is formed with its porous, brittle outer layer leading to increased overall corrosion rates and localized metal attack.

In a sodium heated steam generator, there is a large driving force for hydrogen to diffuse through the tube wall into the sodium, thus yielding Bloom-type scale. In a water heated system, a more exaggerated Potter-Mann situation can exist owing to corrosion on the two metal surfaces. Such a condition would lead to larger hydrogen gradients in the inner diameter scale than a tube corroding only on the inner diameter.

To minimize the extent of hydrogen gradient formation some design precautions were taken. The evaporator corrosion test will use superheated water as its heating fluid, but the space between the heat transfer tube and its metal shell will be flushed with helium. This will minimize any hydrogen build-up and more closely simulate the sodium-heated evaporator tube. Grooves will be machined into the outside diameter of the heat transfer tube to allow for helium flushing. With hydrogen gradients minimized, a more prototypic scale can be expected to form on each tube section.

Post-Exposure Examination

The exposed tube sections will be destructively examined to assess the relative corrosion rates of the three sections. Extensive metallography will be performed to identify and examine areas of localized corrosive attack and to gain more knowledge about evaporator scales and their formation mechanisms.

FOULING/CLEANING

As previously reported[9], fouling of steam generator tubing surfaces may have major impact on both heat transfer and corrosion. The problem, while common to all steam generation systems, has more pronounced effects in an LMFBR because of the high heat flux required of such a system. Further, in the case of CRBR, recent analytical studies indicate that fouling may have a major, but unknown, impact on DNB itself. Roberts[10] indicates that there is insufficient data on the effects of fouling to decide whether DNB may be eliminated or made worse. DNB could be eliminated by requiring heat to vaporize liquid in the deposit voids in the nucleate boiling zone. DNB could become much worse if fouling improves heat conductance in nucleate boiling while degrading it in the film boiling region.

Specific activities on this topic have included:

Measurement of Particulate Levels

Fouling is predominantly the deposition onto the evaporator tubes of metallic oxides arising from corrosion of piping and heater surfaces in the feedwater train. (Deposits of condensate salts may aggravate the problem somewhat.) The amounts deposited are proportional to the amount dissolved/suspended in the feedwater. Specifications for the CRBR system, which are identical to those for once-through plants, limit the amount of Fe and Cu to 10 and 2 ppb, respectively. It is important to determine the actual value for these species for a number of reasons. For example, such data permits better estimates of plant fouling coefficients in performance calculations. The data are needed to provide realistic values for iron and copper additives in tests of fouling effects on corrosion. They are also essential to the formulation of cleaning solvents and methods. Relatively few plants currently

in operation use stainless steel feedwater heaters, demineralization and volatile chemistry, thus data on feedwater chemistry typical of CRBR is unavailable.

As discussed in the previous work on sodium content of feedwater, the Neuces Bay Plant of Central Power and Light does have the feedwater characteristics desired. Negotiations have been in progress to resume testing at the plant. Permission has been obtained to carry out the work. It is not clear yet that it will be physically possible to install the type of in-line probe needed to provide a representative sample of coolant. The high pressure sampler being fabricated to accept the water from the probe is shown schematically in Figure 3 and pictorially in Figure 4. The water is cooled and passed through filter holders which will contain papers impregnated with anion and cation exchange resins to concentrate soluble ionic corrosion products. A membrane filter will collect the suspended materials in the sample stream.

Cleaning of Boiler Deposits

Negotiations are in progress with American Electric Power, Canton, Ohio to obtain a piece of evaporator tubing which has been fouled in a manner analagous to that expected for CRBR. Philo I, the first of the Universal Pressure Type Boilers (once through) built by Babcock and Wilcox is currently in lay-up. There are sections of 2 1/4 Cr - 1 Mo tubing in a 316°C (600°F) region which have not been cleaned for several years prior to shutdown. Apparently water chemistry was of the volatile type. AEP has agreed to remove a section of tubing provided we bear the cost of replacement. Discussions are continuing to ensure the suitability of the tube prior to initiating purchasing procedures.

General discussions on boiler tube cleaning have been carried out with Dow Chemical and Halliburton, two of the leading vendors of this service. Considerable literature on the topic has been accumulated, and an actual chemical cleaning has been witnessed during this period. Some purchase of specific cleaning reagents has begun.

REFERENCES

1. Dutina, D., "A Survey of Modern Boiler Water Practice", General Electric Report GEAP-14042, April 1975.

2. Dutina, D., Peterson, J. R., and Van Hoesen, D., "Evaluation and Testing for Cyclic Thermal Strain and Accelerated Corrosion Damage Due to Operation with Critical Heat Flux in Sodium Heated Steam Generators", presented at 68th Annual Meeting AICHE, Los Angeles, California, November 16 - 20, 1975.

3. Personal Communication, L. V. Hampton to J. Clevenger (T.V.A.).

4. Gaul, G. to Kruger, G., "Recommendation of Stainless Steel as the Feedwater Train Material in CRBRP", 490-CR-DD01, November 1974.

5. Fitzsimmons, M. D., et. al., "Simulated Boiler Water Reactor and Superheat Corrosion Facility", Nucl. Sci. Eng., 17, 18, (1963).

6. Berge, P., et. al., "The Effect of Hydrogen on the Corrosion of Steels in High Tempe ature Water", presented at the NACE Corrosion Meeting, Chicago, Illinois, March 1974.

7. Friggons, H. A., et. al., "Nucleation and Growth of Magnetite Films on Fe in High Temperature Water", Corrosion Science, Vol. 8, No. 12, December 1968, pp. 871 - 881.

8. Harrison, P. L., et. al., "The Kinetics of the Oxidation of Steels in High Temperature Aqueous Solutions", Corrosion Science, Vol. 10, 1970, pp. 585 - 594.

9. Casey, D., and Dutina, D., "Investigation of the Water Purity Requirements and Fouling for the CRBR Steam Generator", Transactions of the American Nuclear Society, Vol. 21, p. 178, New Orleans, Louisiana, June 1975.

10. Letter, J. M. Roberts and J. R. Leonard to Distribution, "Cycle Adjustments VS. Power Level for DNB Strain Cycle Analysis", D790-75-96R, 9/26/75.

TABLE I

FEEDWATER SODIUM ION CONCENTRATION

Neuces Bay Plant

A. SODIUM ION PROBE* - (Milton Roy, Ammonia pH Control)

Na Concentration	Time
< .4 ppb	168 hours
> .4; < .8 ppb	216 hours
> .8; < 1.0 ppb	48 hours
> 1.0 ppb	6 hours

B. SHORT TERM (24 hour) EVAPORATED SAMPLES

No. 1A	0.4 ppb	(10 1)
No. 1B	0.25 ppb	(10 1)

C. FLAME IONIZATION DETECTOR

<1 ppb measured on 6 different days

---

* Calibration of Probe
- Laboratory Standards (by dilution)
- ~Weekly One Point Standardization
- ~Monthly 4 - 5 Point Standardization

TABLE II

CONCENTRATED SAMPLE RESIDUES

(Boiler Samples, Neuces Bay Plant)

NUMBER	1	ID	2	3
Na*	2380	1040	11	103
Cl*	2530	800	3	43
PO_4*	66	31	2	9
SO_4*	37	21	2	4
pH	9.4	7.0	6.9	9.85
Volume**	3.3	2.2	31.8	35.0
Mg Residue	19.1	--	4.5	26.3
% as NaCl	70	50	34	33

* ppb in Boiler Water

** Liters

TABLE III

FEEDWATER SPECIFICATION - BULL RUN STEAM PLANT[3]

pH	9.0 - 9.5
Conductivity	3.0 - 8.0 μmho
Cation Conductivity	0.3 (max)
Hydrazine	10 - 15 ppb
O_2	5 ppb (max)
SiO_2	20 ppm
Na	2 ppb (max)
Fe	10 ppb (max)
Cu	2 ppb (max)

TABLE IV

EVAPORATOR CORROSION TEST CONDITIONS

	NUCLEATE BOILING	DNB	FILM BOILING	CRBR 100% POWER DNB ZONE
Length	262 cm (8.6')	122 cm (4')	61 cm (2')	---
Steam Quality	0 - 21.4%	21.4 - 35%	35 - 45%	---
Steam Temp	328°C (622°F)	328°C	328°C	331°C (628°F)
Flow	0.14 kg/s (1120 lb/hr)	---	---	---
Heat Flux	797,500 wah/m^2 (~ 253,000 B/hr-ft^2)	397,152 (~ 126,000)	972,800 (~ 150,000)	841,584 (267,000)
Metal Temperature	316°C (~ 600°F)	397/352°C (747/666°F)	388°C (730°F)	379/336°C (714/636°F)
$\Delta(\Delta T)$		44°C (~ 80°F)		33°C (~ 60°F)

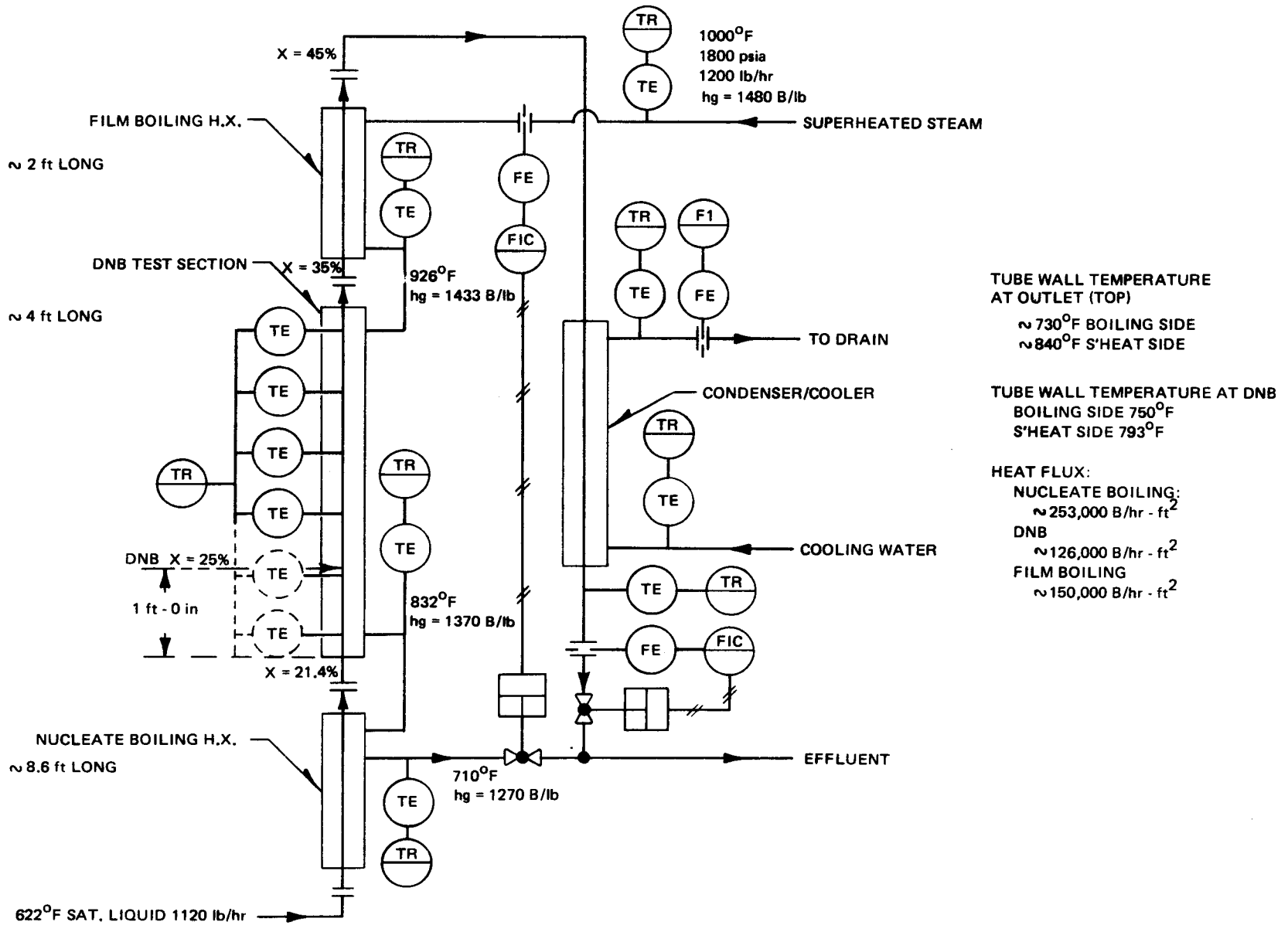

Figure 1. DNB Test Schematic

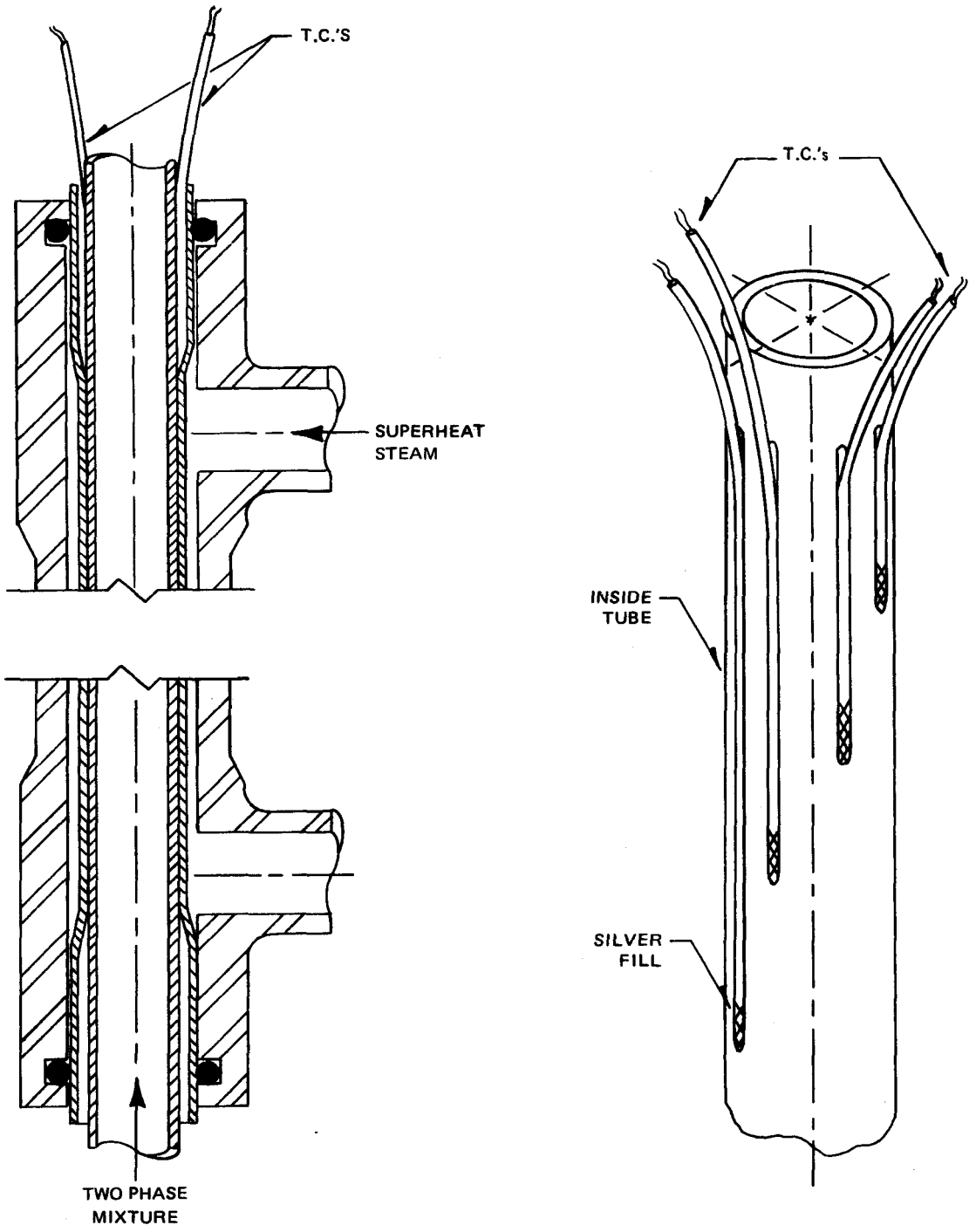

Figure 2. DNB Test Section Concept

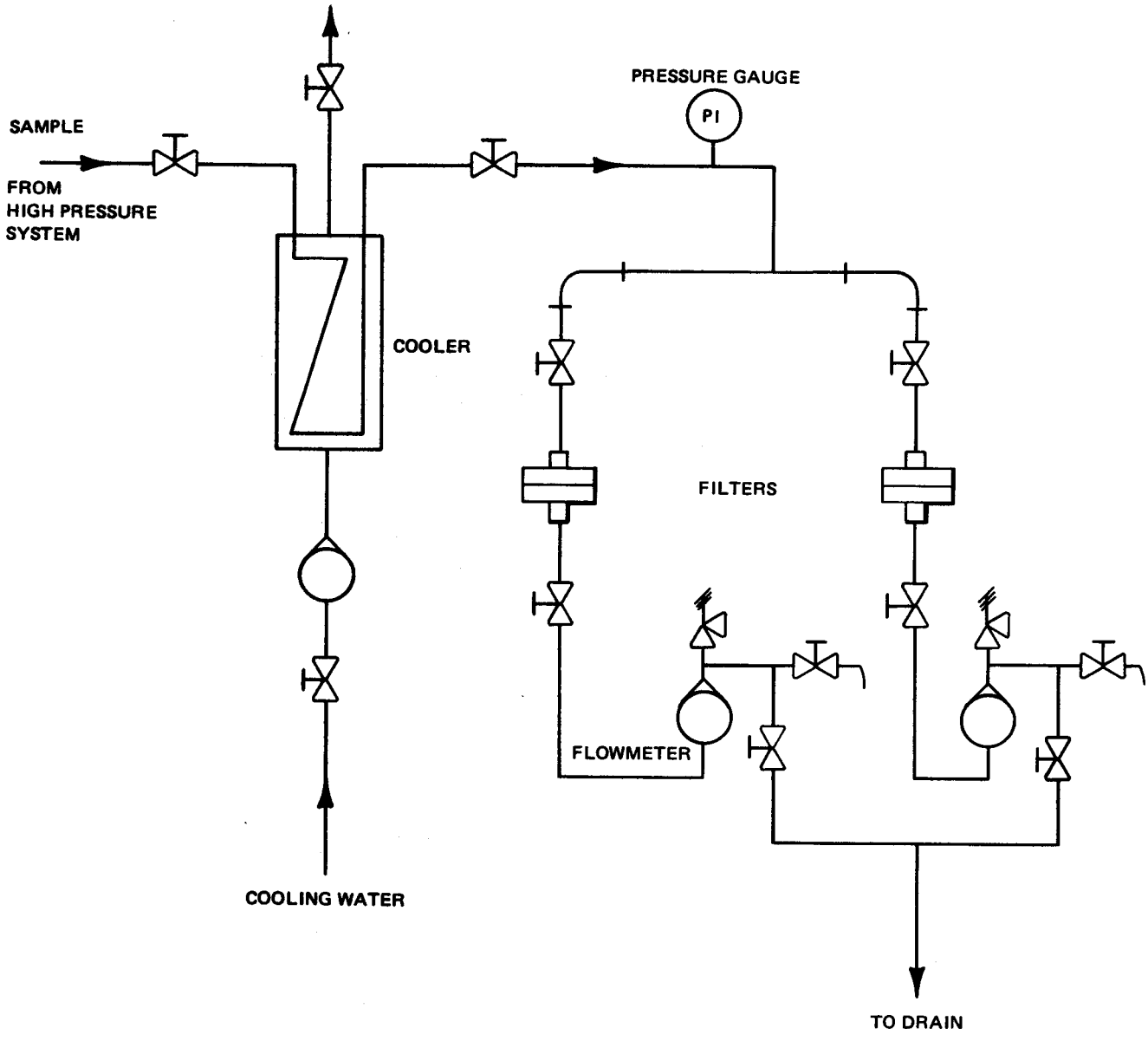

Figure 3. Particulate Sampler

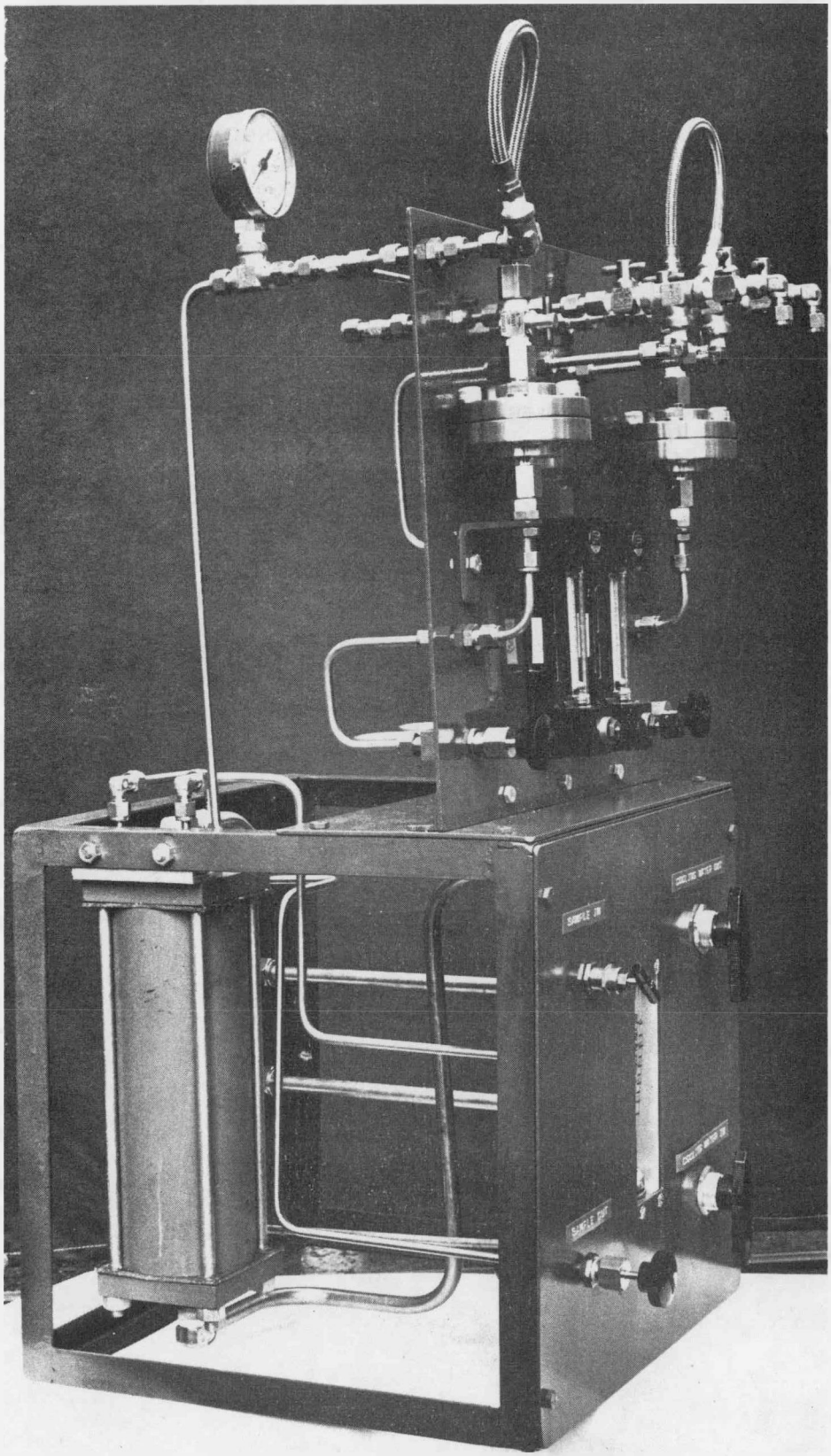

Figure 4. Particulate Sampler

VII. TRANSITION JOINT DEVELOPMENT

WELD PROCESS DEVELOPMENT

The hot-wire Gas Tungsten Arc (GTA) process has been selected for fusion welding of the 457 mm (18 in.) and 660 mm (26 in.) diameter transition joints for CRBRP. A description of the process and advantages for this application was included in the previous report in this series, July 1975.

A hot-wire GTA welding system has been installed at GE-FBRD specifically for transition weld development. A photograph of the system is shown in Figure 1 and a brief description of the major components is provided below.

DESCRIPTION

Power Supply and Programmer

Direct current is supplied to the GTA torch by a TekTran LSC 300 power supply. This is a solid state, silicon control rectified, closed-loop type power supply with variable current and voltage characteristics capable of supplying constant current or constant voltage. Current pulsing up to 30 Hz is provided. Accuracy of 1% of the dial setting is claimed by the manufacturer.

The programmer controls the current levels and interval times for each zone of the weld cycle. The weld cycle (shown in Figure 2) includes gas prepurge, initial current, upslope, weld current, current taper, down slope, and post purge. In addition, start and stop signals are provided for wire feed, fixture travel, arc oscillation, automatic voltage control system (AVC), and the hot-wire power supply. Accuracy of 1% of the dial settings for interval timers and level controllers is claimed by the manufacturer.

Hot-Wire Power Supply

A separate power supply is used for the hot-wire system. Presently a Linde VAC 501 AC constant voltage machine is being used. Feedback loops are not incorporated in this machine, therefore current control is not precise.

Wire Feeder

A wire feeder with 0.5% speed control has been built by GE to ensure constant wire feed rate. Commercially available units could not guarantee the required speed control for automatic welding. A ServoTek DC motor with tachometer feedback provides precise speed control from 100 - 3600 rpm. The motor is coupled to a gear reducer and wire drive unit to feed wire at 17.8 to 635 cm/min (7 to 250 in/min).

Oscillator

A Celesco Model 80A magnetic oscillator is used to sweep the arc across the weld. Oscillation amplitude, speed, and side wall dwell are independently adjustable.

Torches and Shielding

A Linde HW-27 GTA torch is used for the main arc, and a model #598512 torch is used for hot-wire. A trailing shield is used to ensure adequate gas coverage during welding. The standard Linde trailing shield required extensive modification to provide desired torch position and weld puddle visibility.

Linear Travel and Pipe Rotation

A Jetline precision side-beam carriage moves the torch linearly during plate welding. A specially designed turning fixture is used to rotate pipe under the weld head for circumferential pipe welds. Both positioners are driven with ServoTek motors to provide 0.5% speed control.

OPERATION

The system is designed for automatic operation after the start signal is given by the operator. All time intervals, current levels, and fixture motions are pre-programmed. The operator is required to start the weld sequence and monitor the system during the welding, but is not required to make adjustments to the system during welding.

The system was installed in late September 1975. Since then, considerable testing, de-bugging, and modification of the system components has been required. Two of the main concerns have been with the automatic voltage control system and the lack of weld puddle visibility because of the design of the trailing shield.

The AVC system has not been able to maintain a constant stand-off distance or stable, repeatable torch positioning during a normal welding sequence. The manufacturer is investigating the problem and is confident a solution can be found. Presently, the AVC system is not being used in weld development. Interactions of the oscillator magnetic field with the AVC system are expected to cause additional problems because of arc length changes as the arc is swept across the weld by the magnetic field. A system which senses stand-off distance with an electro-mechanical probe and provides a correction signal to a servomotor-operated positioning slide is being investigated as an alternative to the AVC system.

Weld procedure development has been hampered by poor weld puddle visibility. The trailing gas shield as delivered by the vendor blocked direct observation from most angles. The standard trailing shield has been extensively modified to include a viewing window, (see Figure 3). This arrangement provides good visibility even during the root pass.

With the exception of the AVC, the weld system is working well and is used daily for weld development. Dissimilar metal welds between 2 1/4 Cr - 1 Mo and Alloy 800 using Inco 82 filler metal, and between Alloy 800 and 316SS using 16-8-2 filler are presently being developed. The present emphasis is on performing the latter welds in order to demonstrate the capability of depositing low-dilution, fissure-free weld metal. These welds will be sent to ORNL for extensive mechanical characterization.

WELD TESTING

Guide bend tests were performed according to ASME Section IX on several plates welded by a crude system used prior to the new system. A preliminary procedure was used to help determine to what extent further development was

necessary. Three root bends and four face bends were dye penetrant tested before and after bending. Typical specimens are shown in Figure 4. The results are given in Table I. One face bend specimen suffered a fusion boundary separation at the Cr-Mo/Inco 82 interface. All other specimens were acceptable by ASME standards.

Weld metal dilution was determined on two of the bend specimens with the electron microprobe. Concentration of Ni, Cr, and Fe were measured at 16 points at regular intervals in the weld. The average composition at various points in these two welds is shown in Figure 5. Iron concentration serves as a good measure of dilution because the filler metal itself contains only about 3%. It is seen that most dilution occurs at the root of the weld and along the side walls. In no case was the dilution greater than 25%, even at the root. In comparison, up to 50% Fe may be found in the root pass of a cold-wire GTA weld.

STRESS ANALYSIS

The object of the analysis is to develop a weld joint design that minimizes the thermal stresses generated at the dissimilar metal interface. In the last semiannual report, it was stated that the tri-metallic joint, 2 1/4 Cr - 1 Mo/ Incoloy 800/316, with a 30° included weld angle was found to be optimum. A useage evaluation has been made for the 2 1/4 Cr - 1 Mo in this configuration according to ASME Code Case 1592. The evaluation, based on anticipated creep and fatigue damage for normal operation and 315 cycles from 538 to 343°C (1000 to 650°F), showed that the 2 1/4 Cr - 1 Mo has a useage factor of about 65%. When start-ups were considered, the useage went beyond 100%. As a result, new designs that lowered the useage factor were proposed and examined. The most promising to date is a four material joint, 2 1/4 Cr - 1 Mo/Inconel 600/Incoloy 800/ 316. Elastic analysis of this joint showed that the hoop stresses at the 2 1/4 Cr - 1 Mo interface were reduced by 35% - 50%. Useage for steady state operation and 315 cycles from 538°C to 343°C was reduced to 25%. Useage evaluation has not yet been done for start-ups.

The four material joint is effective because the thermal expansion of Inconel 600 closely matches the thermal expansion of the Cr-Mo, thereby greatly

reducing thermal stresses in the Cr-Mo. In this joint the major mismatch in thermal expansion occurs between the Inconel 600 and the Incoloy 800. These austenitic alloys are better able to accommodate the induced stresses because of their high temperature strength.

Although the new design has been shown to significantly reduce the useage, the tri-metallic joint is still the reference design for SCTI and CRBRP because these are the only materials allowed for high temperature service in ASME Code Case 1592. Inclusion of Inconel 600 in the piping system will require ASME Code approval, an expensive and time consuming process. Development of the four material joints will continue for possible use as a replacement, or for future applications.

ALTERNATIVE JOINING METHODS

A study was undertaken to investigate methods other than fusion welding for fabricating multi-material transition joints. Methods studied were inertia welding, co-extrusion, and explosive welding. In addition, two non-welded transition joints, a continuously-graded composition joint and a torroidal expansion joint, were considered. The study is summarized in Table II. The major conclusions and recommendations are:

1. Conventional fusion welding is the most practical method for fabricating 457 mm (18 in.) and 660 mm (26 in.) diameter joints. The hot-wire GTA process should continue to be the primary method for the large diameter joints.

2. Inertia welding offers several advantages over fusion welding for the 152 mm (6 in.), 76 mm (3 in.), and 25 mm (1 in.) transition joints. This process is recommended for further development. (There is no technical reason why larger pipe cannot also be welded by this process. However, there is currently no machine large enough to join the 18 and 26 in. pipes.)

TABLE I

SUMMARY OF GUIDE BEND TESTS FOR 0.5 IN. PLATES
OF 2 1/4 Cr - 1 Mo AND 304SS WELDED
WITH INCONEL 82 BY THE HOT-WIRE GTA PROCESS

(Preliminary Procedures Were Used)

SPECIMEN	CRACK DESCRIPTION	CRACK LOCATION	PRE-BEND PENETRANT INDICATION
RB-1	None	---	No
RB-2	1 .005" long	.090" from SS boundary	No
RB-3	5 < .030" long	WM near Cr-Mo/I82 boundary	Yes
RB-4	3 < .050" long	WM near SS/I82 boundary	Yes
	1 .005" long	WM near Cr-Mo/I82 boundary	No
FB-2	1 .187" long	Cr-Mo/I82 boundary separation	No
FB-3	None	---	No
FB-4	1 .015" long	WM near Cr-Mo/I82 boundary	Yes

TABLE II

SUMMARY OF ALTERNATE DISSIMILAR METAL JOINING METHODS FOR CRBRP TRANSITION JOINTS

METHOD	ADVANTAGES	DISADVANTAGES	RECOMMENDATION
Fusion Weld	1. Common, versatile, proven process; much experience is available. 2. Any pipe diameter and wall may be welded. 3. Low heat input, low dilution welds are possible. 4. Excellent repeatability is possible with proper equipment.	1. Liquid metal mixing can cause hot cracking, decarburization, and low ductility. 2. Process variables must be closely controlled for long periods to avoid defects. 3. Sensitization can occur at HAZ. 4. Diametral shrinkage up to 2% is expected.	Continue as primary joining method for large diameter pipe
Inertia Weld	1. Liquid metal mixing problems eliminated. 2. Short weld times, low peak temperatures result in narrow HAZ, minimal carbon transport, and sensitization. 3. Excellent process repeatability. 4. Relatively smooth weld interface closely approximates that assumed in stress analysis. 5. Vertical weld interface, a characteristic of this process, has been shown to reduce hoop stresses.	1. Welding machine capacity limits weld area to about 142 cm^2 (22 in^2). 2. Grain flow reorients longitudinal defects perpendicular to pipe axis. 3. No long term service experience available although 5000 hr. stress rupture data is comparable to GTA welds.	Develop process for smaller transition joints.
Explosive Weld	1. Liquid metal mixing problems eliminated. 2. Short weld times, low peak temperatures eliminates HAZ, carbon transport and sensitization. 3. Relatively smooth weld interface closely approximates that assumed in stress analyses.	1. Joint configurations for circumferential pipe welds are difficult to explosive weld. 2. Long tapered weld interface results in higher hoop stresses. 3. No service or fabrication experience is available.	Not recommended for development.
Co-extrusion	1. Liquid metal mixing problems eliminated. 2. Smooth weld interface closely approximates that assumed in stress analysis.	1. Development of large diameter (>457 mm, 18 in.) co-extrusion will be costly because of limited availability of a large extrusion press. 2. Long tapered weld interface will result unless a method can be developed to shorten the taper. 3. Not possible to anneal all materials simultaneously by conventional methods after hot or cold extrusion. Austenitic materials will be severely sensitized.	Not recommended for development.
Continuously-Graded Composition	1. Changes in physical and mechanical properties are gradual and continuous. Sharp interfaces with the accompanying thermal stresses are minimized. 2. Gradients in carbon activity are reduced so that carbon migration does not occur. 3. Process can be applied to large diameter pipe.	1. Requires substantial development to solve metallurgical and fabrication problems. 2. Experience is limited to laboratory testing. 3. Difficult to characterize physical and mechanical properties of discrete regions in the joint, making theoretical analysis difficult. 4. Extensive testing required to prove reliability.	Long range solution requiring much development. Develop as a back-up method if step-graded joints fail.
Torroidal Expansion Joint	1. Pipe ends not rigidly restrained so thermal stresses don't build up. 2. Fabrication of 660 mm (26 in.) diameter and larger joints is common.	1. Design basis must be established. 2. Presently not allowed by ASME Code for primary pressure boundary. 3. External restraints may be required to prevent certain types of pipe movements. 4. Provisions must be made to prevent Na stagnation and freezing during service and draining.	Continue preliminary investigation on a low level basis.

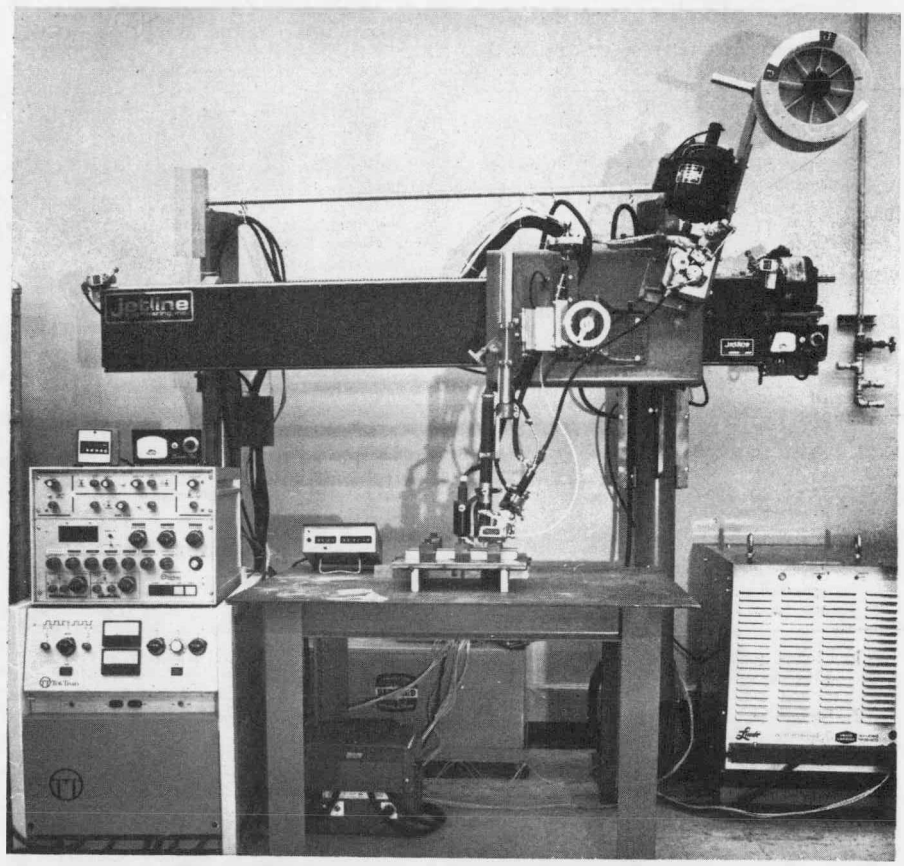

Figure 1. Hot-Wire GTA Weld System for Plate Welding

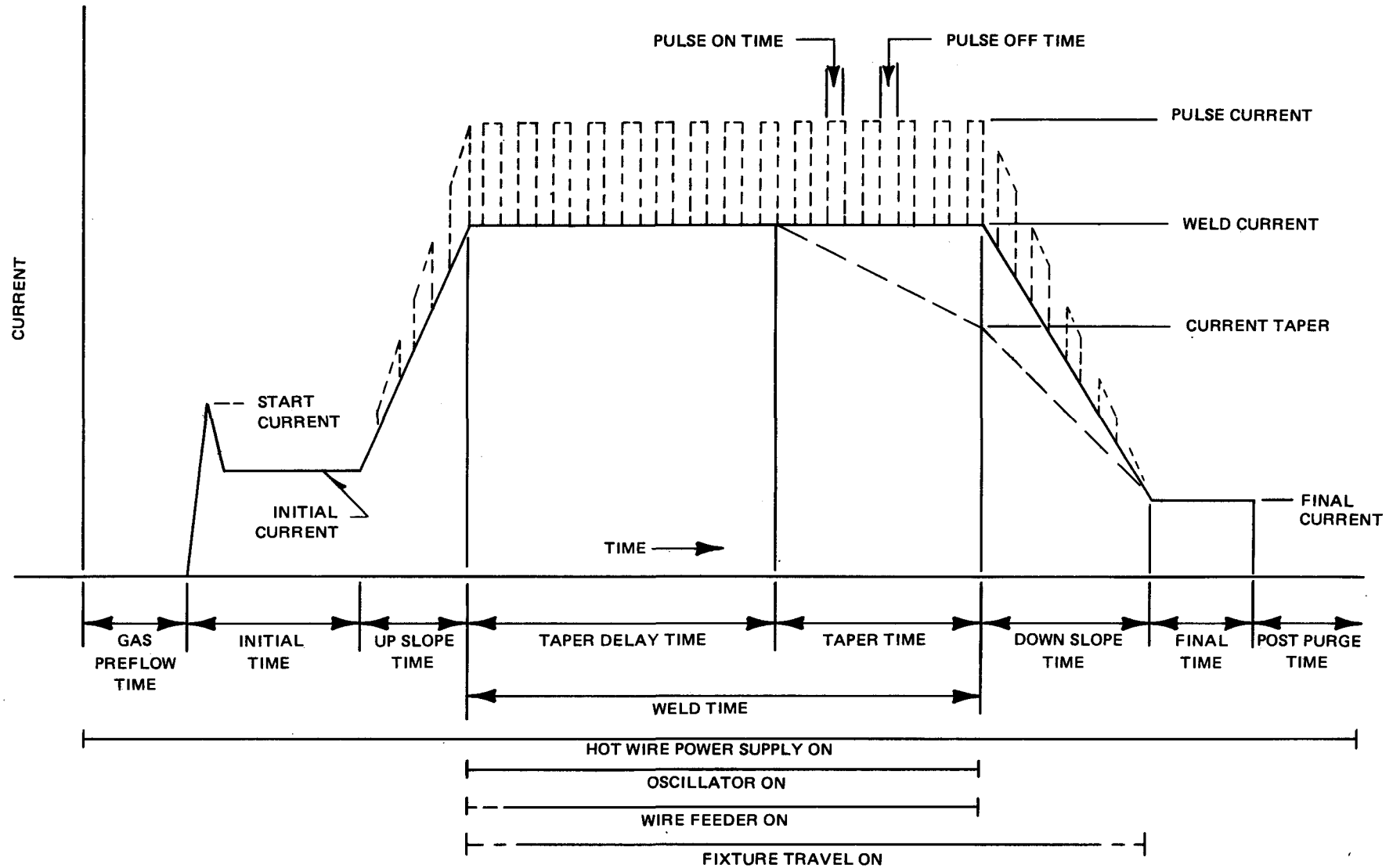

Figure 2. Weld Cycle for Hot-Wire GTA Weld System

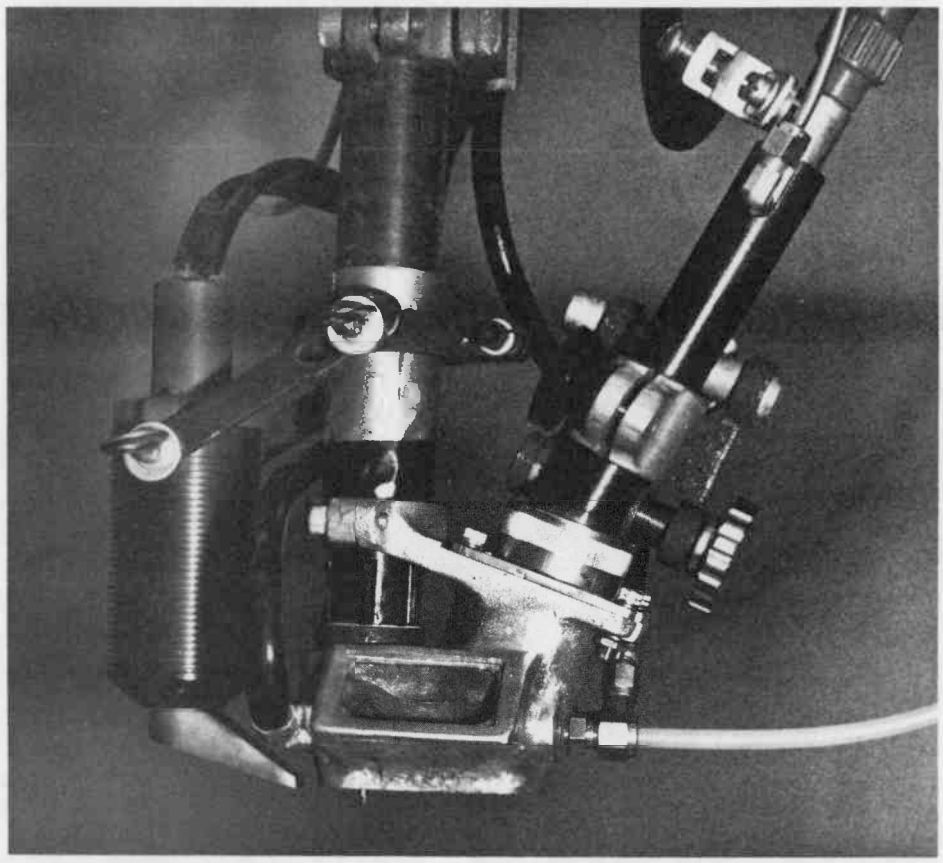

Figure 3. Gas Trailing Shield modified to Provide greater Visibility

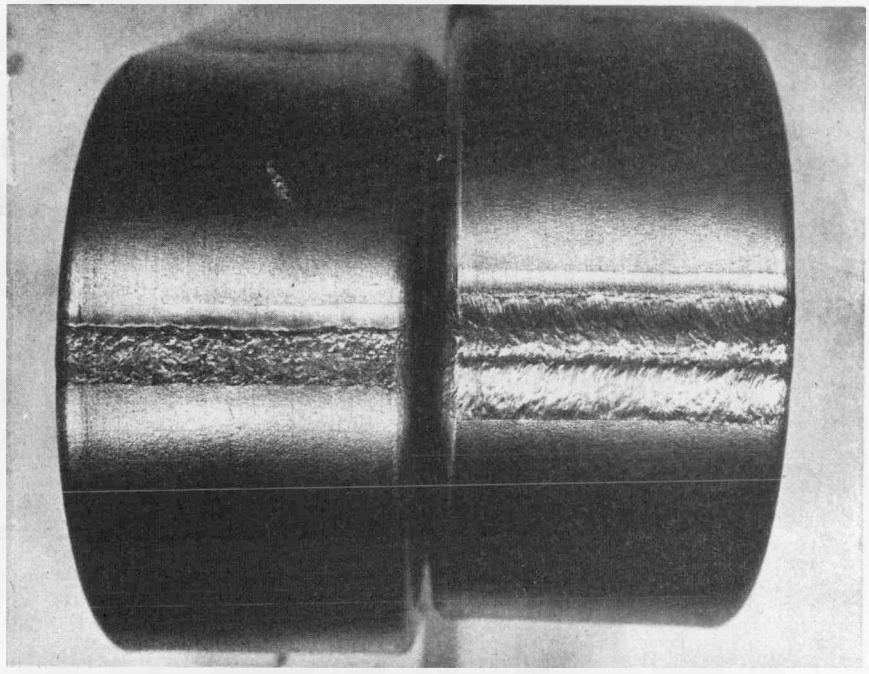

a. ROOT BEND

b. FACE BEND

Figure 4. Guide Bend Specimens, 2¼ Cr – 1 Mo welded to 304SS with INCONEL 82 after 1350°F, 1 hr PWHT

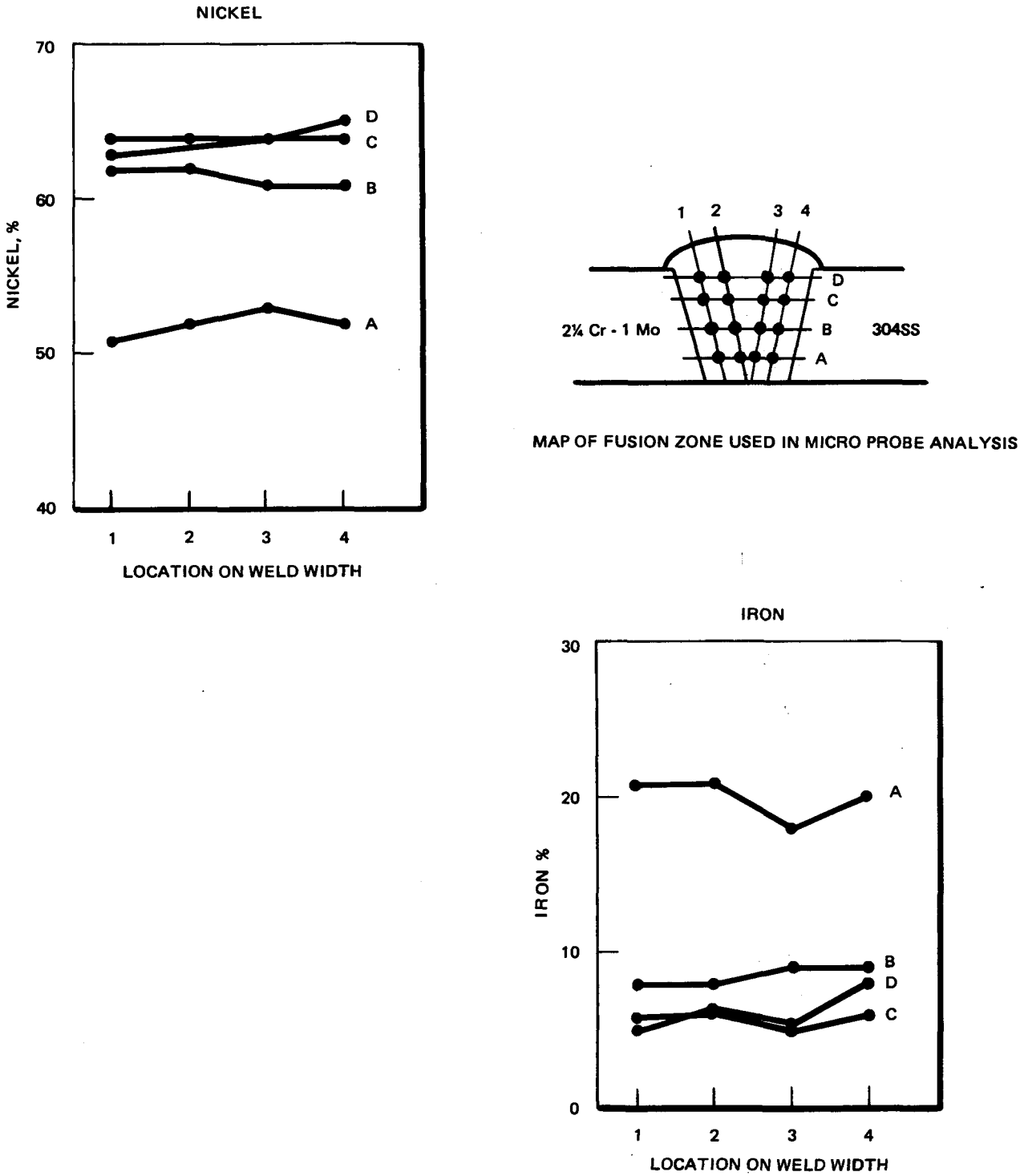

Figure 5. Microprobe Determination of Composition of ERNiCr-3 Filler Metal in 2¼ Cr – 1 Mo/304SS, Hot-Wire GTA Weld

APPENDIX A

TECHNICAL MEMORANDUM
ASSESSMENT OF THE EFFECT OF USING LOW CARBON 2¼Cr-1Mo PIPING IN THE INTERMEDIATE SYSTEM MOCKUP LOOP (ISML)

K. D. Challenger
J. L. Krankota

SUMMARY

The ISML was constructed in fiscal year 1975 to study the carburization and decarburization kinetics of the materials to be used to construct the Intermediate Heat Transport System (IHTS) of the Clinch River Breeder Reactor (CRBR). A low carbon variety*of 2¼Cr-1Mo has been used in place of normal carbon 2¼Cr-1Mo in the construction of the ISML in order to meet a very critical construction schedule. The completion of the loop was crucial for the verification of the plant design and the delay would have been a minimum of nine months. The delay was due to lead times required to purchase piping of the desired specifications. (The latter part of calendar '74 and early part of '75 were the most difficult times to obtain commitments for tubing deliveries.) At that time, the introduction of low carbon piping was believed to have no effect on the overall objective of the program. However, recent data indicate that the low carbon piping is acting as a weak carbon sink instead of the originally assumed carbon source.

General Electric believes that the original design objectives of the ISML must be completely restored. A study was made to evaluate alternate schemes and recommend a fix. It is recommended that normal carbon* 2¼Cr-1Mo be added to the loop in an amount equivalent in surface area to that of the low carbon piping present in the loop. This additional material will be placed in the loop in locations that are in the same temperature regime as that of the low carbon piping it is intended to replace.

The cost of this fix is insignificant and there are no schedule delays, as the normal carbon 2¼Cr-1Mo parts needed for the fix are already on hand.

---

*Low Carbon: 0.03%
Normal Carbon: 0.07-0.12%

This report describes the present condition of the loop, lists recent results, provides an analysis of data, examines the impact of recommended action, and provides the analysis to support the recommended action to restore the loop to achieve original objectives.

INTRODUCTION

In 1970, results obtained in static sodium tests indicated that, at the design temperature of the CRBR - IHTS, 2¼Cr-1Mo would not decarburize significantly.[1] A recommendation to design was subsequently made that resulted in a small penalty on the allowable design stresses for 2¼Cr-1Mo steam generator tubes to reflect the 300-400 ppm carbon loss predicted for the 30-year life. Reanalysis of data from other sodium test programs confirmed the results from the static pot tests.[2]

However, since most of the data used to make the decarburization correlation were obtained from tests in small static pots, it was decided that a bimetallic loop should be constructed to confirm the results obtained in static sodium. The ISML (Fig. 1) was designed to simulate the critical parameters believed to be controlling the carbon transport process, i.e., the temperature gradient through the heat exchangers and the surface area ratio of austenitic stainless steel to 2¼Cr-1Mo in the loop. At the time of the ISML design, the design of the CRBR-IHTS was not finalized requiring that an approximation of the temperature gradients and surface area ratio be used in designing the ISML.

Not until the spring of 1974, were plans made to begin construction of the test loop with a required completion date of June 1975. The completion date of June 1975 was crucial in order to recover early confirmation data for the plant design. During the pre-procurement planning phase, it was learned that delivery of 2¼Cr-1Mo piping was about nine months or more; this delay could not be accepted. General Electric had on site, at that time, a sufficient quantity of piping of the correct size that had been left over from the construction of the SGTR under a GE/ESADA contract. This piping was a low carbon variety of 2¼Cr-1Mo but qualified to ASTM A213 T22. Samples from this piping had been previously exposed in sodium pots and were found to decarburize at approximately the same rate as 2¼Cr-1Mo with higher carbon contents.[1,2] Further, the mechanical properties of this steel generated during the same ESADA program indicated that it had adequate strength for the moderate loading expected in the ISML. This piping was, therefore, selected for construction of the ISML.

STATEMENT OF THE PROBLEM

One of the primary objectives for the ISML (as it is constructed) is not presently fulfilled. The use of the low carbon 2¼Cr-1Mo piping has resulted in an effective surface area ratio of austenitic stainless steel (γ) to 2¼Cr-1Mo ferritic steel (α) in the ISML which is not prototypic of the Intermediate Heat Transport System (IHTS) of the Clinch River Breeder Reactor (CRBR); $(\gamma/\alpha)_{ISML} = 5$, $(\gamma/\alpha)_{CRBR} = 2$.

DISCUSSION OF THE PROBLEM

The approximate γ/α for an IHTS typical of the CRBR for an operating temperature equal to or greater than 800F is 2 (800F is selected as a point of reference as the kinetics of carbon transport are exponential with temperature, e.g., the rate of decarburization at 950F is an order of magnitude greater than that at 800F. Thus, those materials exposed to sodium at temperatures below 800F do not contribute significantly to the carbon transport process). The overall γ/α for the same typical IHTS is 1.

The ISML was constructed to model the parameters of the IHTS which were believed to control the carbon transport process, namely, temperatures and balance of materials, Fig. 2. As such, the ISML presently has a γ/α for $T \geq$ 800F of 1.7 and an overall ratio of 2. Thus, the γ/α in the critical temperature region of $T \geq$ 800F is very nearly the same as the IHTS. However, of the approximately 1600 in^2 of 2¼Cr-1Mo above 800F, only 550 in^2 has a carbon content prototypical of that to be used for the CRBR (0.07 to 0.12%C). The remainder of the 2¼Cr-1Mo in the ISML contains only 0.030%C resulting in an effective γ/α of 5. As discussed in the introduction, the technical impact of using the low carbon 2¼Cr-1Mo was assessed prior to its use and based on previous experience (data) with this material it was decided that it could be used without compromising any of the program's objectives. Specifically, it was assumed that the low carbon piping would decarburize at rates similar to the normal carbon.

However, recent data generated at WARD[3] and in the ISML itself (data in this report) indicate that the low carbon 2¼Cr-1Mo carburizes slightly. In the WARD tests, samples previously decarburized to 630 ppm carbon during 100 hour exposure to 1100F Na subsequently carburized to 690 ppm after 5000 hours exposure at 950F.

Data generated in the ISML are shown in Fig. 3 and tabulated in Table I. All data shown except that for the low carbon 2¼Cr-1Mo represents approximately 600 hour exposure (Run B-1), the low carbon 2¼Cr-1Mo has been exposed for 1000 hours (Run B-2). Thin foil (0.003") samples of the low carbon 2¼Cr-1Mo were prepared from archive piping, isothermally annealed per RDT-M3-33, and exposed in ISML for 1000 hours in sample holders SH-2 (isothermal 950F) and HX-3 (heat transfer 940-800F). Eleven carbon analyses were performed on archive unexposed 0.003" foils and seven on the exposed foils. The samples in SH-2 carburized 90 ppm from a mean value of 285 to 375 ppm. Statistical analysis of these data indicates that the 90 ppm carburization is statistically significant with 90% confidence.

The samples of 2¼Cr-1Mo with normal carbon content exposed for 600 hours demonstrate the expected decarburization behavior. Two different heats of 2¼Cr-1Mo have been exposed; one has an unstable microstructure (contains a large amount of bainite) and the other a stable microstructure (polygonal ferritic + pearlite). The unstable microstructure decarburizes at a faster rate than the stable one consistent with other published results.[4,5] The stainless steel is carburizing, but after 600 hours the degree of carburization is too small to accurately estimate rates.

These data indicate that the carbon activity in the ISML is very near that for 2¼Cr-1Mo containing 400 ppm carbon.

The French have observed similar behavior in their Carnacier Sodium Loops. Here samples of 2¼Cr-1Mo, one group with 500 ppm and the other group with 1400 ppm carbon, were exposed simultaneously in the same sodium loop at temperatures ranging from 932 to 1022F for 17,000 hours.[8] The 1400 ppm carbon 2¼Cr-1Mo decarburized at a rate predicted by the GE correlation while the carbon content of the samples starting with only 500 ppm carbon did not change. Type 316 SS samples in the same loop carburized significantly. These facts indicate that a similar carbon activity exists in the French Carnacier Loops.

Based on these recent observations, there are two concerns over the desired prototypicality of the ISML that must be resolved:

1. *Will the presence of the low carbon 2¼Cr-1Mo result in a lower carburization rate of the 304 SS by acting as a competing source for carbon?*

2. *Will the overall carbon transport process be altered by the change in effective γ/α?*

ANALYSIS OF CONCERNS

1. There are two reasons why the carburization of the low carbon 2¼Cr-1Mo will not effect the carburization behavior of the austenitic stainless steel specimens:

- The total amount of carbon that can possibly be picked up by the low carbon 2¼Cr-1Mo piping during the life of the loop is 0.138 grams of carbon. Whereas the stainless steel samples and piping are estimated to remove 4.78 grams of carbon during this same period. Thus, the total carbon removed from the system by the low carbon piping is only 28% of the total removed by both the stainless steel piping and samples. (See Appendix A for the calculations involved).
- The thermodynamic driving force for the carburization of the low carbon 2¼Cr-1Mo is much lower than that for the stainless steel as 2¼%Cr is much less effective at gettering carbon from the sodium than the 18%Cr in the stainless steel.

2. The question of the influence of γ/α ratio can not be answered conclusively. Russian work[6] found that by varying the γ/α from 230 to 2.3 had a significant effect on the amount of decarburization occurring in 2¼Cr-1Mo exposed to sodium in the temperature range of 880 to 1100F for up to 3000 hours. It is, however, difficult to estimate the effect of the comparatively small change in γ/α for ISML; a change from 2 to 5.

It is also difficult to estimate the effect of this ratio on the carburization rate of the austenitic stainless steels.

Therefore, even though the initial data from the ISML are well behaved, (the carburization rate for 304 and decarburization rate of 2¼Cr-1Mo agree with the predictions) there may exist some uncertainty that the measured changes (Fig. 3) are representative of those that will occur in the CRBR-IHTS. Therefore a plan must be implemented to remove all doubt surrounding data generated in the ISML.

RECOMMENDATION

General Electric recommends that the design balance of γ/α be restored by the addition of isothermally annealed 2¼Cr-1Mo per RDT M3-33 in all 2¼Cr-1Mo heat exchangers and sample holders. The amount of surface area of normal carbon content 2¼Cr-1Mo added shall be equivalent to that of the low carbon piping.

Liners ($\sim$0.040" thick) will be inserted into each heat exchanger and sample holder that was originally manufactured from the low carbon 2¼Cr-1Mo pipe; HX-3, HX-4, SH-1, SH-2, and SH-3, Figures 1 and 2. These liners will be installed as shown in Figure 4. The addition of this liner will require a slight modification to the sample configuration; however, modification had already been planned in order to test CRBRP steam generator tubing. These liners will be inserted through the sample exchange port and welded on one end. The weld will prevent sodium flow between the liner and the sample holder and/or heat exchanger wall allowing only one surface of the insert to decarburize. The lack of flow will also prevent carburization of the low carbon 2¼Cr-1Mo in these regions reducing the already small amount of carbon removed from the system by the low carbon piping. The addition of the liner will not require any modification to the loop. These liners will substitute for the low carbon 2¼Cr-1Mo used in the construction of the heat exchangers and sample holders; however, in order to substitute for the surface area of low carbon piping in the hot leg (950F) a coil of $\sim$0.020" foil of normal carbon content 2¼Cr-1Mo with 500 in^2 will be inserted into sample holder SH-2 (950F), Figure 5. The carbon content of the coil will be monitored and the coil replaced when decarburization reaches the center of the foil (approximately 3,000 hrs.).

This recommendation restores the γ/α in all temperature regimes.

However, preparation of the inserts and coils will require approximately one month. Thus, an interim action is required.

The γ/α has been temporarily restored by the addition of 1500 in^2 of isothermally annealed 2¼Cr-1Mo containing 1200 ppm carbon into sample holders SH-2, SH-3 and SH-4 (Figures 1 and 2) in the form of 0.045" diameter wire.

Six coils of these wires have been inserted over thermocouples in each sample holder as illustrated in Figure 6. The total surface area of the coils (1500 in^2) will be divided equally among SH-2, SH-3, and SH-4 not only restoring the overall γ/α balance, but proportioningly placing the substitute 2¼Cr-1Mo in the same temperature regions as that of the low carbon piping. The wire in SH-2 substitutes for the hot leg cross over piping at 950F (450 in^2), SH-3 for the heat exchanger, HX-3 and sample holder SH-3 operating in the temperature range of 800-950F (550 in^2) and SH-4 for the cold leg piping, heat exchanger HX-4 and sample holder SH-4 (500 in^2).

The recommended interim modification restores both the originally designed γ/α in the high temperature range ($T \geq 800F$) and overall γ/α.

Since at most only 1% of the total carbon transferred in the ISML will be used in the carburization of the low carbon 2¼Cr-1Mo piping, its influence on the carbon transport processes is viewed as quite innocuous. This alteration has been completed without any delay in the loop operation or additional costs.

POSSIBLE ADVERSE CONSEQUENCES OF INTERIM ACTION

1. *Small diameter wires will "run out" of carbon during the time necessary to complete the permanent fix.*
2. *Lower sodium velocity on the inside of the samples will alter the carbon transport process.*
3. *Diffusion bonding of the wires to the test samples will occur.*

DISCUSSION OF CONSEQUENCES

Using the GE correlation for decarburization[2] (presently believed to over estimate the actual decarburization which is slowed down by thermal aging), will reach the center of the wire altering the carbon activity gradient in the wire after a comparatively short time (4,000 hrs.). However, this time period is much larger than the time period required to fabricate the materials for the permanent fix; the loop will operate with these wires for only 1,000 hours.

In regards to the second concern, the effect of Na velocity on decarburization has been shown by Thorley[7] to negligible in the range of ½ to 32 fps. They found no effect of Na velocity in this range after Na exposures of 4,000 hours at 930F. During this experiment, the 0.040" thick samples decarburized from about 1200 ppm to 900 ppm with no discernible effect of Na velocity. Therefore, it is not believed that the sodium velocity change will influence the decarburization kinetics.

The third concern addresses the possibility of diffusion bonding between the wire coils and the samples. Inevitably there will be contact between the coils and the samples, however the contact area will be very small, and the loads between coils and samples should be very low. Therefore diffusion bonding of the samples should not occur. Also, this approach of using coils of wire inside sample holders has been employed many times in the past without difficulty.

The loop will be operated with these coils serving to restore the γ/α for 1,000 hours as the loop is scheduled for shut-down at that time for modification of sample holders to allow testing of CRBRP steam generator tubing. During this scheduled shut-down, the liners will be installed into all 2¼Cr-1Mo sample

holders and heat exchangers. The incorporation of the inserts will delay the loop operation approximately one week. However, all modifications can be completed with the existing funding for this task.

REFERENCES

1. Armijo, J. S., Krankota, J. L., Lauritzen, T. A. and Yukawa, S., "Materials Evaluation and Fabrication Studies, Steam Generator Development", NEDL-13655, Oct. 1970.

2. Krankota, J. L. and Armijo, J. S., "Decarburization Kinetics of Low-Alloy Ferritic Steels in Sodium", Met. Trans. (1972), 3, 2515.

3. Private communication S. Shields to J. Krankota, July 1975.

4. Matsumoto, K. et.al., "Carbon Transfer Behavior of Materials for LMFBR Steam Generators" presented at the International Conference on Steam Generators, Gatlinsburg, Tenn., Sept. 9-12, 1975.

5. Natesan, K., Chopra, O. K., and Kassuer, T., "Compatibility of 2¼Cr-1Mo Steel in Sodium Environment", ibid.

6. Bykov, V. N. et.al., "The Problems of Corrosion Resistance of Structural Materials in Sodium", CEMA Symposium of Atomic Power Stations with Fast Reactors Vol. I", Joint Publications Research Translation JPRS 48330, 427, July 1969.

7. Thorley, A. et.al., "Effect of Sodium Exposure on the Mechanical Properties and Structure of Some Ferritic Austenitic and Nickel Alloys", T6R Report 1909(C), 1969.

8. Trip Report, C. N. Spalaris and D. Green to Distribution, Trip to Cadarache, Oct. 23, 1975.

Table I Carbon Contents of All Samples Removed From Run B-1 (591 hrs.) and Selected Sample From Run B-2 (912 hrs.)

Run	Material	Location	Sample	Temperature		Carbon (ppm)		
				°F	°C	Co	C_f	ΔC
B-1	304SS	HX-1	H201	666	352	325	349	+24
							388	+63
	304SS	HX-1	H221	705	374	325	351	+26
							303	-22
	304SS	SH-1	S201	807	431	623	634	+11
							631	+8
	2¼Cr-1Mo	SH-1	S221*	807	431	1345	1150	-195
							1157	-188
	304SS	HX-2	H401	807	431	623	740	+117
							722	+99
	304SS	HX-2	H421	857	458	623	726	+103
							757	+134
	304SS	SH-2	S401	967	520	325	405	+80
							430	+111
	2¼Cr-1Mo	SH-2	S421*	967	520	1345	916	-429
							944	-401
	2¼Cr-1Mo	HX-3	H601*	945	507	1345	1128	-217
							1132	-213
	2¼Cr-1Mo	HX-3	H621*	875	468	1345	1216	-129
							1212	-133
	304SS	SH-3	S601	776	413	623	657	+34
							694	+71
	2¼Cr-1Mo	SH-3	S621**	776	413	1083	743	-340
							752	-331
	2¼Cr-1Mo	HX-4	H801**	805	429	1083	761	-322
							764	-319

Table I Carbon Contents of All Samples Removed From Run B-1 (591 hrs.) and Selected Sample From Run B-2 (912 hrs.)

Continued

Run	Material	Location	Sample	Temperature °F	Temperature °C	Carbon (ppm) Co	Carbon (ppm) C_f	Carbon (ppm) ΔC
B-1	2¼Cr-1Mo	HX-4	H821**	762	406	1083	787	-296
							801	-282
	304SS	SH-4	S801	670	354	623	721	+98
							720	+97
	2¼Cr-1Mo	SH-4	S821*	670	354	1345	1258	-87
							1301	-44
B-2	2¼Cr-1Mo L.C.	SH-2	L.C.2	967	520	264	392	
						350	353	
						267	380	
						342	409	
						269	322	
						201	360	
						319	399	
						319		
						260		
						250		
						300		
					Mean	285	375	+90

NOTE: 1) All samples are 0.010 in. (0.025 cm) from Run B-1 and 0.003 in. (0.007 cm) from Run B-2.

2) * Stable microstructure (20% Tempered Pearlite, 80% Ferrite)

** Unstable microstructure (15% Bainite, 85% Ferrite)

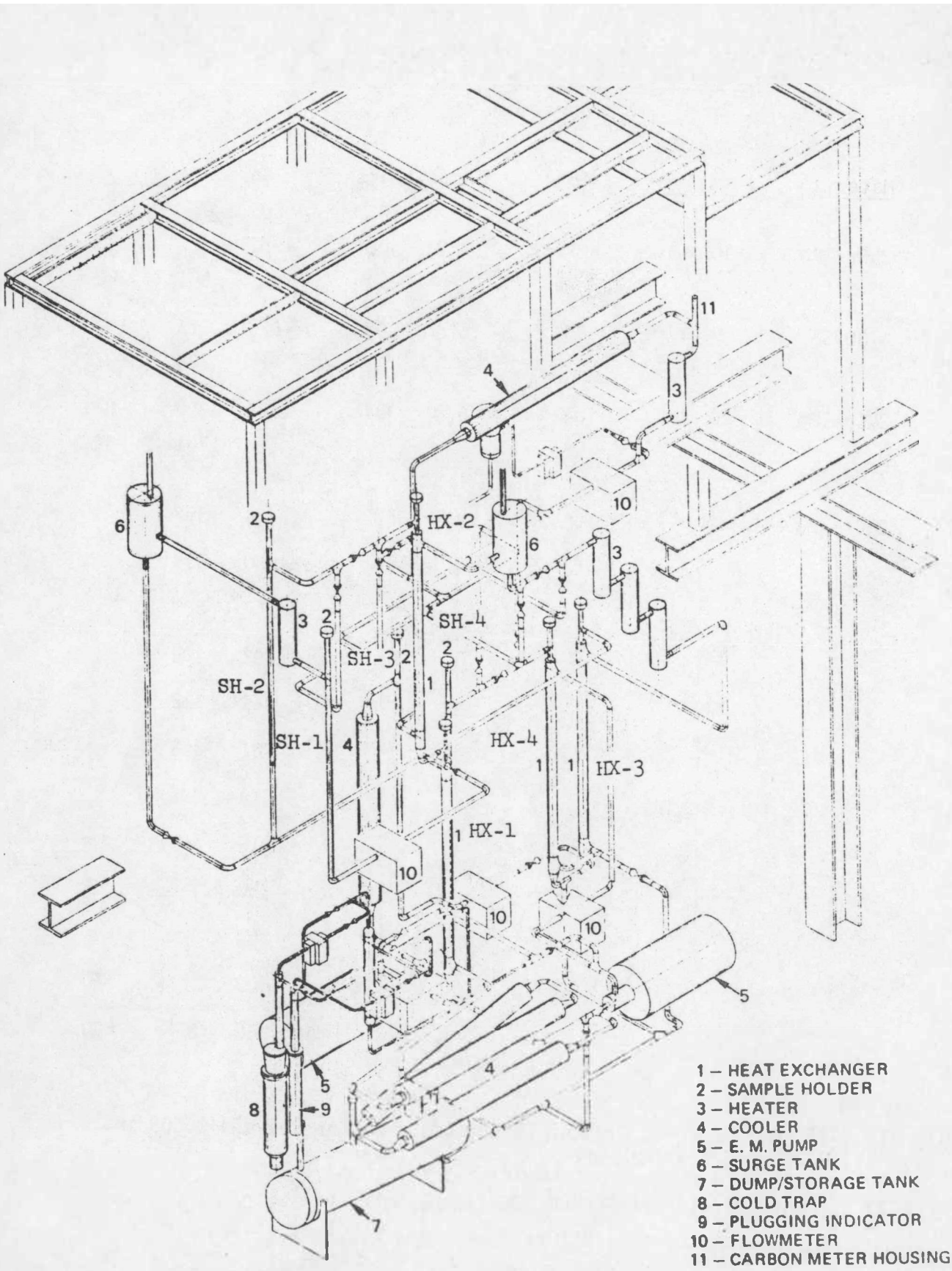

Figure 1 Intermediate System Mockup Loop

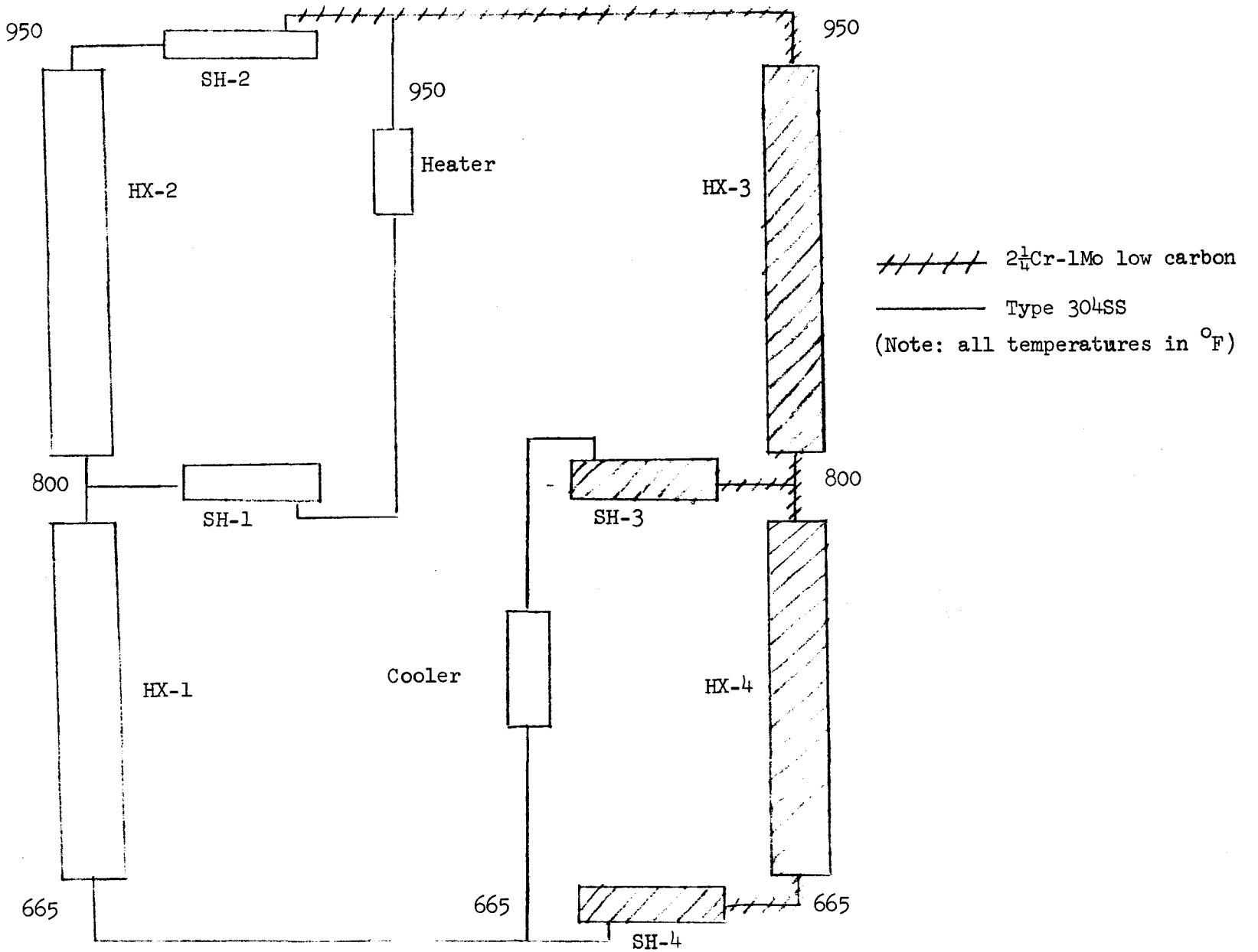

Figure 2 Test loop of the Intermediate System Mockup Loop (ISML)

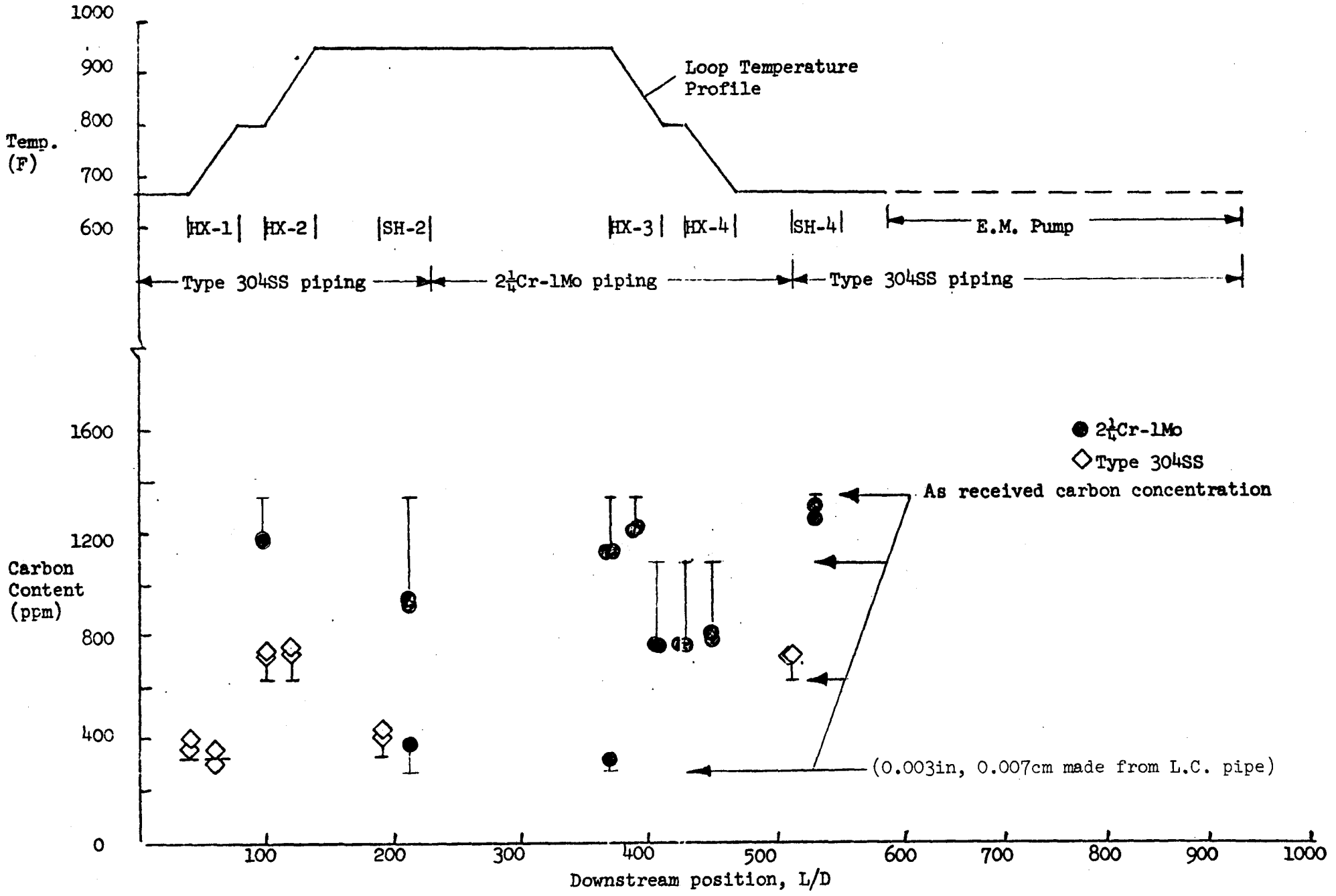

Figure 3 Carbon concentration profile in ISML after first test run (Run B-1, 591 hours)
Note: All samples are 0.025cm (0.010in) thick (except as noted).

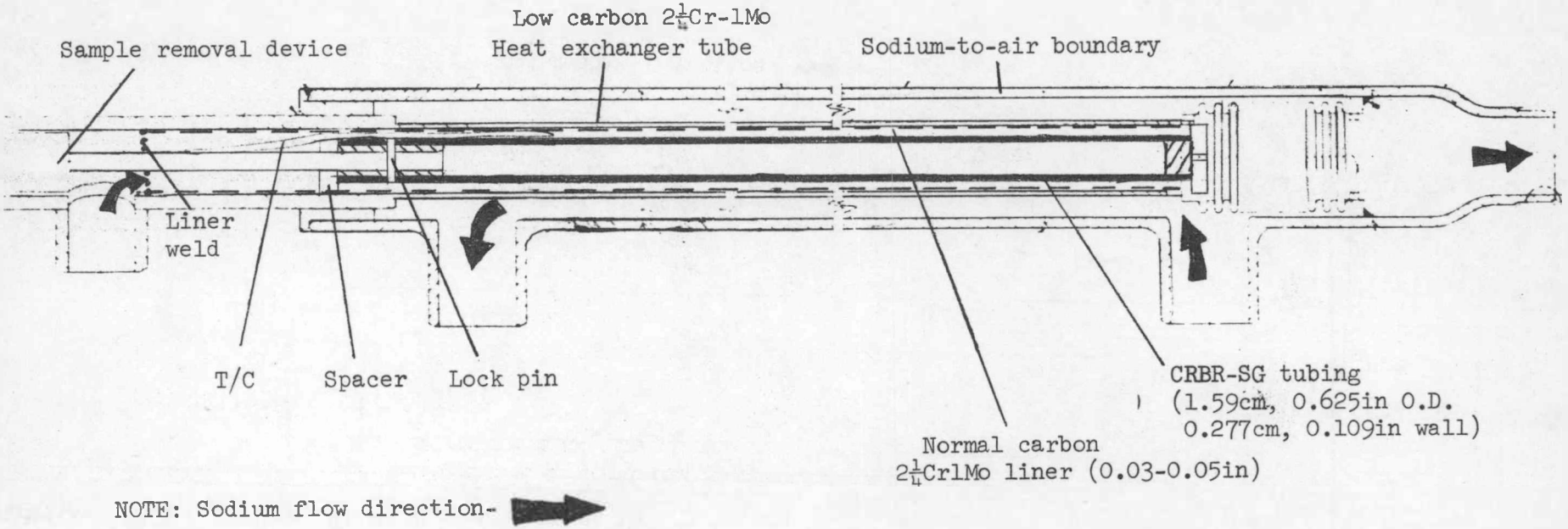

Figure 4 Sample and sample holder for the ISML heat exchanger sample holder (planned for run B-4 and beyond)

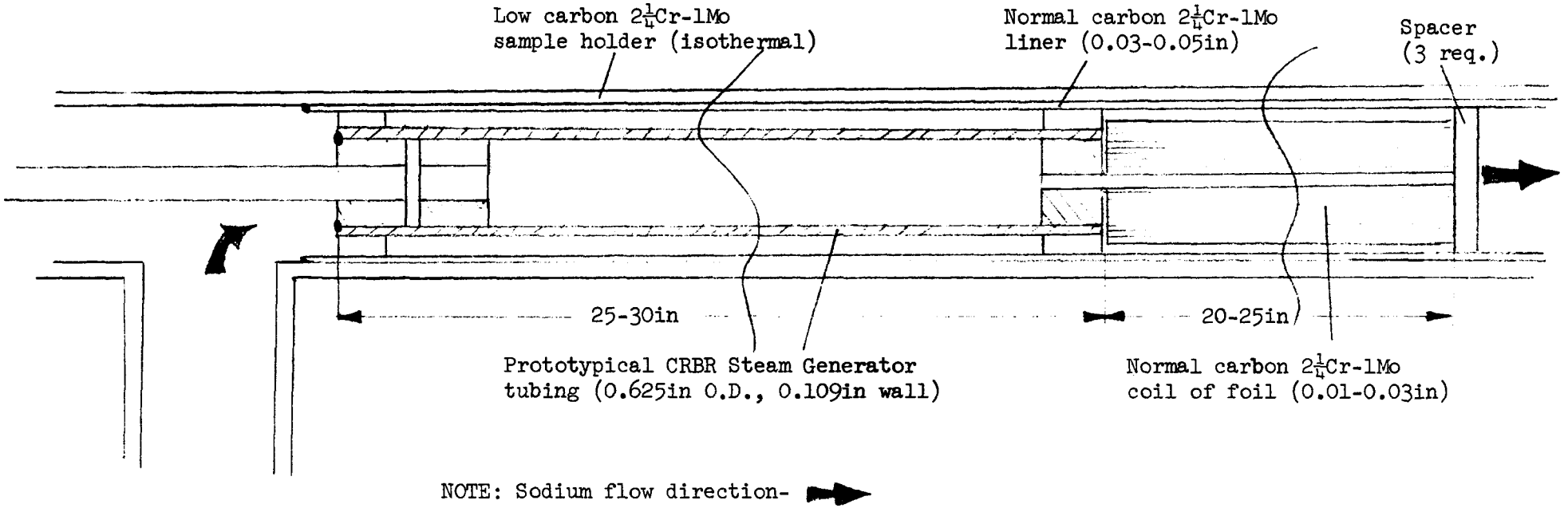

Figure 5 Sample and sample holder for the ISML isothermal sample holder (planned for run B-4 and beyond)

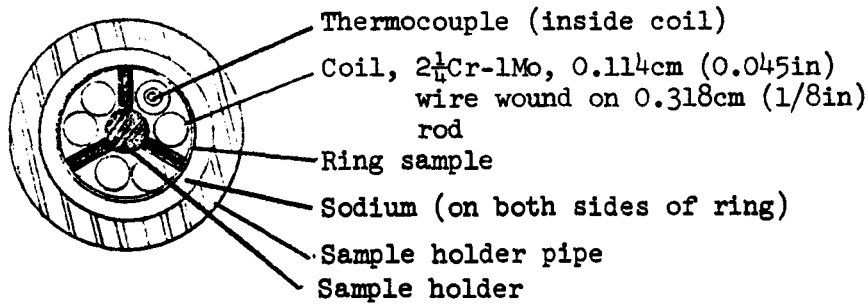

Figure 6 ISML sample holder containing normal carbon level 2¼Cr-1Mo wire coils.

APPENDIX B

ANALYSIS OF CARBON SINKS IN THE ISML

I Carburization of Low Carbon 2¼Cr-1Mo in the ISML

The amount of carbon picked up by the low carbon 2¼Cr-1Mo can be expressed in terms of grams C per cm^2 surface;

$$M = \frac{\Delta C\ \Delta X\ \rho}{2}$$

Where: $\Delta C = 60X10^{-6}$gm c/gmFe (WARD Ref. 3)

$\Delta X = 0.003in = 0.0076cm$

$\rho = 7.8gmFe/cm^3Fe$

$$M = \frac{(60X10^{-6})(0.0076)(7.8)}{2}$$

$$M = 1.78X10^{-6}gm\ c/cm^2Fe$$

This influx of carbon occured during 5000 hours of exposure in the WARD CEL sodium loop. The rate constant from which the predicted carbon pickup in the ISML is determined is calculated from these data assuming parabolic carburization behavior;

$$K = \frac{M}{t^{\frac{1}{2}}}$$

Where: $t^{\frac{1}{2}} = (5000\ hours\ X\ 3600\ sec/hr)^{\frac{1}{2}}$

$t^{\frac{1}{2}} = 4242\ sec^{\frac{1}{2}}$

and $K = \frac{1.78X10^{-6}}{4242}$

$K = 4.2X10^{-10}gmC/cm^2\text{-}sec^{\frac{1}{2}}$

The assumption of parabolic behavior is conservative because the carburization rate of WARDs low carbon 2¼Cr-1Mo was slower than that predicted by WARD based on simple diffusion.

The amount of carbon picked up by the ISML low carbon 2¼Cr-1Mo piping is;

$$W_1 = (M)(A)$$

Where: A = $9062cm^2$ of sodium-exposed low carbon 2¼Cr-1Mo piping.

and $M = Kt^{\frac{1}{2}}$

$t^{\frac{1}{2}} = (25,000\ hours\ X\ 3600\ sec/hr)^{\frac{1}{2}}$

$t^{\frac{1}{2}} = 9487\ sec^{\frac{1}{2}}$

$W_1 = (8.4X10^{-10})(9487)(9062)$

$W_1 = 0.035$

A value of W_1 = 0.138gmC is calculated using ΔC = 90ppm; the amount picked up by the L.C. Foils during Run B-2.

II Carburization of Stainless Steel in Loop B (GE Data Compilation Figure A-1)

As before, the amount of carbon picked up by the stainless steel is expressed in terms of grams C per cm^2 surface, which in this case can be read from the data correlation in Figure A-1; here M equals 0.15 mgm/cm^2 after 25,000 hours. The amount of carbon picked by the ISML stainless steel piping and samples is;

$W_2 = (M)(A)$ Where: A = 31580cm^2 of sodium exposed stainless steel piping and samples.

$W_2 = (1.5X10^{-4})(31580)$

$W_2 = 4.7gmC$

Of the total predicted carbon pickup in the ISML the amount picked up by the low carbon 2¼Cr-1Mo piping is negligible;

$$f_{2\frac{1}{4}Cr} = \frac{.138}{.138 + 4.7}(100)$$

$f_{2\frac{1}{4}Cr} = 2.8\%$

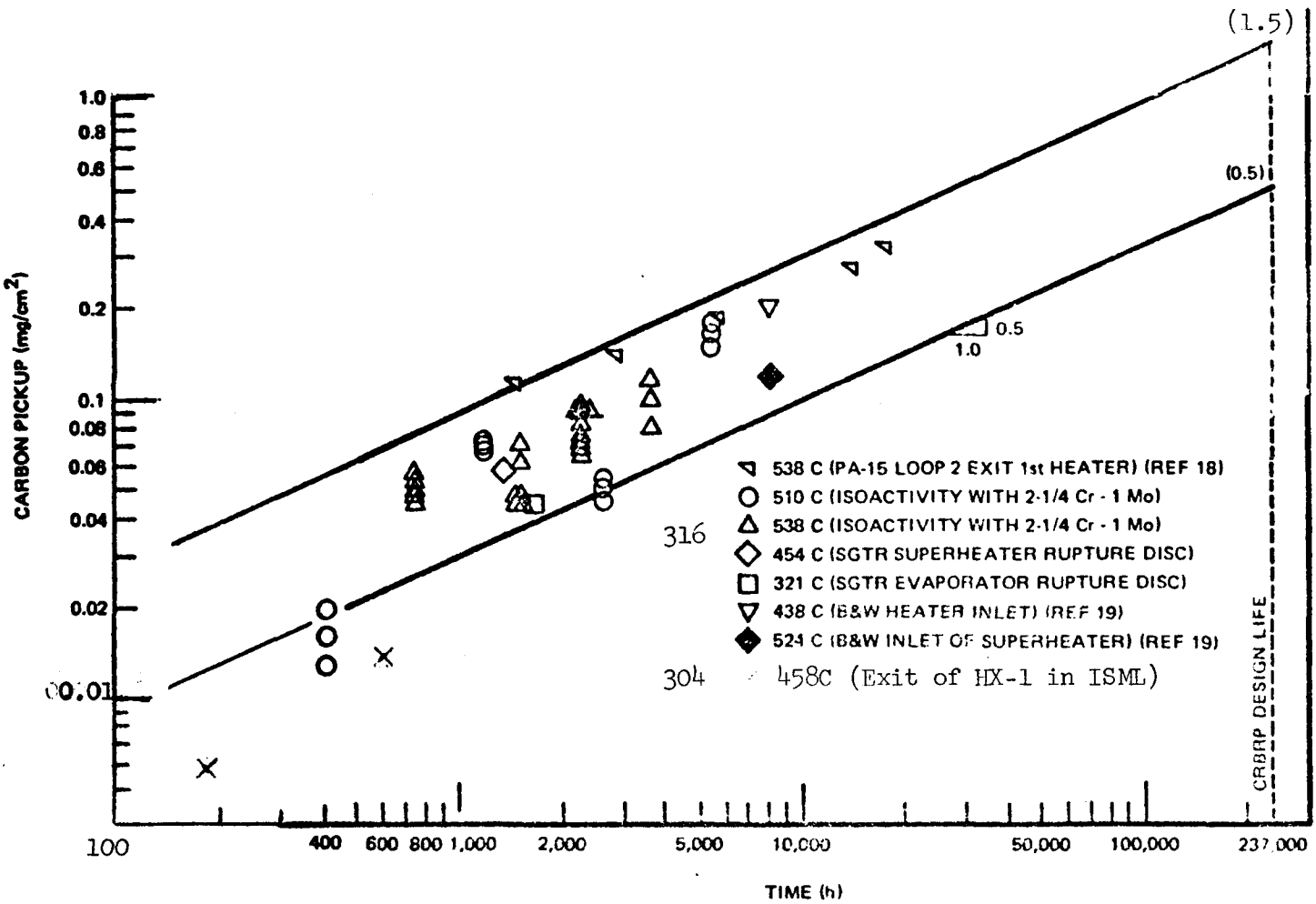

Figure A-1 Carburization of stainless steels in sodium in bimetallic ($2\frac{1}{4}$Cr-1Mo/stainless steel) loops.

CONTRACT NO. AT(04-3)-893-10 TASK G

189-SG029 FY76

STEAM GENERATOR MATERIALS QUALIFICATION

CONTRIBUTORS

H. J. Busboom

J. F. Copeland

R. A. Day

D. Dutina

R. T. Hartle

M. D. Mitchell

H. P. Offer

P. J. Ring

D. N. Rodgers

D. W. Sandusky

C. N. Spalaris

M. D. Sullivan

T. Yang